Thèse de Doctorat

Mention : Sciences Agronomiques et Ecologiques

Spécialité : Sciences de la mer : Océanographie physique

Présentée à **l'Ecole Doctorale en Sciences Technologie et Santé (ED 585)**

de l'Université du Littoral Côte d'Opale

par :

SALAH SALAH Ikram

pour obtenir le grade de Docteur de l'Université du Littoral Côte d'Opale

Caractérisation de la dynamique biogéochimique des eaux côtières brésiliennes via l'analyse des archives satellites « couleur de l'eau »

Soutenue le 06/03/2026, après avis des rapporteurs, devant le jury d'examen :

M. Bertrand Lubac, Maître de conférences, EPOC, Bordeaux	**Rapporteur**
M. Pierre Gernez, Maître de conférences, MMS, Nantes	**Rapporteur**
M. Cédric Jamet, Professeur, LOG, ULCO	**Président**
Mme Aline de Matos Valerio, Docteur, Indiana université	**Examinatrice**
M. Milton Kampel, Directeur de recherche, INPE	**Examinateur**
M. Hubert Loisel, Professeur, LOG, ULCO	**Directeur de thèse**
M. Vincent Vantrepotte, Chargé de recherche, LOG, ULCO	**Co-encadrant**

PhD Thesis

Major Agricultural and Ecological Sciences

Specialty: Marine Sciences: Physical Oceanography

presented at **the Doctoral School of Science, Technology and Health (ED 585)**

of the Université du Littoral Côte d'Opale

by

SALAH SALAH Ikram

To obtain the degree of Doctor of the Université du Littoral Côte d'Opale

Characterization of the biogeochemical dynamics of Brazilian coastal waters through the analysis of ocean color satellite archives

Defended on the 06/03/2026, after approval of the reviewers, in front of the jury

Mr. Bertrand Lubac, Associate Professor, EPOC, Bordeaux University	**Reviewer**
Mr. Pierre Gernez, Associate Professor, MMS, Nantes University	**Reviewer**
Mr. Cédric Jamet, Professor, LOG, ULCO	**President**
Mrs. Aline de Matos Valerio, Doctor, Indiana University	**Examiner**
Mr. Milton Kampel, Researcher Director, INPE	**Examiner**
Mr. Hubert Loisel, Professor, LOG, ULCO	**Thesis supervisor**
Mr. Vincent Vantrepotte, Researcher, LOG, ULCO	**Co-supervisor**

ACKNOWLEDGEMENTS

As I come to the end of my doctoral journey, I realize how deeply this work has been shaped by the support, guidance, and trust of many people. This thesis is not solely the result of individual effort, but of a collective commitment that I am sincerely grateful for.

I would like to express my deepest gratitude to my primary supervisor, **Vincent Vantrepotte**. His unwavering support, availability, and confidence were essential throughout this PhD. His thoughtful guidance, rigorous feedback, and constant encouragement played a decisive role in my scientific development and personal growth. I truly believe that this work would not have been possible without him.

I am also profoundly thankful to my co-supervisor, **Hubert Loisel**, for his insightful ideas, careful reading of my thesis and papers, and constructive remarks. His scientific rigor and clarity of thought greatly enriched this research, and I hold him in the highest esteem.

I gratefully acknowledge **ULCO**, **ANR**, and **LOG** for their financial support and for providing an excellent research environment in which this work could be carried out.

I would like to thank the members of the jury, **Cédric Jamet**, **Pierre Gernez**, **Aline de Matos Valerio**, and **Milton Kampel**, for accepting the responsibility of evaluating my work and for the time and attention they devoted to it. My sincere thanks also go to the members of my thesis monitoring committee, **David Doxaran** and **Milton Kampel**, for their valuable advice, careful follow-up, and continued support throughout the course of my PhD.

I would like to extend special thanks to **Manh, Joao** and **Daniel** for always being available to exchange ideas, offer guidance, and share their experience whenever I needed it.

I am grateful to my colleagues and friends **Yasmine, Naziha, Wafa, Bahdja, Rosa**, **Carina**, **Marie**, **Corentin**, **Kévin**, and **Raed**, whose friendship, encouragement, and shared moments made these three years of doctoral study both enriching and memorable.

To my mother, my sisters, and my brother, I owe my deepest gratitude for their unwavering emotional support, their faith in me, and the pride they have always shown in my achievements. Their presence has been a constant source of strength. To my beloved nieces and nephews, for the joy and light they bring.

Finally, in loving memory of my father. Even in his absence, I know he would have been proud of me, and this work is dedicated to him.

TABLE OF CONTENTS

ACKNOWLEDGEMENTS…… 3
TABLE OF CONTENTS…… 4
LIST OF ACRONYMS……... 8
LIST OF FIGURES……. 9
LIST OF TABLES…….16
INTRODUCTION…….17
CHAPTER 1: STATE OF THE ART…… 22
1.1. Study area: Brazilian coastal waters……..23
1.1.1. General setting and geographical extent……23
1.1.2. Coastal morphology and ecosystem complexity……24
1.1.3. Climatic and hydrological conditions…… 25
1.1.4. Ocean circulation and hydrodynamic processes…… 25
1.1.5. Biogeochemical variability of Brazilian coastal waters…… 27
1.1.6. Anthropogenic pressures and the need for long-term monitoring……. 28
1.2. Satellite ocean color remote sensing and coastal biogeochemistry…….....29
1.2.1. Satellite ocean color observations and mission continuity…… 29
1.2.2. Atmospheric correction and retrieval of remote sensing reflectance…….32
1.2.3. Optical properties and bio-optical inversion of biogeochemical variables…….....36
1.2.4. Optical complexity of coastal waters and implications for long-term monitoring.....38
1.2.5. Biogeochemical descriptors of coastal water quality…….41
1.2.6. Key biogeochemical descriptors of coastal water quality……...42
1.3. Time series analysis of ocean color observations for assessing coastal ecosystem variability and change……45
1.4. Conclusion…….51
CHAPTER 2: BRAZILIAN COASTAL WATERS DATASET DEVELOPMENT AND GENERAL SPATIOTEMPORAL DYNAMICS……...53
2.1. Introduction……... 53
2.2. COCOBRAZ database (2002-2022)……..54
2.2.1. Description of the in situ database…… 54
2.2.2. Description of the COCOBRAZ MODIS 1km satellite database…….. 57
2.2.2.1. MODIS-Aqua data (1 km) OC-SMART processing (2002-2022)……. 57

2.2.2.2. MODIS-Aqua (1km) NIR-SWIR processing (2002-2022)…… 59
2.2.2.3. Bio-optical models applied on MODIS (OC-SMART)…….. 60
2.2.2.4. Ancillary data…….65
2.2.2.5. Time series decomposition and trend analysis of the COCOBRAZ dataset…66
2.3. Brazilian Coastal ecosystems…….69
2.3.1. MODIS aqua advantage and limitations…… 69
2.3.2. Comparison of satellite ocean-colour products in Brazilian coastal waters……72
2.3.2.1. Comparison based on red-band reflectance and coastal coverage……..72
2.3.2.2. Comparison based on Chl-a estimation in coastal waters……...77
2.3.2.3. Impact of satellite product choice on long-term chlorophyll-a trends in coastal waters…… 83
2.3.3. Hotspot detection in Brazilian coastal waters (2002-2022)……86
2.3.4. Selected example of human-induced pressures on Brazilian coastal waters……..…91
2.3.4.1. Agriculture and farming impact……. 91
2.3.4.2. Dam construction impact……... 92
2.3.4.3. Industrialisation and urbanisation impacts…….94
2.4. Conclusion…….96
CHAPTER 3: IMPACT OF INDUSTRIALIZATION ON THE EVOLUTION OF SUSPENDED PARTICULATE MATTER FROM MODIS DATA (2002-2022): CASE STUDY OF AÇU PORT, BRAZIL……98
3.1. Introduction……...98
3.2. Materials and Methods…….100
3.2.1. Study area……...100
3.2.2. Ocean color satellite data…… 101
3.2.2.1. Atmospheric correction……. 101
3.2.2.2. Bio-optical model for SPM estimation…….. 102
3.2.3. Ancillary data…….. 105
3.2.4. Statistical analysis……107
3.2.4.1. Statistical indicators……...107
3.2.4.2. Time series decomposition method……108
3.3. Results…….109
3.3.1. A combined bio-optical model for SPM estimation based on OWTs…… 109
3.3.2. Spatio-temporal dynamics of SPM……. 111

3.3.2.1. SPM seasonal variation…… 111
3.3.2.2. SPM interannual variability……...114
3.3.3. Evolution of the environmental conditions…….. 118
3.3.3.1. Land use and cover…… 118
3.3.3.2. Combined impact of industrialization and environmental forcings on the regional SPM dynamics……...118
3.4. Discussion……... 123
3.4.1. A combined bio-optical model for SPM estimation based on OWTs……..123
3.4.2. Spatio-temporal dynamics of SPM……..124
3.4.2.1. Seasonal variation of SPM and environmental forcings……125
3.4.2.2. Interplay between port development and environmental forcing in shaping SPM interannual variability……127
3.4.3. Limitations and Perspectives for Multi-Scale Monitoring……..130
3.5. Conclusions…….131
CHAPTER 4: IMPACTS OF DEFORESTATION AND PASTURE EXPANSION ON SUSPENDED PARTICULATE MATTER AND CHLOROPHYLL-A IN THE COASTAL WATERS OF MARANHÃO, NORTHERN BRAZIL, DERIVED FROM 20 YEARS OF MODIS OBSERVATIONS (2002-2022)…… 133
4.1. Introduction…….133
4.2. Materials and Methods…… 135
4.2.1. Study area……135
4.2.2. Ocean Color Satellite data……137
4.2.3. Bio-optical models for SPM and Chl-a estimation……..138
4.2.3.1. Chl-a model CONNECT……138
4.2.3.2. SPM bio-optical model……..138
4.2.4. Ancillary data…….. 139
4.2.5. Statistical analysis……140
4.2.5.1. Time series decomposition method and trend analysis…….. 140
4.2.5.2. Generalized Additive Model Analysis……... 141
4.3. Results…….142
4.3.1. Chl-a and SPM climatological distribution…… 142
4.3.2. Chl-a and SPM general variability patterns…… 145
4.3.3. Seasonal Variation of Chl-a and SPM and environmental factors…… 148

4.3.3.1. River discharge and precipitation…….. 148
4.3.3.2. Currents and winds…… 150
4.3.4. Interannual variation of Chl-a and SPM…….. 152
4.3.4.1. Trend Analysis……...152
4.3.4.2. Anthropogenic treats (land use and land cover)…… 153
4.3.4.3. Interannual Variation of Chl-a/SPM…….. 156
4.3.5. Relative importance of climate and human pressures on interannual Variation of Chl-a and SPM……157
4.4. Discussion……... 159
4.4.1. Chl-a and SPM general patterns…….. 159
4.4.2. Chl-a and SPM seasonal variability (2002-2022)…… 160
4.4.3. Interannual variability of Chl-a and SPM driven by anthropogenic and environmental factors……..162
4.5. Conclusion……...165
CHAPTER 5: GENERAL DISCUSSION……...168
5.1. Synthesis of the main findings……..168
5.2. Relative roles of natural forcing and anthropogenic pressures…….169
5.3. Methodological contribution and implications…….169
5.4. Limitations and uncertainties……170
5.5. Implications for coastal monitoring and management……..171
5.6. Concluding remarks……..171
GENERAL CONCLUSION……172
PERSPECTIVES…….175
REFERENCES……...177
ANNEX……...205
RÉSUMÉ SUBSTANTIEL EN FRANÇAIS……...213
ABSTRACT……227
RÉSUMÉ…….229

LIST OF ACRONYMS

APIC	Açu Port Industrial Complex
CDOM	Colored Dissolved Organic Matter
Chl-a	Chlorophyll-a
NIR	Near-Infrared
OWT	Optical Water Type
POC	Particulate Organic Carbon
SPM	Suspended Particulate Matter
$\boldsymbol{R_{rs}}$	Remote Sensing Reflectance
RC	Rate of Change
$\boldsymbol{\lambda}$	Wavelength

LIST OF FIGURES

Figure 1.1. Conceptual framework of anthropogenic impacts on coastal water quality. The diagram illustrates the pathways from land-based pressures (nutrient enrichment, pollutants) to ecosystem degradation (eutrophication, harmful algal blooms, and oxygen depletion), highlighting the risks to biodiversity and human activities (Dai *et al.*, 2023)……..22

Figure 1.2. Geographic framework of Brazilian coastal and shelf waters, showing the Exclusive Economic Zone and continental shelf (200 m depths) (Freire *et al.*, 2014)……..23

Figure 1.3. Summary of the different coastal types/ecosystems and forcing parameters acting on Brazilian waters (adapted from Kerr et al., 2016, MAPIOMAS, https://mapbiomas.org/)....24

Figure 1.4. Main sea surface ocean currents flowing along the Brazilian continental margin. North Equatorial Current (NEC), North Equatorial Countercurrent (NECC), northern (nSEC), central (cSEC), and southern South Equatorial Current (sSEC), South Equatorial Countercurrent (SECC), North Brazil Current (NBC), North Brazil Ring (NBR), North Brazil Undercurrent (NBUC), Brazil Current (BC), Malvinas Current (MC), South Atlantic Current (SAC). Circles inside the South Brazil Bight are quasi-stationary cyclonic meanders (AMORIM et al., 2024; CAMPOS; GONÇALVES; IKEDA, 1995). The division of the Brazilian continental margin into five regions is also shown (North, Northeast, Abrolhos, South Brazil Bight, South). Adapted from da Silveira et al. (da Silveira et al., 2020)……26

Figure 1.5. Medium spatial resolution sensors (300 m - 1km) used by multisensor time series……..30

Figure 1.6. Schematic representation of the irradiance propagation paths to the sensor: (a) direct or multiple scattering within the atmosphere; (b) specular reflection at the sea surface; (c) water-leaving radiance, after interaction with the water column, reaching the sensor. Adapted from IOCCG, (2000) and Cardoso Dos Santos, (2025)……34

Figure 1.7. Mean relative contributions of Detritus, Phytoplankton, CDOM, and Water to total light absorption at wavelengths between 300 and 700 nm for the NAAMES dataset. Error bars represent one standard deviation for these estimates (Allen et al., 2020)……..35

Figure 1.8. Conceptual illustration of the main categories of inversion models applied to marine reflectance signals for the retrieval of biogeochemical products from satellite ocean-color observations (adapted from IOCCG, 2000)……..38

Figure 1.9. Illustration of the optical diversity of Brazilian waters and selected coastal/shelf areas (MERIS GlobCoast global dominant OWT; processing, Mélin and Vantrepotte, 2015 typology: classes 1-2 ultra-turbid waters, 3-9 coastal waters, waters for which standard oceanic

OCR products are not adapted, 10-17 oceanic-like waters)……..40
Figure 1.10. Example of a probabilistic OWT based combination of empirical chlorophyll-a algorithms in coastal waters. The relative difference between probabilistic and non-probabilistic algorithm combinations illustrates the reduction of spatial discontinuities when class membership probabilities are explicitly considered (adapted from Tran et al., 2023)……41
Figure 1.11. Time series decomposition illustrating the separation of an observed signal into seasonal, interannual (trend-cycle), and irregular components…….48
Figure 1.12. Illustration of an initial application of the Census X-11 method to detect the impact of climatic modulations on interannual variations of SeaWiFS Chl-a over the period 1997-2007 (Vantrepotte and Mélin, 2011). Blue areas indicate the presence of negative monotonic trends, red areas indicate positive monotonic trends, while green pixels denote the presence of significant interannual modulations (X-11 Tt component)……49
Figure 2.1. COCOBRAZ in situ data distribution along the Brazilian coastal waters. Red dots indicate the 3646 sampling stations for Chl-a, SPM, POC, DOC, and turbidity……..55
Figure 2.2. Frequency distribution histograms of biogeochemical variables included in the COCOBRAZ in situ dataset: (a) Chl-a, (b) POC, (c) DOC, (d) SPM, and (e) TUR…….56
Figure 2.3. Processing chain of MODIS-Aqua dataset (2002-2022) by COCOBRAZ project for the Brazilian margin (adapted from Cardoso Dos Santos, 2025)……58
Figure 2.4. Distribution of the in situ dataset. (a) Frequency distribution histograms of in situ POC validation data, (b) Frequency distribution histograms of in situ POC matchup data…..62
Figure 2.5. Optical water type classification. Average standardized reflectance spectra corresponding to the five OWTs defined from the in situ dataset (N = 440) according to Tran et al. (Tran *et al.*, 2023)…….63
Figure 2.6. Validation of the new inversion algorithm for estimating POC from $R_{rs}(\lambda)$: Tran et al. (2019) and Le et al. (2017) combination based on OWTs (OWTs 1-3 and 4-5, respectively). (a) in situ validation, (b) satellite matchup validation (MODIS - OC-SMART)……..65
Figure 2.7. Example of monthly MODIS-Aqua R_{rs} (667 nm) showing the diversity of Brazilian coastal ecosystems detectable at 1 km resolution……...70
Figure 2.8. Distribution of identified coastal systems along the Brazilian coastline…….71
Figure 2.9. Effect of spatial resolution on coastal and estuarine chlorophyll-a patterns. (a) MODIS-Aqua (1 km). (b) Sentinel-3 OLCI (300 m). (c) MODIS-Aqua zoom over river mouths. (d) Corresponding Sentinel-3 OLCI zoom……72
Figure 2.10. Spatial distribution and cross-shelf variability of $R_{\mathrm{rs}}\ (\lambda)$ in the São Francisco River coastal region derived from different satellite products. (a) R_{rs} (670 nm) from GlobColour

(4 km). (b) R_{rs} (665 nm) from OC-CCI (1 km). (c) R_{rs} (667 nm) from MODIS OC-SMART (1 km). (d) Coastal-offshore transect of logR_{rs} (λ) in the blue, green, and red spectral bands extracted from Globcoulor, OC-CCI and MODIS OC-SMART along the transect shown in panels (a, b and c; White line)……73

Figure 2.11. Comparison of red-band remote sensing reflectance (R_{rs} (λ)) in embayed coastal environments derived from GlobColour, OC-CCI, and MODIS OC-SMART. (a) R_{rs} (670 nm) from GlobColour (4 km). (b) R_{rs} (665 nm) from OC-CCI (1 km). (c) R_{rs} (667 nm) from MODIS OC-SMART (1 km)……..75

Figure 2.12. Global satellite-in situ matchups of retrieved R_{rs} (λ) with the OC-SMART atmospheric correction algorithm. Adapted from Tran et al. (2025)……..77

Figure 2.13. Spatial distribution of satellite-derived Chl-a in Sepetiba and Guanabara bays from different products. (a) Monthly Chl-a from GlobColour (4 km). (b) Monthly Chl-a from OC-CCI (1 km). (c) Monthly Chl-a from MODIS processed with OC-SMART and estimated using the CONNECT model (1 km)……78

Figure 2.14. Spatial distribution of relative differences (%) between OC-CCI and MODIS OC-SMART (CONNECT) Chl-a in optically complex coastal waters……79

Figure 2.15. Point-based analysis of satellite-derived Chl-a at representative coastal locations: (a-b) long-term time series from GlobColour, OC-CCI, and MODIS OC-SMART, and (c-d) scatter-based comparison between OC-CCI and MODIS OC-SMART at points A and B (Figure 14)…….80

Figure 2.16. Performance of satellite-derived chlorophyll-a estimates in Brazilian coastal waters based on matchups with COCOBRAZ in situ observations. (a) Matchup between OC-CCI Chl-a and in situ measurements. (b) Matchup between Chl-a estimated using the CONNECT model applied to MODIS OC-SMART and in situ measurements. Point colors indicate OWT class membership, ranging from turbid waters (C1) to ultra-oligotrophic waters (C17). (Cardos Dos Santos, 2025)…….82

Figure 2.17. Comparison of satellite-derived rates of change (RC, % year^{-1}) in chlorophyll-a over selected Brazilian coastal regions ($P < 0.05$). (a-c) São Francisco River coastal region derived from (a) GlobColour (4 km), (b) OC-CCI (1 km), and (c) MODIS-Aqua processed with OC-SMART and estimated using the CONNECT model (1 km).(d-f) Guanabara Bay and Sepetiba Bay derived from (d) GlobColour (4 km), (e) OC-CCI (1 km), and (f) MODIS-Aqua processed with OC-SMART and estimated using the CONNECT model (1 km)……84

Figure 2.18. Distribution of long-term trends in Chl-a, SPM, and POC across Brazilian coastal systems (2002-2022). (a) Chl-a variability 2002-2022, (b) SPM variability 2002-2022 and (c)

POC variability 2002-2022……87
Figure 2.19. Examples of biogeochemical hotspots in Brazilian coastal bays identified from significant rates of change (RC, $p < 0.05$) in Chl-a, SPM, and POC over the 2002–2022 period. (a) Bay of Santa Catarina Island, showing increasing trends in Chl-a, SPM, and POC. (b) Guanabara Bay, exhibiting decreasing trends in Chl-a, SPM, and POC……88
Figure 2.20. Examples of biogeochemical hotspots in Brazilian estuaries and river mouths identified from significant rates of change (RC, $p < 0.05$) in Chl-a, SPM, and POC over the 2002-2022 period. (a) River mouths south of the São Francisco River (Sergipe, Vaza-Barris, Castro, and Real rivers). (b) Cananéia-Iguape estuarine-lagoon complex……89
Figure 2.21. Examples of biogeochemical hotspots in Brazilian coastal lagoons identified from significant rates of change (RC, $p < 0.05$) in Chl-a, SPM, and POC over the 2002-2022 period. (a) Araruama Lagoon, showing trends in Chl-a, SPM, and POC. (b) Southern Brazilian lagoonal systems (Patos Lagoon, Mangueira Lagoon, and Mirim Lagoon), exhibiting trends in Chl-a and POC and SPM……90
Figure 2.22. Chl-a variation along the western coast of Maranhão State (2002-2022). (a) RC of Chl-a ($p<0.05$). (b) Census X-11 decomposition method outputs at point A……92
Figure 2.23. SPM variation at Sao Francisco River plume (2002-2022). (a) RC of SPM ($p<0.05$). (b) Census X11 decomposition method outputs at point A……93
Figure 2.24. (a) Correlation map between SPM interannual variation and river discharge. (b) Correlation graphic between the interannual variation of SPM (red), the interannual variation of POC (black) extracted at point A and the interannual variation of the river discharge (ANA-Hydroweb, Sao Francisco station) (blue)……..93
Figure 2.25. SPM variation near the Açu Port (2002-2022). (a) RC of SPM ($p<0.05$). (b) Census X11 decomposition method outputs at point A……..94
Figure 2.26. POC variation in Sepetiba bay (2002-2022). (a) RC of POC ($p<0.05$). (b) Census X11 decomposition method outputs at point A……..95
Figure 2.27. Correlation graphic between the interannual variation of SPM (blue), the interannual variation of POC (black) and the urbanization (MapBiomas) (red)……96
Figure 3.1. Location of the study area. (a) Location of northern coast of Rio de Janeiro state, highlighted in red, (b) Regional map showing bathymetry and major rivers, with a red box indicating the position of Açu Port, (c) Satellite view of Açu Port, the specific area analyzed in this study……..101
Figure 3.2. Distribution and classification of GLORIA in situ dataset. (a) Frequency distribution histograms of in situ SPM validation data, (b) Frequency distribution histograms

of in situ SPM matchup data……102
Figure 3.3. Optical water type classification. (a) Average standardized reflectance spectra corresponding to the five OWTs defined from the GLORIA dataset (N = 489) according to Tran et al. (Tran *et al.*, 2023); (b) Geographical distribution of the in-situ SPM data……..104
Figure 3.4. Validation of the new inversion algorithm for estimating SPM from R_{rs} (λ): Siswanto et al. (Siswanto *et al.*, 2011)and Han et al. (Han *et al.*, 2016) combination based on optical water types (OWT 1-3 and 4-5, respectively). (a) in situ validation, (b) satellite matchup validation (MODIS – OC-SMART)……111
Figure 3.5. (a, b) Satellite-derived monthly mean surface suspended particulate matter (SPM) concentrations (mg. L^{-1}) from MODIS OC-SMART (2002-2022) illustrating SPM distribution during (a) austral summer (e.g. December) and (b) austral winter (e.g. July). (c, d) Coefficient of variation (%) of SPM concentrations during (c) austral summer (December) and (d) austral winter (July). White arrows represent current circulation during (a) austral summer (December 2019) and (b) austral winter (July 2019)……112
Figure 3.6. (a) Time series of Seasonal variation (X11 outputs) of SPM (black), meridional current (blue), (b) Time series of Seasonal variation (X11 outputs) of SPM and meridional wind (green) extracted at Point A, located offshore (20 m depth) the Açu Port (Figure 3.5a)…….113
Figure 3.7. Temporal Rate of Change (RC) in SPM between 2002-2022 within the study area, showing only statistically significant changes ($p < 0.05$)……115
Figure 3.8. (a) Map showing the spatial extent of the surface area used for extracting the time series. (b)Time series of the raw SPM (c) and Census X11 interannual term from 2002 to 2022, both (b and c) averaged over the area within the Açu Port where the RC is positive (RC > 0) and statistically significant ($p < 0.05$, N = 246)……116
Figure 3.9. (a) Correlation map ($p < 0.05$, N = 246) between the interannual variation of SPM in the entire study area and the referenced time series of interannual variation extracted from the Açu Port region exhibiting significant SPM increase shown in Figure 8c. (b) RC of SPM including both significant and non-significant variations……117
Figure 3.10. Land use and land cover maps for the years 2002 and 2022 within the Açu Port (MapBiomas)). (a) 2002 land cover map, (b) 2022 land cover map……118
Figure 3.11. Impact of industrialization (Açu) on the SPM variation. (a) Correlation map between industrialization and SPM interannual variation between 2002 and 2022. (b) Time series of the interannual variation of SPM (black) and the industrialization growth (red)…..119
Figure 3.12. Correlation maps between interannual components of SPM, wind and current. (a) correlation map between the interannual component of SPM and meridional current (V). (b)

correlation map between the interannual component of SPM and zonal current (U). (c) correlation map between the interannual component of SPM and meridional wind (V). (d) correlation map between the interannual component of SPM and zonal wind (U). Only significant correlations ($p < 0.05$, $N = 246$) are shown……121

Figure 3.13. (a) Time series of the interannual variation of SPM (black) and interannual variation of V current (red) at point A parallel to the APIC. (b) Time series of the interannual variation of SPM (black) and interannual variation of V wind (red) at point A parallel to the APIC (bathy = 20 m)……123

Figure 4.1. Study area location. (a) Maranhão State. (b) Northern Brazilian coastal region with the red box highlighting western Maranhão. (c) Detailed view of the study area and main rivers. (d) True-color image of the study area from Google Satellite imagery……136

Figure 4.2. Dominant Optical Water Types distribution over the MODIS 2002-2022 time period (17 classes; Mélin and Vantrepotte, 2015, Jorge et al., 2021). (a) OWT distribution along the northern Brazilian coast. (b) in the study area on the western coast of Maranhão State…..138

Figure 4.3. Seasonal average (2002-2022) of Chl-a (a-d) and SPM (e-h) during the rainy season (December-May) and dry season (June–November) for the western coast of Maranhão State(a-b) Mean Chl-a for the rainy and dry seasons; (c-d) Chl-a coefficient of variation for the rainy and dry seasons; (e-f) Mean SPM for the rainy and dry seasons; (g-h) SPM coefficient of variation for the rainy and dry seasons. Dominant surface currents indicated by black arrows……..144

Figure 4.4. Relative contributions (%) of seasonal, interannual, and irregular components derived from Census X-11 decomposition (2002–2022) to the total variance of Chl-a (a–d) and SPM (e–h) along the western coast of Maranhão State: (a) Chl-a coefficient of variation (%); (b) seasonal contribution to Chl-a total variance (%); (c) interannual contribution to Chl-a total variance (%); (d) irregular contribution to Chl-a total variance (%); (e) SPM coefficient of variation (%); (f) seasonal contribution to SPM total variance (%); (g) interannual contribution to SPM total variance (%); (h) irregular contribution to SPM total variance (%)……..147

Figure 4.5. Time series of the seasonal variation (Census X-11 outputs) of the Pindaré River (Figure 1) discharge and the mean precipitation over the study area (2002-2022)…….148

Figure 4.6. Correlation between the seasonal variation (Census X-11 outputs) of river discharge and Chl-a and SPM over the western coast of Maranhão State: (a–b) spatial correlation maps between the seasonal variation of Chl-a and SPM and the seasonal variation of river discharge; (c–d) time series of the seasonal variation of Chl-a and SPM extracted at point A with the seasonal variation of river discharge (2002–2022)……..150

Figure 4.7. Correlation maps between the seasonal variation (Census X-11 outputs) of Chl-a and SPM and the seasonal variation of the zonal component of current and wind (U-current, U-wind) over the western coast of Maranhão State: (a) correlation between Chl-a and U-current; (b) correlation between SPM and U-current; (c) correlation between Chl-a and U-wind; (d) correlation between SPM and U-wind……151

Figure 4.8. Correlation maps between the seasonal variation (Census X-11 outputs) of Chl-a and SPM and the seasonal variation of the meridional component of current and wind (V-current, V-wind) over the western coast of Maranhão State: (a) correlation between Chl-a and V-current; (b) correlation between SPM and V-current; (c) correlation between Chl-a and V-wind; (d) correlation between SPM and V-wind……..152

Figure 4.9. Rate of change (RC) of Chl-a and SPM between 2002-2022 over the western coast of Maranhão State: (a) RC of Chl-a; (b) RC of SPM, showing only statistically significant changes ($p < 0.05$); (c) Time series of Census X-11 interannual variation of Chl-a; (d) standardized time series of Census X-11 interannual variation of SPM, both averaged over the areas with positive and statistically significant RC ($RC > 0$, $p < 0.05$, $N = 246$)……153

Figure 4.10. Land use and land cover maps for 2002 and 2022 within the study area (MapBiomas): (a) land cover map for 2002; (b) land cover map for 2022……..154

Figure 4.11. Correlation between land use and the interannual variation of Chl-a and SPM over the western coast of Maranhão State: (a) correlation map between the interannual variation of Chl-a and pasture; (b) correlation map between the interannual variation of SPM and pasture; (c) time series of the interannual variation of Chl-a (blue) and SPM (black) extracted at point A together with forest (green) and pasture (red) areas from 2002 to 2022…….155

Figure 4.12. RC of the Chl-a:SPM ratio between 2002-2022 over the western coast of Maranhão State: (a) RC of the Chl-a:SPM ratio, showing only statistically significant changes ($p < 0.05$); (b) time series of the Census X-11 interannual variation of the Chl-a:SPM ratio from 2002 to 2022, averaged over areas where RC is negative and statistically significant ($RC < 0$, $p < 0.05$)…….156

Figure 4.13. Partial effects of river discharge on Chl-a and SPM obtained from the GAM analysis: (a) smooth function of river discharge for Chl-a; (b) smooth function of river discharge for SPM……...159

LIST OF TABLES

Table 2.1. List of in situ oceanographic missions used in the COCOBRAZ compilation……54

INTRODUCTION

Coastal zones are dynamic interfaces between land and ocean, where physical, biogeochemical, and biological processes interact across a wide range of spatial and temporal scales (Longhurst et al., 1995; Gattuso et al., 1998; Levin et al., 2015). Although their relatively limited spatial extent, coastal environments play a fundamental role in the Earth system by regulating fluxes of matter and energy between terrestrial watersheds and the open ocean (Bauer et al., 2013; Regnier et al., 2013), while sustaining high levels of biological productivity (Pauly and Christensen, 1995; Cloern et al., 2014). These regions also hold major socio-economic importance, as they host dense human populations, ports, industrial facilities, and a wide range of economic activities, and provide essential ecosystem services, such as fisheries production, coastal protection, and carbon sequestration (Small and Nicholls, 2003; Costanza et al., 2014; Neumann et al., 2015).

Over recent decades, increasing anthropogenic pressures have profoundly altered the functioning of coastal systems worldwide (Halpern et al., 2015; IPCC, 2022). Land-use and land-cover changes such as deforestation, pasture expansion, agricultural intensification, urban growth, dam construction, and the development of industrial and port infrastructures have substantially increased the export of sediments, nutrients, and organic matter from land to sea (Beusen et al., 2005; Syvitski et al., 2005). These enhanced fluxes modify the optical and biogeochemical properties of coastal waters, affect light availability and primary production, and ultimately alter ecosystem structure and functioning (Cloern, 2001; Bowers and Binding, 2006; Cloern et al., 2014). Understanding the magnitude, variability, and drivers of these changes has become a major scientific challenge, particularly in the context of global environmental change and the growing need for sustainable coastal management (Doney, 2010; Duarte, 2014).

The characterization of key biogeochemical variables, including chlorophyll-a (Chl-a), suspended particulate matter (SPM), and particulate organic carbon (POC), is central to assessing coastal water quality and ecosystem dynamics (Groom et al., 2019; Schroeder et al., 2015). SPM is a key descriptor of water turbidity and particle transport, strongly controlling light availability and sediment dynamics in coastal environments, and playing a major role in the transport of nutrients and contaminants (Kineke et al., 1996; Doxaran et al., 2002; Miller and McKee, 2004). POC represents the organic fraction of suspended matter and provides essential information on coastal carbon cycling, organic matter inputs, and anthropogenic

influence (Blair and Aller, 2012; Bauer et al., 2013). Chl-a is widely used as an indicator of phytoplankton biomass and primary production and constitutes a key proxy for trophic status and nutrient enrichment in coastal waters (Kasprzak et al., 2008; Cloern et al., 2014). These variables integrate the combined influence of natural forcing mechanisms, such as river discharge, hydrodynamics, and climate variability, and human-induced perturbations. However, long-term and spatially representative in situ observations remain scarce in many coastal regions, especially along extensive and heterogeneous coastlines (Henson, Beaulieu and Lampitt, 2016; Breitburg et al., 2018; Muller-Karger et al., 2018). This lack of observations severely limits the capacity to quantify long-term trends and to disentangle anthropogenic signals from natural variability.

In addition to direct anthropogenic pressures, coastal zones are highly vulnerable to climate change. Rising sea surface temperatures and the increasing occurrence of marine heatwaves affect stratification, phytoplankton dynamics, and biogeochemical processes, while changes in precipitation regimes modify river discharge and terrestrial runoff, altering the magnitude and timing of sediment, nutrient, and organic matter inputs to coastal waters (Milliman et al., 2008; Hobday et al., 2016; IPCC, 2022). Extreme rainfall events enhance soil erosion, leaching, and particulate transport from continental watersheds, whereas droughts can reduce freshwater inputs and increase residence times in coastal systems, with direct consequences for water quality (Dai et al., 2009; Ward et al., 2017). Climate-driven and anthropogenic pressures often act simultaneously and interact non-linearly: land-use changes such as deforestation, pasture expansion, and agricultural intensification can amplify the sensitivity of coastal systems to climatic forcing, while climate variability may modulate or obscure anthropogenic signals. This interplay complicates the attribution of observed biogeochemical changes to specific drivers and reinforces the need for long-term, spatially consistent observations to disentangle climatic and human-induced impacts in coastal environments (Syvitski et al., 2005; Doney et al., 2012; Regnier et al., 2013).

Satellite ocean color remote sensing provides a unique and powerful means to overcome these limitations (McClain, 2009; Dutkiewicz et al., 2019; Sathyendranath et al., 2019). By delivering synoptic, repetitive, and internally consistent observations over decadal time scales, satellite sensors enable the analysis of seasonal, interannual, and long-term variability in coastal biogeochemical properties (Franz et al., 2007; Siegel et al., 2013). Among the available satellite missions, MODIS-Aqua offers the longest continuous and internally consistent ocean color time series currently available, making it particularly suitable for long-term trend analyses in coastal

environments. Alternative multi-sensor products, such as GlobColour (4 km) and the Ocean Color Climate Change Initiative (OC-CCI, 1 km), provide global coverage but remain limited in optically complex coastal waters due to coarser spatial resolution and reduced performance in highly turbid environments (Cardoso Dos Santos et al., 2025).

Nevertheless, the application of ocean color techniques in coastal environments remains challenging. Coastal waters are often optically complex, with variable contributions from phytoplankton, mineral particles, and colored dissolved organic matter (Morel and Prieur, 1977; Prieur and Sathyendranath, 1981). As a result, algorithms originally developed for clear oceanic waters often perform poorly in coastal zones, highlighting the need for adapted atmospheric corrections and bio-optical approaches capable of handling strong optical heterogeneity (IOCCG, 2000; Dierssen, 2010; Odermatt et al., 2012). The analysis of such long satellite-derived time series further requires robust statistical frameworks to separate long-term trends from seasonal and interannual variability, as well as flexible models such as Generalized Additive Models (GAMs) to explore potentially non-linear relationships between biogeochemical variables and environmental drivers in highly dynamic coastal systems (Hastie and Tibshirani, 1986; Pezzulli et al., 2005; Vantrepotte and Mélin, 2011; Wood, 2017).

The Brazilian coastal zone represents a particularly relevant natural laboratory to address these challenges. Extending over nearly 8,000 km, it spans equatorial, tropical, and subtropical regions and encompasses a wide diversity of geomorphological, hydrodynamic, and biogeochemical settings (Castro and Miranda, 1998; Spalding et al., 2007). Brazilian coastal waters are influenced by major river plumes, such as those of the Amazon and La Plata rivers, complex estuarine systems, and energetic western boundary currents, as well as by mesoscale and sub-mesoscale processes that regulate exchanges between the continental shelf and the open ocean (Molinier et al., 1993; Piola et al., 2005; Rudorff et al., 2011; Araujo et al., 2017). At the same time, the Brazilian coastline is subject to increasing anthropogenic pressures related to deforestation, pasture expansion, agricultural development, industrialization, and port construction (Marques et al., 2019; Souza et al., 2020; MapBiomas, 2021).

Despite their ecological and socio-economic importance, Brazilian coastal waters remain poorly documented by sustained in situ monitoring programs (Brandini et al., 2018). Existing observations are fragmented in space and time, which limits the assessment of large-scale patterns and long-term changes. In this context, the systematic exploitation of satellite ocean color archives, combined with the development of bio-optical algorithms specifically adapted

to optically complex coastal waters, offers an essential pathway to improve the understanding of biogeochemical dynamics at regional to national scales.

This PhD thesis is conducted within the framework of the COCOBRAZ project, funded by the São Paulo Research Foundation (FAPESP, Brazil) and the French National Research Agency (ANR, France), which aims to assess the long-term evolution of the biogeochemical quality of Brazilian coastal and shelf waters and to identify the respective roles of natural and anthropogenic drivers in support of environmental policy development.

In this context, this PhD thesis addresses the following scientific questions:

1. How reliably can MODIS-Aqua ocean color observations, combined with adapted atmospheric correction and bio-optical models, represent Chl-a, SPM and POC dynamics across optically complex Brazilian coastal waters?
2. What spatio-temporal changes and coastal hotspots can be identified in the biogeochemical properties of Brazilian coastal waters using MODIS-Aqua 1 km time series (2002-2022)?
3. What is the relative importance of anthropogenic pressures and climatic forcing in driving long-term changes in Brazilian coastal water quality, based on regional case studies along the Brazilian coast?

This PhD thesis addresses these issues by investigating the spatio-temporal variability and long-term evolution of coastal biogeochemistry along the Brazilian margin using satellite ocean color observations. The work relies on more than two decades of MODIS-Aqua (1 km) data processed using the OC-SMART (Ocean Color - Simultaneous Marine and Aerosol Retrieval Tool) atmospheric correction method (Fan et al., 2021) and combined with bio-optical models specifically designed for coastal environments. A particular emphasis is placed on approaches based on Optical Water Types (OWTs), which explicitly account for the strong optical heterogeneity of Brazilian coastal waters and enable robust retrievals of biogeochemical variables across contrasted environments (Vantrepotte et al., 2012; Moore et al., 2014; Spyrakos et al., 2018). Within this framework, dedicated retrieval algorithms for SPM and POC were developed during this PhD for MODIS applications in coastal waters. These algorithms rely on an OWT based approach, combining and weighting existing bio-optical models according to their performance across contrasted optical conditions, in order to ensure robust applicability along the land-sea continuum.

The scientific objectives of this thesis are threefold. First, it aims to establish a coherent and homogeneous observational framework for Brazilian coastal waters by integrating long-term satellite observations with available in situ data, in order to characterize large-scale spatial patterns and temporal variability of key biogeochemical variables. Second, it seeks to identify long-term trends and coastal hotspots of change, and to distinguish the respective roles of natural forcing mechanisms and anthropogenic pressures. Third, through targeted regional case studies, the thesis examines the specific impacts of human activities such as deforestation and pasture expansion in northern Brazil, and industrial and port development in southeastern Brazil on sediment dynamics and phytoplankton biomass.

The structure of the thesis reflects this scientific progression. Chapter 1 presents the state of the art on coastal biogeochemical variability, satellite ocean color remote sensing, and methodological challenges associated with optically complex waters, with a specific focus on the Brazilian coastal context. Chapter 2 describes the development of the COCOBRAZ observational framework, including the compilation of in situ data, the processing of the full MODIS-Aqua archive, and the analysis of the general spatiotemporal variability of Chl-a, SPM, and POC along the Brazilian coast over the 2002-2022 period. Chapter 3 examines the influence of industrialization and port development on SPM dynamics, using the Açu Port Industrial Complex as a case study. Chapter 4 focuses on the Amazonian Equatorial Coast of Maranhão and investigates the impact of deforestation and pasture expansion on suspended sediments and phytoplankton biomass.

By combining large-scale satellite analyses with regional process-oriented studies, this thesis provides new insights into the biogeochemical functioning of Brazilian coastal waters and demonstrates the capability of long-term satellite ocean color observations to detect and interpret anthropogenic impacts in highly dynamic coastal environments. The results contribute to the scientific basis required to support integrated coastal management strategies and evidence-based public policies aimed at preserving coastal water quality and ecosystem sustainability.

CHAPTER 1: STATE OF THE ART

Coastal zones constitute key transitional environments where interactions between terrestrial, marine, and atmospheric processes generate strong physical and biogeochemical variability (Crossland et al., 2005; Ramesh et al., 2015). Throughout history, these regions have played a central role in human development, hosting major settlements, ports, and resource-extraction activities (e.g. fisheries, mining, and offshore energy production), and supporting a wide range of socioeconomic uses (Figure 1.1). Despite their relatively limited spatial extent, coastal ecosystems are among the most productive on Earth and provide a disproportionately high share of ecosystem goods and services compared to many larger marine and terrestrial systems (Millennium Ecosystem Assessment, 2005; Luisetti et al., 2014).

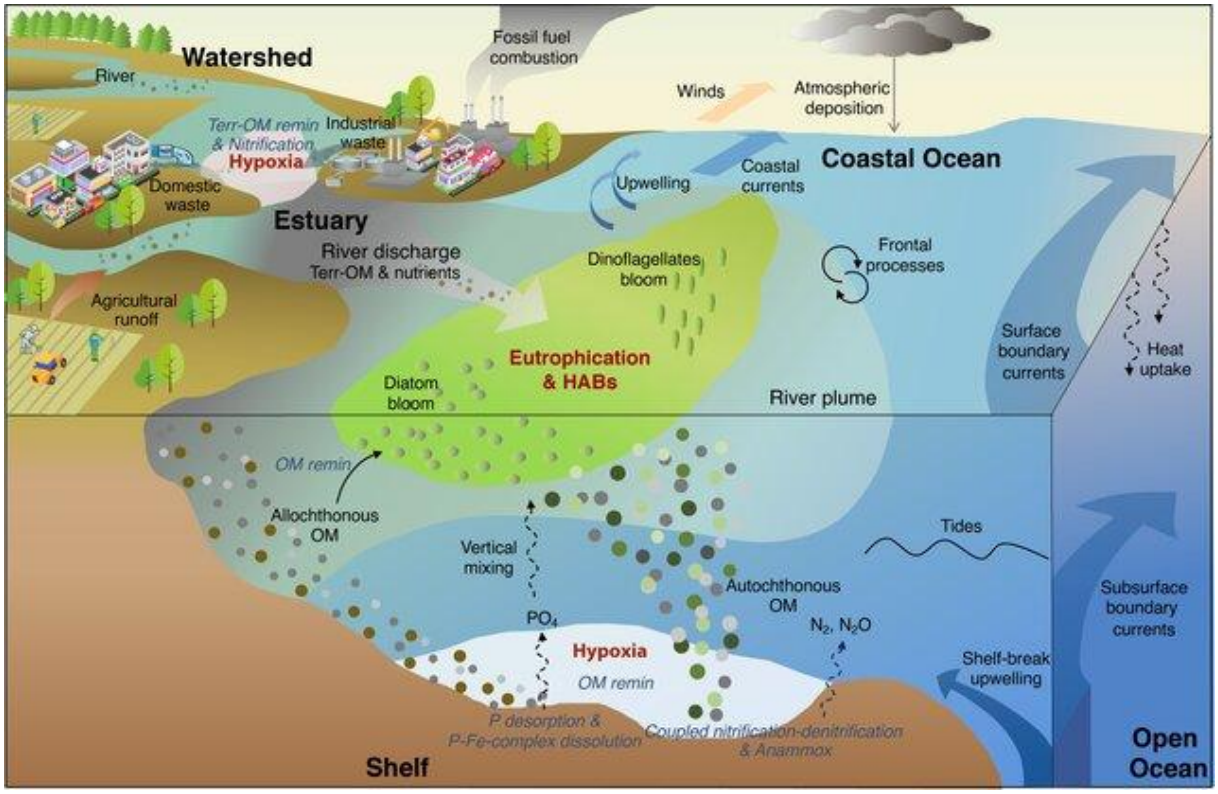

Figure 1.1. Conceptual framework of anthropogenic impacts on coastal water quality. The diagram illustrates the pathways from land-based pressures (nutrient enrichment, pollutants) to ecosystem degradation (eutrophication, harmful algal blooms, and oxygen depletion), highlighting the risks to biodiversity and human activities (Dai et al., 2023).

This combination of high productivity, intense human use, and environmental sensitivity makes coastal and marginal seas priority areas for environmental monitoring. Improving the understanding of their dynamics, detecting changes in their properties, and evaluating the effectiveness of environmental management policies require sustained and spatially extensive observations. However, existing observation networks remain unevenly distributed in space and

time, with many coastal regions insufficiently sampled and certain periods poorly represented due to logistical constraints (Muller-Karger et al., 2018; Marcos et al., 2019). In this context, satellite ocean color remote sensing offers a cost-effective approach for the frequent and global monitoring of coastal waters, providing a valuable complement to in situ observations (Mélin et al., 2011; Blondeau-Patissier et al., 2014; Majid et al., 2025).

1.1. Study area: Brazilian coastal waters

1.1.1. General setting and geographical extent

The Brazilian coastal zone is one of the most extensive and diverse coastal systems in the world (Figure 1.2), extending from approximately 4° N to 34° S and spanning nearly 8,000 km of coastline (Ab'Sáber, 2003; Bernardes et al., 2012). This vast latitudinal range encompasses equatorial, tropical, and subtropical regions, generating a strong environmental gradient that fundamentally shapes the physical, ecological, and biogeochemical characteristics of Brazilian coastal waters. The interface between the continent and the ocean includes an exceptional diversity of geomorphological and oceanographic settings, which has motivated several classifications of the Brazilian coast based on geological, climatic, hydrographical, and sedimentological criteria (Ekau and Knoppers, 1999).



Figure 1.2. Geographic framework of Brazilian coastal and shelf waters, showing the Exclusive Economic Zone and continental shelf (200 m depths) (Freire et al., 2014).

The Brazilian continental shelf displays large spatial variability in width and depth (Figure 1.2). It reaches its widest extension near the Amazon region, where the shelf spans up to ~330 km, while narrowing drastically to less than 20 km along portions of the northeastern and eastern coast, before widening again toward the southeast and south (Coutinho, 1995; Castro and Miranda, 1998; Castro et al., 2006). Shelf depths typically range from 40 m to about 180 m, influencing light availability, nutrient dynamics, and water mass interactions. This heterogeneous shelf morphology plays a central role in modulating circulation patterns, sediment transport, and primary productivity along the coast.

1.1.2. Coastal morphology and ecosystem complexity

Brazilian coastal waters host a wide variety of coastal systems, including estuaries, coastal bays, lagoons, and open shelf environments (Figure 1.3). These systems are embedded within a mosaic of geomorphological features such as muddy seabeds, tidal flats, wetlands, coastal dune fields, and reef structures (Dominguez, 2009). In addition, Brazil supports a remarkable diversity of coastal and marine habitats, including mangroves, salt marshes, seagrass meadows, rhodolith beds, and coral reefs (Kerr et al., 2016). The spatial distribution and functioning of these ecosystems vary strongly along the coast, driven by differences in climate, hydrodynamics, sediment supply, and freshwater inputs.

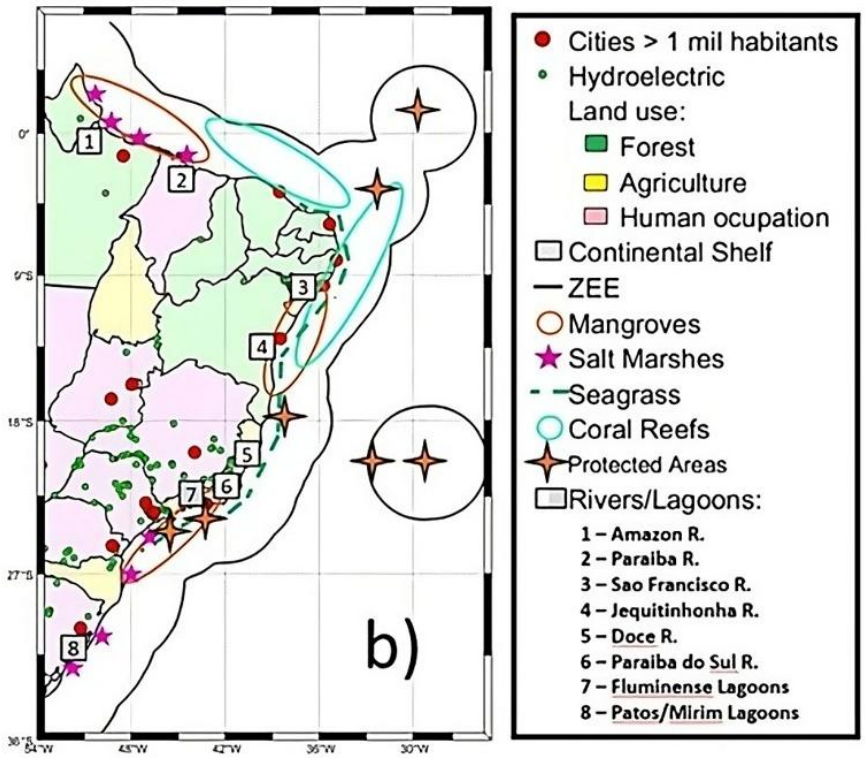

Figure 1.3. Summary of the different coastal types/ecosystems and forcing parameters acting on Brazilian waters (adapted from Kerr et al., 2016, MAPIOMAS, https://mapbiomas.org/).

The wide latitudinal extent of the Brazilian coast induces pronounced heterogeneity in ecosystem structure and biogeochemical functioning (Ekau and Knoppers, 1999; Kerr et al., 2016). Northern coastal waters are strongly influenced by large river plumes, particularly the Amazon River (Figure 1.3), leading to turbid, nutrient-rich, and highly productive waters characterized by elevated suspended matter and organic carbon concentrations (Ciotti et al., 2010; Molleri et al., 2010; Bernardes et al., 2012). In contrast, large portions of the northeastern and eastern shelves are dominated by oceanic water masses and limited continental runoff, resulting in clearer and generally oligotrophic conditions (Ekau and Knoppers, 1999; Castro et al., 2006; Brandini et al., 2018). Southern coastal waters exhibit strong seasonal variability linked to freshwater discharge from the La Plata River system and adjacent coastal lagoons, producing marked gradients in salinity, turbidity, and primary productivity (Ciotti, Garcia and Jorge, 2010; Burone et al., 2021).

1.1.3. Climatic and hydrological conditions

Climatic conditions along the Brazilian coast vary substantially from north to south, reflecting the transition from equatorial and humid tropical climates in the northern and northeastern regions to warm temperate and subtropical climates in the southeastern and southern sectors (Ekau and Knoppers, 1999; Bernardes et al., 2012; Kerr et al., 2016). These climatic gradients control precipitation regimes, wind patterns, and seasonal variability, thereby strongly modulating river discharge, water column stratification, and mixing processes in coastal waters (Castro et al., 2006; Brandini et al., 2018).

Brazilian coastal waters are shaped by a complex interplay between atmospheric forcing, freshwater inputs, and oceanic circulation. The magnitude and seasonality of river discharge vary widely among regions, with large drainage basins such as the Amazon and La Plata exerting a dominant control on coastal salinity, nutrient availability, and suspended matter concentrations (Castro et al., 2006; Ciotti et al., 2010; Burone et al., 2021). Smaller river systems, although individually less influential, collectively contribute to the spatial heterogeneity of land-sea interactions along the Brazilian coast (Bernardes et al., 2012; Kerr et al., 2016).

1.1.4. Ocean circulation and hydrodynamic processes

Large-scale ocean circulation along the Brazilian margin is dominated by two major western boundary currents (Figure 1.4): the North Brazil Current (NBC) and the Brazil Current (BC), both originating from the bifurcation of the South Equatorial Current (SEC) near 10° S

(Castro et al., 2006; Brandini et al., 2018). The NBC flows northwestward along the northern and northeastern margin, interacting strongly with the Amazon River plume and exporting freshwater and suspended material toward the equatorial Atlantic. The BC, a comparatively weaker current, flows southward along the eastern and southeastern coast, transporting Tropical Water at the surface and South Atlantic Central Water at subsurface levels (de Souza et al., 2020).

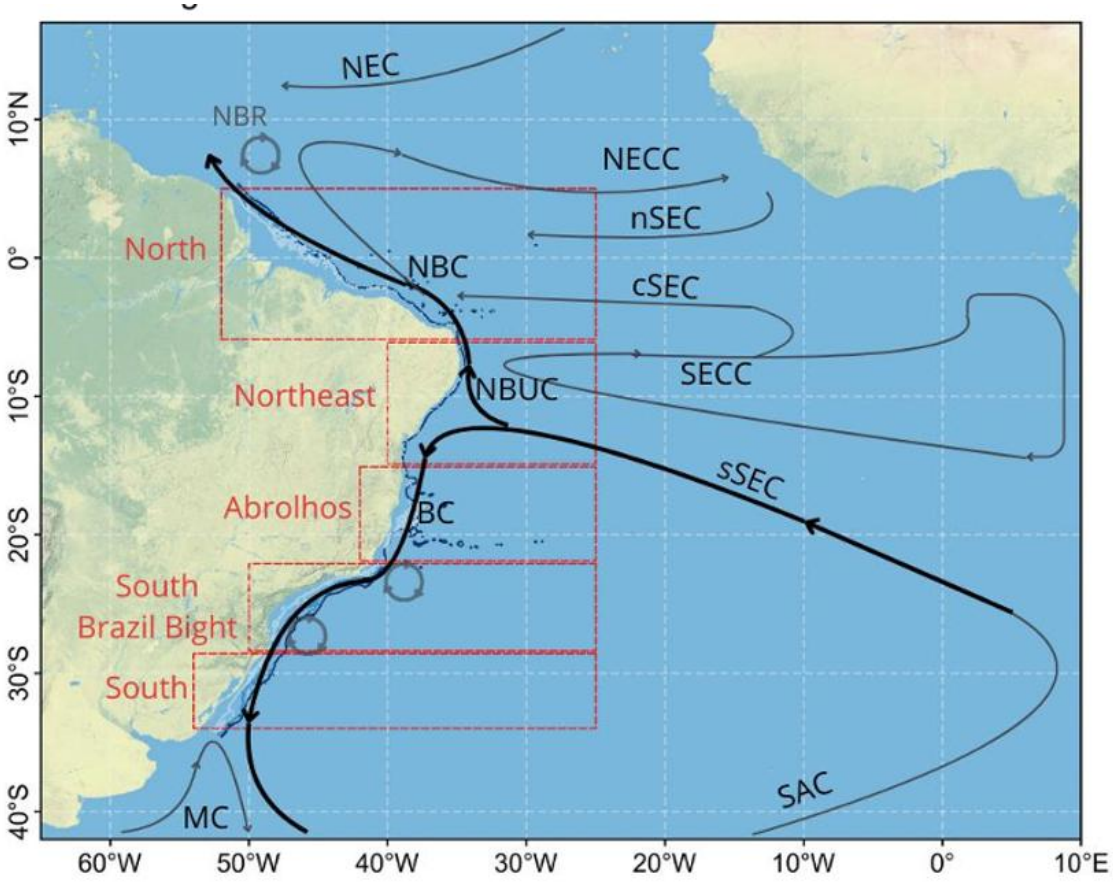

Figure 1.4. Main sea surface ocean currents flowing along the Brazilian continental margin. North Equatorial Current (NEC), North Equatorial Countercurrent (NECC), northern (nSEC), central (cSEC), and southern South Equatorial Current (sSEC), South Equatorial Countercurrent (SECC), North Brazil Current (NBC), North Brazil Ring (NBR), North Brazil Undercurrent (NBUC), Brazil Current (BC), Malvinas Current (MC), South Atlantic Current (SAC). Circles inside the South Brazil Bight are quasi-stationary cyclonic meanders (Amorim et al., 2024; Campos; Gonçalves; Ikeda, 1995). The division of the Brazilian continental margin into five regions is also shown (North, Northeast, Abrolhos, South Brazil Bight, South). Adapted from da Silveira et al. (da Silveira et al., 2020).

Mesoscale processes, including eddies, meanders, and coastal upwelling events, play a key role in modulating nutrient supply and biological productivity along the Brazilian continental shelf by enhancing exchanges between shelf and open-ocean waters (Castro et al., 2006; Brandini, Tura and Santos, 2018). These processes are particularly prominent along the southeastern coast near Cape Frio, where favorable wind conditions and interactions between the Brazil Current and shelf morphology promote the intrusion of nutrient-rich South Atlantic

Central Water onto the shelf, leading to enhanced phytoplankton biomass and primary production (Rodrigues and Lorenzzetti, 2001; Amorim et al., 2024).

Tidal regimes also vary markedly along the Brazilian coast, ranging from macrotidal conditions in the north to microtidal environments in the south, and further contribute to regional differences in vertical mixing, sediment resuspension, and coastal turbidity (Ekau and Knoppers, 1999; Bernardes et al., 2012).

1.1.5. Biogeochemical variability of Brazilian coastal waters

As a consequence of the strong physical and ecological heterogeneity of the Brazilian coastal zone, coastal waters exhibit pronounced spatial and temporal variability in key biogeochemical properties, including suspended particulate matter (SPM), chlorophyll-a (Chl-a), colored dissolved organic matter (CDOM), and particulate organic carbon (POC) (Ekau and Knoppers, 1999; Ciotti et al., 2010; Da Silva et al., 2021). This variability reflects the coexistence of highly contrasted environments, ranging from turbid, nutrient-rich waters influenced by major river plumes and estuarine systems to clearer and generally oligotrophic offshore and eastern shelf waters (Molleri et al., 2010; Bernardes et al., 2012; Brandini et al., 2018).

The interaction between freshwater inputs, shelf circulation, and oceanic water masses governs the distribution and mixing of Coastal Waters, Tropical Water, and South Atlantic Central Water along the Brazilian shelf, generating complex biogeochemical gradients at regional and national scales (Ekau and Knoppers, 1999; Castro et al., 2006; Ciotti et al. 2010). These gradients are further modulated by climate variability, including natural oscillations such as ENSO and longer-term climate trends that affect precipitation, wind patterns, and upwelling intensity, thereby influencing sediment dynamics and biological productivity (de Souza et al., 2020; Tavora et al., 2020).

At regional scales, the temporal variability of coastal biogeochemical properties is driven by a combination of seasonal hydrological cycles, mesoscale circulation, wind-induced resuspension, and episodic events such as storms and extreme river discharge. In northern Brazil, large river plumes such as the Amazon generate persistent high-SPM and high-POC waters extending over hundreds of kilometers, with strong seasonal modulation linked to river discharge (Molleri et al., 2010; Bernardes et al., 2012). In contrast, southeastern and southern coastal regions are more strongly influenced by coastal circulation, wind forcing, and localized resuspension processes associated with storms and wave activity (Castro et al., 2006; Brandini et al., 2018). Phytoplankton blooms can develop seasonally in estuarine and nearshore

environments, particularly in eutrophic bays and regions affected by nutrient enrichment or coastal upwelling, such as the Cabo Frio region (Valentin et al., 1987; Brandini, 1990; Andrade and Gonzalez, 2018). These blooms may persist from several days to several weeks and can extend from local estuarine scales to large shelf areas depending on environmental conditions and circulation patterns.

1.1.6. Anthropogenic pressures and the need for long-term monitoring

Brazilian coastal zones host a large fraction of the national population and concentrate major socioeconomic activities, including tourism, fisheries, aquaculture, port infrastructure, and industrial development. Rapid urbanization since the 1960s, together with deforestation, dam construction, and the expansion of intensive agriculture, has led to increased nutrient inputs, sediment fluxes, and chemical contamination in many coastal environments (Bernardes et al., 2012; de Andrés et al., 2018). These anthropogenic pressures have been shown to affect a wide range of coastal ecosystems, including bays (Fistarol et al., 2015; Cotovicz et al., 2019), coastal lagoons (Knoppers and Kjerfve, 1999; Cotovicz et al., 2021), estuaries (Rudorff et al., 2011; Mourão et al., 2020), and mangrove systems (Ferreira and Lacerda, 2016). The magnitude and nature of these impacts vary widely among regions, depending on land-use practices, hydrological conditions, and ecosystem vulnerability (Bernardes et al., 2012; Cotovicz et al., 2021).

Despite recent efforts to expand in situ monitoring networks and marine protected areas, the assessment of long-term and large-scale biogeochemical changes in Brazilian coastal waters remains limited by the scarcity of sustained and spatially representative observations (Garcia et al., 2016; CEMBRA, 2019). This limitation is particularly critical given the strong regional heterogeneity of anthropogenic pressures and natural forcing mechanisms. In this context, satellite ocean color remote sensing has emerged as a key complementary tool for monitoring coastal water quality over multidecadal time scales, allowing synoptic assessment of spatial patterns, seasonal variability, and long-term trends in biogeochemical properties (Gonzalez-Silvera et al., 2004; Ciotti, Garcia and Jorge, 2010; Kampel et al., 2019). Continuous satellite archives such as those provided by MODIS offer a unique opportunity to investigate the evolution of optically and biogeochemically contrasted coastal waters across the entire Brazilian shelf.

However, satellite ocean color observations are subject to several well-documented limitations, particularly in optically complex coastal environments. Major sources of uncertainty include atmospheric correction, sensor calibration, and bio-optical inversion

algorithms, with errors generally increasing in turbid and coastal waters (Gordon and Wang, 1994; IOCCG, 2000; Mobley et al., 2016). Spatial resolution constraints (typically 300 m to 1 km for medium-resolution sensors) limit the detection of fine-scale coastal features, while cloud cover, sun glint, and high aerosol loads can significantly reduce data availability (Mélin et al., 2017; Groom et al., 2019). In addition, satellite ocean color observations are inherently restricted to the near-surface layer, as the detected signal originates from the upper optical depth of the water column, generally corresponding to the first light attenuation depth, which varies with water clarity and optical properties (Kirk, 1994; IOCCG, 2000). Consequently, satellite-derived products provide an integrated view of surface optical and biogeochemical properties and do not directly resolve vertical structure or subsurface processes.

Overall, the exceptional spatial heterogeneity, strong land-sea coupling and increasing anthropogenic pressures make Brazilian coastal waters a priority region for sustained environmental monitoring. However, despite this recognized importance, long-term in situ observations remain sparse, and most regional assessments rely on limited spatial coverage or short time series, restricting the capacity to resolve coastal variability and long-term trends. Improving the understanding of biogeochemical dynamics at regional to national scales is therefore essential to support coastal management, conservation strategies, and science-based policy initiatives, including recent national programs dedicated to ocean sustainability and marine spatial planning (Eberhard et al., 2016; Giglio et al., 2018; Gonçalves et al., 2021; Magris et al., 2021).

1.2. Satellite ocean color remote sensing and coastal biogeochemistry

1.2.1. Satellite ocean color observations and mission continuity

Satellite ocean color remote sensing has become a cornerstone for observing marine and coastal biogeochemical processes at regional to global scales. By providing synoptic and repetitive measurements of water-leaving radiance, satellite observations enable the monitoring of key biogeochemical variables, such as Chl-a, SPM, and POC, over a wide range of temporal and spatial scales (McClain, 2009; Blondeau-Patissier et al., 2014).

The first proof-of-concept satellite ocean color mission was the Coastal Zone Color Scanner (CZCS), launched in 1978 aboard Nimbus-7. Operating between 1978 and 1986, CZCS demonstrated for the first time that quantitative estimates of marine biogeochemical parameters, particularly Chl-a concentration, could be retrieved from spaceborne optical measurements

(McClain, 2009). Although limited in spatial and temporal coverage, CZCS laid the foundations for modern ocean color remote sensing.

The modern era of global ocean color observations began in the late 1990s with the launch of the Sea-viewing Wide Field-of-view Sensor (SeaWiFS, 4 km, 1 km resolution) in 1997, which ensured near-continuous global ocean color measurements from polar-orbiting satellites. SeaWiFS was followed by a succession of dedicated sensors, including the Moderate Resolution Imaging Spectroradiometer (MODIS, 1 km resolution), the Medium Resolution Imaging Spectrometer (MERIS, 300 m and 1km resolution), and more recently the Ocean and Land Colour Instrument (OLCI, 300 m and 1 km resolution) onboard Sentinel-3A and Sentinel-3B satellites, with continuity expected from the forthcoming Sentinel-3C mission. These sensors typically provide global coverage within one to two days, with spatial resolutions ranging from approximately 300 m to 1 km at nadir, making them well suited for large-scale and long-term analyses (Figure 1.5).

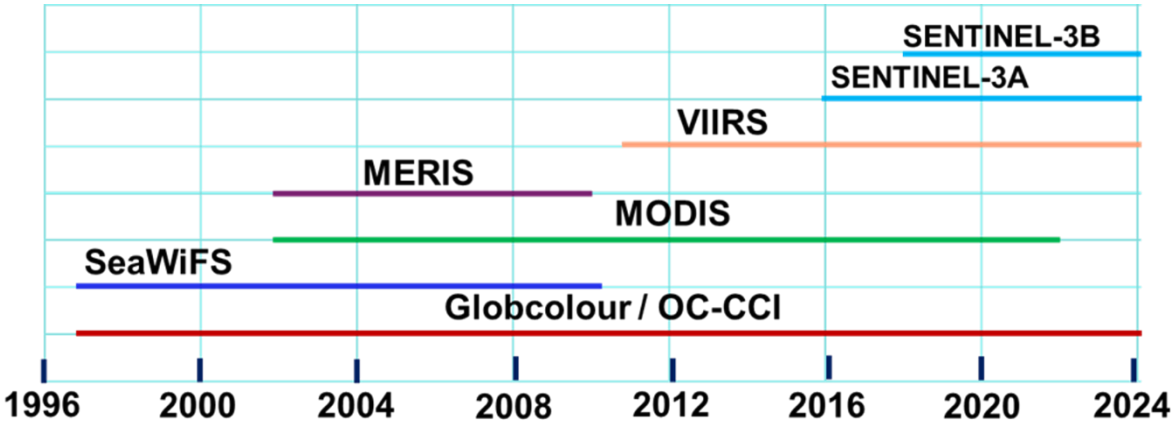

Figure 1.5. Medium spatial resolution sensors (300 m - 1km) used by multi-sensor time series.

The continuity of ocean color observations is essential for the construction of multi-decadal time series, particularly because the operational lifetime of individual sensors is generally limited to five to ten years (with the notable exception of MODIS). As a result, long-term studies increasingly rely on the combination of observations from multiple sensors to ensure temporal consistency and sufficient data availability (Henson et al., 2010; Mélin et al., 2017).

Early efforts to combine multi-sensor ocean color observations were initiated in the late 1990s, notably by Gregg and Woodward, (1998), as summarized in the IOCCG, (1999) report. These studies demonstrated that merging data from different sensors could significantly increase spatial coverage and observation frequency. For instance, the combined use of SeaWiFS and MODIS provided daily valid observations over up to 23% of the global ocean, compared to approximately 16-18% when using each sensor independently.

During the early 2000s, several methodological approaches were developed to generate multi-sensor ocean color products, particularly for Chl-a, including inter-sensor bias correction, spectral band shifting, and statistical harmonization techniques (Kwiatkowska and Fargion, 2003; Pottier et al., 2006; Mélin and Zibordi, 2007; Maritorena et al., 2010). These approaches are comprehensively described in the IOCCG, (2007) report and paved the way for the operational production of merged ocean color datasets.

Among the major initiatives resulting from these developments, the GlobColour and Ocean Colour Climate Change Initiative (OC-CCI) projects stand out. GlobColour, initiated in 2005 under the coordination of the European Space Agency (ESA), was designed to deliver consistent, user-oriented ocean color products by merging data from multiple sensors. Since 2015, GlobColour has also contributed to the Copernicus Marine Environment Monitoring Service (CMEMS), providing downscaled remote sensing products to end users (Garnesson et al., 2019).

The OC-CCI project, launched by ESA in 2009, aims to generate long-term, climate-quality time series of ocean color essential climate variables (ECVs), in response to the needs of the Global Climate Observing System (GCOS), the UNFCCC, and the IPCC (Sathyendranath et al., 2017, 2019). OC-CCI provides harmonized remote sensing reflectance, Chl-a, and related products derived from a multi-sensor processing chain designed to minimize inter-sensor inconsistencies and temporal discontinuities.

Despite these advances, several studies have shown that long-term trends derived from multi-sensor ocean color products can vary substantially depending on the dataset used. Differences in acquisition geometry, spatial resolution, spectral configuration, overpass time, and sensor availability can introduce biases that affect trend detection, particularly in optically complex coastal waters (Saulquin et al., 2013; Mélin, 2016; Hammond et al., 2020; Yu et al., 2023; Pauthenet et al., 2024). Consequently, the use of multi-sensor datasets for long-term analyses requires careful performance evaluation to avoid misinterpretation of observed trends.

This issue is especially critical in coastal environments, where strong spatial heterogeneity and rapid temporal variability challenge standard open-ocean algorithms. In this context, higher-resolution sensors, such as the Multi-Spectral Instrument (MSI) onboard Sentinel-2, have opened new perspectives for coastal ocean color studies. With spatial resolutions of 10-60 m and frequent revisit times, Sentinel-2 MSI (10, 20 and 60 m resolution) is particularly suited for resolving fine-scale coastal features, river plumes, and nearshore gradients that cannot be captured by kilometer-scale sensors. Although not originally designed as a dedicated ocean

color mission, Sentinel-2 has increasingly been used for coastal water quality applications, complementing traditional ocean color sensors.

In this context, several national and international initiatives have been developed to improve the exploitation of ocean color remote sensing for coastal and shelf environments, where optical complexity challenges standard retrieval approaches. In 2021, the COCOBRAZ project was launched through a collaboration between the National Institute for Space Research (INPE, Brazil), the Institute of Oceanography of the University of São Paulo (IOUSP), and the Laboratory of Oceanology and Geosciences (LOG, France), with funding from FAPESP (2021/04128-8) and the French National Research Agency (ANR-21-CE01-0026).

The primary objective of the COCOBRAZ project, of which this PhD work is part, is to provide a comprehensive assessment of water quality in the Brazilian marine domain at a spatial resolution of 1 km, explicitly accounting for the strong optical heterogeneity of coastal and shelf waters. Within this framework, several biogeochemical variables are retrieved from MODIS-Aqua single-sensor observations.

Despite major advances in satellite ocean color remote sensing and the availability of multi-decadal archives from sensors such as SeaWiFS, MODIS, MERIS, and OLCI, the assessment of long-term biogeochemical variability in Brazilian coastal waters remains limited. Existing studies are often restricted to local or regional scales, short time periods, or a single biogeochemical variable, and are frequently constrained by the scarcity of in situ data for algorithm calibration and validation. In addition, the strong optical heterogeneity of Brazilian coastal and shelf waters challenges the direct application of global multi-sensor products, whose performance and consistency remain insufficiently evaluated in these optically complex environments. As a result, there is still a lack of spatially consistent, long-term, and regionally adapted satellite-based assessments of key coastal biogeochemical properties at the national scale. Addressing these limitations requires dedicated approaches that explicitly account for optical diversity, ensure algorithm robustness in coastal waters, and critically evaluate the suitability of widely used multi-sensor datasets for trend analysis. These needs motivate the development and application of tailored satellite-based methodologies, such as those implemented in the present PhD, to improve the monitoring of biogeochemical variability along the Brazilian continental margin.

1.2.2. Atmospheric correction and retrieval of remote sensing reflectance

Ocean color remote sensing relies on the measurement of the spectral light field emerging from the ocean after the interaction of solar radiation with the atmosphere, the sea surface, and

the water column. The signal detected by a satellite sensor is therefore not a direct measurement of biogeochemical variables, but an optical response controlled by the absorption and scattering properties of seawater and its constituents. In ocean optics, these properties are commonly separated into inherent optical properties (IOPs) and apparent optical properties (AOPs). IOPs depend only on the medium and include absorption, scattering, and backscattering coefficients, whereas AOPs also depend on the geometry and intensity of the ambient light field. Remote sensing reflectance, R_{rs} (λ), is an AOP and represents the main quantity used in ocean color applications to infer surface biogeochemical properties (Morel and Prieur, 1977; Gordon et al., 1988; Mobley, 1999; IOCCG, 2000).

The spectral shape of R_{rs} (λ) is controlled by the relative contribution of optically active constituents. Phytoplankton pigments, especially chlorophyll-a, strongly absorb light in the blue and red spectral domains, while suspended particulate matter enhances scattering and backscattering, particularly in the green to red wavelengths. Colored dissolved organic matter mainly absorbs light in the ultraviolet and blue spectral regions. These different optical signatures form the basis for the retrieval of for instance Chl-a, SPM, CDOM, POC proxies from satellite observations. However, in coastal waters, these constituents often vary independently, which complicates the interpretation of the satellite signal and reduces the performance of algorithms developed for open-ocean waters (IOCCG, 2000; Mobley et al., 2016; Werdell et al., 2018).

Satellite sensors measure the radiance at the top of the atmosphere, but only a small fraction of this signal originates from the water column, while most of it results from atmospheric scattering by molecules and aerosols, as well as surface effects such as sun glint, making atmospheric correction a critical step for ocean color applications (Gordon and Wang, 1994; IOCCG, 2010). Accurate retrieval of oceanic information therefore relies on robust correction procedures designed to isolate the water-leaving radiance component.

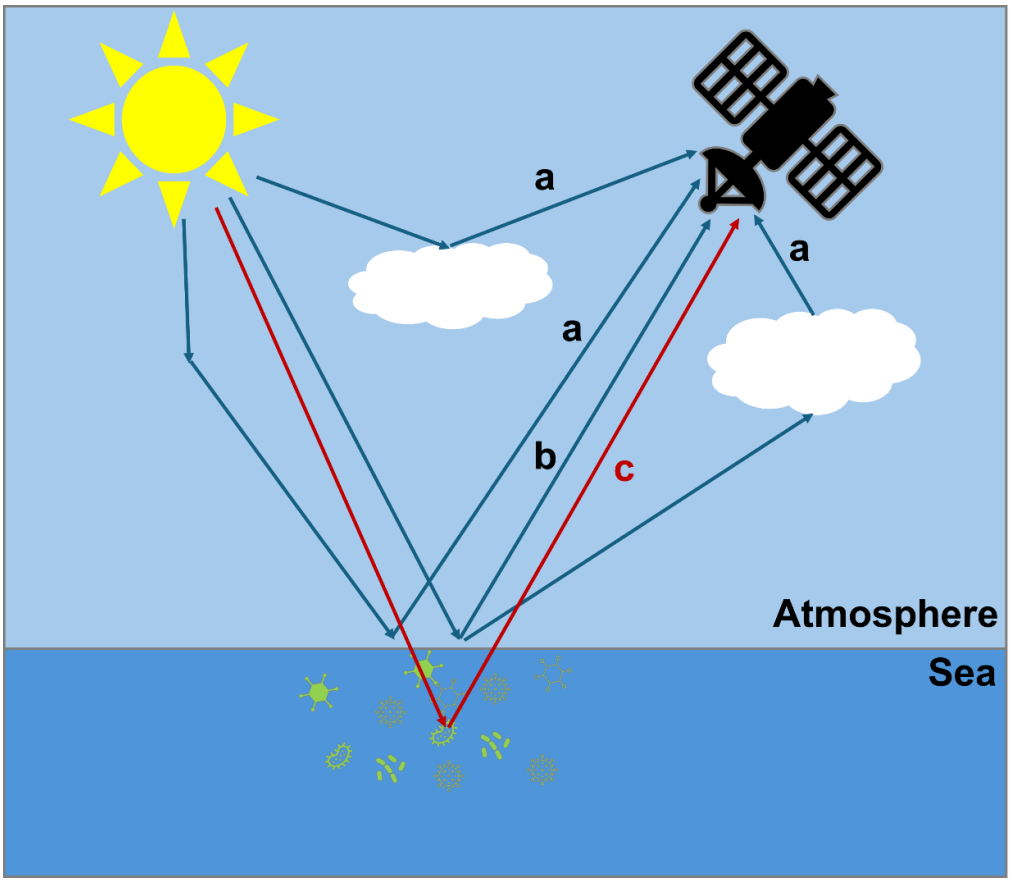

Figure 1.6. Schematic representation of the irradiance propagation paths to the sensor: (a) direct or multiple scattering within the atmosphere; (b) specular reflection at the sea surface; (c) water-leaving radiance, after interaction with the water column, reaching the sensor. Adapted from IOCCG, (2000) and Cardoso Dos Santos, (2025).

Atmospheric correction aims to remove atmospheric and surface contributions in order to derive the remote sensing reflectance, $\boldsymbol{R_{rs}}(\boldsymbol{\lambda})$, which constitutes the fundamental input for all ocean color bio-optical algorithms (Mobley et al., 2016). Remote sensing reflectance is classically defined as:

$$\boldsymbol{R_{rs}}(\boldsymbol{\lambda}) = \frac{\mathbf{L_w}(\boldsymbol{\lambda})}{\mathbf{E_d}(\boldsymbol{\lambda})} \quad \textbf{(1.1)}$$

where $\mathbf{L_w}(\boldsymbol{\lambda})$ is the water-leaving radiance just above the sea surface and $\mathbf{E_d}(\boldsymbol{\lambda})$ is the downwelling irradiance incident on the surface (Mobley, 1999; IOCCG, 2010). By construction, $\boldsymbol{R_{rs}}$ represents the spectral fingerprint of the water column and directly links satellite observations to the optical and biogeochemical properties of surface waters.

Spectral variations in remote-sensing reflectance are closely related to variations in the inherent optical properties (IOPs) of seawater (Gordon et al., 1975; Morel and Prieur, 1977):

$$\boldsymbol{R_{rs}}(\boldsymbol{\lambda}) = \boldsymbol{g} \cdot \frac{\boldsymbol{b_b}(\boldsymbol{\lambda})}{\boldsymbol{a}(\boldsymbol{\lambda}) + \boldsymbol{b_b}(\boldsymbol{\lambda})} \quad \textbf{(1.2)}$$

where (g) is a parameter that depends on the illumination geometry and scattering properties of the water column. The total absorption coefficient, (**a(λ)**) is expressed as:

$$\mathbf{a(\lambda) = a_w(\lambda) + a_{ph}(\lambda) + a_{cdom}(\lambda) + a_{nap}(\lambda)} \quad \textbf{(1.3)}$$

where $\mathbf{a_w}$, $\mathbf{a_{ph}}$, $\mathbf{a_{cdom}}$ and $\mathbf{a_{nap}}$ denote the absorption coefficients of pure water, phytoplankton, colored dissolved organic matter (CDOM), and non-algal particles (NAP), respectively (Figure 1.7). Similarly, the total backscattering coefficient ($\mathbf{b_b(\lambda)}$) is given by:

$$\mathbf{b_b(\lambda) = b_{bw}(\lambda) + b_{bp}(\lambda)} \quad \textbf{(1.4)}$$

where $\mathbf{b_{bw}(\lambda)}$ and $\mathbf{b_{bp}(\lambda)}$ represent the backscattering contributions of seawater and suspended particles, respectively. Consequently, the spectral shape and magnitude of $\boldsymbol{R_{rs}}$ are governed by the balance between absorption and backscattering processes, providing a direct link between optical measurements and the composition of the water column.

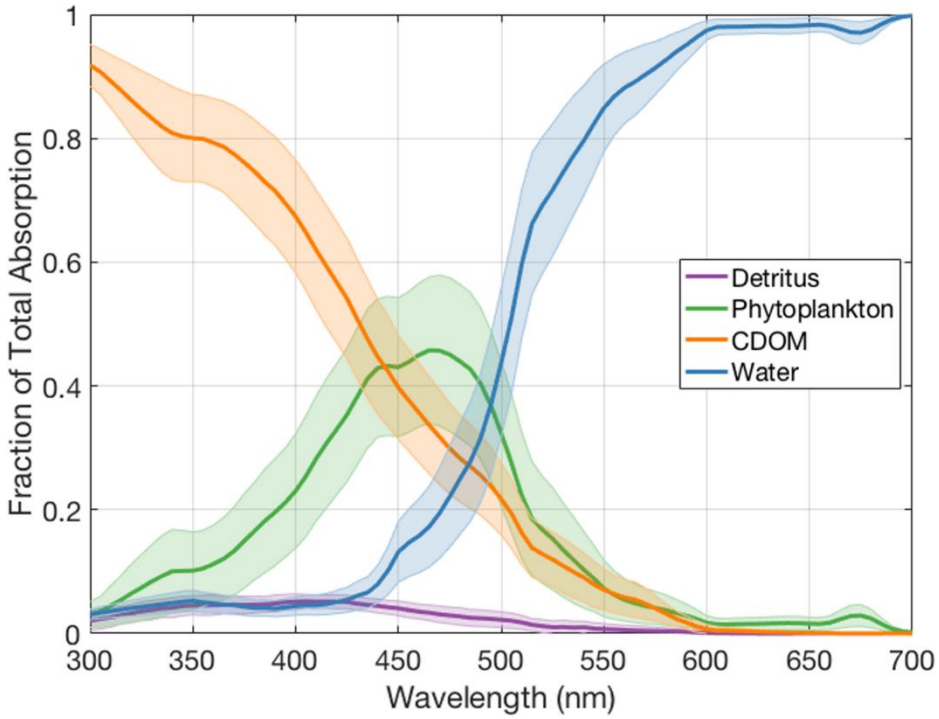

Figure 1.7. Mean relative contributions of Detritus, Phytoplankton, CDOM, and Water to total light absorption at wavelengths between 300 and 700 nm for the NAAMES dataset. Error bars represent one standard deviation for these estimates (Allen et al., 2020).

Early atmospheric correction schemes were developed primarily for open-ocean conditions and relied on the assumption that water-leaving radiance is negligible in the near-infrared spectral domain. This assumption is generally valid for open-ocean Case-1 waters, defined as waters in which optical variability is dominated by phytoplankton and covarying substances (Gordon and Morel, 1983). However, it often breaks down in coastal and shelf Case-2 waters, where optical properties are influenced by additional, independently varying constituents such

as suspended particulate matter and colored dissolved organic matter (Gordon and Morel, 1983; IOCCG, 2000). In these environments, scattering by suspended particles can produce a significant near-infrared water signal, violating the dark-pixel assumption commonly used for atmospheric correction (Ruddick et al., 2000; IOCCG, 2010). Therefore, numerous refinements and alternative approaches have been proposed to improve atmospheric correction in optically complex waters, including modified NIR-based methods, shortwave infrared techniques, and coupled atmosphere-ocean inversion schemes (Wang and Shi, 2007; Steinmetz, Deschamps and Ramon, 2011; Mobley et al., 2016). Despite these advances, atmospheric correction remains one of the main sources of uncertainty in coastal ocean color applications.

Within the COCOBRAZ project, two main atmospheric correction approaches were implemented and evaluated for coastal waters: the Ocean Color - Simultaneous Marine and Atmospheric Retrieval Tool (OC-SMART) (Fan et al., 2021) and a combined near-infrared to shortwave infrared (NIR-SWIR) approach (Wang and Shi, 2007). Both methods are described in detail in Chapter 2. In the context of this PhD, the analysis primarily focuses on the use of OC-SMART applied to MODIS data at 1 km spatial resolution, which constitutes the core dataset for the development, evaluation, and application of coastal biogeochemical algorithms.

Despite substantial progress in atmospheric correction methodologies, the accurate retrieval of remote sensing reflectance in coastal waters remains challenging. The strong optical complexity of coastal and shelf environments, driven by high concentrations of suspended particles, variable CDOM, and intense land-sea interactions, often violates the assumptions underlying standard open-ocean correction schemes. As a result, residual atmospheric contamination and uncertainties in R_{rs} retrieval persist, particularly in turbid and highly dynamic coastal regions such as those encountered along the Brazilian continental margin. These uncertainties directly propagate into bio-optical inversion algorithms and can significantly affect the reliability of derived biogeochemical products and long-term trend analyses. Consequently, the evaluation and selection of atmospheric correction approaches adapted to optically complex coastal waters constitute a critical prerequisite for robust satellite-based assessments of coastal biogeochemical variability.

1.2.3. Optical properties and bio-optical inversion of biogeochemical variables

The interpretation of ocean color observations is grounded in radiative transfer theory and the optical properties of seawater. Optical properties are commonly divided into inherent optical properties (IOPs), which depend solely on the medium and its constituents, and apparent optical properties (AOPs), which also depend on the ambient light field (Kirk, 1994; Mobley, 1999).

IOPs include absorption and scattering coefficients associated with pure seawater, phytoplankton pigments, non-algal particles, and colored dissolved organic matter, and they control the spectral shape and magnitude of the upwelling light field detected by satellite sensors (Mobley, 1999). In practice, the absorption coefficient determines how light is removed from the water column, while the backscattering coefficient controls the fraction of light redirected upward toward the sensor. The balance between absorption and backscattering therefore determines the magnitude and spectral shape of R_{rs} (λ).

Among AOPs, remote sensing reflectance plays a central role, as it provides the physical link between satellite measurements and the biogeochemical characteristics of surface waters (Morel and Prieur, 1977; Gordon et al., 1988). Variations in R_{rs} reflect changes in the relative contributions of absorption and backscattering processes, which form the basis for the inversion of biogeochemical variables from space.

Bio-optical algorithms establish quantitative relationships between R_{rs} and properties of the water column. A wide range of approaches has been developed, including empirical band-ratio algorithms, semi-analytical models based on simplified radiative transfer equations (Figure 1.8), and more recent machine-learning techniques (O'Reilly et al., 1998; Lee, Carder and Arnone, 2002; Werdell et al., 2018). In open-ocean environments, where optical variability is largely driven by phytoplankton, standard chlorophyll-a algorithms have demonstrated robust performance and form the basis of most global products (O'Reilly et al., 1998; Hu et al., 2012). In contrast, coastal waters are optically complex, as multiple constituents contribute independently to absorption and scattering, often leading to degraded performance of standard products, particularly for chlorophyll-a, suspended particulate matter, and dissolved organic matter (IOCCG, 2000; Werdell et al., 2018).

Despite the diversity of bio-optical inversion approaches developed over the past decades, the retrieval of biogeochemical variables in coastal waters remains subject to substantial uncertainty. The decoupling between optical properties and phytoplankton biomass in optically complex environments limits the applicability of standard open-ocean algorithms and reduces the robustness of global products when applied to coastal and shelf regions. In areas characterized by strong spatial heterogeneity, variable particle composition, and intense land-sea interactions, such as the Brazilian coastal zone, algorithm performance may vary markedly in space and time. This highlights the need for inversion strategies that explicitly account for optical diversity and for systematic evaluations of algorithm suitability across contrasted coastal water types, particularly when long-term variability and trend analyses are targeted.

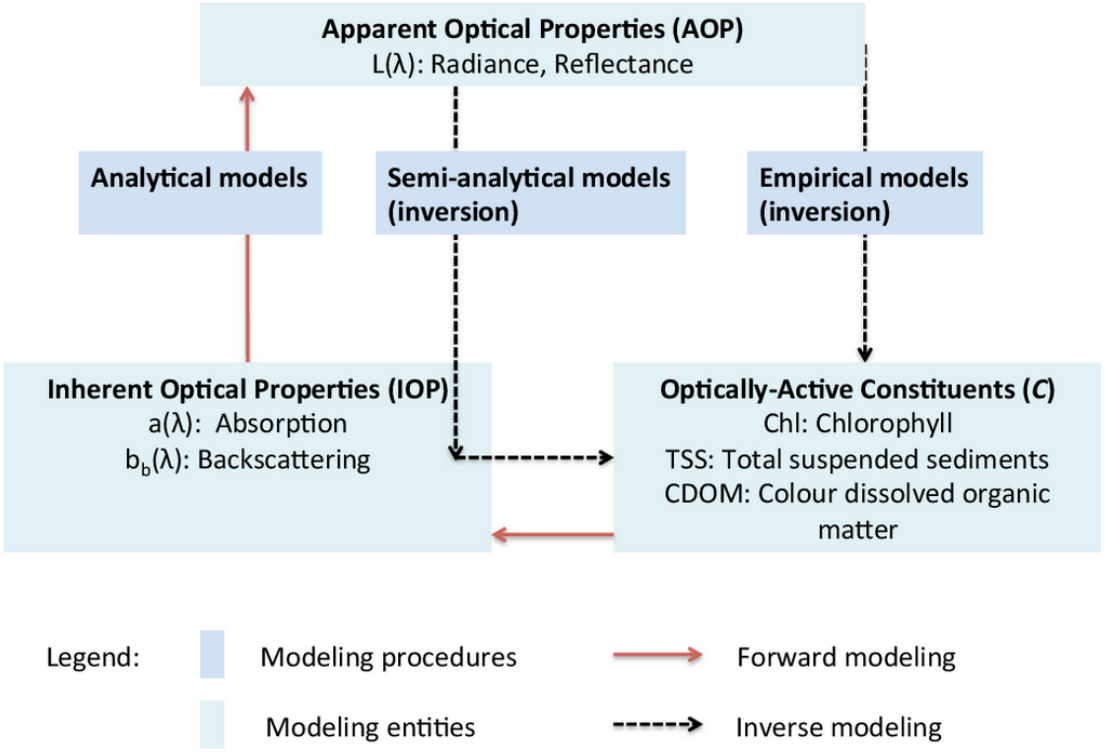

Figure 1.8. Conceptual illustration of the main categories of inversion models applied to marine reflectance signals for the retrieval of biogeochemical products from satellite ocean-color observations (adapted from IOCCG, 2000).

1.2.4. Optical complexity of coastal waters and implications for long-term monitoring

The strong optical heterogeneity of coastal waters represents a major challenge for the consistent exploitation of long-term satellite ocean color archives. Variations in suspended sediments, riverine inputs, CDOM, phytoplankton communities, and hydrodynamic processes generate pronounced spatial and temporal variability in optical properties, directly affecting atmospheric correction and bio-optical inversion (IOCCG, 2000; Mobley et al., 2016; Spyrakos et al., 2018). These effects are particularly critical for multi-decadal analyses, where small systematic biases may accumulate and compromise the interpretation of long-term trends (Mélin, 2016; Hammond et al., 2020; Pauthenet et al., 2024).

A classical framework for describing ocean optical variability distinguishes between Case-1 and Case-2 waters (Morel and Prieur, 1977). In Case-1 waters, optical properties are primarily driven by phytoplankton and covary with chlorophyll-a concentration, whereas in Case-2 waters, additional optically active constituents such as mineral particles and dissolved organic matter contribute significantly to the optical signal, leading to a decoupling between optical properties and phytoplankton biomass (Morel, 1988; Mobley et al., 2004). Most coastal and shelf environments fall into the Case-2 category, limiting the applicability of global bio-optical algorithms originally developed for open-ocean conditions (IOCCG, 2000; Mélin and Zibordi, 2007).

To better capture the diversity of optical conditions, Optical Water Type (OWT) classification schemes have been developed to group water masses according to similarities in their remote sensing reflectance spectra (Moore, Campbell and Feng, 2001; Moore, Campbell and Dowell, 2009; Spyrakos et al., 2018). Among these, the OWT classification proposed by Mélin and Vantrepotte (2015) constitutes a widely used global framework applicable to both open-ocean and coastal waters. This classification was subsequently adapted at the global scale by Jorge et al. (2021), while preserving its original conceptual basis.

This OWT framework has been applied to assess optical variability and algorithm performance in Brazilian waters (Figure 1.9). Santos et al. (2023) applied the Mélin and Vantrepotte (2015) classification, adapted by Jorge et al. (2021), along the Brazilian continental margin to evaluate chlorophyll-a estimates, highlighting the limitations of global Chl-a products in optically complex coastal environments (Cardoso Dos Santos, 2025). In parallel, region-specific optical classifications have been developed for Brazilian waters, such as the classification conducted by Valerio et al. (2021) in the Lower Amazon region and its tributaries, which identified dominant optical classes associated with hydrological variability.

In this context, OWT-based frameworks provide a consistent basis for evaluating ocean color retrieval performance and for developing algorithms adapted to optically complex coastal waters. By accounting for the dominant optical characteristics of water masses, OWT classifications support the selection and application of appropriate retrieval strategies, thereby improving the reliability and consistency of satellite-derived biogeochemical products for long-term coastal monitoring.

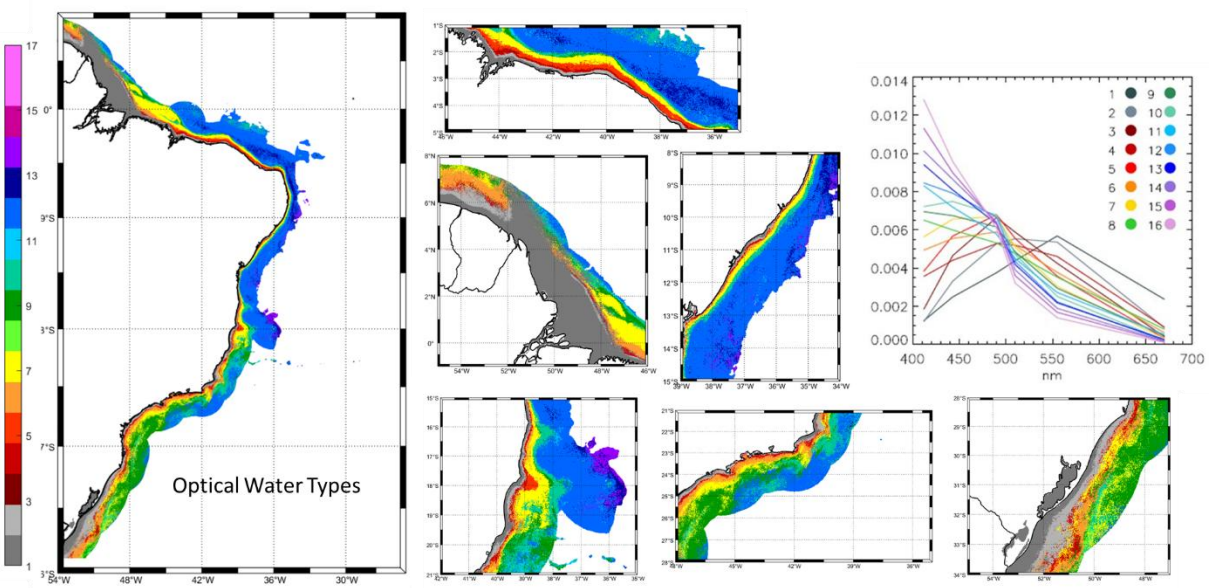

Figure 1.9. Illustration of the optical diversity of Brazilian waters and selected coastal/shelf areas (MERIS GlobCoast global dominant OWT; processing, Mélin and Vantrepotte, 2015 typology: classes 1-2 ultra-turbid waters, 3-9 coastal waters, waters for which standard oceanic OCR products are not adapted, 10-17 oceanic-like waters).

Recent developments have demonstrated that combining bio-optical algorithms within an OWT framework can be further improved by explicitly accounting for the probabilistic nature of water mass classification. Using a global in situ dataset, Tran et al. (2023) showed that weighting chlorophyll-a estimates by the probability of pixel membership to multiple OWTs leads to smoother spatial transitions and reduced inconsistencies between adjacent optical regimes. As illustrated in Figure 1.10, probabilistic combinations outperform simple, non-probabilistic averaging, particularly in coastal transition zones where optical properties vary continuously rather than discretely. These results highlight the importance of probabilistic OWT-based approaches for improving the robustness of satellite-derived chlorophyll-a products in optically heterogeneous coastal waters.

While Optical Water Type frameworks provide an effective means to characterize optical diversity and improve the evaluation of ocean color products in coastal environments, their systematic integration into long-term monitoring strategies remains limited. In highly heterogeneous regions such as the Brazilian coastal zone, where multiple optical regimes coexist and vary seasonally and interannually, the lack of approaches explicitly combining OWT information with biogeochemical retrieval and trend analysis constrains the interpretation of satellite-derived time series. In particular, the extent to which optical regime variability influences long-term biogeochemical signals at regional to national scales remains insufficiently quantified. Addressing this gap requires the consistent use of OWT-based

methodologies to disentangle natural optical variability from genuine biogeochemical trends and to enhance the robustness of satellite-based coastal monitoring.

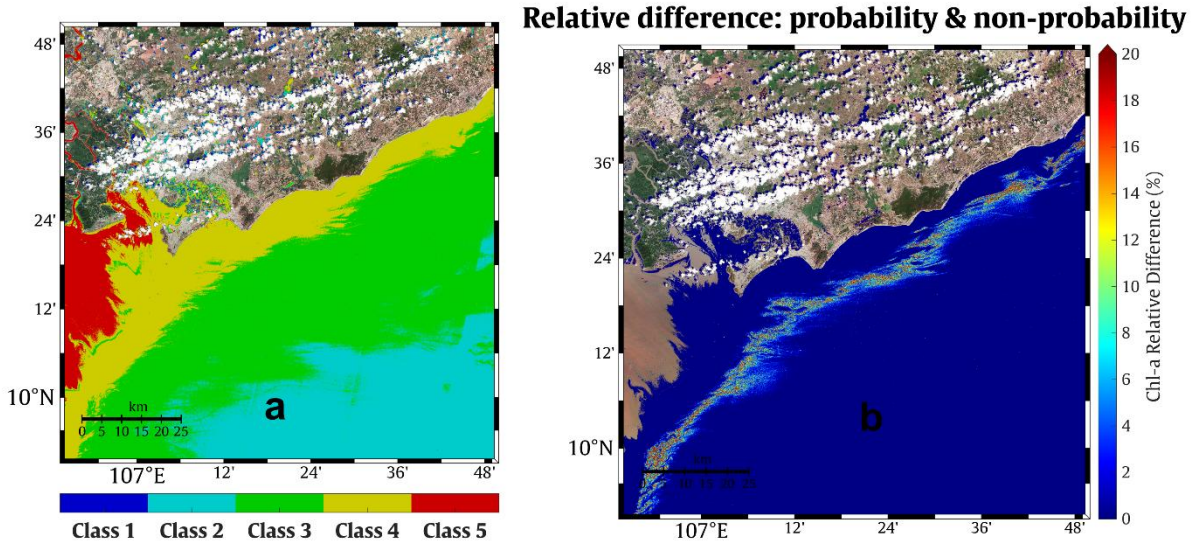

Figure 1.10. Example of a probabilistic OWT based combination of empirical chlorophyll-a algorithms in coastal waters. The relative difference between probabilistic and non-probabilistic algorithm combinations illustrates the reduction of spatial discontinuities when class membership probabilities are explicitly considered (adapted from Tran et al., 2023).

1.2.5. Biogeochemical descriptors of coastal water quality

Monitoring coastal water quality involves the acquisition and analysis of physical, chemical, and biological parameters in order to assess environmental status, detect long-term trends, identify degradation processes, and support informed decision-making. Coastal ecosystems are among the most productive and valuable components of the marine environment, providing essential services for biodiversity conservation, fisheries, aquaculture, recreation, and coastal economies. Maintaining water quality is therefore critical for ecosystem functioning, public health, and the sustainability of human activities in coastal zones (Bierman et al., 2011).

Coastal waters are increasingly impacted by anthropogenic pressures, including nutrient enrichment, land-based pollution, and hydrological alterations, which often result in eutrophication and the proliferation of harmful algal blooms (Anderson et al., 2002). Water quality degradation may also arise from elevated concentrations of pollutants such as oil residues, heavy metals, and organic contaminants (Shahidul Islam and Tanaka, 2004), as well as from increases in turbidity (Orpin et al., 2004) and changes in dissolved oxygen levels (Sánchez et al., 2007). These processes pose significant risks to coastal ecosystems and to the human communities that depend on them (Figure 1.1).

The spatial and temporal variability of coastal water quality indicators occurs over a wide range of scales. Short-term variability, from hours to days, is often associated with tides, storms, sediment resuspension, and transient phytoplankton blooms, while seasonal to interannual variability is generally linked to river discharge, precipitation regimes, coastal upwelling, and climate oscillations (Cloern and Jassby, 2008; Vantrepotte and Mélin, 2011). In coastal waters, suspended particulate matter plumes generated by storms, wave-induced resuspension, or river floods can extend over several tens to hundreds of kilometers and strongly modify water turbidity and light availability (Doxaran et al., 2009; Shi and Wang, 2010). Similarly, phytoplankton blooms may develop rapidly in nutrient-enriched coastal waters and represent key indicators of ecosystem response to both natural forcing and anthropogenic pressures (Anderson et al., 2002; Cloern et al., 2014).

Given the strong spatial and temporal variability of coastal environments, continuous monitoring of water quality is essential to distinguish long-term trends from short-term natural variability and to assess the relative contributions of anthropogenic and natural forcing. In this context, the characterization of the spatiotemporal distribution of biological, biogeochemical, and physical parameters is of fundamental importance for coastal management applications, many of which involve substantial economic and societal interests, and for improving our understanding of coastal ecosystem dynamics and associated biogeochemical cycles (Loisel et al., 2023).

1.2.6. Key biogeochemical descriptors of coastal water quality

- **Chl-a**

Chl-a is a fundamental indicator of phytoplankton biomass and primary production and is widely used as a proxy for trophic status and nutrient availability in coastal waters (Kasprzak et al., 2008). Chlorophyll-a is the main photosynthetic pigment present in all phytoplankton and is responsible for light absorption in the visible spectral domain, which forms the basis of its use in ocean-color remote sensing (Morel and Prieur, 1977; Kirk, 1994). Because Chl-a concentration is expressed per unit volume of seawater, it is commonly used as an indirect proxy for phytoplankton biomass, although this relationship is not strictly linear.

Chl-a concentration varies not only with phytoplankton biomass but also with light conditions and nutrient availability, which can modify the chlorophyll content of phytoplankton cells without proportional changes in carbon biomass (Geider et al., 1997; Behrenfeld et al., 2005). Phytoplankton plays a central role in the marine carbon cycle by assimilating

atmospheric CO_2 through photosynthesis, thereby contributing to climate regulation (Bopp et al., 2002; Wang et al., 2023).

From a remote-sensing perspective, Chl-a is not directly measured by satellite sensors but is estimated from remote sensing reflectance R_{rs} (λ) using bio-optical inversion algorithms, most commonly based on blue–green band ratios or semi-analytical approaches (O'Reilly et al., 1998; Lee et al., 2002; Werdell et al., 2018). In optically complex (Case-2) waters, however, R_{rs} (λ) is strongly affected by other water constituents such as suspended particulate matter (SPM) and colored dissolved organic matter (CDOM), which alters the relationship between R_{rs} and Chl-a and reduces the performance of algorithms developed for open-ocean conditions (IOCCG, 2000; Groom et al., 2019; Lavigne et al., 2021).

- **SPM**

SPM is a key parameter for water quality monitoring and plays a central role in coastal and shelf systems (Håkanson et al., 2004). It strongly influences water turbidity and underwater light availability and is closely linked to morphodynamic processes such as coastal erosion, sediment resuspension, transport, and deposition. SPM also acts as an efficient vector for the transport of nutrients, trace metals, and contaminants from land to the ocean (Miller and Cruise, 1995; Velegrakis et al., 1997; Kroon et al., 2012).

It is composed of a mixture of organic particles (e.g., phytoplankton, bacteria, detrital organic matter) and inorganic mineral particles suspended in the water column (Stramski et al., 2004). SPM encompasses a broad particle size spectrum, typically ranging from submicron particles (<1 μm) to coarse particles and aggregates exceeding 100 μm, including clays, silts, biogenic particles, and flocs formed through aggregation processes (Babin et al., 2003; Woźniak et al., 2010). This wide size distribution directly affects scattering and backscattering coefficients and makes SPM one of the dominant drivers of optical variability in coastal waters, particularly in turbid environments (Stramski et al., 2004; IOCCG, 2000).

- **Organic carbon pools (POC and DOC)**

Organic carbon, present in both particulate (POC) and dissolved (DOC) forms, plays a fundamental role in marine biogeochemical cycles and has important implications for ecosystem functioning and environmental quality (Dhillon and Inamdar, 2014). Although continental shelves represent only a small fraction of the global ocean surface, they contribute disproportionately to marine organic matter production, accounting for approximately 20% of total oceanic primary production. Coastal zones receive organic carbon from multiple sources, including riverine inputs (Cauwet, 2002), groundwater discharge (Burnett et al., 2003), and atmospheric deposition (Willey et al., 2000).

POC constitutes a major pool of organic matter in coastal waters and includes living biomass (phytoplankton, zooplankton, heterotrophic bacteria) as well as detrital material (Loisel et al., 2023). The distribution and dynamics of POC are key indicators of biological productivity in the euphotic zone (Behrenfeld et al., 2005) and provide valuable information on carbon export processes and trophic transfer. In human-impacted coastal regions, elevated POC concentrations may also reflect pollution events or enhanced terrestrial inputs (Tran et al., 2019; Li et al., 2023).

DOC represents the largest organic carbon reservoir in the ocean and plays a crucial role in the global carbon cycle. DOC dynamics in coastal and continental margin systems are controlled by terrestrial inputs, in situ biological production, microbial degradation, and export to the open ocean (HEDGES, 2002; Hansell and Carlson, 2014; Vantrepotte et al., 2015). Although DOC accounts for a relatively small fraction of the total carbon inventory in the water column, which is largely dominated by dissolved inorganic carbon (DIC), it constitutes the largest exchangeable organic carbon pool and is a key component of both surface and deep-ocean carbon budgets (Druffel et al., 1992; Hansell and Carlson, 1998, 2014; Barrón and Duarte, 2015).

DOC is operationally defined as the fraction of organic carbon that passes through fine filters (typically 0.2-0.7 μm) and consists of a complex mixture of low- and high-molecular-weight organic compounds dissolved in seawater (Carlson and Hansell, 2015). DOC represents the largest organic carbon reservoir in the ocean and plays a crucial role in the global carbon cycle. DOC dynamics in coastal and continental margin systems are controlled by terrestrial inputs, in situ biological production, microbial transformation, and export to the open ocean (Ji, 2002; Hansell et al., 2014; Vantrepotte et al., 2014).

Although DOC does not directly contribute to vertical particulate carbon export, which is primarily driven by POC, in the water column, making it the largest exchangeable organic carbon pool in the ocean and a key component of both surface and deep-ocean carbon budgets (Druffel et al., 1992; Hansell and Carlson, 2014; Barrón and Duarte, 2015).

- **CDOM**

CDOM is a major contributor to light absorption in coastal and inland waters (Stedmon et al., 2000; Valerio et al., 2018). It consists of complex mixtures of aliphatic and aromatic compounds derived from the degradation of terrestrial and aquatic organic matter (Kirk, 1994). CDOM strongly influences underwater light availability and primary production and is commonly used as an optical proxy for non-optically measured carbon pools, including DOC,

as well as for processes related to carbon cycling and air-sea CO_2 exchange (Valerio et al., 2018).

Although Chl-a, SPM, organic carbon pools, and CDOM constitute key descriptors of coastal water quality, their consistent observation and interpretation in coastal environments remain challenging. In optically complex waters, the strong co-variability and partial decoupling among these constituents complicate their retrieval from satellite observations and limit the direct applicability of algorithms developed for open-ocean conditions. Moreover, existing studies often focus on individual variables or restricted regions, providing limited insight into the coupled variability of biogeochemical pools and their long-term evolution at broader spatial scales. In regions such as the Brazilian coastal zone, where terrestrial inputs, hydrodynamic forcing, and anthropogenic pressures vary markedly along the margin, there remains a need for integrated, satellite-based assessments that jointly address multiple biogeochemical descriptors using approaches adapted to coastal optical complexity. Such assessments are essential to improve the understanding of coastal carbon dynamics and water quality variability over seasonal to decadal time scales.

1.3. Time series analysis of ocean color observations for assessing coastal ecosystem variability and change

Time series analysis of satellite ocean color observations has become a fundamental approach for investigating the temporal dynamics of marine ecosystems in both coastal and open-ocean environments. The availability of long-term satellite records enables the assessment of ecosystem variability across multiple temporal scales and provides a unique opportunity to detect ecosystem responses to environmental forcing, including climate variability and anthropogenic pressures (Behrenfeld et al., 2005; Henson et al., 2010, 2018; Gregg et al., 2017; Dutkiewicz et al., 2019; Capotondi et al., 2024).

Detecting climate-driven signals from ocean color time series generally requires long observational records, typically on the order of several decades, to separate low-frequency trends from natural variability, particularly in the open ocean (Henson et al., 2010; Dutkiewicz et al., 2019). Recent studies have shown, however, that climate-driven signals can emerge earlier in ocean color reflectance. Using a 20-year MODIS-Aqua time series, Cael et al. (2023) demonstrated that statistically significant trends in remote-sensing reflectance $R_{rs}(\lambda)$ can be detected after approximately two decades over a large fraction of the global ocean. In coastal environments, ecosystem responses to environmental forcing are often faster due to strong land-

sea interactions and shorter biogeochemical adjustment times. While this increased sensitivity may facilitate earlier manifestations of change, it also enhances short-term variability, making the interpretation of long-term signals more challenging and highlighting the need for robust analytical frameworks adapted to coastal conditions.

A key objective of ocean color time series analysis is the detection and quantification of changes across different temporal scales, including long-term changes, in key biogeochemical variables such as Chl-a, SPM, and organic carbon pools. Trend analysis represents one of the approaches used to characterize variability at long time scales and provides direct information on whether these variables increase or decrease over time, on the rate of change, and on the statistical significance of observed variations, thereby offering insights into ecosystem trajectories under changing environmental conditions (Mélin et al., 2017; Loisel et al., 2017; Brito et al., 2020). Such analyses form one basis for linking observed variability to underlying climatic or anthropogenic drivers.

However, interpreting trends in ocean color time series is particularly challenging in coastal and shelf environments. These regions are characterized by strong seasonal cycles, high short-term variability, episodic events (e.g. river floods, storms, phytoplankton blooms), and irregular data availability related to cloud cover, acquisition geometry, and sensor limitations (Pahlevan et al., 2016; Alvera-Azcárate et al., 2025). As a result, simple parametric approaches may be inadequate, and robust analytical frameworks are required to reliably distinguish long-term changes from natural variability and observational noise.

In coastal environments, ecosystem responses to environmental forcing can take different temporal forms, including gradual changes, abrupt events, and regime shifts, depending on the nature and intensity of the driving mechanisms. Gradual changes typically reflect long-term trends associated with persistent forcings, such as progressive warming, sustained increases in nutrient inputs from agriculture, or long-term land-use change, leading for instance to slow increases in Chl-a or POC concentrations over decadal scales (Mélin et al., 2017; Brito et al., 2020). Abrupt events, in contrast, correspond to short-lived but intense perturbations, such as extreme river discharge, storms, or anomalous rainfall, which can cause sharp, transient increases in turbidity or phytoplankton biomass in coastal waters (Pahlevan et al., 2016; Alvera-Azcárate et al., 2025). Beyond these responses, regime shifts involve rapid transitions between distinct ecosystem states that persist over time and are often associated with threshold behavior, resulting from cumulative climatic forcing, circulation changes, or sustained anthropogenic pressures such as eutrophication or river regulation (Vantrepotte and Mélin, 2011; Racault et al., 2017).

In this context, multi-scale analysis of ocean color time series plays a central role. The decomposition of observed signals into seasonal, interannual (trend-cycle), and irregular components (Figure 1.11) allows the separation of recurring seasonal patterns from low-frequency variability and long-term change (Pezzulli et al., 2005; Dagum, 2010). This decomposition facilitates the interpretation of trend shape and timing and provides a framework for linking biogeochemical variability to environmental forcing mechanisms. As illustrated by the Census X-11 application in Figure 1.12, separating monotonic trends from significant interannual modulations helps reveal spatially coherent patterns of change that may be consistent with gradual shifts, event-driven perturbations, or more abrupt transitions in ecosystem functioning, depending on the regional context and forcing history (Vantrepotte and Mélin, 2011).

However, although the Census X-11 approach is particularly effective for separating seasonal and interannual components in strongly seasonal environmental datasets, its performance may be reduced in systems characterized by complex non-stationary variability, abrupt regime shifts, or multi-year cyclic oscillations that do not follow regular seasonal patterns (Dagum, 2010; Wang et al., 2020). In such situations, part of the low-frequency variability may be distributed between the trend-cycle and irregular components, potentially complicating the interpretation of long-term changes. Nevertheless, the method remains highly suitable for coastal ocean color applications due to its robustness to noisy datasets and strong seasonal signals.

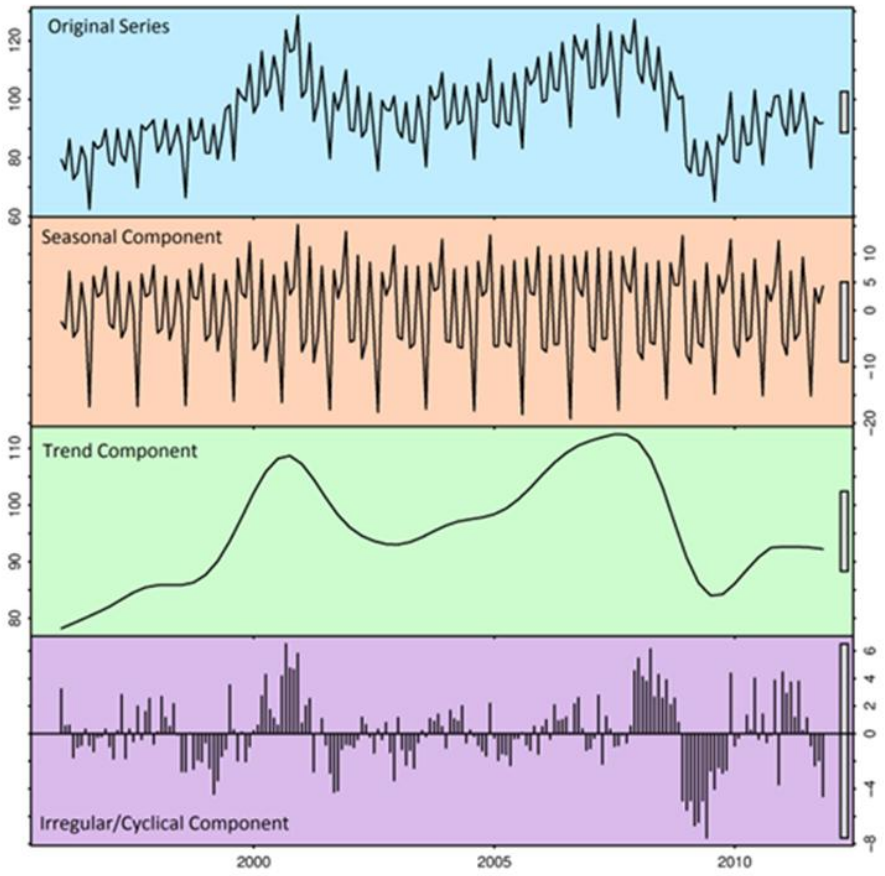

Figure 1.11. Time series decomposition illustrating the separation of an observed signal into seasonal, interannual (trend - cycle), and irregular components.

Complementary to decomposition approaches, trend detection methods are widely used to formally assess the direction, magnitude, and significance of long-term changes in ocean color time series. Non-parametric techniques have become standard in environmental applications due to their robustness to non-normal distributions, missing data, and outliers, which are common features of satellite datasets (Hirsch et al.,1982; Vantrepotte and Mélin, 2011; Wang et al., 2020). Together, decomposition and trend analysis provide a comprehensive framework for characterizing coastal ecosystem dynamics, from seasonal variability to persistent long-term change.

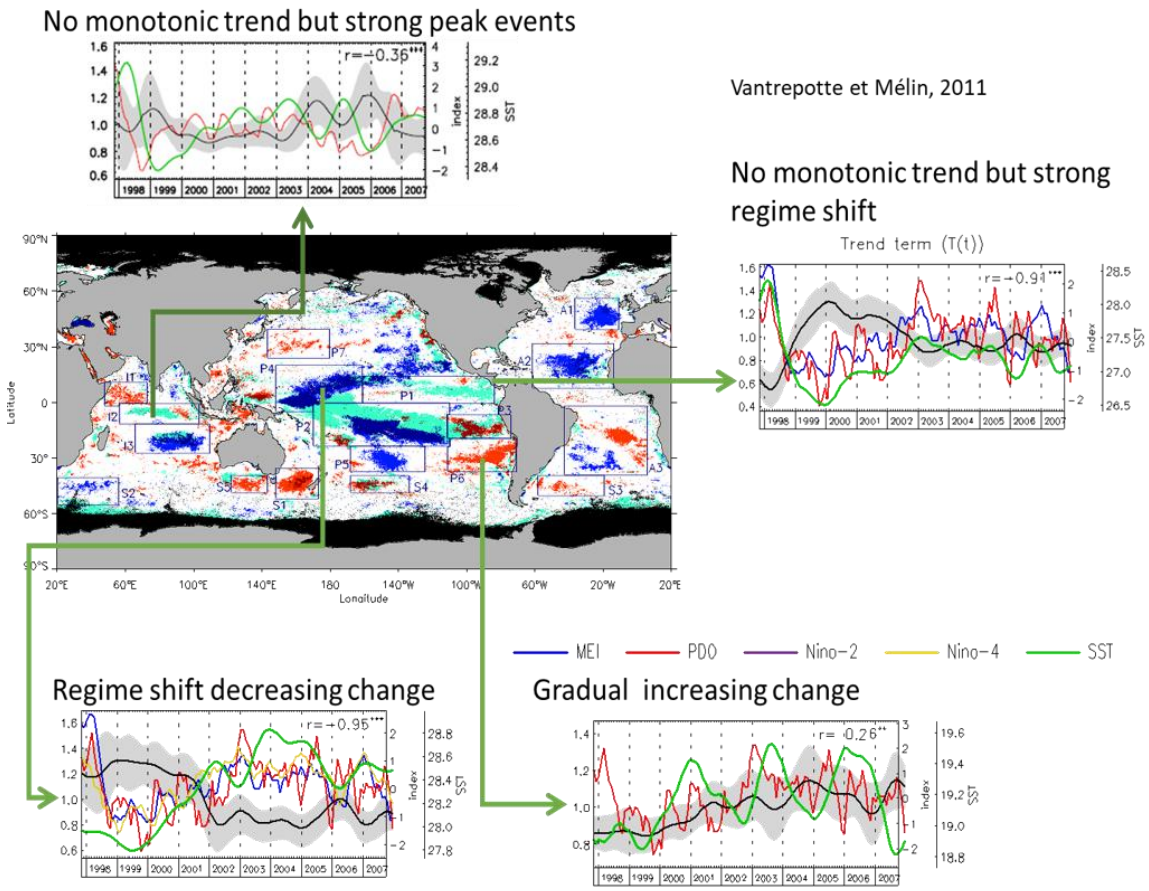

Figure 1.12. Illustration of an initial application of the Census X-11 method to detect the impact of climatic modulations on interannual variations of SeaWiFS Chl-a over the period 1997-2007 (Vantrepotte and Mélin, 2011). Blue areas indicate the presence of negative monotonic trends, red areas indicate positive monotonic trends, while green pixels denote the presence of significant interannual modulations (X-11 T(t) component).

The relevance of such approaches is particularly high in coastal regions, where strong land-sea interactions, intense human pressures, and climate variability interact to shape biogeochemical dynamics. In the Brazilian coastal zone, the combination of pronounced spatial heterogeneity, optically complex waters, and uneven in situ data coverage makes satellite-based time series analysis a critical tool for assessing ecosystem variability and detecting long-term changes at regional to national scales. Robust trend detection and multi-scale analysis are therefore essential to improve the understanding of coastal ecosystem responses to environmental change and to support monitoring and management efforts along the Brazilian continental margin.

In practice, the analysis of ocean color time series relies on a combination of complementary approaches to characterize variability across temporal scales and to detect long-term changes. Decomposition methods, such as the Census X-11 procedure, are commonly used to separate seasonal, interannual (trend - cycle), and irregular components (Shiskin, Young and Musgrave, 1965; Pezzulli, Stephenson and Hannachi, 2005; Vantrepotte and Mélin, 2009),

while non-parametric trend detection techniques, including the seasonal Mann-Kendall test and Sen's slope estimator, provide robust estimates of trend direction and magnitude (Sen, 1968; Hirsch, Slack and Smith, 1982; Vantrepotte and Mélin, 2011). These methods are particularly well suited to satellite ocean color data, which are affected by missing values, non-Gaussian distributions, and strong seasonality (Mélin, 2016; Wang et al., 2020). The methodological framework adopted in this study is described in detail in Chapter 2.

Beyond the characterization of temporal variability, a major challenge in coastal ocean color time series analysis is to disentangle the relative contributions of climate variability and anthropogenic forcing to observed biogeochemical changes. Statistical and machine-learning approaches have increasingly been used to address this issue by explicitly modeling non-linear relationships between ocean color variables and multiple environmental drivers. Methods such as generalized additive models (GAMs) allow the quantification of smooth, non-linear responses to climatic and hydrological variables, while ensemble techniques such as random forests provide flexible frameworks to assess variable importance and rank the relative influence of different forcings, including river discharge, precipitation, sea surface temperature, and land-use indicators (De'ath and Fabricius, 2000; Breiman, 2001; Wood, 2017; Hengl et al., 2018). When combined with long-term satellite time series, these approaches offer powerful tools to move beyond trend detection and toward a more causal understanding of coastal ecosystem responses to interacting climatic and anthropogenic pressures.

To date, no systematic study has comprehensively assessed recent changes in coastal water quality along the Brazilian coast by fully exploiting long-term ocean color archives using multi-scale time series analysis and statistical attribution techniques. In the Brazilian coastal zone, the application of such integrative time series approaches therefore remains relatively limited despite the strong exposure of coastal ecosystems to both climate variability and rapidly intensifying human pressures. Large river systems, extensive agricultural expansion, dam construction, and coastal urbanization generate complex and spatially heterogeneous forcings, while long-term in situ biogeochemical observations remain sparse and unevenly distributed. As a result, satellite-based multi-scale time series analysis, combined with statistical attribution methods, represents a critical avenue for advancing the assessment of coastal ecosystem change in Brazil. Expanding these approaches at regional to national scales is essential to improve the detection of long-term trends, to quantify the relative impact of climate and land-based drivers, and to provide a scientific basis for coastal monitoring and management strategies along the Brazilian continental margin (Mélin et al., 2017; Sathyendranath et al., 2019).

1.4. Conclusion

This chapter has provided a comprehensive overview of the physical, optical, and biogeochemical complexity of Brazilian coastal waters, as well as the current state of satellite ocean color observations and time-series analysis approaches applied to coastal environments. The Brazilian coastal zone stands out as one of the most heterogeneous coastal systems worldwide, shaped by strong latitudinal gradients, diverse hydrodynamic regimes, large riverine inputs, and increasing anthropogenic pressures. This complexity poses major challenges for the accurate retrieval and interpretation of satellite-derived biogeochemical variables.

Despite the availability of multi-decadal ocean color archives and the growing number of regional and global studies, significant gaps remain in the assessment of long-term biogeochemical variability along the Brazilian coast. Existing studies are often limited to specific regions, short time periods, or individual variables, and frequently rely on global algorithms or multi-sensor merged products whose performance in optically complex coastal waters is not systematically evaluated. In particular, the strong optical heterogeneity of Brazilian waters limits the direct applicability of standard open-ocean algorithms and introduces uncertainties in long-term trend analyses. Moreover, few studies explicitly combine multiple biogeochemical descriptors with robust time-series decomposition methods to disentangle seasonal variability from long-term change at regional to national scales.

Within this context, this PhD addresses several of these limitations by developing and applying satellite-based methodologies specifically adapted to Brazilian coastal waters. Retrieval algorithms for SPM (Chapter 3) and POC (Chapter 2) were developed using an OWT-based framework, allowing the inversion schemes to be tailored to the diversity of optical conditions encountered along the coast. In parallel, Chl-a, DOC, and CDOM were estimated using existing ocean color algorithms selected and adapted for optically complex coastal environments. This combination of newly developed and adapted approaches enables a consistent characterization of coastal biogeochemical variability while explicitly accounting for spatial heterogeneity.

MODIS observations constitute the core satellite dataset of this work, providing a consistent basis for algorithm development and long-term analysis. A dedicated comparison between OC-CCI products at 1 km resolution and GlobColour products at 4 km resolution, using MODIS-based products as a reference (Chapter 2), allows an objective evaluation of the consistency and suitability of widely used multi-sensor merged datasets for coastal applications

in Brazil. This assessment highlights the need for caution when using merged products for trend detection in optically complex coastal waters.

Beyond product development, this chapter introduces the time-series analysis framework applied throughout the thesis. The combination of Census X-11 decomposition and the non-parametric Mann–Kendall test, applied to Chl-a, SPM, and POC time series (Chapter 2), provides a robust basis for separating seasonal, interannual, and long-term components. This approach proved effective in detecting significant trends and identifying several biogeochemical hotspots along the Brazilian coast.

Two contrasted examples are explored in the following chapters: a hotspot primarily influenced by industrialization and port infrastructure (Chapter 3), and a second hotspot associated with the impacts of deforestation and pasture expansion on coastal Chl-a and SPM dynamics (Chapter 4). Together, these case studies demonstrate how satellite ocean color time-series analysis can reveal spatially explicit signatures of anthropogenic pressures in Brazilian coastal waters.

Overall, this State of the Art highlights the need for regionally adapted satellite-based approaches to improve the monitoring of Brazilian coastal ecosystems. By integrating OWT-based retrieval algorithms, robust time-series decomposition methods, and a critical evaluation of existing datasets, this PhD contributes to filling key methodological and observational gaps and provides a framework for future large-scale and long-term assessments of coastal biogeochemical change in Brazil.

CHAPTER 2: BRAZILIAN COASTAL WATERS DATASET DEVELOPMENT AND GENERAL SPATIOTEMPORAL DYNAMICS

2.1. Introduction

This PhD work is conducted within the framework of the Franco-Brazilian COCOBRAZ project (ANR, PRCI, FAPESP), which includes among its main objectives the development of an innovative, coherent, and accessible observational framework for Brazilian coastal waters. The project addresses a critical limitation in coastal research in Brazil: the scarcity and fragmentation of in situ observations, both spatially and temporally, which constrain the characterization of biogeochemical variability along the country's extensive and highly dynamic coastline.

To address this limitation, COCOBRAZ relies on the combined use of in situ measurements and long-term satellite observations. In situ data provide essential information at local and process scales, while satellite observations ensure continuous spatial coverage and long-term temporal consistency. Together, these complementary data sources enable the analysis of coastal biogeochemical variability at regional to national scales (Groom et al., 2019).

Within this context, an initial step of this PhD work was the assembly of a consistent observational framework integrating available in situ data with the complete MODIS-Aqua 1-km archive over Brazilian coastal waters. This framework supports the investigation of large-scale spatial patterns, long-term variability, and changes in key biogeochemical variables along the Brazilian coast.

Building on this observational basis, this chapter provides a general overview of Brazilian coastal waters at the national scale. It introduces the data framework used in this thesis, describes the satellite-derived biogeochemical products and analysis methods, and examines the general spatiotemporal variability of Chl-a, SPM, and POC over the 2002-2022 period. Particular emphasis is placed on the identification of major coastal hotspots of change, which reflect the combined influence of natural processes and anthropogenic pressures and serve as a basis for the more detailed regional analyses developed in the following chapters.

2.2. COCOBRAZ database (2002-2022)

2.2.1. Description of the in situ database

The database compiles in situ data from numerous oceanographic missions conducted between 2000 and 2023 across different coastal regions (Table 2.1). This data varies in scope and instrumentation: some include only Chl-a, others provide POC, DOC, SPM… and a few also offer remote-sensing reflectance ($R_{rs}(\lambda)$), contributing to a heterogeneous yet complementary dataset.

Table 2.1. List of in situ oceanographic missions used in the COCOBRAZ compilation

Mission	Year	Source
Abracos	2015, 2017	Farias et al. (2015)
Abrolhos	2013, 2016	INPE collection
ACEx/SIMTECO	2012	Gonçalves-Araújo et al. (2015)
AMAZONMIX	2021	Arnaud et al. (2021)
AMBES-INVERNO	2013	Petrobras, INPE collection
Anacondas	2012	INPE collection
Araruama	2017-2018, 2021	Personal communication
CANANEIA (ECOS Project)	2013-2014, 2021-2023	Personal communication
Chlorophyll-North	2012	Personal communication
COSTANORTE	2017	USP collection
DEPROAS	2001-2002	Kampel (2003)
DEVRED	2003	Personal communication
Guanabara	2000-2020	Oliveira et al. (2016), Cotovicz et al. (2015), Cotovicz et al. (2018), INPE
Guyane	2009-2010, 2012, 2014-2017	Vantrepotte et al. (2012), LOG
ILHAS2	2017	USP collection
M-TECH	2018	USP collection
MARANHAO (ECOS Project)	2022	Personal communication
MARSEAL	2014	Kampel et al. (2019)
Nomad-ioffe	2001-2002	LOG
Oceano-Norte	2009	Santos (2013)
Paraiba do Sul River	2017-2018	Cotovicz et al. (2020)
Sanagu	2021-2022	Kutner et al. (2023)
SEPEITIBA-ILHAGRANDE	2021-2022	Miranda et al. (2024)
Saquarema	2019-2020	Erbas et al. (2021)
TARA	2010	LOG collection
Trans-Atlantico	2009	IOUSP, INPE collection
Ubatuba-Antares	2005-2018	INPE collection

The COCOBRAZ in situ dataset comprises 3646 sampling points distributed along the Brazilian coastal zone (Figure 2.1), spanning estuarine regions, river plumes, inner and outer shelf environments, and oceanic waters. Each record includes core metadata such as mission name, station number, date, time, latitude, and longitude, ensuring full traceability and reproducibility across the database.

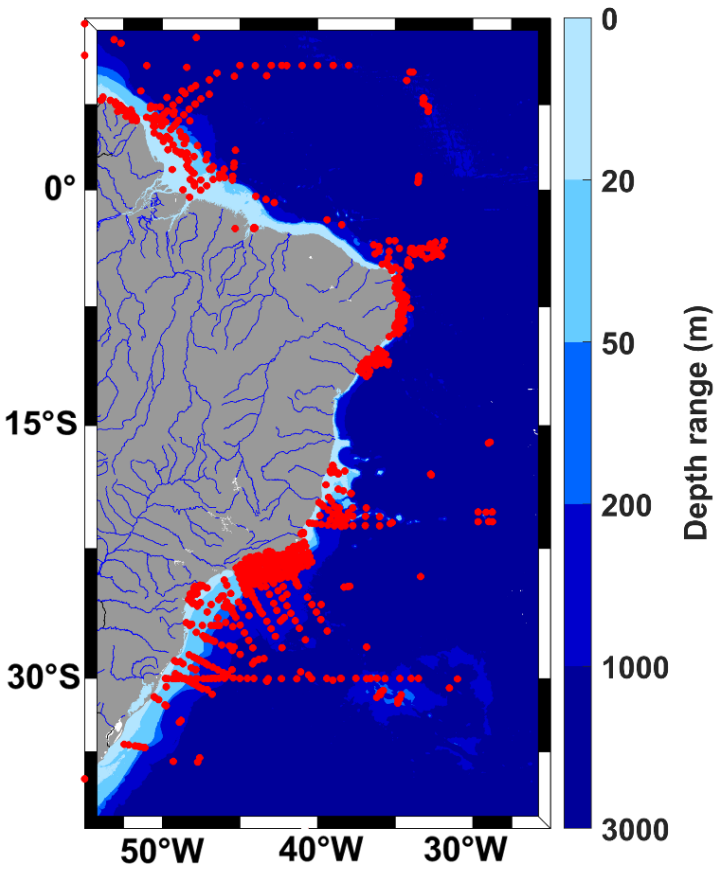

Figure 2.1. COCOBRAZ in situ data distribution along the Brazilian coastal waters. Red dots indicate the 3646 sampling stations for Chl-a, SPM, POC, DOC, and turbidity.

A wide range of biogeochemical variables was compiled between 2000 and 2023 (Figure 2.2). Among these variables, Chl-a is the most represented, with 3170 observations (Figure 2.2a). Chl-a values cover an extremely broad range of conditions, from oligotrophic offshore waters to highly productive and turbid environments, with concentrations varying between 0.02 µg. L^{-1} and 974.05 µg. L^{-1}, and an average of 39.3 µg. L^{-1}.

Measurements of POC are available for 353 stations (Figure 2.2b), ranging from 0.16 to 68.60 mg. L^{-1} (mean = 3.47 mg. L^{-1}), while DOC is documented 406 stations (Figure 2.2c), with values between 0.04 and 27.58 mg. L^{-1} (mean = 5.20 mg. L^{-1}). These carbon-related variables provide essential information on organic matter dynamics across contrasting coastal systems.

The dataset also includes measurements of SPM for 685 stations (Figure 2.2d), displaying strong spatial variability typical of Brazilian coastal waters. Concentrations range from 0.65 mg. L^{-1} in clear waters to extremely high values reaching 1945.34 mg. L^{-1} in highly turbid regions, with an average of 41.57 mg. L^{-1}. Similarly, turbidity (TUR) measurements are available for 176 stations (Figure 2.2e), with values spanning 0.1 to 258 NTU (mean = 24.76

NTU), diversely reflecting the influence of river discharge, sediment resuspension, and tidal mixing.

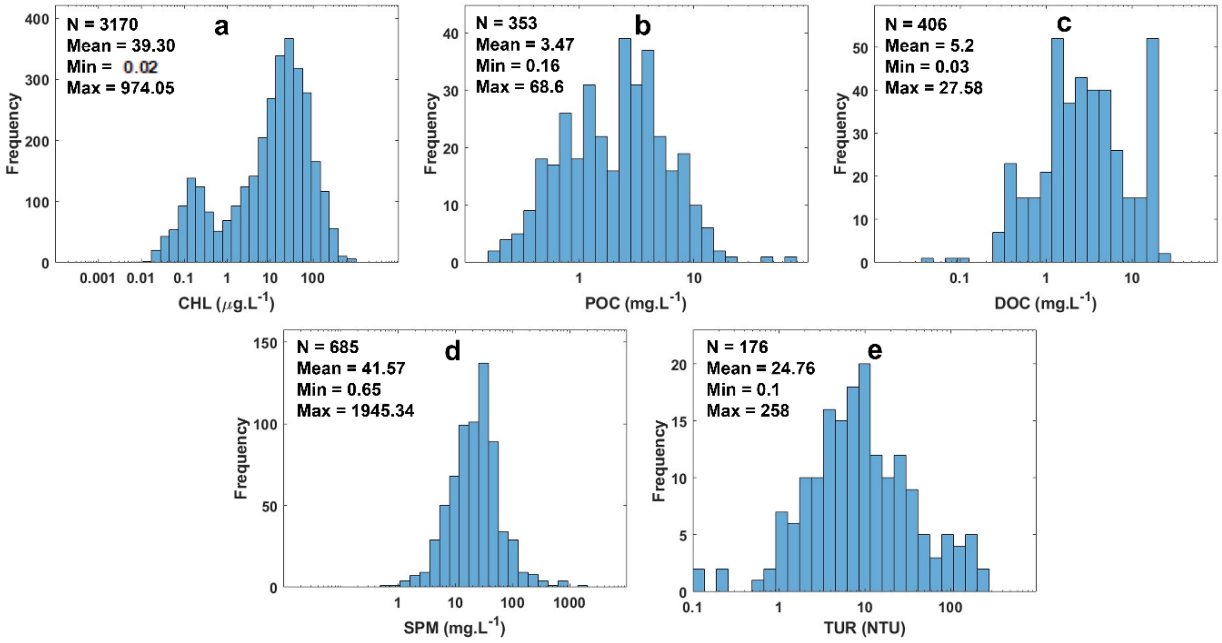

Figure 2.2. Frequency distribution histograms of biogeochemical variables included in the COCOBRAZ in situ dataset: (a) Chl-a, (b) POC, (c) DOC, (d) SPM, and (e) TUR.

A subset of missions also provides $R_{rs}(\lambda)$ measurements, available for 762 stations. Most reflectance samples correspond to stations where chlorophyll-a was also measured, offering valuable matchups for validating bio-optical algorithms and satellite-derived products. Such radiometric observations remain scarce along the Brazilian coast, making their inclusion particularly important for algorithm development.

Additional physical and optical descriptors, including temperature, salinity, a_{CDOM}, and absorption coefficients, are available for a smaller number of stations. Although these measurements are less frequent, they provide critical context for interpreting biogeochemical variability and characterizing water masses.

Overall, the in situ dataset assembled in COCOBRAZ offers a comprehensive and unprecedented overview of Brazilian coastal waters. Despite the heterogeneity of sampling strategies across missions, the resulting compilation fills a major observational gap for Brazil and provides a robust foundation for evaluating satellite retrievals and examining large-scale biogeochemical patterns along the coast.

Within the scope of this thesis, the in situ dataset is presented as part of the COCOBRAZ observational framework but is not used directly for algorithm development or validation within this work. These in situ observations were, however, used for the validation of the CONNECT

Chl-a algorithm (Cardoso Dos Santos, 2025; Tran et al., 2025) in the framework of associated studies. Beyond the analyses presented here, the COCOBRAZ in situ compilation is intended to be made available as part of a broader dataset for Brazilian coastal waters and to be further complemented and used in future studies. The analyses presented in this thesis primarily rely on long-term satellite-derived products, while the in situ data provide contextual support and ensure consistency with existing observational frameworks.

2.2.2. Description of the COCOBRAZ MODIS 1km satellite database

Although the in situ dataset remains spatially and temporally limited with respect to the extent and diversity of the Brazilian coastline, its compilation provided an essential observational basis for supporting the development and interpretation of the satellite-based dataset. Satellite observations therefore play a crucial role in extending this information across space and time, enabling the detection of changes, the characterization of coastal heterogeneity, and a more comprehensive understanding of biogeochemical dynamics along the coast. The combined use of satellite products and in situ measurements thus offers a robust framework for investigating coastal processes and supporting environmental management and policy development in Brazil.

2.2.2.1. MODIS-Aqua data (1 km) OC-SMART processing (2002-2022)

The satellite component of the COCOBRAZ database relies on a structured and consistent processing chain applied to the full MODIS-Aqua mission (2002-2022), as illustrated in Figure 2.3. This workflow transforms the raw satellite acquisitions into a homogeneous long-term archive suitable for coastal applications along the entire Brazilian shoreline. The process begins with the download of daily Level-1A (L1A) scenes (~3000 scenes/year), which provide complete coverage of the Brazilian coastal waters through multiple overlapping swaths. These files form the basis of the satellite dataset and initiate the sequence of preprocessing steps.

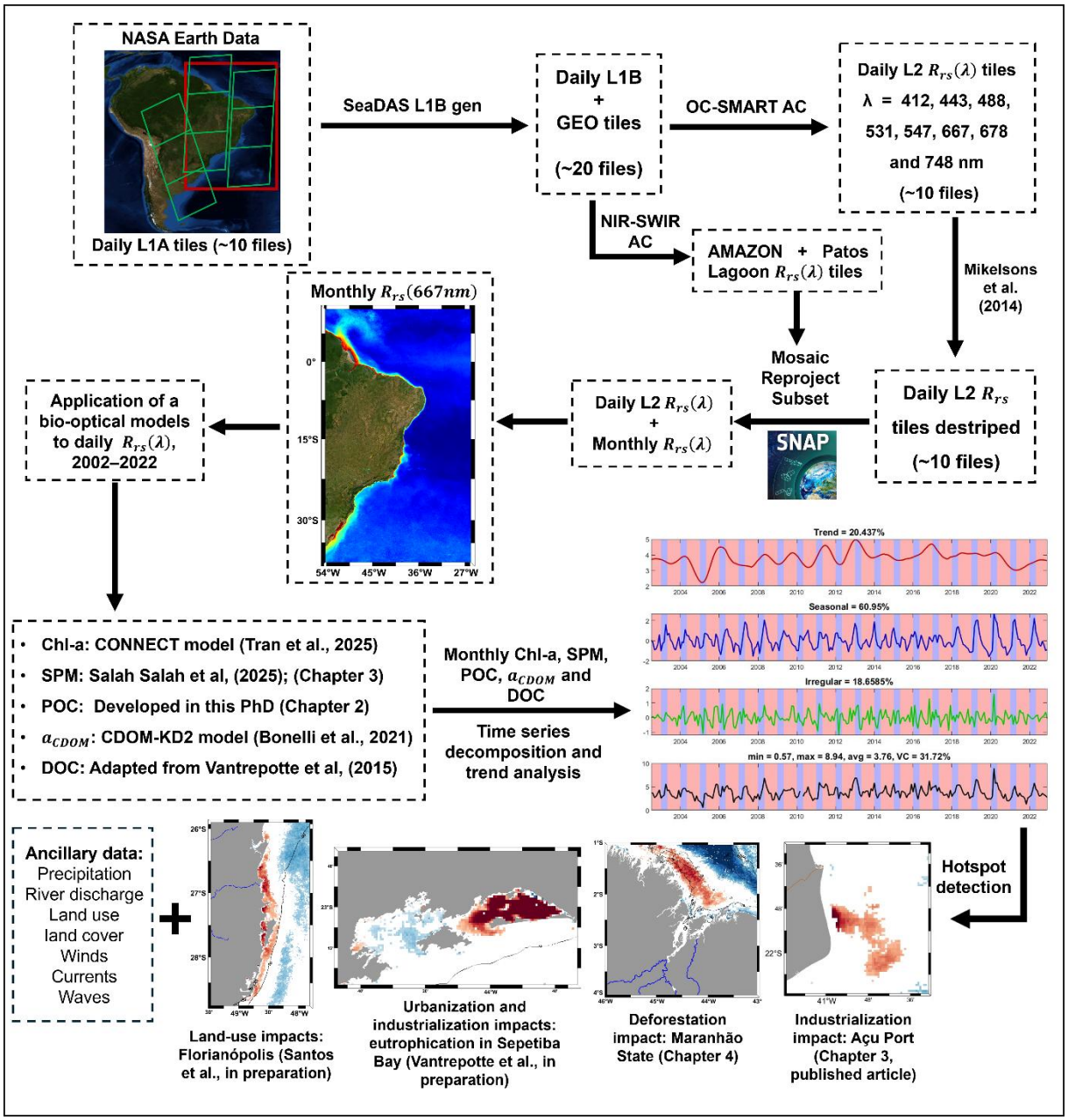

Figure 2.3. Processing chain of MODIS-Aqua dataset (2002-2022) by COCOBRAZ project for the Brazilian margin (adapted from Cardoso Dos Santos, 2025).

The processing chain begins with the conversion of Level-1A (L1A) raw scenes into Level-1B (L1B) and GEO formats using the *l1bgen_modis* tools in SeaDAS. These files are then corrected for atmospheric effects using OC-SMART (Fan et al., 2021) that combines multilayer neural networks with detailed radiative transfer simulations and has demonstrated strong performance in optically complex waters (Tran et al., 2025, IOCCG, 2025). The algorithm produces $R_{rs}(\lambda)$, for the MODIS spectral bands at 412, 443, 488, 531, 547, 667, 678, and 748 nm.

To improve the consistency of the daily products, the $R_{rs}(\lambda)$ tiles were destriped using a tool based on the method of Mikelsons et al., (2014), available from the NESDIS STAR Center.

This step reduces the characteristic striping noise often present in MODIS imagery and leads to cleaner and more reliable ocean-color fields. The destriped tiles were merged into daily mosaics, reprojected onto a regular WGS84 grid at ~1 km resolution, and cropped to the region spanning 25°W to 55°W and 11°N to 38°S. These operations were performed in SNAP (version 10).

The resulting data set consists in a coherent and continuous two-decade archive of daily $R_{\mathrm{rs}}(\lambda)$ maps for all Brazilian coastal waters (~7400 images). Monthly composites (246 images) were then generated using the geometric mean to balance the influence of extreme values and uneven sampling. This long-term dataset forms the backbone of the COCOBRAZ satellite archive, supporting the derivation of biogeochemical variables such as Chl-a, SPM, POC, DOC, and a_{cdom} (used algorithms are described in section 2.2.2.3). More broadly, it provides a consistent observational framework for understanding the spatial heterogeneity and temporal dynamics that characterize the Brazilian coastal ocean.

2.2.2.2. MODIS-Aqua (1km) NIR-SWIR processing (2002-2022)

While OC-SMART provides high-quality atmospheric correction for most Brazilian coastal waters, it faces important limitations in extremely turbid environments. MODIS does not include a 510 nm band, and several of its visible and NIR channels, particularly 551, 667, 678, 748 and 869 nm, are known to saturate in very high-turbidity waters (Zhang *et al.*, 2010; Doxaran *et al.*, 2014). In contrast, the 555 nm and 645 nm bands are less prone to saturation and are especially valuable for retrieving reliable reflectance in turbid regions. This characteristic became particularly relevant when developing SPM and POC algorithms, which depend on stable red wavelengths.

A practical challenge encountered during the MODIS processing was that OC-SMART does not provide access to the 645 nm red band. Saturation at 667 nm in highly turbid waters, including the Amazon River plume and the Patos Lagoon, results in a complete loss of information. In the Patos Lagoon, OC-SMART generally provides valid retrievals; however, under extreme turbidity, partial information loss may occur and can be effectively complemented using a NIR-SWIR atmospheric correction. OC-SMART relies on a neural network trained on full spectral inputs, so the saturation of even one band affects the retrieval of all other wavelengths. This explains why large parts of the Amazon plume appear missing or masked in OC-SMART outputs: the sensor saturates in the red and near-infrared channels, and the algorithm cannot generate valid $R_{\mathrm{rs}}(\lambda)$ values for the remaining spectrum.

To recover these missing regions and obtain non-saturated reflectance in environments where OC-SMART fails, an additional NIR-SWIR atmospheric correction was applied. This method retrieves the 645 nm band, which is crucial for turbid waters, and reconstructs valid $R_{\mathrm{rs}}(\lambda)$ fields even under extreme optical conditions. The correction was applied only to two specific subsets. One subset covers the Amazon River mouth in the north and the other covers the Patos Lagoon in the south. Both areas frequently experience strong saturation in standard MODIS bands and therefore cannot be properly represented using OC-SMART alone.

The NIR-SWIR processing followed the same general workflow as the main MODIS processing chain. Level-1 scenes were converted to Level-1B, atmospherically corrected using the NIR-SWIR method, mosaicked, reprojected onto a 1 km grid, and cropped to the boundaries of each regional subset. This process produced a complete daily reflectance record for both regions from 2002 to 2022, along with monthly composites generated using the same geometric-mean approach applied in the OC-SMART archive.

These additional NIR-SWIR products are included in the COCOBRAZ database as complementary information. They were not used directly in the analyses presented in this thesis, which focus on the MODIS archive processed with OC-SMART. However, their inclusion preserves critical observations from the most turbid Brazilian waters, where standard OC-SMART processing systematically loses data. This ensures that COCOBRAZ provides a complete and realistic representation of the full range of optical conditions along the Brazilian coast, from clear offshore environments to some of the most turbid estuarine systems in the world.

2.2.2.3. Bio-optical models applied on MODIS (OC-SMART)

Using the 20-year MODIS-Aqua R_{rs} archive processed with OC-SMART, a set of bio-optical models was applied to generate daily and monthly maps of Chl-a, SPM, POC, DOC and a_{CDOM} for all Brazilian coastal waters. These models are suitable for optically complex environments and have shown good performance when applied to MODIS reflectance. *Some of them were developed specifically as part of this work, including the new POC and SPM algorithms, while others are existing approaches adapted for coastal domain.*

The resulting products form a consistent biogeochemical archive covering the period from 2002 to 2022, offering a unique long-term perspective on the spatial and temporal variability of the main optical and biogeochemical components of Brazilian coastal waters. The inversion algorithms used for each of the products developed in the frame of COCOBRAZ data set developments are described below:

- **Chl-a bio-optical model**

To generate Chl-a concentrations for the full 2002-2022 MODIS-Aqua archive, the CONNECT model was applied (Tran et al., 2025). This neural-network approach is designed to operate across a broad range of optical water conditions, which makes it suitable for the strong gradients observed along the Brazilian coast. The model relies on two complementary neural-network structures: one trained on blue, green and red wavelengths for clearer waters, and another that incorporates the near-infrared region to account for turbid environments. The selection between the two configurations is guided by the optical water type assigned to each pixel, ensuring that the most appropriate network is used for the local conditions. Through this strategy, a consistent 20-year Chl-a dataset was generated for all Brazilian coastal waters, allowing large-scale and long-term patterns in phytoplankton biomass to be explored.

- **SPM bio-optical model**

To estimate SPM concentration, an OWT-based bio-optical models combination was specifically developed on the frame of this PhD. The method combines two complementary algorithms: the Siswanto model (Siswanto et al., 2011) for oligotrophic to mesotrophic conditions and the Han (Han et al., 2016) model for turbid to highly turbid waters. Both algorithms were recalibrated for MODIS-Aqua spectral bands, and their outputs were integrated using an OWT probability-weighted scheme to ensure robust retrievals across the full range of optical environments along the Brazilian coast. The detailed steps of the model development are presented in Chapter 3, Section 3.2, and the validation procedure is described in Chapter 3, Section 3.3.

- **$a_{\mathrm{CDOM}}(443)$ bio-optical model**

The absorption by colored dissolved organic matter (CDOM) at 443 nm, ($a_{\mathrm{CDOM}}(443)$), was estimated using the CDOM-KD2 bio-optical model. This approach is based on a semi-analytical formulation introduced by Loisel et al. (2014), which relates CDOM absorption to the vertical attenuation coefficient of downwelling irradiance, Kd. The CDOM-KD2 algorithm, as implemented for coastal applications by Bonelli et al. (2021), was applied to the MODIS-Aqua reflectance archive to retrieve $a_{\mathrm{CDOM}}(443)$ across all Brazilian coastal waters. This method provides estimates in regions influenced by strong CDOM gradients, such as river plumes and estuarine systems and enabled the generation of a continuous 20-year $a_{\mathrm{CDOM}}(443)$ dataset.

- **DOC bio-optical model**

DOC concentrations were estimated using the method proposed by Vantrepotte et al. (2015) and adapted by Montero et al., (2025) which links DOC to the $a_{\mathrm{CDOM}}(443)$. This relationship is widely used in coastal systems where a_{CDOM} is a strong optical indicator of DOC. After retrieving $a_{\mathrm{CDOM}}(443)$ from the MODIS reflectance data, the DOC model was applied directly to the entire MODIS-Aqua time series, producing a continuous 20-year dataset for Brazilian coastal waters.

- **POC bio-optical model**

A specific model has been developed for estimating POC in coastal waters in the frame of this PhD using existing formulations and OWTs.

In practice, an independent global in situ dataset was used for the development and validation of the POC retrieval algorithm, comprising paired measurements of $R_{\mathrm{rs}}(\lambda)$ and POC collected between 1997 and 2015 across a wide range of coastal environments (Tran et al., 2019). The subset used for in situ validation (Figure 2.4a) includes 440 samples, with POC concentrations ranging from 45.4 to 5743.5 mg.m^{-3} and a mean value of 666.1 mg.m^{-3}, reflecting highly turbid and optically complex waters.

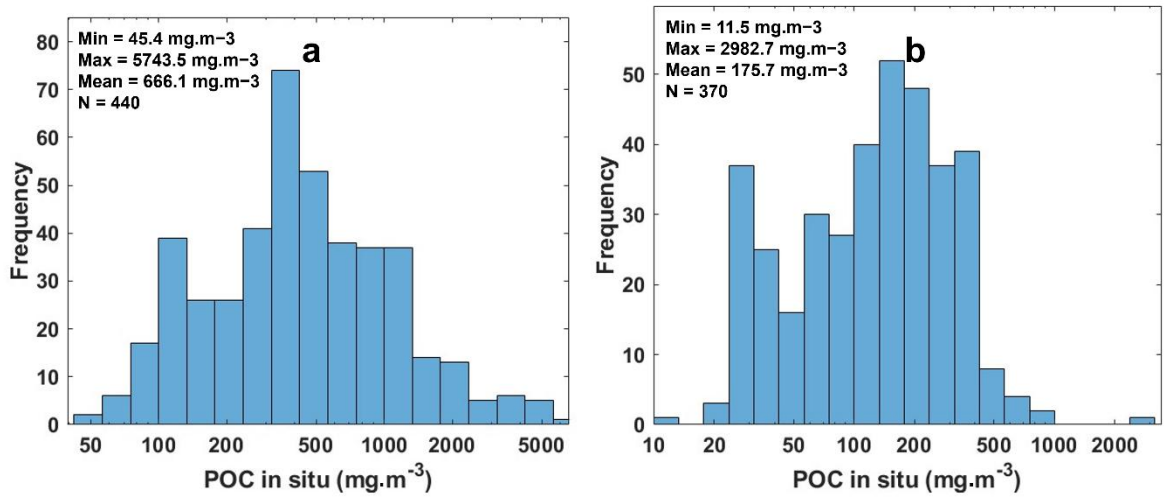

Figure 2.4. Distribution of the in situ dataset. (a) Frequency distribution histograms of in situ POC validation data, (b) Frequency distribution histograms of in situ POC matchup data.

A second subset was used for satellite matchup validation (Figure 2.4b), consisting of 370 in situ-satellite pairs generated following the classical matchup quality-control procedure described by

Werdell et al. (2009), including spatial homogeneity and temporal collocation criteria, after applying OC-SMART quality flags to MODIS $R_{rs}(\lambda)$ data. This matchup dataset spans POC values from 11.5 to 2982.7 mg.m^{-3}, with a mean concentration of 175.7 mg.m^{-3}. Together, these datasets cover broad biogeochemical gradients and provide a robust basis for assessing algorithm performance in coastal waters.

$R_{rs}(\lambda)$ spectra from this dataset were subsequently classified into five OWTs using unsupervised hierarchical clustering following Vantrepotte et al. (2012) and Mélin and Vantrepotte (2015). The Ward (1963) method was applied for its robustness in identifying optically coherent groups (Ferreira and Hitchcock, 2009). The resulting OWTs represent distinct water masses, from clear to highly turbid (Figure 2.5).

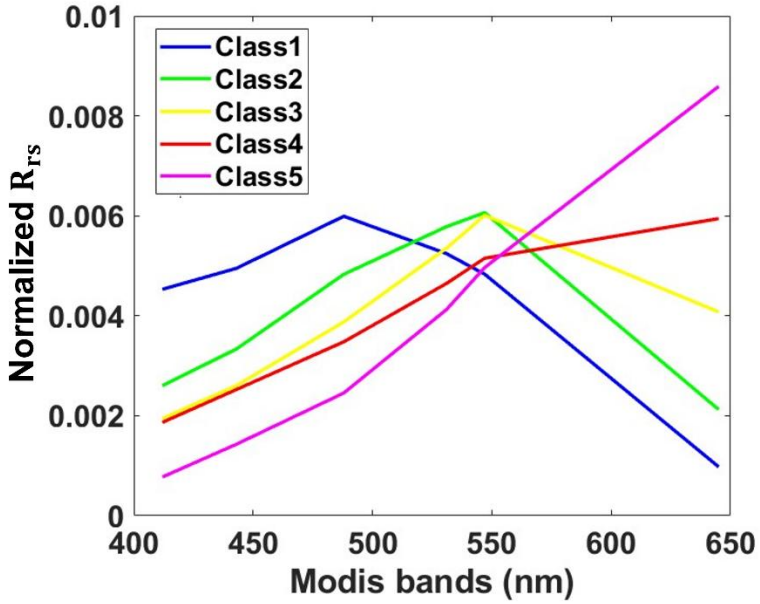

Figure 2.5. Optical water type classification. Average standardized reflectance spectra corresponding to the five OWTs defined from the in situ dataset (N = 440) according to Tran et al. (Tran *et al.*, 2023).

For POC estimation, the algorithms proposed by Le et al. (2017) and Tran et al. (2019) were selected based on their demonstrated performance in turbid coastal environments, particularly in French Guiana (Tran, 2023). An evaluation across the five OWTs showed that the Tran et al. (2019) algorithm provides more accurate estimates in clear to moderately turbid waters (OWTs 1 to 3), whereas the Le et al. (2017) algorithm performs better under highly turbid conditions (OWTs 4 and 5).

Both algorithms were therefore recalibrated and adapted to the MODIS OC-SMART spectral configuration and to the OWT-based framework. The coefficients of the Tran et al. (2019) algorithm were recalculated using data associated with OWTs 1-3, while the Le et al. (2017) algorithm was recalibrated using data corresponding to OWTs 4 and 5.

The adapted Tran et al. (2019) formulation (R^2 = 0.49, N = 363) for MODIS OC-SMART (POC_{Tran}) is expressed as:

$$\boldsymbol{X = log10\ \frac{R_{rs}667}{R_{rs}488}} \quad \textbf{(2.1)}$$

$$\boldsymbol{log10(POC_{Tran}) = aX + b} \quad \textbf{(2.2)}$$

with $a = 0.75$ and $b = 2.81$, yielding:

$$\boldsymbol{POC_{Tran} = 10^{0.75X+2.81}} \quad \textbf{(2.3)}$$

The adapted the Le et al. (2017) algorithm (R^2 = 0.51, N = 74) for MODIS OC-SMART (POC_{Le}) is defined as:

$$\boldsymbol{log_{10}(POC_{Le}) = a_0 + a_1X_1 + a_2X_2 + a_3X_3 + a_4X_4} \quad \textbf{(2.4)}$$

where $a_0 = 3.47$, $a_1 = -107.85$, $a_2 = 707.46$, $a_3 = -617.38$ and $a_4 = 50.91$, and $X_1 = R_{rs}(488)$, $X_2 = R_{rs}(531)$, $X_3 = R_{rs}(551)$ and $X_4 = R_{rs}(667)$

$$\boldsymbol{POC_{Le} = 10^{3.47-107.85R_{rs}(488)+707.46R_{rs}(531)-617.38R_{rs}(551)+50.91R_{rs}(667)}} \quad \textbf{(2.5)}$$

The final POC estimate is obtained by combining the two models using the same probability-weighted approach applied to the SPM algorithm in Chapter 3, based on OWT membership probabilities described in Section 3.2.2.2:

$$\boldsymbol{POC = \frac{W_1POC_{Tran} + W_2POC_{Le}}{W_1 + W_2}} \quad \textbf{(2.6)}$$

where $W_1 = p_{OWT_1} + p_{OWT_2} + p_{OWT_3}$, and $W_2 = p_{OWT_4} + p_{OWT_5}$, with $p(\mathrm{OWT}_i)$ representing the membership probability of each pixel to OWT_i, computed following the method described in Section 3.2.2.2 (Chapter 3). The combined model was subsequently validated using both in situ and satellite-derived $R_{rs}(\lambda)$data.

Figure 2.6 illustrates the validation performance of the combined POC retrieval model based on Le et al. (2017) and Tran et al. (2019), using both in situ observations (Figure 2.6a) and OC-SMART satellite-derived reflectance data (Figure 2.6b). For the in situ validation (Figure 2.6a), the combined model shows a strong agreement between estimated and measured POC concentrations (R^2 = 0.65, slope = 0.69; N = 440), with low uncertainty metrics (RMSD = 0.24, MAPD = 6.52%). The dispersion of points across OWTs highlights improved performance in highly turbid waters (OWTs 4 and 5), confirming the complementarity of the two algorithms under elevated particulate conditions.

The satellite matchup validation using OC-SMART reflectance data (Figure 2.6b) yields comparable, and slightly improved, performance statistics (R^2 = 0.73, slope = 0.69; N = 370), with similarly low errors (RMSD = 0.21, MAPD = 6.33%). Despite the additional sources of uncertainty associated with atmospheric correction and satellite-derived $R_{rs}(\lambda)$, the combined model maintains stable accuracy. It should be noted that matchup data remain limited for the most optically complex water classes (4-5).

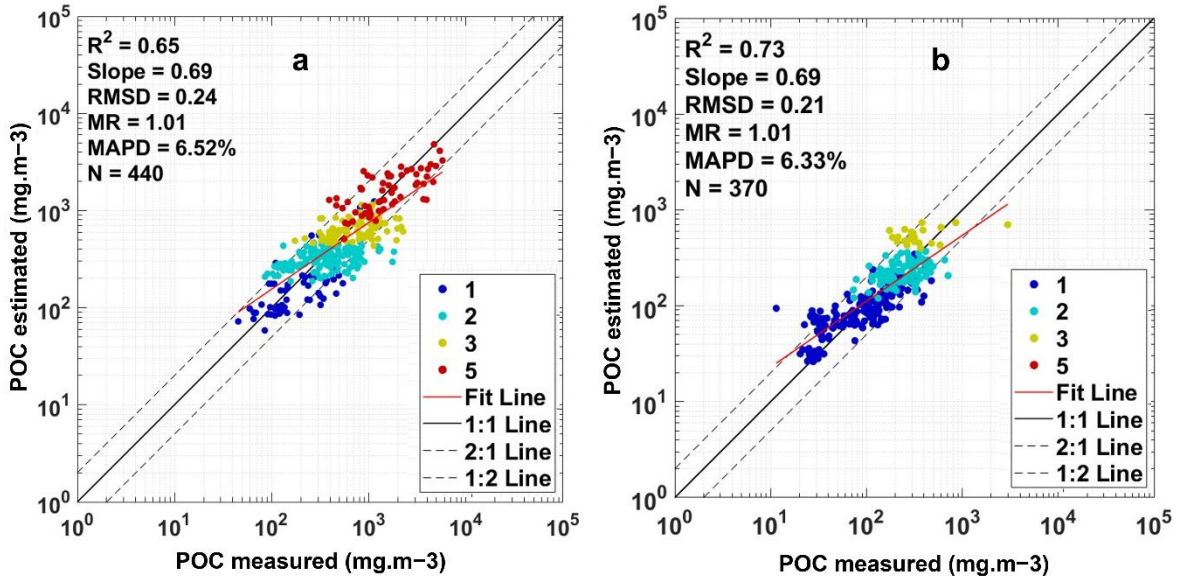

Figure 2.6. Validation of the new inversion algorithm for estimating POC from $R_{rs}(\lambda)$: Tran et al. (2019) and Le et al. (2017) combination based on OWTs (OWTs 1-3 and 4-5, respectively). (a) in situ validation, (b) satellite matchup validation (MODIS - OC-SMART).

Overall, these results demonstrate the robustness of the combined POC retrieval strategy in optically complex coastal waters. The validated model was subsequently applied to 20 years of MODIS-Aqua OC-SMART data (2002-2022) to investigate long-term variability and spatial patterns of POC in Brazilian coastal environments.

This model will be integrated into ongoing work by Loisel et al. (in preparation), in which a third algorithm will be added to the present combination to estimate POC in clear waters using the Loisel *et al.* (2002) model, leading to a complete OWT-based POC retrieval scheme spanning conditions from very clear to highly turbid waters.

The statistical indicators used to validate this algorithm are described in detail in Section 3.2.4.

2.2.2.4. Ancillary data:

The complete COCOBRAZ database also includes wind fields, surface currents, and precipitation datasets. These environmental variables provide essential context for interpreting the observed biogeochemical variability and changes in coastal water quality and are presented

in detail in Chapters 3 and 4. Wind and current information are used to characterize circulation patterns, mixing processes, and transport pathways, while precipitation data supports the analysis of freshwater inputs and land-sea exchanges. All datasets cover the full study area and are provided as monthly products spanning the 2002-2022 period, ensuring consistency with the satellite-derived biogeochemical time series. At the regional scale, additional ancillary data such as river discharge, land use and land cover, and wave parameters were used to investigate anthropogenic impacts and environmental variability, as described in Chapters 3 and 4.

2.2.2.5. Time series decomposition and trend analysis of the COCOBRAZ dataset

Time series of Chl-a, SPM, POC, DOC, and $a_{\mathrm{CDOM}}(443)$, derived from MODIS-Aqua observations and complemented by ancillary environmental data from the COCOBRAZ database, were analyzed to investigate the spatio-temporal variability and long-term evolution of Brazilian coastal waters over the 2002-2022 period.

- **Time series representation and decomposition framework**

Time series analysis is widely used to investigate temporal variability in ocean color remote sensing (OCRS) data and other environmental observations. A time series $Y(t)$ can be expressed as the sum of additive components representing distinct temporal signals:

$$\boldsymbol{Y(t) = T(t) + S(t) + R(t)} \quad \textbf{(2.7)}$$

where $T(t)$ denotes the trend-cycle component, $S(t)$ the seasonal component, and $R(t)$ the residual or irregular variability (Pezzulli et al., 2005).

The trend-cycle term integrates both long-term changes and low-frequency oscillations. In this study, low-frequency oscillations are referred to as the interannual component, while the persistent monotonic increase or decrease over time is defined as the trend. The residual component includes short-term fluctuations and unexplained variability.

- **Time series decomposition using the Census X-11 method**

To separate seasonal, interannual, and irregular components, the Census X-11 decomposition method was applied to each monthly time series. X-11 is an extension of classical moving-average decomposition techniques, based on iterative filtering procedures combined with autoregressive integrated moving average (ARIMA) modeling (Dagum, 1983, 2010).

For monthly data ($m = 12$), classical decomposition estimates the interannual component using a centered moving average:

$$\widehat{T}_t = MA_{2\times12} = \frac{Y_{t-6} + 2Y_{t-5} + \cdots + 2Y_t + \cdots + 2Y_{t+5} + Y_{t+6}}{24} \quad (2.8)$$

However, such moving-average approaches cannot be applied at the boundaries of the time series and assume a stationary seasonal cycle. The X-11 method overcomes these limitations by:

- allowing gradual temporal changes in the seasonal component,
- estimating components over the full time series, including boundary periods,
- applying data transformations when necessary to stabilize variance.

These characteristics make X-11 particularly suitable for long-term environmental and climate-related datasets and for OCRS time series affected by irregular sampling and noise (Pezzulli et al., 2005; Vantrepotte and Mélin, 2011).

- **Trend detection using the Seasonal Mann-Kendall test**

To detect monotonic trends while accounting for strong seasonality, the Seasonal Mann-Kendall (sMK) test was applied to each variable. Unlike linear regression, the sMK test does not assume normality, homoscedasticity, or independence of residuals, making it well suited for environmental time series characterized by non-normal distributions, outliers, missing values, and irregular sampling (Mann, 1945; Hirsch et al., 1982; Hirsch and Slack, 1984).

In the sMK framework, the monthly time series is reorganized into a matrix with 12 columns (months) and n rows (years). For each month m, the Mann–Kendall statistic S_m is computed as:

$$S_m = \sum_{j=1}^{n-1} \sum_{i=j+1}^{n} sgn(Y_{i,m} - Y_{j,m}) \quad (2.9)$$

with the sign function defined as:

$$\mathbf{sgn}(Y_{i,m} - Y_{j,m}) = \begin{cases} +1, & \text{if } (Y_{i,m} - Y_{j,m}) > 0 \\ 0, & \text{if } (Y_{i,m} - Y_{j,m}) = 0 \\ -1, & \text{if } (Y_{i,m} - Y_{j,m}) < 0 \end{cases} \quad (2.10)$$

The monthly statistics are aggregated to obtain the global statistic:

$$S_k = \sum_{m=1}^{12} S_m \quad (2.11)$$

The variance of each monthly statistic is given by:

$$\mathbf{var}(S_m) = \frac{n(n-1)(2n+5)}{18} \tag{2.12}$$

and the variance of the global statistic is:

$$\mathbf{var}(S_k) = \sum_{m=1}^{12} \mathbf{var}\,(S_m) \tag{2.13}$$

The standardized test statistic is then computed as:

$$Z_{S_k} = \begin{cases} \dfrac{S_k - 1}{\sqrt{\mathbf{var}(S_k)}}, & \text{if } S_k > 0 \\ 0, & \text{if } S_k = 0 \\ \dfrac{S_k + 1}{\sqrt{\mathbf{var}(S_k)}}, & \text{if } S_k < 0 \end{cases} \tag{2.14}$$

The null hypothesis of no monotonic trend is rejected when $|\ Z_{S_k}\ | > |\ Z_{1-\alpha/2}\ |$, where α is the chosen significance level.

- **Trend magnitude estimation using Sen's slope**

When a significant trend is detected, its magnitude is estimated using Sen's slope estimator (Sen, 1968). This method computes slopes between all possible pairs of observations:

$$\beta = \mathbf{median}\left(\frac{Y_j - Y_i}{j - i}\right), \text{for } j > i \tag{2.15}$$

Sen's slope is robust to outliers and missing data and is therefore well adapted to OCRS and environmental time series (da Silva *et al.*, 2015). Positive values indicate increasing trends, while negative values indicate decreasing trends.

- **Analytical scope**

This combined decomposition and trend analysis framework enables the identification of spatial and temporal patterns, as well as hotspots of significant change along the Brazilian coastal zone. Particular attention is given to the spatio-temporal variability and long-term evolution of Chl-a, SPM, and POC, which are key indicators of coastal biogeochemical processes and human-induced pressures over the 2002-2022 period.

2.3. Brazilian Coastal ecosystems

2.3.1. MODIS aqua advantage and limitations

MODIS-Aqua observations at 1 km spatial resolution provide an effective tool for monitoring long-term variability in Brazilian coastal waters. Brazil hosts a wide range of coastal ecosystems, including bays, estuaries, and lagoons. The use of this medium-resolution sensor, processed with the OC-SMART atmospheric correction, enables the observation of many of these ecosystems, as illustrated in Figure 2.7.

Figure 2.7 shows an example of monthly R_{rs} at 667 nm, highlighting the diversity of coastal environments that can be identified using MODIS-Aqua at 1 km resolution. Although this spatial resolution does not allow observation inside rivers and inner estuaries, it enables the detection of river mouths and associated coastal plumes, as well as bays and lagoons.

Several bays are clearly identifiable (Figure 2.7), including Marajó Bay (Subset a), São Marcos Bay (Subset b), Todos os Santos Bay (Subset f), and the Guanabara and Sepetiba bays (Subset j). River mouths such as the Acaraú and Apodi rivers (Subset c), Rio Grande do Norte river (Subset d), the São Francisco, Sergipe, Vaza-Barris, Castro, and Real rivers (Subset e), and the Paraíba do Sul River (Subset h) are also detectable. In addition, several lagoons can be identified, including Feia Lagoon (Subset h), the Araruama and Saquarema lagoons (Subset i), Imaruí Lagoon (Subset l), and the Patos, Mirim and Mangueira lagoons (Subset m).

Overall, MODIS-Aqua at 1 km resolution provides a synoptic view of the Brazilian coastline, allowing the identification of both large coastal systems and smaller-scale features, such as the ria-type estuaries in Maranhão State (Subset b). Within this framework, more than 40 river mouths and estuaries, 17 bays, and 17 coastal lagoons were identified across the study area in the context of this thesis (Figure 2.8).

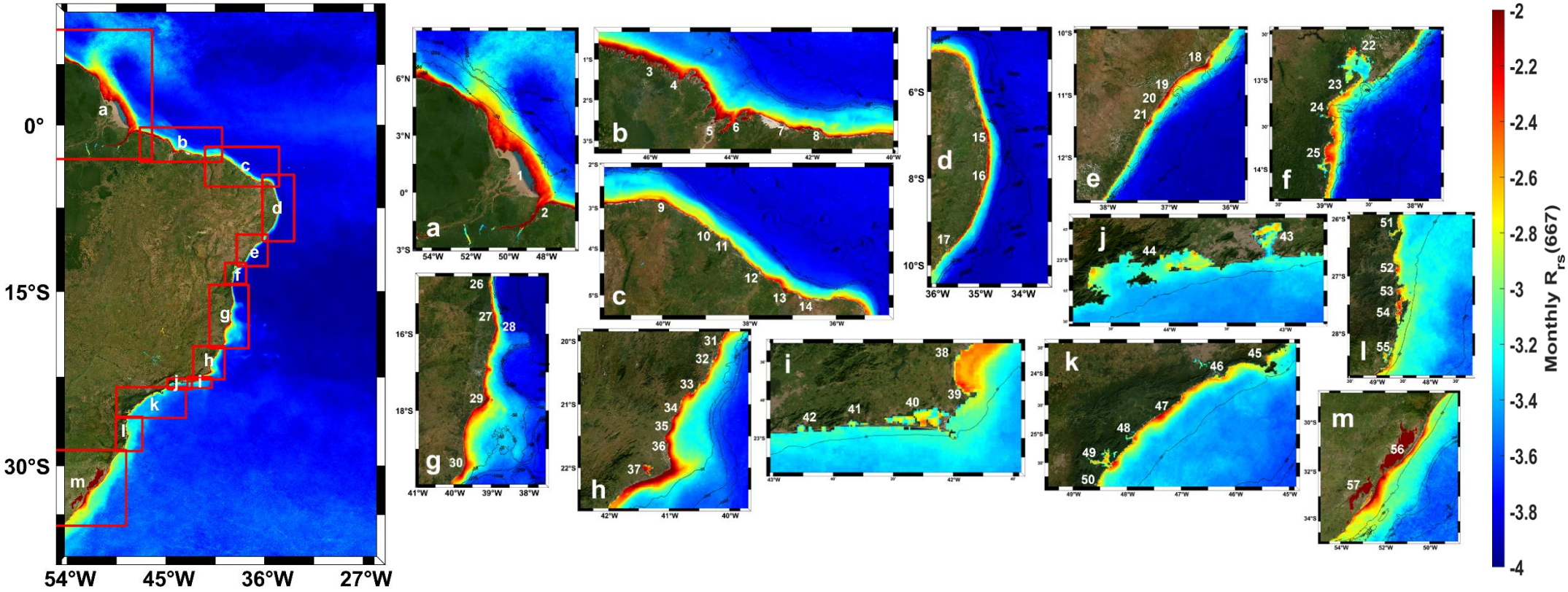

1. Amazon River; **2.** Marajó Bay; **3.** Gurupi River; **4.** Turiaçu Bay; **5.** São Marcos Bay; **6.** Arraial Bay; **7.** Preguiças River; **8.** Parnaíba River; **9.** Acaraú River; **10.** Curu River; **11.** Ceará River; **12.** Jaguaribe River; **13.** Apodi River; **14.** Conchas and Piranhas Rivers; **15.** Rio Grande do Norte River; **16.** Trachunhaém River; **17.** Manguaba and Mundaú Lagoons; **18.** São Francisco River; **19.** Sergipe River; **20.** Vaza-Barris River; **21.** Castro and Real Rivers; **22.** Todos os Santos Bay; **23.** Jaguaripe River; **24.** Das Almas River; **25.** Orojo River; **26.** Almada and Cachoeira Rivers; **27.** Salsa River; **28.** Jequitinhonha River; **29.** Caravelas Estuary; **30.** Doce River; **31.** Fundão River; **32**. Vitória Bay; **33.** Benevente River; **34.** Novo River; **35.** Itabapoana River; **36.** Paraíba do Sul River; **37.** Feia Lagoon; **38.** Das Ostras River; **39.** Una River; **40.** Araruama Lagoon; **41.** Saquarema Lagoon; **42.** Maricá Lagoon; **43.** Guanabara Bay; **44.** Sepetiba Bay; **45.** Caraguatatuba Bay; **46.** Santos Bay; **47.** Ribeira de Iguape River; **48.** Mar Pequeno; **49.** Paranaguá Bay; **50.** São João River; **51.** Babitonga Bay; **52.** Itajaí-Açu River; **53.** Metropolitan Bay; **54.** Bays of Santa Catarina Island; **55.** Imaruí Lagoon; **56.** Patos Lagoon; **57.** Mirim and Mangueira Lagoons.

Figure 2.7. Example of monthly MODIS-Aqua R_{rs} (667 nm) showing the diversity of Brazilian coastal ecosystems detectable at 1 km resolution.

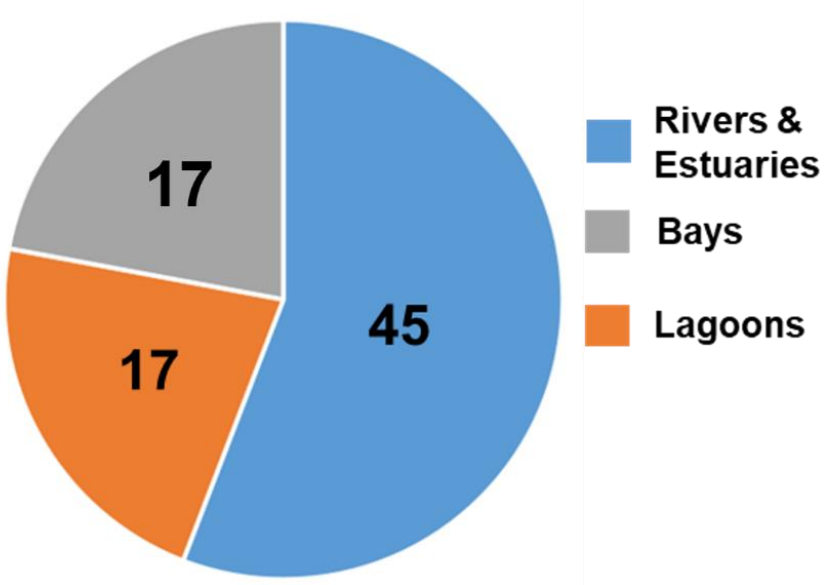

Figure 2.8. Distribution of identified coastal systems along the Brazilian coastline.

Despite its ability to capture a wide range of coastal systems, the 1 km spatial resolution of MODIS-Aqua imposes constraints on the observation of fine-scale processes within narrow estuaries and river channels (Doxaran et al., 2009). In these environments, the sensor footprint often exceeds the width of the water bodies, leading to partial land contamination, commonly referred to as adjacency effects, and to the absence of valid observations within inner estuarine and fluvial domains (Santer and Schmechtig, 2000; Beltrán-Abaunza et al., 2014). As a consequence, MODIS-Aqua primarily resolves the offshore expression of riverine inputs, such as river mouths and associated coastal plumes, rather than the internal estuarine gradients. This limitation is illustrated by the comparison shown in Figure 2.9, where the 300 m resolution of the Ocean and Land Colour Instrument (OLCI) reveals estuarine structures and nearshore gradients that remain unresolved at the MODIS spatial scale (Cazzaniga et al., 2019; Tilstone et al., 2021).

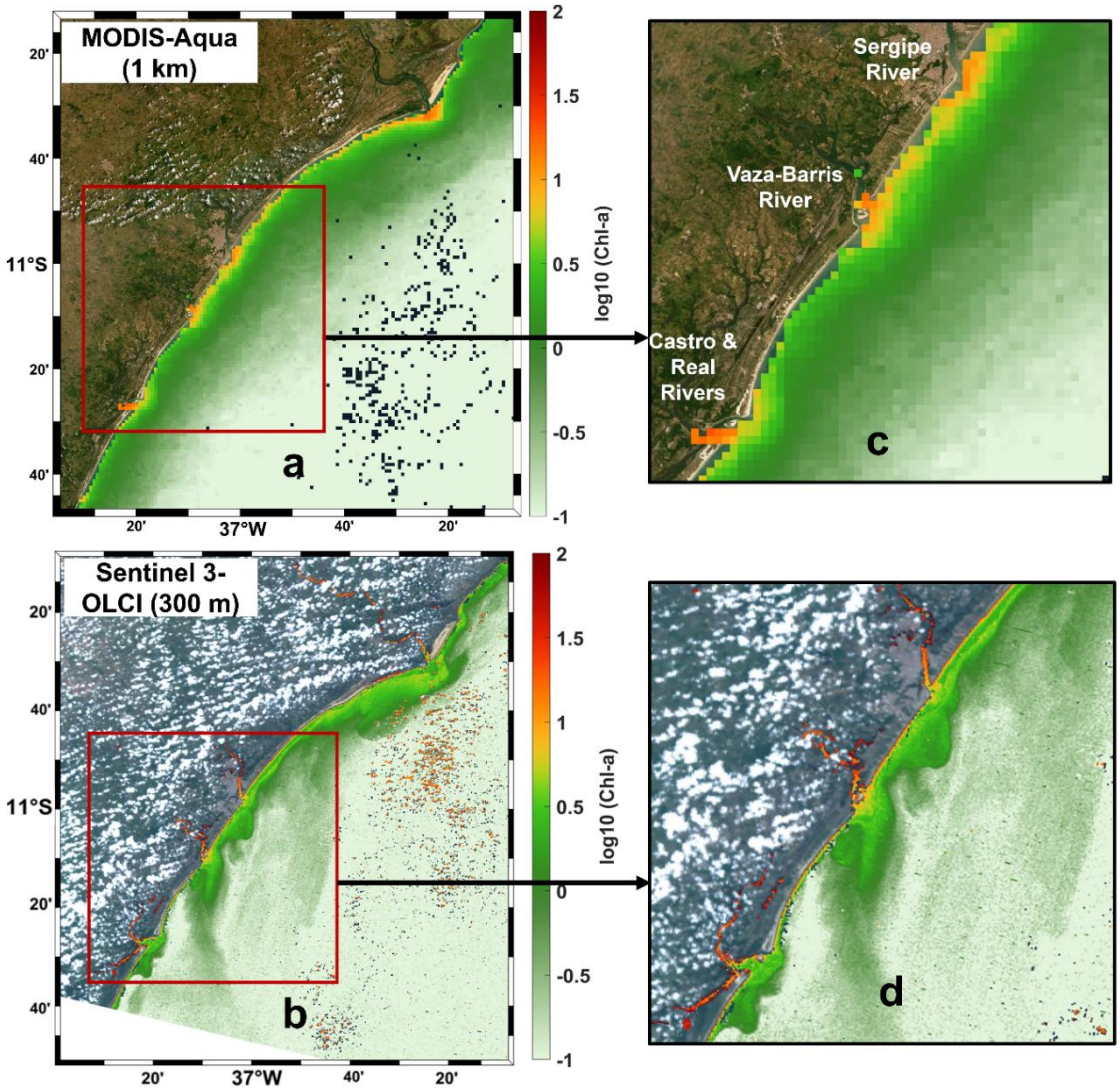

Figure 2.9. Effect of spatial resolution on coastal and estuarine chlorophyll-a patterns. (a) MODIS-Aqua (1 km). (b) Sentinel-3 OLCI (300 m). (c) MODIS-Aqua zoom over river mouths. (d) Corresponding Sentinel-3 OLCI zoom.

2.3.2. Comparison of satellite ocean-colour products in Brazilian coastal waters

2.3.2.1. Comparison based on red-band reflectance and coastal coverage

Figure 2.10 compares the spatial distribution of $R_{rs}(\lambda)$ in the red spectral domain derived from GlobColour (4 km), OC-CCI (1 km), and MODIS processed with OC-SMART (1 km) over the São Francisco River coastal region, together with a coastal-offshore transect extracted across the river plume. All three products show a consistent large-scale pattern, characterized by higher R_{rs} (λ) values in the nearshore zone and a progressive decrease offshore. This cross-shelf gradient reflects the strong influence of riverine discharge and suspended material in coastal waters, which increases backscattering and red-band reflectance (Ody et al., 2016; Simão et al., 2024).

In Figure 2.10a, the GlobColour product exhibits a broad and spatially smoothed band of elevated red-band R_{rs} along the coast. High reflectance values are not restricted to the immediate vicinity of the São Francisco River mouth but extend along large portions of the coastline, including areas influenced by adjacent river systems and general coastal turbidity. The offshore decrease in $R_{rs}(\lambda)$ is gradual, and the boundary between coastal and offshore waters appears diffuse. Fine-scale spatial variability associated with individual river plumes or localized coastal features is not resolved. This spatial smoothing is consistent with the coarse spatial resolution of GlobColour (4 km), which averages sub-pixel variability and attenuates sharp optical gradients in heterogeneous coastal environments (Bissett et al., 2004; Mouw et al., 2015).

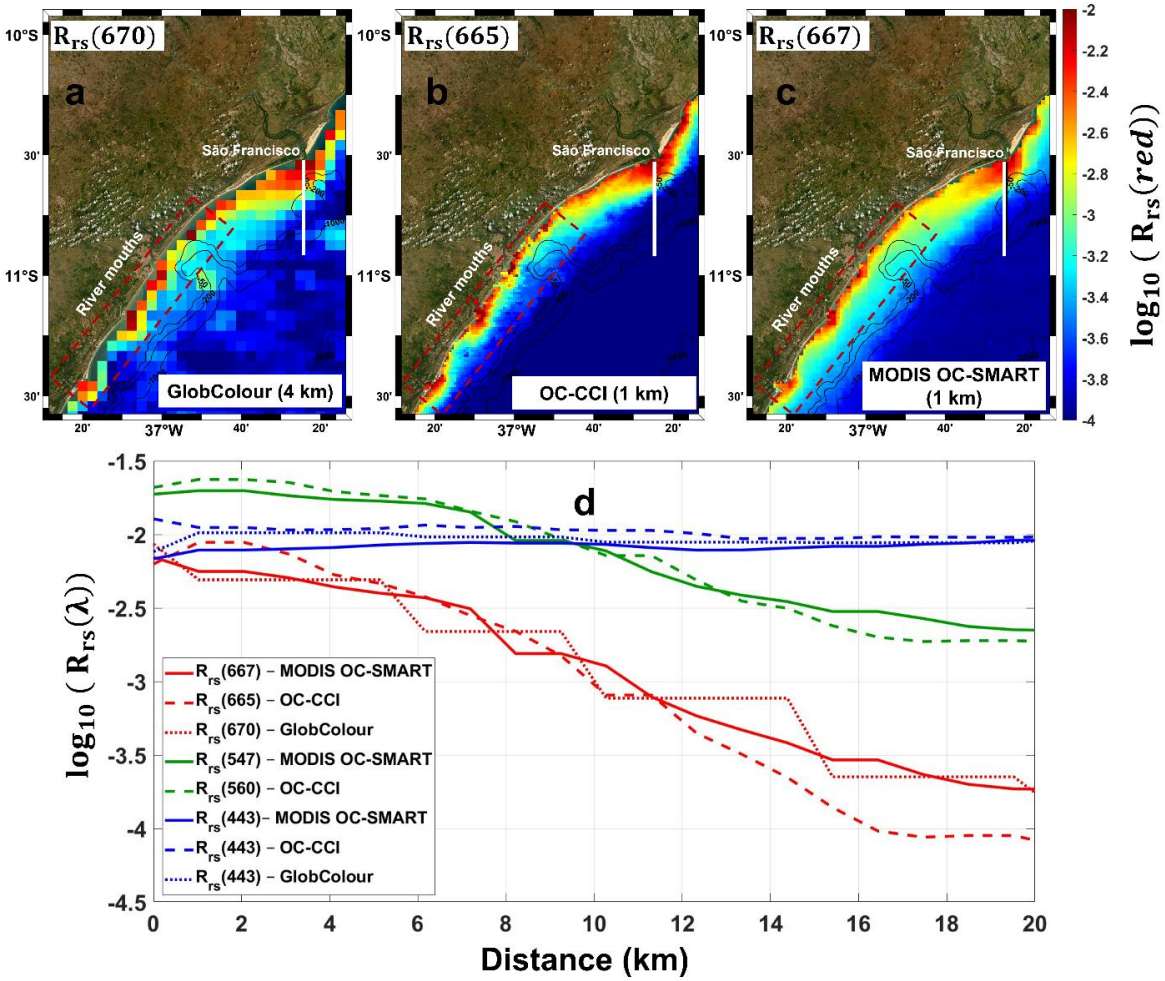

Figure 2.10. Spatial distribution and cross-shelf variability of R_{rs} (λ) in the São Francisco River coastal region derived from different satellite products. (a) R_{rs}(670 nm) from GlobColour (4 km). (b) R_{rs}(665 nm) from OC-CCI (1 km). (c) R_{rs}(667 nm) from MODIS OC-SMART (1 km). (d) Coastal-offshore transect of log R_{rs} (λ) in the blue, green, and red spectral bands extracted from Globcoulor, OC-CCI and MODIS OC-SMART along the transect shown in panels (a, b and c; White line).

Figures 2.10b and 2.10c show the same region as observed by OC-CCI and MODIS OC-SMART at 1 km resolution. In both products, the coastal band of elevated $R_{\mathrm{rs}}(\lambda)$ is narrower and more clearly constrained to the inner shelf compared to GlobColour. Individual coastal features, including the São Francisco River plume and signals associated with other nearby river mouths, are more distinctly expressed. The cross-shelf gradient is sharper, with a more abrupt transition between high nearshore $R_{\mathrm{rs}}(\lambda)$ and lower offshore values. Despite this overall consistency, clear differences are visible between the two 1 km products. The OC-CCI $R_{\mathrm{rs}}(\lambda)$ field appears more spatially heterogeneous, with stronger small-scale variability along the coast, while the MODIS OC-SMART product displays smoother spatial transitions and a more continuous coastal signal.

These differences are further highlighted by the coastal-offshore transect shown in Figure 10d, which is extracted along the white line indicated in Figures 2.10a-c. The transect is shown for the blue, green, and red spectral bands for OC-CCI and MODIS OC-SMART, while for GlobColour only the blue and red bands are included, as no green-band $R_{\mathrm{rs}}(\lambda)$ product is available for this dataset.

In all datasets and available bands, $R_{\mathrm{rs}}(\lambda)$ decreases offshore, confirming the strong nearshore influence of suspended material and optically complex waters. The blue band exhibits the weakest offshore gradient, remaining relatively stable across the transect, whereas the green and red bands show a more pronounced decrease with increasing distance from the coast. This spectral behavior is consistent with the higher sensitivity of longer wavelengths to particle backscattering in turbid coastal waters (Ruddick et al., 2006).

Along the transect, OC-CCI-derived $R_{\mathrm{rs}}(\lambda)$ displays stronger point-to-point variability in all available bands, particularly in the red and green wavelengths, resulting in a more irregular offshore evolution. In contrast, MODIS OC-SMART $R_{\mathrm{rs}}(\lambda)$ decreases more smoothly with distance, producing a more regular cross-shelf profile. The GlobColour transect follows the same overall offshore-decreasing trend but is characterized by a coarser spatial structure, consistent with its 4 km spatial resolution.

These differences are directly visible in Figure 2.10d and primarily reflect differences in processing strategies rather than spatial resolution alone, since OC-CCI and MODIS OC-SMART are both provided at 1 km resolution. The smoother behavior of MODIS OC-SMART suggests stronger spatial coherence in the retrieved $R_{\mathrm{rs}}(\lambda)$ fields, whereas OC-CCI and GlobColour preserve higher local variability along the transect.

Figure 2.11 extends the $R_{rs}(\lambda)$ comparison to embayed coastal environments. In Figure 11a, the GlobColour product shows limited capability to resolve the internal optical structure of the bays. The $R_{rs}(\lambda)$ field is dominated by large pixels that integrate mixed signals from shallow waters, land adjacency, and adjacent offshore areas, leading to a suppression of internal spatial gradients. In Figures 11b and 11c, the OC-CCI and MODIS OC-SMART products provide a more detailed representation of the bays, although missing pixels are still present in narrow or highly complex coastal zones in both datasets. Within the bays, MODIS OC-SMART maintains more spatial continuity in the $R_{rs}(\lambda)$ field, while OC-CCI shows a more fragmented pattern with higher small-scale variability.

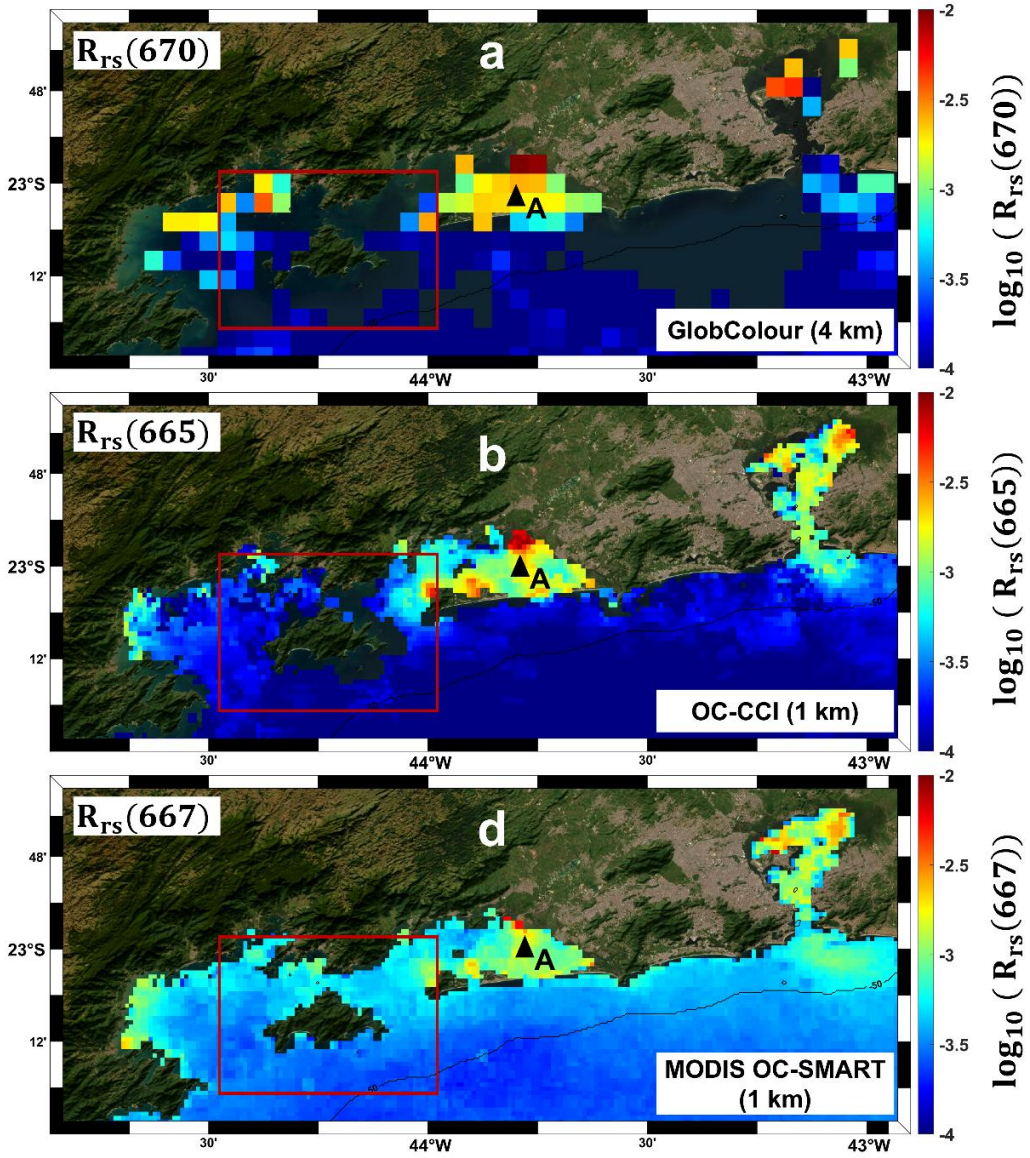

Figure 2.11. Comparison of red-band remote sensing reflectance ($R_{rs}(\lambda)$) in embayed coastal environments derived from GlobColour, OC-CCI, and MODIS OC-SMART. (a) R_{rs}(670 nm) from GlobColour (4 km). (b) R_{rs}(665 nm) from OC-CCI (1 km). (c) R_{rs}(667 nm) from MODIS OC-SMART (1 km).

Taken together, Figures 2.10 and 2.11 demonstrate that all three products capture the large-scale coastal-offshore $R_{rs}(\lambda)$ gradient associated with riverine influence and coastal turbidity. However, the representation of spatial variability strongly depends on both spatial resolution and processing strategy. The coarse resolution of GlobColour limits its ability to resolve individual river plumes and embayed environments, whereas the 1 km products better capture coastal heterogeneity. Differences between OC-CCI and MODIS OC-SMART, particularly in terms of spatial smoothness and variability, highlight the sensitivity of $R_{rs}(\lambda)$ retrievals to algorithmic choices and atmospheric correction approaches in optically complex coastal waters (IOCCG, 2010; Bui et al., 2022)

In addition to the regional comparison presented here, the overall consistency of the MODIS OC-SMART $R_{rs}(\lambda)$ fields is supported by independent global matchup analyses against in situ measurements. Using a large and globally distributed dataset, Tran et al. (2025) evaluated OC-SMART $R_{rs}(\lambda)$ retrievals against in situ observations across multiple visible and near-infrared wavelengths and reported good agreement between satellite-derived and measured reflectance. Their analysis shows that OC-SMART achieves comparable or slightly improved accuracy relative to the standard SeaDAS (l2gen) atmospheric correction, particularly in the visible spectral domain, while also reducing the occurrence of negative $R_{rs}(\lambda)$ values.

The scatterplots (Figure 2.12) presented by Tran et al. (2025) indicate that OC-SMART retrieves $R_{rs}(\lambda)$ with a robust overall performance at the global scale, with the best agreement observed in the green bands and decreasing performance toward the blue and near-infrared wavelengths. This behavior is consistent with earlier validation studies and reflects the increased sensitivity of atmospheric correction uncertainties at shorter and longer wavelengths. Although this global validation does not directly discriminate between OC-CCI and MODIS OC-SMART, it confirms that the OC-SMART atmospheric correction applied to MODIS data provides physically consistent and reliable $R_{rs}(\lambda)$ estimates, supporting its use in optically complex coastal environments such as the São Francisco River plume examined in this study.

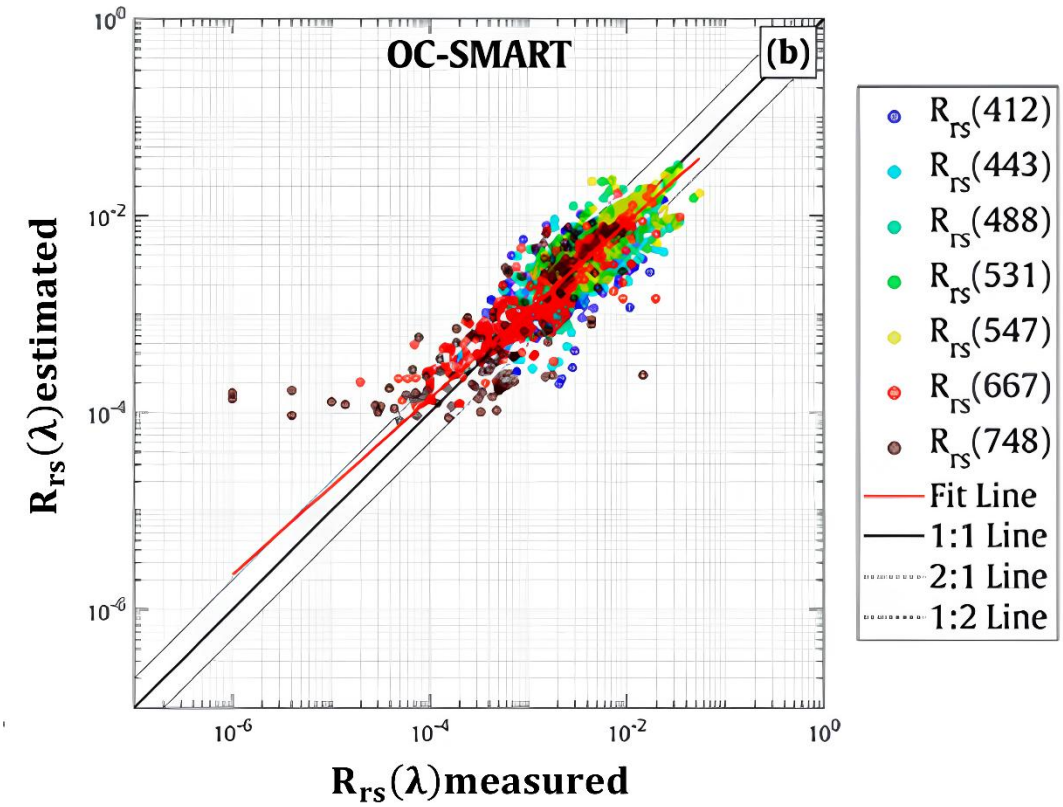

Figure 2.12. Global satellite-in situ matchups of retrieved R_{rs} (λ) with the OC-SMART atmospheric correction algorithm. Adapted from Tran et al. (2025).

2.3.2.2. Comparison based on Chl-a estimation in coastal waters

Figure 2.13 compares the spatial distribution of monthly satellite-derived Chl-a concentrations from the three products over the embayed coastal region encompassing Sepetiba Bay and Guanabara Bay. Chl-a from GlobColour (4 km) and OC-CCI (1 km) is obtained from merged multi-sensor datasets that apply standard open-ocean Chl-a algorithms (e.g., OCx and CI/OCI; O'Reilly et al., 1998; Hu et al., 2012), primarily optimized for Case-1 waters, which may result in larger uncertainties in optically complex coastal environments (IOCCG, 2000; Mélin et al., 2017). In contrast, the MODIS Chl-a product used here is estimated with the CONNECT algorithm (Tran et al., 2025) adapted for coastal waters and validated for MODIS processed with OC-SMART atmospheric correction.

Despite differences in spatial resolution and processing strategies, the three products depict a coherent large-scale pattern, with elevated Chl-a concentrations within the bays and in nearshore waters, and lower values offshore. This spatial organization is consistent with the strong influence of confined circulation, riverine inputs, and anthropogenic nutrient sources in these semi-enclosed systems, which promote phytoplankton biomass accumulation in coastal waters (Cloern, 2001; Paerl, 2006).

The GlobColour product (Figure 2.13a) shows broad areas of elevated Chl-a within both Sepetiba and Guanabara bays, but with a markedly smoothed spatial structure. Internal gradients within the bays are weakly resolved, and transitions between high-Chl-a coastal waters and lower offshore concentrations appear diffuse. This reflects the combined effect of the coarse spatial resolution (4 km) and spatial averaging, which limits the ability to represent sharp gradients and small-scale variability typical of embayed coastal environments (Mouw et al., 2015).

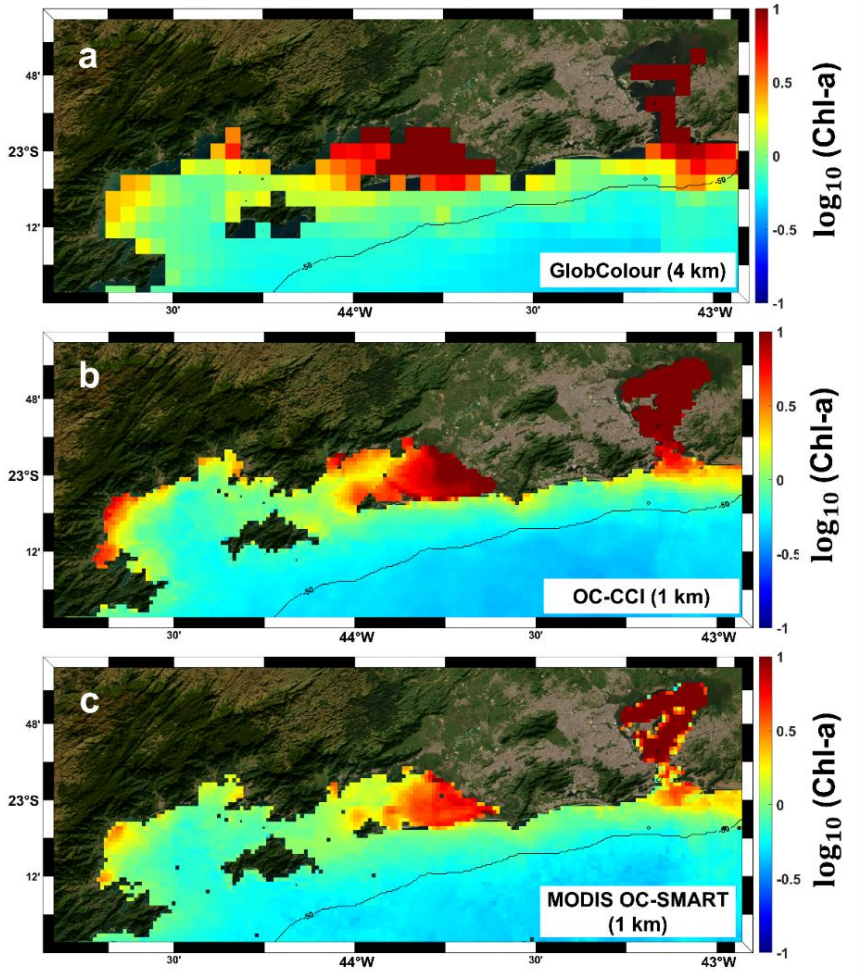

Figure 2.13. Spatial distribution of satellite-derived Chl-a in Sepetiba and Guanabara bays from different products. (a) Monthly Chl-a from GlobColour (4 km). (b) Monthly Chl-a from OC-CCI (1 km). (c) Monthly Chl-a from MODIS processed with OC-SMART and estimated using the CONNECT model (1 km).

The OC-CCI product (Figure 2.13b), provided at 1 km resolution, resolves the embayments more clearly and captures stronger coastal-offshore gradients compared to GlobColour. Elevated Chl-a concentrations are more distinctly confined within the bays and along the inner coastal zone. However, spatial heterogeneity within the bays appears patchy, and localized discontinuities are visible, particularly in narrow or semi-enclosed areas. These features indicate increased sensitivity to complex optical conditions and land-water adjacency effects

that are characteristic of highly turbid and optically complex coastal waters (Zibordi et al., 2009; Odermatt et al., 2012).

The MODIS OC-SMART product using the CONNECT algorithm (Figure 2.13c) exhibits a spatially coherent Chl-a distribution across both bays and the adjacent coastal zone. Gradients within Sepetiba and Guanabara bays are smoother and more continuous, and the transition from inner-bay waters to the open shelf is more consistently represented. While fine-scale variability remains limited by the 1 km resolution, the MODIS-based product preserves the main spatial contrasts observed in the embayed environments without the strong smoothing evident in GlobColour.

Figure 2.14 presents the spatial distribution of relative differences between OC-CCI and MODIS OC-SMART (CONNECT) chlorophyll-a products in Sepetiba Bay and Guanabara Bay. The relative difference map reveals strong and spatially coherent contrasts, with deviations locally exceeding ± 50% in coastal waters.

Two distinct regimes are clearly identified. In Sepetiba Bay (point A), OC-CCI exhibits predominantly positive relative differences, indicating systematically higher Chl-a concentrations compared to MODIS OC-SMART. In contrast, in Guanabara Bay (point B), negative relative differences dominate, reflecting substantially lower OC-CCI values relative to MODIS OC-SMART. These spatial patterns are not randomly distributed but are strongly structured and confined to optically complex coastal environments, suggesting systematic differences in the response of the two products rather than noise or sampling effects.

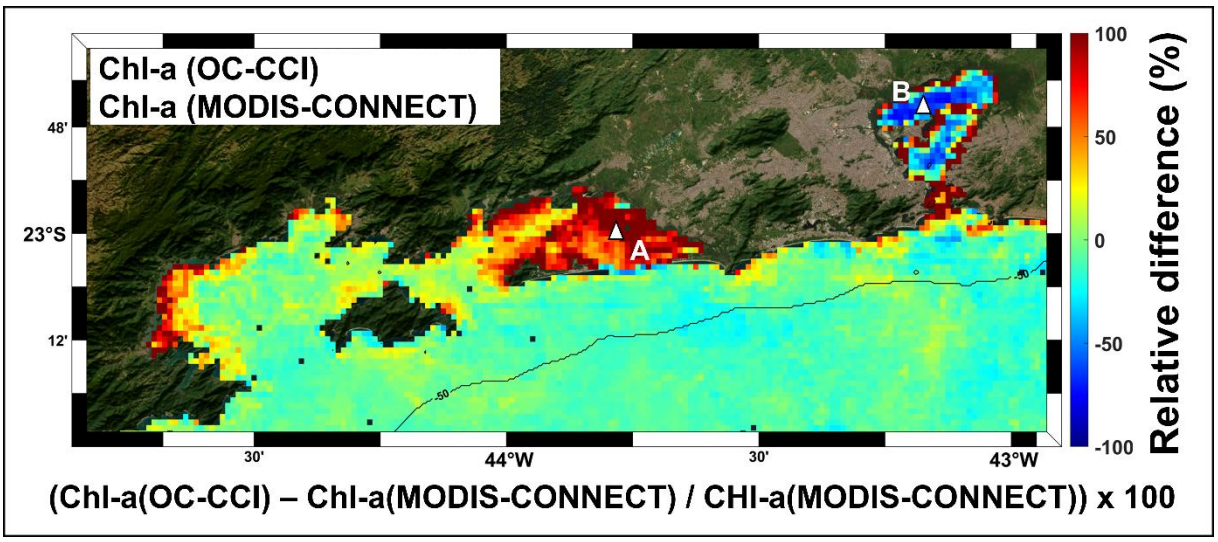

Figure 2.14. Spatial distribution of relative differences (%) between OC-CCI and MODIS OC-SMART (CONNECT) Chl-a in optically complex coastal waters.

OC-CCI Chl-a estimates are primarily derived from blue-to-green band-ratio algorithms (OCx family), which rely on the assumption that variations in water-leaving radiance in the blue and green spectral regions are predominantly driven by phytoplankton absorption (O'Reilly et al., 1998; Sathyendranath et al., 2019). In optically complex coastal waters, however, elevated concentrations of SPM and CDOM strongly affect the blue and green reflectances, violating this assumption. As a result, OCx-type algorithms may exhibit systematic biases, including overestimation or reduced sensitivity, depending on the dominant optical regime (Garnesson *et al.*, 2019).

Figure 2.15 presents the long-term (2002-2022) Chl-a variability extracted at two representative locations, points A and B, selected based on the spatial patterns observed in Figure 14. Panels (a) and (b) show the Chl-a time series from GlobColour (4 km), OC-CCI (1 km), and MODIS OC-SMART (1 km), while panels (c) and (d) display the corresponding scatter plots comparing OC-CCI and MODIS OC-SMART.

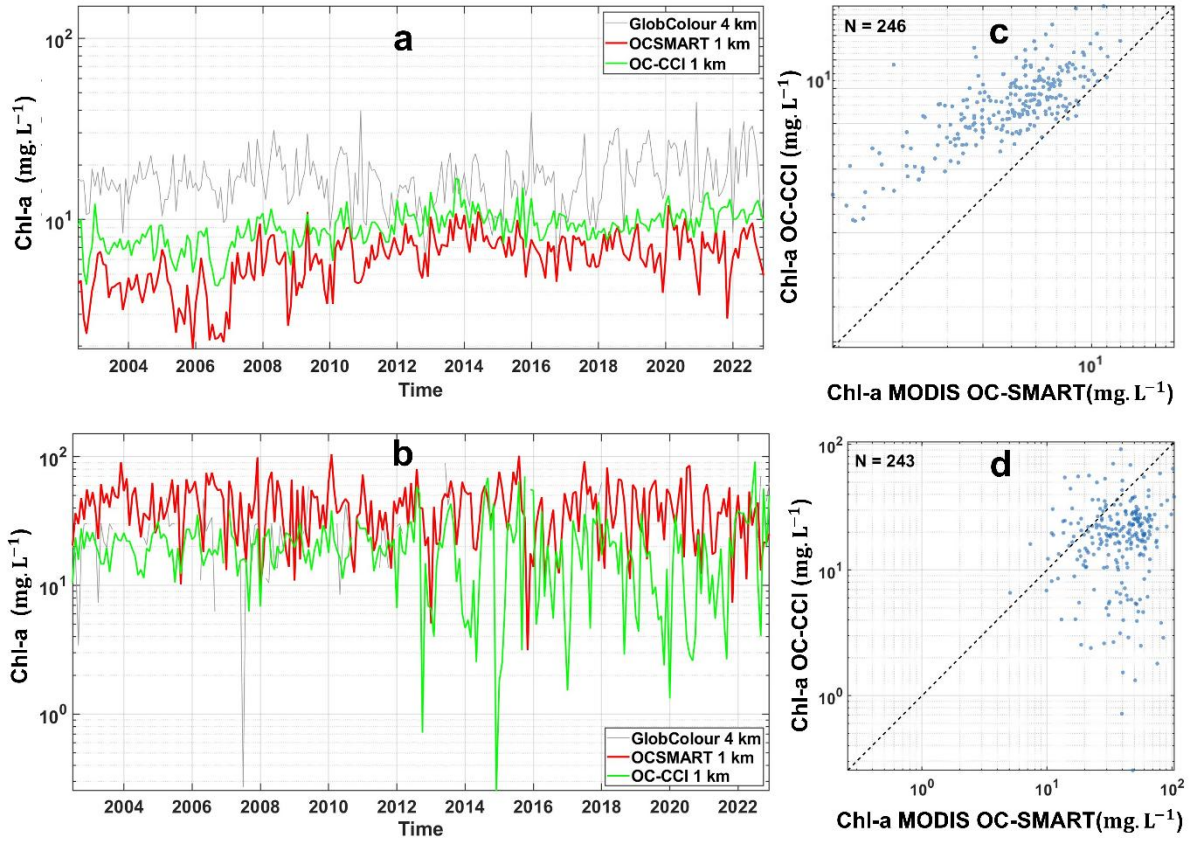

Figure 2.15. Point-based analysis of satellite-derived Chl-a at representative coastal locations: (a-b) long-term time series from GlobColour, OC-CCI, and MODIS OC-SMART, and (c-d) scatter-based comparison between OC-CCI and MODIS OC-SMART at points A and B (Figure 14).

At point A, located in Sepetiba Bay (Figure 2.15a), all three products capture similar temporal variability at seasonal to interannual scales, with synchronous peaks and troughs

throughout the 2002-2022 period. However, systematic differences in magnitude are evident. GlobColour generally reports the highest Chl-a concentrations, while OC-CCI consistently yields higher values than MODIS OC-SMART.

The corresponding scatter plot (Figure 2.15c) shows that most data points lie above the 1:1 line, indicating a systematic positive bias of OC-CCI relative to MODIS OC-SMART. Importantly, the relationship remains monotonic across the full concentration range, with OC-CCI continuing to increase as MODIS OC-SMART increases. This behavior indicates a systematic overestimation of Chl-a by OC-CCI at point A, rather than a saturation effect, and is consistent with the known limitations of blue-to-green band-ratio algorithms in moderately productive optically complex coastal waters (O'Reilly et al., 1998; Sathyendranath et al., 2019).

At point B, located in Guanabara Bay (Figure 2.15b), the three products still exhibit broadly synchronous temporal variability; however, marked differences in amplitude are observed. While MODIS OC-SMART frequently reaches high Chl-a concentrations, OC-CCI displays a much more compressed range, with abrupt drops and limited maximum values.

This behavior is clearly illustrated in the scatter plot (Figure 2.15d), where OC-CCI values no longer increase proportionally once MODIS OC-SMART exceeds approximately 15-20 mg L^{-1}. Instead, OC-CCI remains confined to a narrower range, resulting in a pronounced deviation below the 1:1 line. This compression reflects a loss of sensitivity or saturation of the OCx blue-to-green approach under highly optically complex conditions, where high Chl-a concentrations coexist with extreme turbidity and strong CDOM absorption, and where the blue-green signal becomes increasingly dominated by non-phytoplankton constituents (Garnesson et al., 2019; Sathyendranath et al., 2019).

Overall, Figures 2.14 and 2.15 demonstrate that the spatial patterns of relative differences between OC-CCI and MODIS OC-SMART reflect two distinct algorithmic regimes in optically complex coastal waters. OC-CCI exhibits a systematic overestimation of chlorophyll-a in moderately productive environments, as illustrated at point A, while a reduced sensitivity or saturation is observed at higher concentrations under extreme optical complexity, as shown at point B. These results highlight the intrinsic limitations of blue-to-green band-ratio algorithms in coastal waters and underscore the need for alternative or regionally adapted approaches in such environments.

Another notable feature in Guanabara time series (Figure 2.15b) is the apparent saturation observed during the early part of the record (approximately 2002–2012) in the OC-CCI and GlobColour products, characterized by a reduced sensitivity to high Chl-a variability relative to MODIS-CONNECT. This behavior is plausibly linked to the sensor composition and

merging strategy underlying multi-sensor products, particularly the dominant contribution of early-generation sensors and cross-sensor harmonization procedures that can limit the effective dynamic range in optically complex and eutrophic coastal waters (Mélin et al., 2017; Sathyendranath et al., 2019).

Santos (2025) compared Chl-a estimates in Brazilian coastal waters using the COCOBRAZ in situ database, the CONNECT model applied to MODIS OC-SMART, and the OC-CCI product (Figure 2.16). While both products showed good overall performance, OC-CCI exhibited a clear saturation effect, with Chl-a estimates asymptotically limited to ~10 mg. L^{-1} and underestimation at higher concentrations associated with OWTs 1 and 2. In contrast, Chl-a CONNECT did not present saturation and maintained a strong agreement with in situ observations over a much wider range, successfully retrieving concentrations up to ~200 mg. L^{-1}.

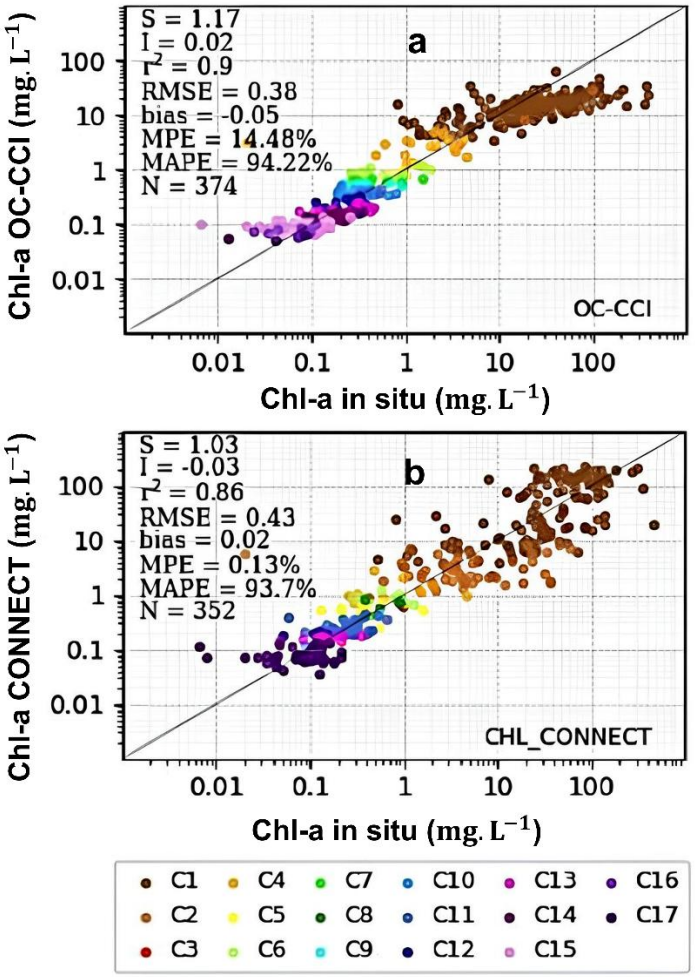

Figure 2.16. Performance of satellite-derived chlorophyll-a estimates in Brazilian coastal waters based on matchups with COCOBRAZ in situ observations. (a) Matchup between OC-CCI Chl-a and in situ measurements. (b) Matchup between Chl-a estimated using the CONNECT model applied to MODIS OC-SMART and in situ measurements. Point colors indicate OWT class membership, ranging from turbid waters (C1) to ultra-oligotrophic waters (C17). (Cardos Dos Santos, 2025).

Chl-a CONNECT estimates were closer to the 1:1 line, with a slope of 1.03, low bias (0.02), and a very low MPE (0.13%), whereas both products showed similarly high MAPE values (~94%). The saturation observed in OC-CCI is consistent with known limitations of global blue-green band-ratio algorithms in optically complex coastal waters, further amplified by spatial resolution and adjacency effects (Dierssen, 2010; Tilstone et al., 2021). These results demonstrate that the CONNECT approach provides more reliable Chl-a estimates in coastal environments characterized by high concentrations and strong continental influence.

An additional limitation affecting both GlobColour and OC-CCI products is the lack of near-infrared (NIR) remote sensing reflectance bands, which are known to be essential for robust retrieval of water quality parameters in turbid coastal environments. The absence of NIR information constrains the capacity of these products to properly characterize highly scattering waters, where Chl-a and SPM signals strongly influence the red-NIR spectral domain (Ruddick et al., 2006; Gurlin et al., 2011). In contrast, MODIS-based processing benefits from access to NIR observations, which contributes to improved performance in embayed and optically complex coastal waters.

Overall, the comparison highlights that while all products reproduce the dominant spatial and temporal patterns of Chl-a in Sepetiba and Guanabara bays, substantial differences remain in their representation of coastal gradients and absolute concentrations. These discrepancies emphasize the importance of spatial resolution and spectral information when analyzing chlorophyll-a dynamics in embayed coastal systems.

2.3.2.3. Impact of satellite product choice on long-term chlorophyll-a trends in coastal waters

The long-term implications of the differences observed among satellite products are illustrated in Figure 2.17, which presents the spatial distribution of the rate of change in Chl-a over the 2002-2022 period derived from GlobColour (4 km), OC-CCI (1 km), and MODIS-Aqua processed with the CONNECT inversion model (1 km). The figure integrates both open coastal environments influenced by riverine inputs and eutrophic embayed systems, allowing a consistent comparison of trend patterns across contrasting coastal settings.

Along the open coast influenced by the São Francisco River and adjacent river systems (Figure 2.17a-c), marked discrepancies emerge among the products. The GlobColour-derived trends (Figure 2.17a) exhibit weak spatial contrasts and a largely diffuse pattern, with limited differentiation between nearshore and offshore waters. This smoothing effect hampers the identification of localized coastal signals and reduces the apparent influence of riverine inputs

on long-term Chl-a variability. The OC-CCI product (Figure 2.17b) reveals clearer coastal signals and a more pronounced nearshore–offshore contrast; however, the spatial continuity of the trends remains fragmented. In particular, coastal features appear discontinuous along the inner shelf, suggesting reduced robustness in resolving fine-scale, river-driven variability in optically complex waters (Dierssen, 2010; Mélin et al., 2011; Eleveld et al., 2017).

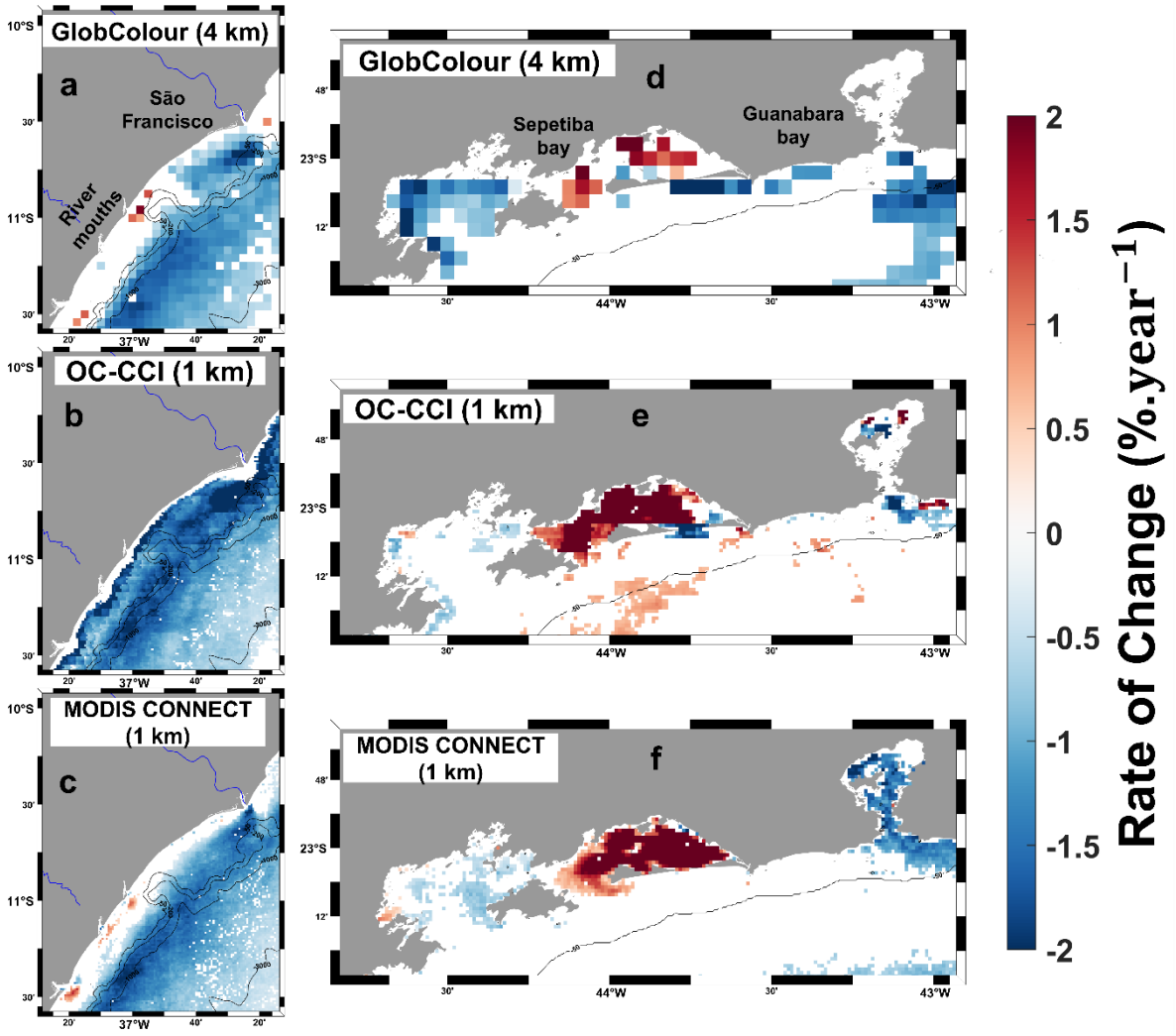

Figure 2.17. Comparison of satellite-derived rates of change (RC, % year^{-1}) in chlorophyll-a over selected Brazilian coastal regions ($P < 0.05$). (a-c) São Francisco River coastal region derived from (a) GlobColour (4 km), (b) OC-CCI (1 km), and (c) MODIS-Aqua processed with OC-SMART and estimated using the CONNECT model (1 km).(d-f) Guanabara Bay and Sepetiba Bay derived from (d) GlobColour (4 km), (e) OC-CCI (1 km), and (f) MODIS-Aqua processed with OC-SMART and estimated using the CONNECT model (1 km).

In contrast, the MODIS-CONNECT product (Figure 2.17c) displays spatially coherent and well-structured Chl-a trends along the inner shelf. Positive rates of change are consistently aligned with the coastal zone and extend alongshore, indicating a cumulative influence of riverine and coastal processes over the two-decade period. The continuity and spatial organization of these trends suggest an improved capacity to capture long-term biogeochemical

changes driven by persistent land-ocean interactions (Cloern and Jassby, 2012; Vantrepotte et al., 2012).

The differences between products become even more pronounced within the embayed environments of Sepetiba Bay and Guanabara Bay (Figure 2.17d-f). In these semi-enclosed systems, the GlobColour product (Figure 2.17d) largely fails to resolve internal spatial variability, resulting in patchy or spatially uniform trend patterns that obscure intra-bay gradients.

The OC-CCI product (Figure 2.17e) shows a clear tendency toward positive Chl-a rates of change within Sepetiba Bay; however, the spatial expression of this signal remains heterogeneous and patchy. Although areas of increasing Chl-a are identifiable within the bay, the spatial organization of the trends is irregular, particularly in confined and nearshore sectors, limiting the interpretation of coherent long-term gradients. This behavior highlights the sensitivity of OC-CCI to optical complexity and local variability in highly eutrophic embayments (Mouw et al., 2015; Tran et al., 2025).

The MODIS-CONNECT trends (Figure 2.17f) reveal well-defined and spatially coherent patterns across both Sepetiba and Guanabara bays. Distinct areas of increasing Chl-a are clearly delineated within the inner bays and along their coastal margins, while offshore waters exhibit weaker or opposite trends. This spatial organization is consistent with long-term eutrophication processes and sustained nutrient enrichment in these systems, suggesting that the MODIS-CONNECT approach provides a more realistic depiction of coastal and embayment-scale biogeochemical evolution.

Both Sepetiba and Guanabara Bays are well documented as highly eutrophic systems resulting from decades of intense anthropogenic pressure. Sepetiba Bay is a shallow, semi-enclosed coastal embayment that has received substantial nutrient inputs from untreated domestic sewage and industrial effluents, leading to persistent eutrophic conditions and recurrent algal blooms (Molisani et al., 2004; Aguiar et al., 2011; Castelo et al., 2021).

Guanabara Bay has similarly experienced severe environmental degradation driven by long-term organic enrichment. However, recent spatially localized decreases in Chl-a, as suggested by the MODIS-CONNECT trends, may be linked to the implementation of targeted sanitation and remediation programs, including the Guanabara Bay Depollution Program (PDBG) and the Social Environmental Sanitation Program (PSAM). These initiatives, accelerated in the context of infrastructure investments prior to the 2016 Olympic Games, aimed to improve sewage collection and treatment in specific sub-basins, potentially reducing nutrient

loads and organic inputs that sustain phytoplankton growth in parts of the bay (Soares et al., 2022).

Overall, Figure 2.17 demonstrates that the choice of satellite product exerts a strong influence on the magnitude, spatial coherence, and interpretability of long-term Chl-a trends in coastal waters. While GlobColour and OC-CCI capture broad-scale tendencies, their limitations in spatial resolution and sensitivity to optically complex conditions constrain their applicability for detailed trend analyses in river-influenced and embayed environments. In contrast, MODIS-CONNECT consistently resolves structured and interpretable Chl-a trends, highlighting its suitability for long-term biogeochemical assessments in heterogeneous coastal systems.

2.3.3. Hotspot detection in Brazilian coastal waters (2002-2022)

To provide an overall picture of biogeochemical dynamics along the Brazilian coastal waters between 2002 and 2022, long-term satellite archives of Chl-a, SPM, and POC were analysed. Trend detection was performed using the non-parametric Mann-Kendall test, allowing the identification of significant increases, decreases, or absence of monotonic trends across distinct coastal environments (river mouths/estuaries, bays, and lagoons). This approach was used as a first step to identify potential biogeochemical hotspots along the Brazilian coast by quantifying the spatial distribution of long-term changes in each variable.

Chl-a (Figure 2.18a) shows contrasted behaviours across coastal systems. Increasing trends were observed in 37% of river mouths and estuaries, 47% of bays, and 29% of lagoons. Decreasing trends affected 35% of river mouths and estuaries, 18% of bays, and 24% of lagoons. A substantial fraction of systems exhibited no significant trend, particularly in lagoons (47%), compared to 35% in bays and 28% in river mouths and estuaries.

SPM (Figure 2.18b) is largely dominated by increasing trends, especially in bays, where 70% showed significant increases. River mouths and estuaries also exhibited a high proportion of increasing trends (49%), while lagoons showed increases in 35% of systems. Decreasing trends were most pronounced in lagoons (59%), compared to 33% in river mouths and estuaries and 18% in bays. Systems showing no significant trend accounted for 18% of river mouths and estuaries, 12% of bays, and only 6% of lagoons.

POC (Figure 2.18c) reveals a predominance of decreasing trends in river mouths and estuaries (44%) and lagoons (59%), whereas bays were mainly characterised by increasing trends (47%). POC increases were observed in 23% of river mouths and estuaries and 24% of lagoons. Systems exhibiting no significant trend represented 33% of river mouths and estuaries, 35% of bays, and 17% of lagoons.

Combining this with Census X11 outputs enabled the detection of several hotspots where some anthropogenic impacts are detected and need to be studied in detail.

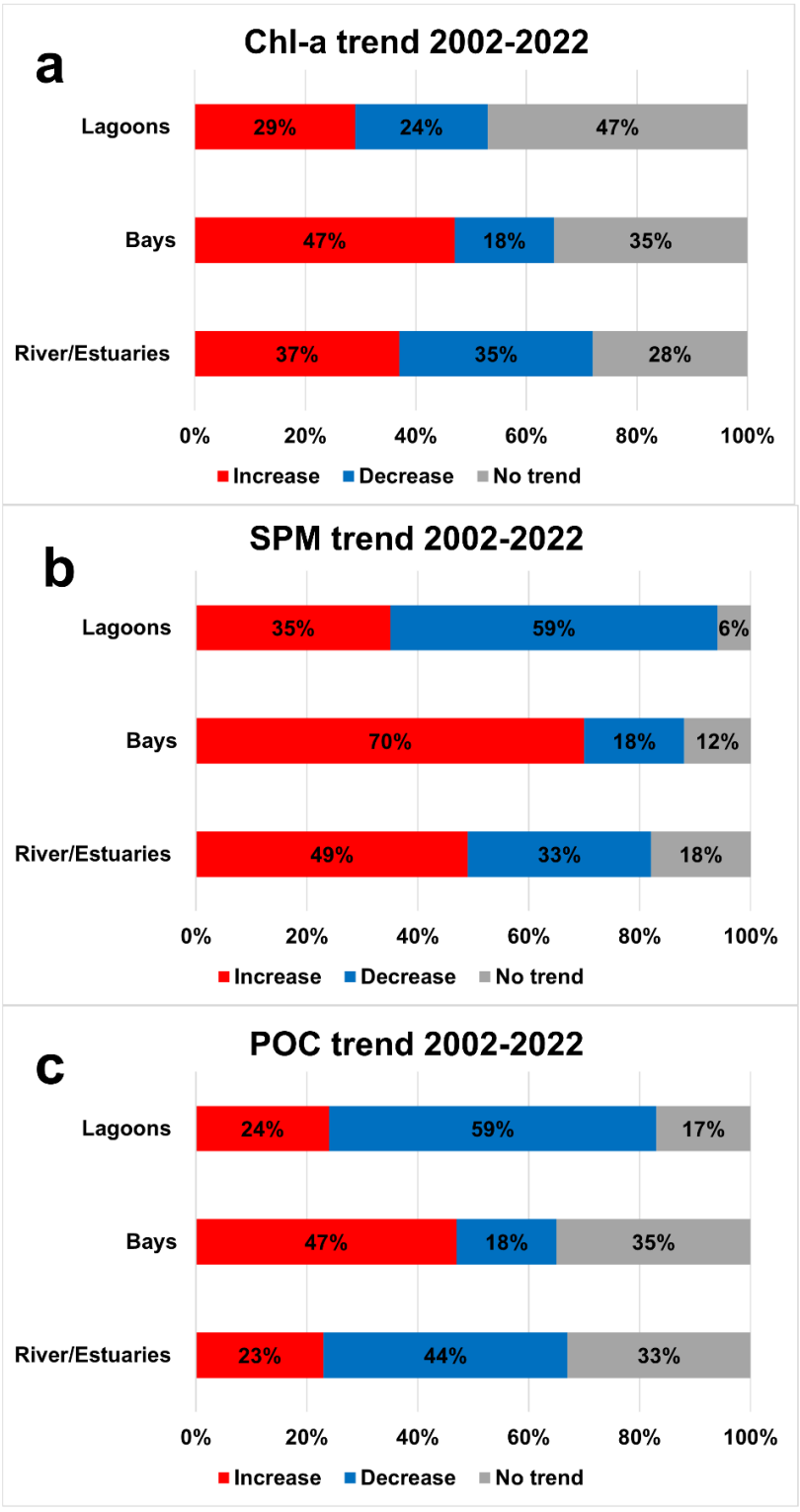

Figure 2.18. Distribution of long-term trends in Chl-a, SPM, and POC across Brazilian coastal systems (2002-2022). (a) Chl-a variability 2002-2022, (b) SPM variability 2002-2022 and (c) POC variability 2002-2022.

Many hotspots were identified along the Brazilian coast, highlighting the diversity of anthropogenic and environmental drivers affecting coastal biogeochemistry. The hotspots were identified based on the significant decreasing or increasing trends for Chl-a, SPM and POC. The variations were observed in the different coastal ecosystems such as bays, lagoons and river mouths.

- **Examples of biogeochemical hotspots in Brazilian coastal bays:**

The Bay of Santa Catarina Island exhibits a marked increase in Chl-a, SPM and POC (Figure 2.19a), primarily associated with urban expansion and agricultural activities in the surrounding watersheds. This hotspot has been investigated in detail by Santos et al. (2025), who attribute the observed trends to land use and land cover changes combined with climate variability.

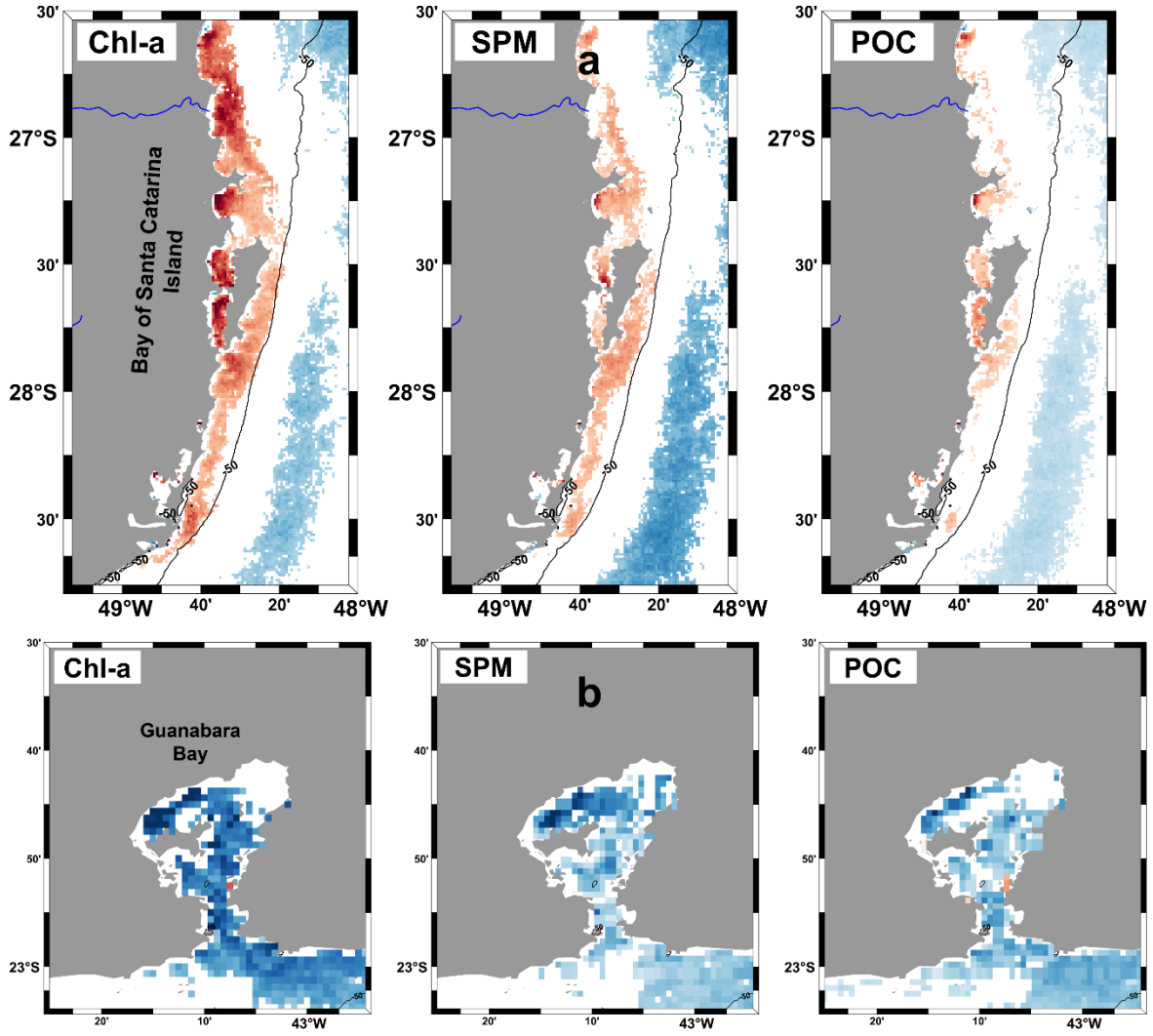

Figure 2.19. Examples of biogeochemical hotspots in Brazilian coastal bays identified from significant rates of change (RC, $p < 0.05$) in Chl-a, SPM, and POC over the 2002–2022 period. (a) Bay of Santa Catarina Island, showing increasing trends in Chl-a, SPM, and POC. (b) Guanabara Bay, exhibiting decreasing trends in Chl-a, SPM, and POC.

Figure 2.19b shows a contrasting pattern, with a decrease in Chl-a, SPM, and POC in Guanabara Bay between 2002 and 2022. Despite being subject to strong anthropogenic pressures related to urbanization and domestic sewage inputs, this decline likely reflects the effects of sanitation and remediation efforts implemented over the past decades. In particular, large-scale initiatives such as the PDBG and the PSAM programs have aimed to reduce pollutant loads entering the bay, which may have contributed to the observed decrease in biogeochemical concentrations (Soares et al., 2022). Guanabara Bay will be included in a future study by Vantrepotte et al. focusing on the main bays of Rio de Janeiro.

- **Examples of biogeochemical hotspots in Brazilian estuaries and river mouths:**

South of the São Francisco River, significant trends in Chl-a, SPM and POC are detected near the river mouths of the Sergipe, Vaza-Barris, Castro and Real rivers (Figure 2.20a). These changes likely reflect modifications in sediment supply linked to land use changes and the combined influence of anthropogenic pressures and environmental drivers. These systems represent relevant targets for future investigations.

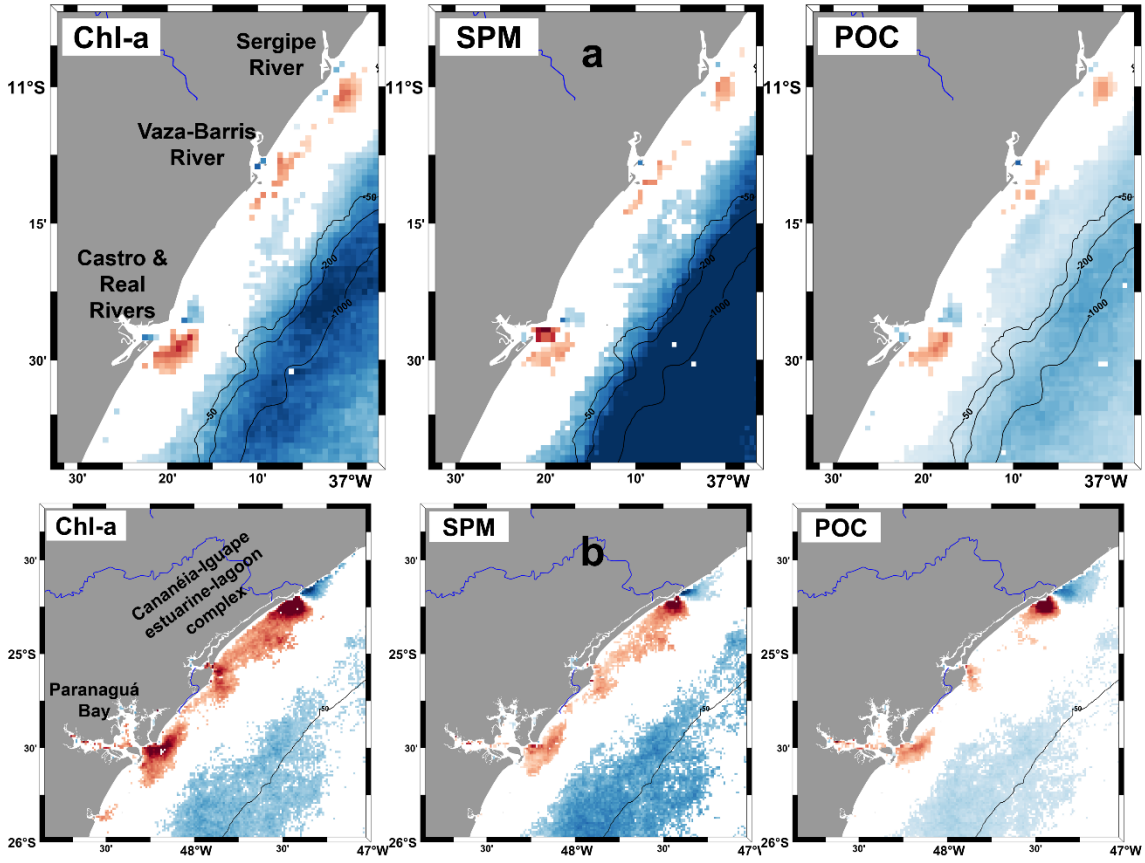

Figure 2.20. Examples of biogeochemical hotspots in Brazilian estuaries and river mouths identified from significant rates of change (RC, $p < 0.05$) in Chl-a, SPM, and POC over the 2002–2022 period. (a) River mouths south of the São Francisco River (Sergipe, Vaza-Barris, Castro, and Real rivers). (b) Cananéia-Iguape estuarine-lagoon complex.

The Cananéia-Iguape estuarine-lagoon complex constitutes another distinct hotspot (Figure 2.20b), characterized by a spatial dipole with increasing rates of change in the southern sector and decreasing values in the northern sector. Such contrasting patterns have been associated with geomorphological processes influencing sediment redistribution in coastal environments. Previous studies indicate that both natural drivers, such as river discharge and wave climate, and long-term human interventions, particularly the Valo Grande artificial channel, play a major role in controlling sediment dynamics in this region (Prado et al., 2019; Silva et al., 2021). A combined assessment of climatic and anthropogenic influences is therefore essential for future management strategies.

- **Examples of biogeochemical hotspots in Brazilian coastal lagoons:**

Figure 2.21a shows a clear decreasing trend in Chl-a, SPM, and POC within the Araruama Lagoon between 2002 and 2022. This decline may be attributed to improved sanitation infrastructure, such as the sewage interceptor belt implemented in the 2000s, and enhanced hydrodynamic flushing with oceanic waters via the Itajuru Channel (Souza et al., 2003; Pereira, Rodrigues and Dias, 2018). However, these trends necessitate detailed future research to further disentangle the specific impacts of anthropogenic drivers and natural fluctuations on the lagoon's biogeochemical cycle.

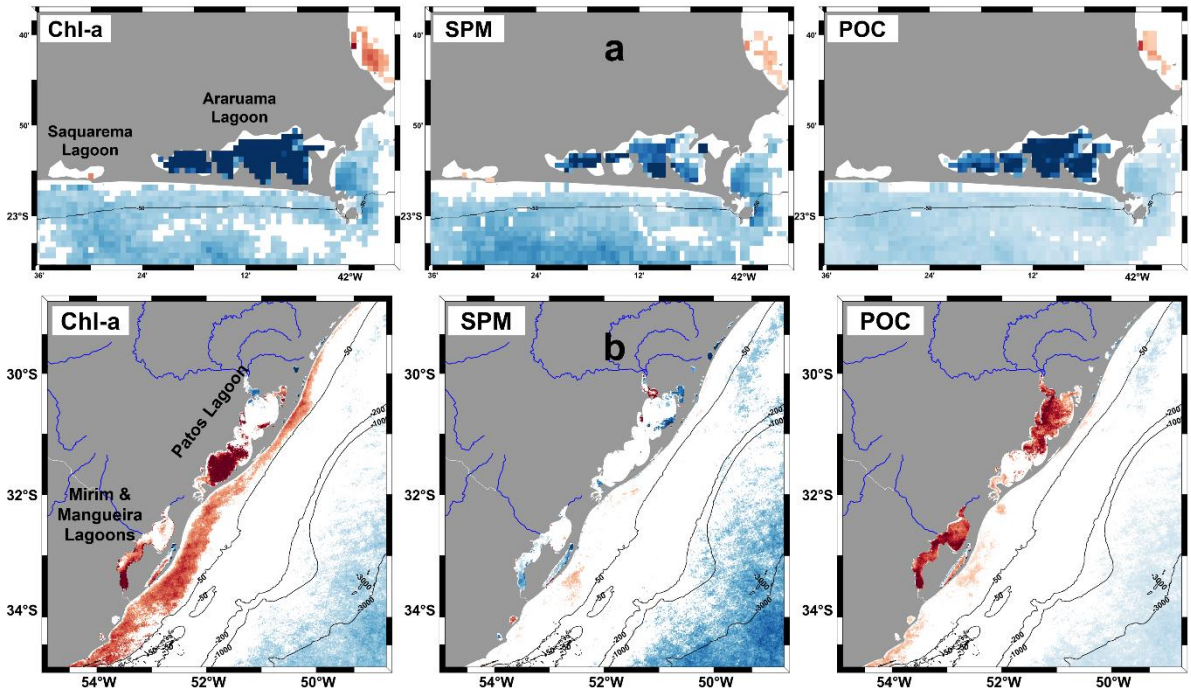

Figure 2.21. Examples of biogeochemical hotspots in Brazilian coastal lagoons identified from significant rates of change (RC, $p < 0.05$) in Chl-a, SPM, and POC over the 2002-2022 period. (a) Araruama Lagoon, showing trends in Chl-a, SPM, and POC. (b) Southern Brazilian lagoonal systems (Patos Lagoon, Mangueira Lagoon, and Mirim Lagoon), exhibiting trends in Chl-a and POC and SPM.

Finally, lagoonal systems such as Patos Lagoon, Mangueira, and Mirim lagoons show a clear increase in Chl-a and POC with no significative trend in SPM (Figure 2.21b). These trends are likely related to land use and land cover changes in the drainage basins, variations in river discharge, and regional climate variability, particularly precipitation. These lagoonal environments represent important natural laboratories for future studies addressing land-sea interactions and carbon dynamics.

The decreasing trend observed along the Brazilian shelf break, potentially linked to geomorphological features and large-scale circulation patterns, is not addressed in this thesis, as it lies beyond the scope and objectives of the present study.

The detected hotspots require association with potential human and environmental pressures to better interpret the observed variability. In this PhD, several hotspots were examined from this perspective, and two of them were further investigated in detail in Chapters 3 and 4.

2.3.4. Selected examples of human-induced pressures on Brazilian coastal waters

The analysis of Census X-11 outputs combined with Mann-Kendall trend tests for Chl-a, SPM, and POC over Brazilian coastal waters enabled the identification of several biogeochemical hotspots associated with anthropogenic pressures, including deforestation, dam construction, urbanization, industrial activities, and agricultural expansion.

2.3.4.1. Agriculture and farming impact

One of the most prominent hotspots is located along the western coast of Maranhão State (Subset b; Figure 2.7). This area exhibits a marked positive rate of change in Chl-a (Figure 2.22a), with an increase of approximately 35% between 2002 and 2022. This trend is primarily attributed to deforestation driven by pasture expansion in the adjacent drainage basins.

The Census X-11 decomposition (Figure 2.22b) indicates that Chl-a variability in this region is dominated by a strong seasonal component, superimposed on a persistent positive long-term trend. These biogeochemical changes are mainly linked to land-use conversion, where enhanced sediment and nutrient inputs are transported from land to the coastal ocean through river discharge.

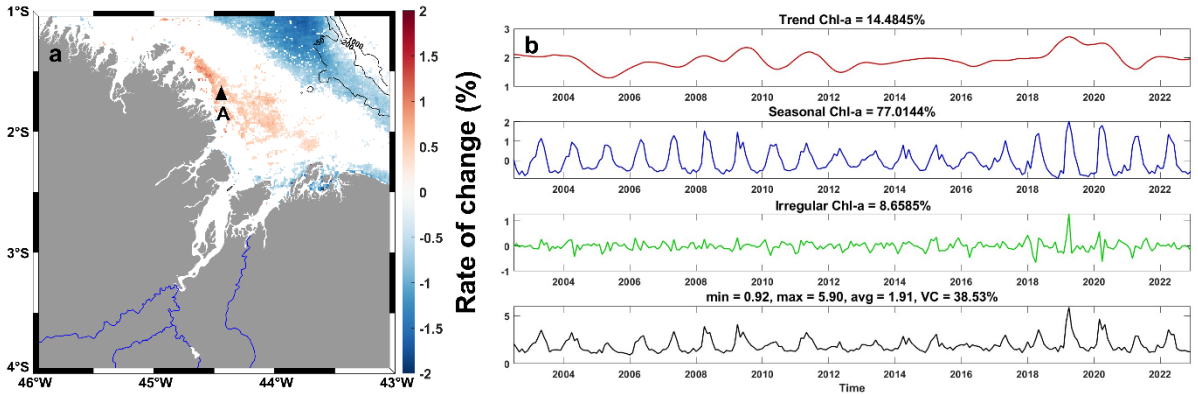

Figure 2.22. Chl-a variation along the western coast of Maranhão State (2002-2022). (a) RC of Chl-a ($p<0.05$). (b) Census X-11 decomposition method outputs at point A.

This hotspot constitutes the focus of Chapter 4, where the impacts of deforestation and pasture expansion on Chl-a and SPM variability are examined in detail.

2.3.4.2. Dam construction impact

The São Francisco River estuary (Subset e; Figure 2.7) represents a major hotspot strongly affected by river regulation. The basin is controlled by a cascade of seven large dams, which regulate approximately 98% of the total drainage area (Knoppers et al., 2006). This extensive regulation has substantially reduced runoff and altered the natural seasonal discharge regime, resulting in profound modifications to sediment transport, water quality, and estuarine ecological dynamics (Melo et al., 2020).

The RC of SPM between 2002 and 2022 is shown in Figure 2.23a, highlighting a marked decline in the particulate matter pool within the São Francisco River plume. Over the study period, both SPM and POC exhibit pronounced negative trends, with decreases of approximately 55% and 35%, respectively. These results indicate a substantial reduction in sedimentary fluxes and carbon export from the river to the coastal ocean.

The Census X-11 decomposition (Figure 2.23b) reveals that interannual variability dominates the SPM signal, reflecting long-term changes in river forcing rather than short-term seasonal fluctuations. Similar behaviour is observed for POC, suggesting a common control on particulate and organic matter dynamics.

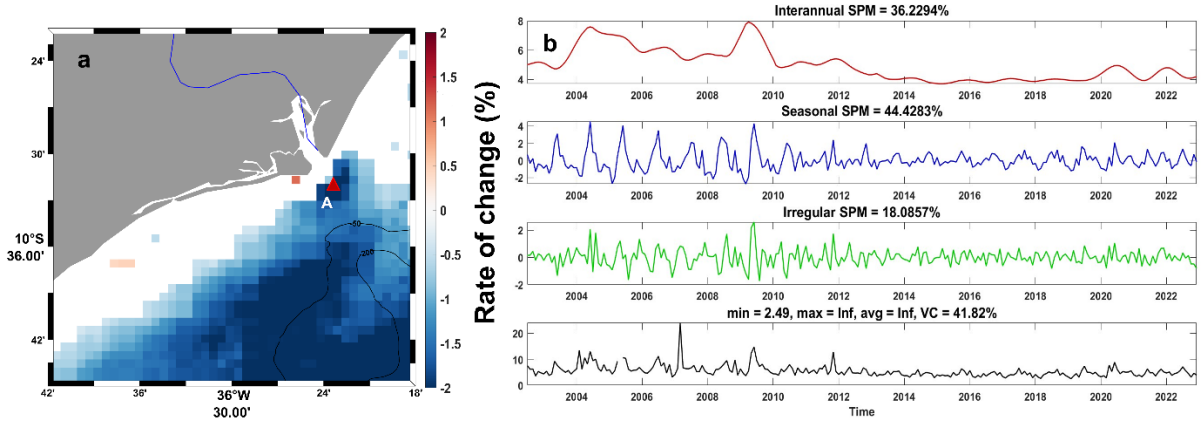

Figure 2.23. SPM variation at Sao Francisco River plume (2002-2022). (a) RC of SPM ($p<0.05$). (b) Census X11 decomposition method outputs at point A.

To explain this decline, a correlation analysis was conducted between the interannual variability of SPM, POC, and river discharge (Figure 2.24b). The results show strong correlations among the three variables, indicating that reductions in river discharge, largely driven by dam regulation, are closely associated with decreases in both particulate matter and organic carbon. This confirms that the altered flow regime directly constrains sediment and carbon availability in the estuarine-coastal system.

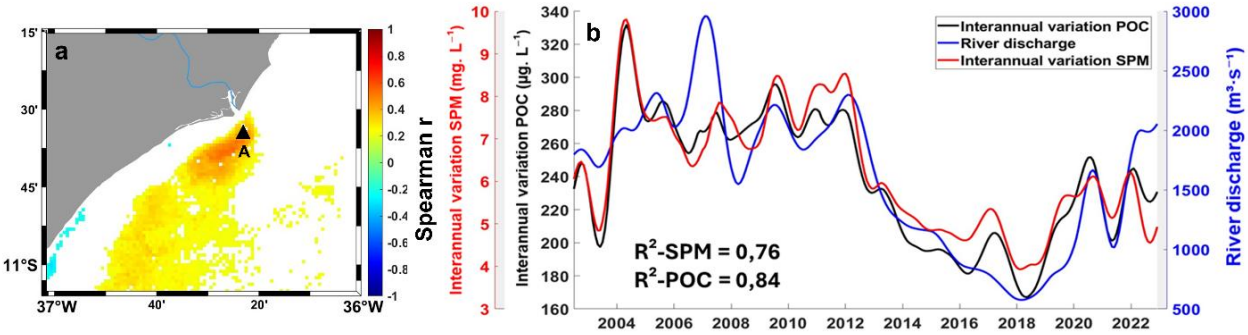

Figure 2.24. (a) Correlation map between SPM interannual variation and river discharge. (b) Correlation graphic between the interannual variation of SPM (red), the interannual variation of POC (black) extracted at point A and the interannual variation of the river discharge (ANA-Hydroweb, Sao Francisco station) (blue).

An extreme decrease occurred in 2012, during one of the most severe droughts recorded in Brazil, which strongly affected the São Francisco Basin (Santos et al., 2017). During this period, intensified dam regulation led to enhanced water retention and a sharp reduction in river discharge, accompanied by an abrupt decline in both SPM and POC. This event highlights the combined impact of climatic extremes and anthropogenic regulation on hydrological and sedimentary dynamics.

Finally, the correlation map between interannual SPM variability and river discharge (Figure 2.24a) shows that the reduction in river inputs affects not only the proximal plume but

also extends offshore, indicating a broader influence on sediment distribution and coastal water quality. Future studies could further refine this analysis by incorporating additional ancillary data, tracking plume dynamics over time, and using higher-resolution satellite observations to better resolve land-sea interactions within the estuary.

2.3.4.3. Industrialisation and urbanisation impacts

The Açu Port, located in the northern region of Rio de Janeiro State (Subset h; Figure 2.7), is the largest deep-water industrial complex in Latin America. Covering approximately 130 km², it has been operational since 2014 (Hora et al., 2021). The port hosts a wide range of industrial activities and plays a strategic role in Brazil's logistics network and oil and gas sector, contributing significantly to regional economic development (Bitencourt et al., 2017).

The rate of change in SPM within the coastal zone adjacent to the Açu Port shows a pronounced positive trend (Figure 2.25a). Over the study period, SPM concentrations increased by approximately 60%, indicating a substantial modification of sedimentary fluxes in the area. This increase suggests a strong influence of port-related activities on sediment dynamics and associated biogeochemical processes in the surrounding coastal environment.

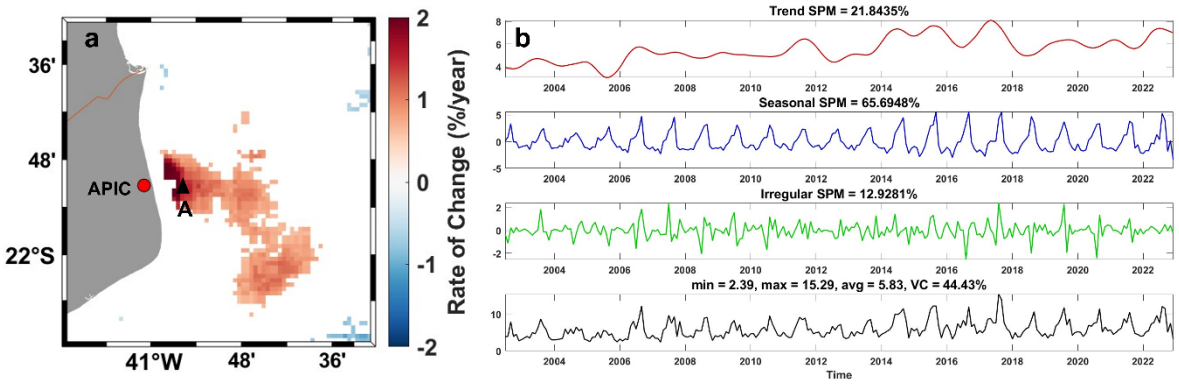

Figure 2.25. SPM variation near the Açu Port (2002-2022). (a) RC of SPM ($p<0.05$). (b) Census X11 decomposition method outputs at point A.

The Census X-11 decomposition extracted at point A near the port (Figure 2.25b) reveals that SPM variability is dominated by a strong seasonal signal with a persistent positive long-term trend, reflecting sustained changes in particulate matter availability.

This hotspot is examined in detail in Chapter 3, where the combined effects of industrial development and environmental drivers on SPM dynamics are investigated.

Sepetiba Bay, located in southeastern Brazil near the metropolitan region of Rio de Janeiro (Subset j; Figure 2.7), represents a major coastal hotspot strongly influenced by urbanization. The bay is surrounded by one of the most densely populated and industrialized regions in Brazil, where urban expansion constitutes the dominant anthropogenic pressure on the coastal environment.

Figure 2.26a illustrates the spatial distribution of POC rate of change in Sepetiba Bay, revealing markedly elevated values within the bay compared to surrounding coastal waters. These high POC levels reflect enhanced organic matter inputs associated with urban activities, including wastewater discharge, industrial effluents, and increased terrestrial runoff. Previous studies have shown that rapid urban growth in the Rio de Janeiro region has substantially altered the biogeochemical conditions of Sepetiba Bay through increased nutrient loading, pollution, and modifications of sedimentation processes (Molisani et al., 2004; Cunha et al., 2006).

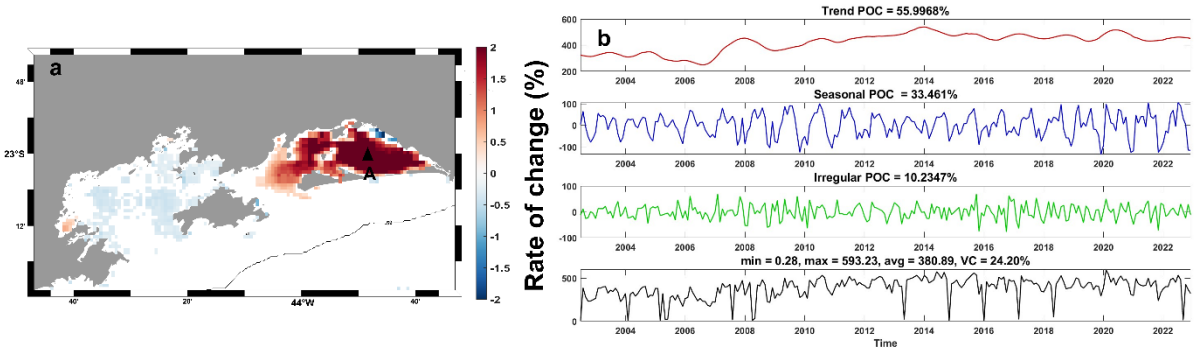

Figure 2.26. POC variation in Sepetiba bay (2002-2022). (a) RC of POC ($p<0.05$). (b) Census X11 decomposition method outputs at point A.

Over the 2002 to 2022 period, the rate of change analysis indicates a pronounced increase of approximately 70% in POC and 45% in SPM within the bay. This intensification is largely confined to Sepetiba Bay, reflecting its semi-enclosed geometry and local hydrodynamic circulation, which favour the retention and accumulation of particulate material. Nevertheless, elevated values observed near the bay mouth suggest that the influence of urbanization and industrialisation may extend to adjacent coastal areas.

The Census X-11 decomposition extracted at point A (Figure 2.26b) shows that POC variability is dominated by a strong long-term trend, with a secondary contribution from seasonal fluctuations. This behaviour indicates a persistent modification of organic carbon dynamics rather than short-term variability alone.

Urbanization represents the primary driver of these changes, with increasing volumes of untreated or partially treated wastewater being discharged into the bay. To assess this influence, a correlation analysis was conducted between urbanization indicators and the interannual

variability of POC and SPM (Figure 2.27). The results reveal strong relationships, demonstrating that the expansion of urban areas (from MapBiomas) is closely associated with increasing concentrations of particulate organic carbon and suspended particulate matter. These findings confirm the significant impact of urban development on the biogeochemical quality of Sepetiba Bay waters.

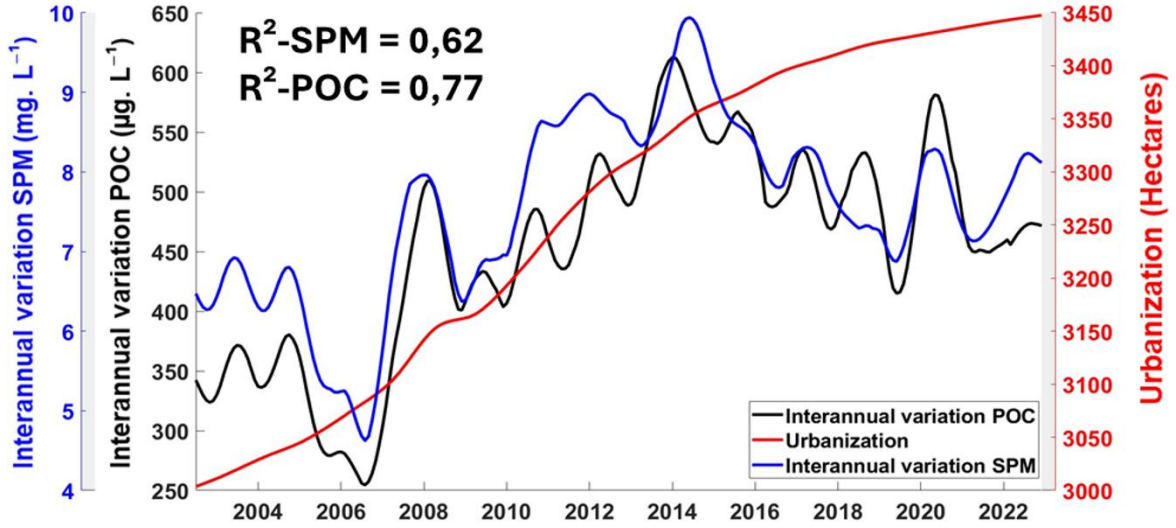

Figure 2.27. Correlation graphic between the interannual variation of SPM (blue), the interannual variation of POC (black) and the urbanization (MapBiomas) (red).

Further investigation of this hotspot is warranted and is currently being addressed in ongoing work led by Vincent Vantrepotte. Future analyses will incorporate Chl-a variability and extend the spatial scope to nearby systems, such as Guanabara Bay, to better characterize regional-scale urban impacts on coastal biogeochemistry.

2.4. Conclusion

This chapter provided an overview of Brazilian coastal waters based on long-term satellite-derived biogeochemical products from MODIS-Aqua. The COCOBRAZ database was introduced as a comprehensive framework that integrates satellite observations and in situ measurements to characterize Brazilian coastal environments at large spatial and temporal scales.

MODIS-Aqua observations at 1 km spatial resolution, processed with the OC-SMART atmospheric correction and combined with dedicated bio-optical models, were shown to offer a consistent and effective observational framework for monitoring Brazilian coastal waters. This approach enables the observation of a wide range of coastal systems, including river

plumes, bays, estuaries, and lagoons, and captures the strong spatial heterogeneity that characterizes the Brazilian coastline.

The analysis of long-term satellite time series using the Census X-11 decomposition and Mann-Kendall trend tests revealed contrasted patterns of variability and significant rates of change in Chl-a, SPM, and POC over the 2002-2022 period. These results highlight the diversity of biogeochemical responses across coastal environments and emphasize the spatial complexity of Brazilian coastal waters.

By combining trend detection and temporal decomposition, several biogeochemical hotspots were identified along the Brazilian coast, associated with major anthropogenic pressures such as deforestation, river regulation, urbanization, industrial development, and agricultural expansion. These hotspots illustrate the capacity of satellite observations to detect large-scale patterns of change and provide a spatial basis for targeted regional analyses.

Two of the detected biogeochemical hotspots, associated with distinct anthropogenic pressures, are examined in detail in Chapters 3 and 4. Chapter 3 focuses on a hotspot linked to industrial development in the Açu Port region, while Chapter 4 investigates a hotspot associated with deforestation and pasture expansion in the coastal waters of Maranhão, northern Brazil, using MODIS observations over the 2002-2022 period.

Overall, this chapter establishes a coherent observational framework for the analysis of Brazilian coastal biogeochemistry at the national scale. The large-scale patterns and hotspots identified here form the basis for the more focused investigations presented in the following chapters.

CHAPTER 3: IMPACT OF INDUSTRIALIZATION ON THE EVOLUTION OF SUSPENDED PARTICULATE MATTER FROM MODIS DATA (2002-2022): CASE STUDY OF AÇU PORT, BRAZIL

3.1. Introduction

Coastal zones are characterized by a diverse array of systems, including estuaries, bays, lagoons, and a variety of geomorphological features (Sullivan Sealey and Bustamante, 1999; Ab'Sáber and Holmquist, 2001; Dominguez, 2009). The biogeochemical dynamics of these systems are significantly influenced by natural processes and anthropogenic activities. On the natural side, land-sea interactions, sediment resuspension and deposition, as well as transport processes driven by waves, tides, winds, and currents, play a central role in regulating the biogeochemical dynamics of coastal waters (Swift et al., 1976; Donker and De Swart, 2013; Andutta et al., 2014; Bianchi et al., 2014). Concurrently, human-driven alterations in land use and cover, including urban expansion, agricultural practices, and dam construction, have the potential to generate substantial pressures, thereby modifying sediment fluxes and nutrient dynamics (Burke, 2001; Bulleri and Chapman, 2010; Barragán and de Andrés, 2015). Suspended particulate matter (SPM) has been identified as a pivotal indicator of these processes, given its direct impact on water quality, turbidity, light penetration, and the transport of nutrients and pollutants (Miller and Cruise, 1995; Velegrakis et al., 1997; Kroon et al., 2012). It is therefore imperative to understand SPM dynamics to improve pollution control, preserve marine ecosystems, and support integrated coastal management (Frascari et al., 1988; Giordani et al., 1992).

In Brazil, coastal ecosystems are particularly vulnerable to both anthropogenic and natural pressures. The accelerated pace of environmental changes can be attributed to a number of factors, including industrialization, deforestation, intensive agriculture, and large-scale infrastructure projects such as dams have accelerated environmental changes (Bernardes et al., 2012). Among the most impactful activities are industrial and port developments, whose construction and operation often involve dredging, land reclamation, and altered sediment fluxes (Ferrari, 1995; Ramessur, 2002; Yudhistira et al., 2022).

An interesting example is the Açu Port, located in São João da Barra, Rio de Janeiro, which is the largest private port-industrial complex in Latin America (Pedlowski, 2013; Pontes Da Silva Júnior and Pedlowski, 2022; Gadotti et al., 2025). A substantial body of research has

examined its socioeconomic and environmental impacts, including heavy metal contamination and effects on local communities (Pedlowski, 2013; Ditty and Rezende, 2014; Gao et al., 2018; Hora et al., 2021; Pontes Da Silva Júnior and Pedlowski, 2022). However, the influence of climate change on sediment transport has received scant attention from the scholarly community. A notable exception is the work of Scheel et al. (2023), who assessed the impacts of climate change on port development. Similarly, Lima et al. (2024) employed integrated hydro-sedimentological modeling to assess port resilience. To date, no study has provided a long-term evaluation of SPM dynamics in the adjacent coastal zone using ocean color remote sensing observations.

Due to the scarcity of long-term and spatially extensive in situ data in Brazilian marine environments, satellite remote sensing of ocean color radiometry (OCR) has become an indispensable tool. However, the elevated optical complexity of coastal waters demands the implementation of robust algorithms capable of retrieving SPM across a range of water clarity levels, from highly turbid to clear (Mélin and Vantrepotte, 2015; Groom et al., 2019). In this context, Optical Water Type (OWT) classification provides an effective approach, allowing the use of water-type-specific algorithms and thus improving retrieval accuracy under variable conditions (Vantrepotte et al., 2012; Carvalho et al., 2014; Tran et al., 2023).

This study utilizes data from the Moderate Resolution Imaging Spectroradiometer (MODIS) sensor onboard the Aqua satellite, with a spatial resolution of 1 km, from 2002 to 2022, to investigate the dynamics of SPM along the northern coast of Rio de Janeiro, with a particular focus on the influence of the Açu port. MODIS provides the longest continuous time series of ocean color available. While alternative datasets such as GlobColour (4 km) and the Ocean Color Climate Change Initiative (OC-CCI, 1 km) offer global coverage, the coarser resolution of GlobColour and the reduced performance of both datasets in turbid environments make them less suitable for this region (Cardoso Dos Santos et al., 2025). Furthermore, the absence of near-infrared (NIR) bands in these sensors is a critical limitation, as NIR bands are indispensable for the retrieval of SPM and chlorophyll-a (Chl-a) in optically complex waters.

The main objective of this study is to depict the recent evolution of the SPM dynamics in the coastal areas adjacent to the Açu Port and assess the relative impact of anthropogenic activities and climate on the regional SPM spatio-temporal patterns from MODIS 1km 2002-2022 data. To do so, an SPM retrieval algorithm based on OWTs was developed. This algorithm was adapted for global coastal waters by integrating existing algorithms according to their performance in specific water types. This algorithm was subsequently implemented on a comprehensive dataset spanning two decades, meticulously processed using the OC-SMART

(Ocean Color – Simultaneous Marine and Aerosol Retrieval Tool) atmospheric correction method (Fan et al., 2021). The resulting SPM time series were then analyzed using the seasonal Mann-Kendall test and Census X11 decomposition method (Pezzulli et al., 2005; Vantrepotte and Mélin, 2011) to detect monotonic trends over 2002-2022 and to characterize temporal variability at multiple scales (seasonal, interannual). Finally, the SPM spatiotemporal patterns were interpreted considering the main natural and anthropogenic drivers of the study area.

3.2. Materials and Methods

3.2.1. Study area

The Açu Port Industrial Complex (APIC) is located in the northern region of Rio de Janeiro State, southeastern Brazil (21.8528° S, 41.0206° W), within the municipality of São João da Barra (Vilani et al., 2021), occupying approximately 40% of its territory (Figure 3.1). The APIC is currently the largest private deep-water industrial port complex in Latin America (Pedlowski, 2013; Pontes Da Silva Júnior and Pedlowski, 2022). It covers an area of 130 km² and includes 11 terminals distributed between offshore and onshore zones. Offshore terminals have been found to have a depth range of 20 to 25 meters, which is sufficient to accommodate large cargo vessels (Gadotti et al., 2025). The APIC construction commenced in late 2006 and early 2007, with official operations initiated in 2014 (Da Silva, Mansur and Borghi, 2018; Hora et al., 2021). The complex is situated in proximity to the Paraíba do Sul River delta, which is the second-largest deltaic system in Brazil (Pontes Da Silva Júnior and Pedlowski, 2022), and in close proximity to the Itabapoana River (see Figure 3.1). The construction of dams and changes in land use have led to a decline in the discharge and plume size of the Paraiba do Sul River. This has resulted in a reduction in the influence on adjacent coastal areas near the river mouths (Rudorff et al., 2011; Oliveira et al., 2012).

The hydrodynamic conditions in the region are mainly influenced by the south-westward flowing Brazil Current, which originates from the bifurcation of the South Equatorial Current (Bernardes et al., 2012; Brandini et al., 2018). Coastal winds are predominantly northeasterly, though southern, southeastern, and southwestern winds are also common during austral autumn and winter (Dereczynski et al., 2019; Lämmle and Bulhões, 2019; Lämmle et al., 2022). The region's climate is classified as humid tropical, with an average annual temperature of approximately 22 °C. However, the region experiences a marked seasonal alternance in its rainfall regime, with wet summers from December to March and drier winters from June to August (Lämmle and Bulhões, 2019).

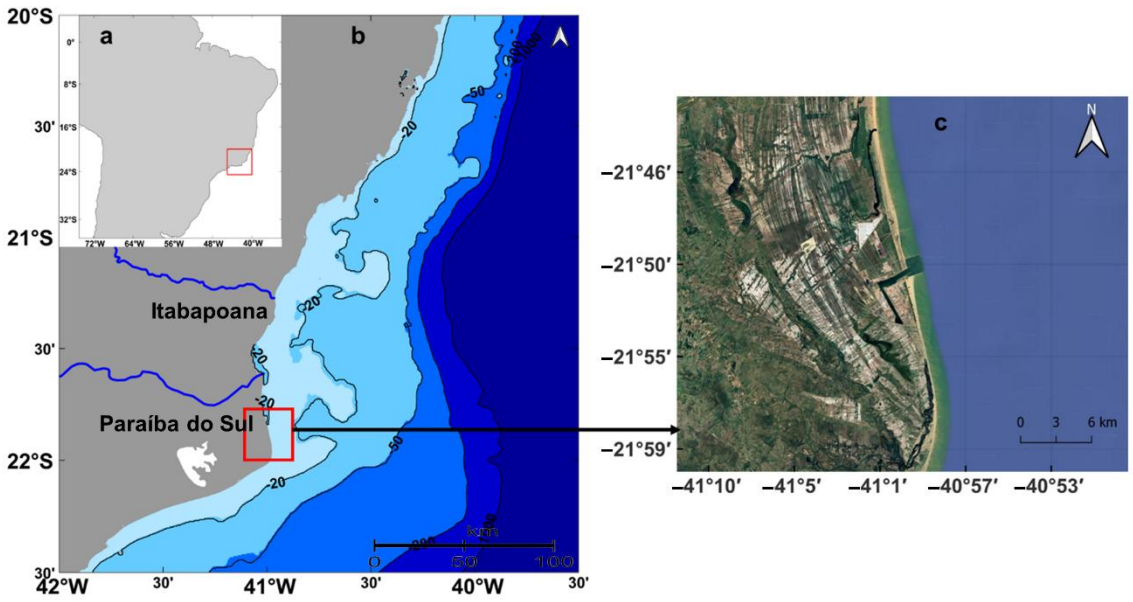

Figure 3.1. Location of the study area. (a) Location of northern coast of Rio de Janeiro state, highlighted in red, (b) Regional map showing bathymetry and major rivers, with a red box indicating the position of Açu Port, (c) Satellite view of Açu Port, the specific area analyzed in this study.

3.2.2. Ocean color satellite data

3.2.2.1. Atmospheric correction

To monitor water quality along the coastal waters of the northern coast of Rio de Janeiro state from 2002 to 2022, MODIS-Aqua Level 1 (L1) images at 1 km spatial resolution were downloaded from the NASA Ocean Biology Processing Group (OBPG) at the Goddard Space Flight Center (https://oceandata.sci.gsfc.nasa.gov/directdataaccess/Level-1A/Aqua-MODIS/ (accessed on 1 December 2022)). This sensor provides the most extensive continuous time series from a single platform, making it particularly valuable for long-term coastal monitoring. The daily L1B data set was processed using the OC-SMART atmospheric correction method (Fan et al., 2021). OC-SMART is an advanced platform based on multilayer neural networks (MLNNs) and extensive radiative transfer simulations based on the AccuRT coupled atmosphere-ocean model to assess the remote sensing reflectance (R_{rs} (λ)) of the water surface (Fan et al., 2021). The atmospheric correction model was selected based on its demonstrated efficacy in retrieving $R_{rs}(\lambda)$ across a broad spectrum of water types. This selection was made following a recent validation study that revealed the model's superior performance in comparison to alternative methods, including Polymer, ACOLITE, and C2RCC (Bui et al., 2022; Pachniak et al., 2023). Additionally, it provides superior spatial coverage, especially in highly turbid waters, due to its advanced cloud screening capabilities. Furthermore, this model demonstrates a diminished sensitivity to contamination from weak to moderate sunglint and

cloud edges (Fan et al., 2021). OC-SMART has also been validated for coastal applications and MODIS-Aqua data by Tran et al. (2025), as well as by a recent IOCCG (2025) evaluation group that assessed atmospheric correction schemes for MODIS using global in situ and synthetic data sets, confirming the method's good overall performance across contrasted environments.

3.2.2.2. Bio-optical model for SPM estimation

- **In situ data**

A bio-optical algorithm for SPM concentration was developed and validated using the Global Reflectance community dataset for Imaging and optical sensing of Aquatic environments (GLORIA) (Lehmann et al., 2023). In practice, this global in situ dataset encompasses 7,572 quality-controlled hyperspectral $R_{rs}(\lambda)$ spectra with 1 nm resolution over the 350-900 nm range collected in both inland and marine waters. Each $R_{rs}(\lambda)$ spectrum is paired with at least one co-located water quality parameter, including Chl-a, SPM, absorption by colored dissolved organic matter (a_{CDOM}), or Secchi depth. SPM measurements encompass a total of 4,149 samples. Subsequent to the implementation of quality control measures and the exclusion of data that had been flagged, a total of 489 points were retained, with each point corresponding to R_{rs} (λ) and SPM measurements. These samples encompassed a range of SPM concentrations, from 0.21 to 844.67 mg·L^{-1}, with a mean value of 25.88 mg·L^{-1} (Figure 3.2a).

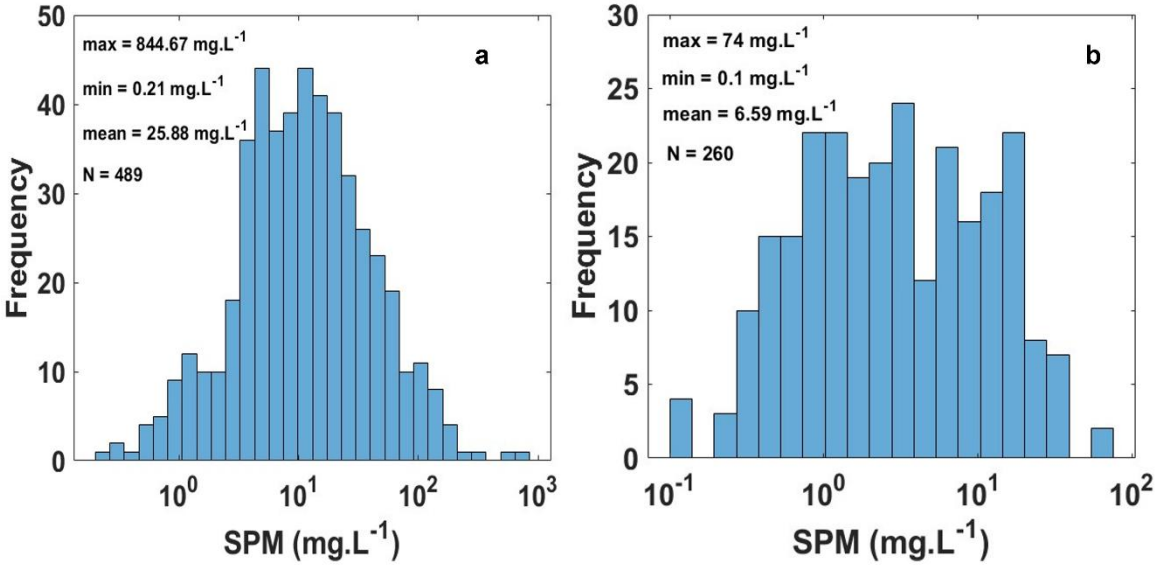

Figure 3.2. Distribution and classification of GLORIA in situ dataset. (a) Frequency distribution histograms of in situ SPM validation data, (b) Frequency distribution histograms of in situ SPM matchup data.

A matchup data set was constructed by extracting the corresponding MODIS OC-SMART $R_{rs}(\lambda)$ data (3x3 pixel window) from the GLORIA SPM stations, which were collected between

2002 and 2022. According to Werdell et al. (Werdell et al., 2009), classical quality control was performed by retaining only the matchups data that demonstrated the following criteria was set for a pixel to be considered valid: 1) at least five valid pixels within the nine pixel subset, 2) a spatial homogeneity of the $R_{rs}(551)$ value within the subset considering a coefficient of variation (CV = standard deviation divided by the mean, multiplied by 100) lower than 30%, and 3) time difference between in situ and satellite observations lower than three hours. Additionally, to remove inaccurate measurements, OC-SMART L2 quality flags were applied, and only valid pixels were retained (flag 0). Pixels with flags 1, 4, 16, 64, 256, and 1024 were excluded (L1 reflectance unavailable; out-of-range geometry; land; cloud; Rayleigh-corrected reflectance (Lrc) out of scope; negative Lrc). Following the implementation of the matchup protocol on the GLORIA data set, the MODIS-validation data set comprises 260 data points, with SPM ranging from 0.1 and 74 $mg \cdot L^{-1}$and an average value of 6.59 $mg \cdot L^{-1}$ (see Figure 3.2b).

- **Optical water types classification**

Optical Water Types offer a practical approach for classifying aquatic environments according to their optical properties (Vantrepotte et al., 2012; Lubac et al., 2008; Da Silva et al., 2021). It is particularly useful in optically complex coastal waters, contributing to water quality monitoring and improving the performance of ocean color algorithms performance (Carvalho et al., 2014; Loisel et al., 2013; Moore et al., 2014; Jackson et al., 2017; Spyrakos et al., 2018).

In this study, OWTs were defined using the methodology described by Vantrepotte et al. (2012), and applied to the GLORIA $R_{rs}(\lambda)$ dataset. Standardized remote sensing reflectance was computed from multispectral R_{rs} (λ) data at six wavelengths in the visible spectrum (412, 443, 488, 531, 547, and 667 nm), corresponding to MODIS bands, to focus on the spectral shape. Standardization was performed by dividing each $R_{rs}(\lambda)$ value by the integral of the reflectance spectrum, as follows:

$$\boldsymbol{R_{rs-N}} = \frac{\boldsymbol{R_{rs}(\lambda)}}{\int_{\lambda_1}^{\lambda_2} \boldsymbol{R_{rs}(\lambda)} \boldsymbol{d\lambda}} \quad \textbf{(3.1)}$$

Where $\boldsymbol{R_{rs-N}}$ is the standardized remote sensing reflectance.

The standardized spectra were then classified into OWTs (see Figures 3.3a and 3.3b) using unsupervised hierarchical clustering using the Ward's method (Ward Jr., 1963), which is less

sensitive to noise and outliers than other methods (Ferreira and and Hitchcock, 2009; Vantrepotte et al., 2012).

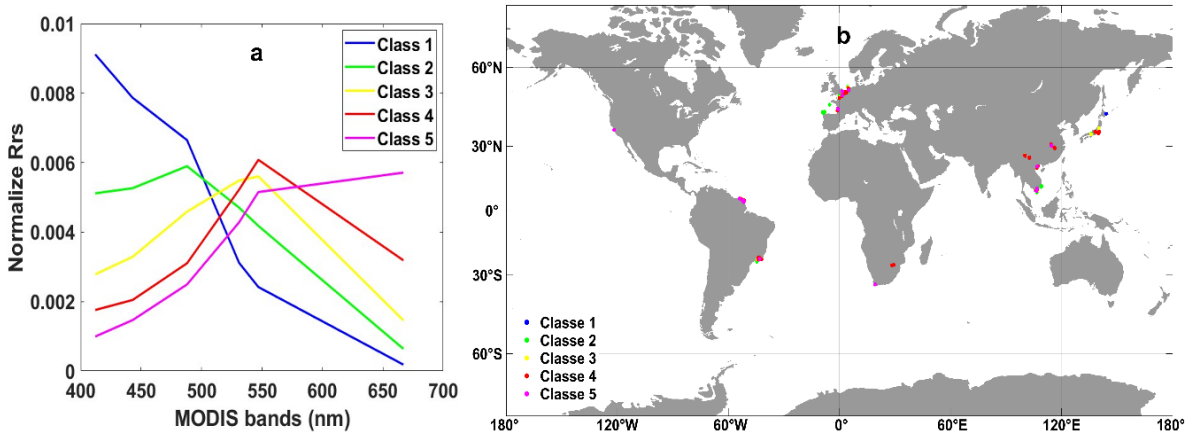

Figure 3.3. Optical water type classification. (a) Average standardized reflectance spectra corresponding to the five OWTs defined from the GLORIA dataset (N = 489) according to Tran et al. (Tran et al., 2023); (b) Geographical distribution of the in-situ SPM data.

In practice, five OWTs were considered, based on a recent classification of a global dataset, including GLORIA data, which was used to develop Chl-a inversion models for Sentinel 2 and 3 (Tran et al., 2023), as well as MODIS data (Tran et al., 2025). This classification resulted in five distinct R_{rs} (λ) spectral shapes. OWTs 1, 2, and 3 (N = 185) correspond to clear oligotrophic-to-mesotrophic waters, with a mean SPM concentration of 5.25 mg·L^{-1}, a minimum of 0.21 mg·L^{-1}, and a maximum of 34.58 mg·L^{-1}. OWTs 4 and 5 (N = 304) represent turbid to highly turbid waters, with mean, minimum and maximum SPM concentrations of 38.44 mg·L^{-1}, 2.37 mg·L^{-1}, and 844.67 mg·L^{-1}, respectively.

- **Principle of algorithms combination based on OWTs**

Five predefined OWTs were used to classify satellite R_{rs} (λ) spectra. This process involves associating each satellite R_{rs} (λ) spectrum with the identified OWTs from the in situ dataset. This association was performed using a detection technique based on the Mahalanobis distance (Bishop, 1993), which has previously been shown to be effective for classifying ocean color data (D'Alimonte et al., 2003; Mélin et al., 2011). Each OWT is characterized by a specific mean vector (μ) and covariance matrix (Σ), computed from standardized, log-transformed R_{rs} (λ) spectra (Mélin et al., 2011; Vantrepotte et al., 2012; Mélin and Vantrepotte, 2015). The Mahalanobis distance (Δ^2) quantifies the similarity between a given satellite spectrum $\boldsymbol{x}$ and each OWT $\boldsymbol{ic}$, and is defined as follows:

$$\Delta_{ic}^{2}(\boldsymbol{x}) = (\boldsymbol{x} - \boldsymbol{\mu_{ic}})^{T}\sum_{ic}^{-1}(\boldsymbol{x} - \boldsymbol{\mu_{ic}}) \quad \textbf{(3.2)}$$

where T indicates the transpose of the matrix.

Using these distances, the class membership probability of spectrum $\boldsymbol{x}$ for OWT $\boldsymbol{ic}$ was computed as (Mélin and Vantrepotte, 2015):

$$\boldsymbol{P_{ic}(x) = 1 - P(\Delta^2_{ic}(x), n)} \quad \textbf{(3.3)}$$

where P is the cumulative χ^2 distribution function with n degrees of freedom (corresponding to the number of spectral bands). In practice, P is defined as follows:

$$\boldsymbol{\left(\Delta^2_{ic}(x), n\right) = \frac{\gamma\left(\frac{n}{2}, \frac{\Delta^2_{ic}(x)}{\Gamma\left(\frac{n}{2}\right)}\right)}{\Gamma\left(\frac{n}{2}\right)}} \quad \textbf{(3.4)}$$

where Γ is the Gamma function and γ is the lower incomplete Gamma function (Gallego *et al.*, 2013).

The probabilities were then standardized to obtain membership values (P*), ensuring that the total sum across all OWTs equaled 1 (Mélin and Vantrepotte, 2015):

$$\boldsymbol{P^*_{ic} = \frac{P_{ic}}{\sum_{ic=1}^{Nc} P_{ic}}} \quad \textbf{(3.5)}$$

These OWT membership values were used to combine several bio-optical algorithms to estimate biogeochemical products using a probability-weighted approach (Mélin et al., 2011; Vantrepotte et al., 2012). When two algorithms are combined to estimate SPM, the final blended product is derived using the following weighted average calculation:

$$\boldsymbol{SPM = \frac{W_1 SPM_1 + W_2 SPM_2}{W_1 + W_2}} \quad \textbf{(3.6)}$$

where $\boldsymbol{W_1}$ and $\boldsymbol{W_2}$ correspond to the probability that each pixel belongs to the OWTs for which models $\boldsymbol{SPM_1}$ and $\boldsymbol{SPM_2}$ should be applied, respectively. Depending on the local water optical properties, this approach enables a smooth and adaptative transition between algorithms, ensuring optimal retrieval performance across the full range of water types present in the study area (Tran et al., 2023).

3.2.3. Ancillary data

In order to support the study of SPM dynamics in the coastal area of the APIC, as well as the observed changes in water quality between 2002 and 2022, several ancillary datasets have been considered, including land use and land cover, river discharge, precipitation, winds, currents, and waves to depict the evolution of marine and land conditions over the MODIS time period.

- **Land use and land cover**

Information on land use and cover was gathered from MapBiomas Project Collection 9.0 (https://brasil.mapbiomas.org/en/ (accessed on 1 January 2025)), which provides annual classifications of land cover and use across Brazil from 1985 to the present day. The area of interest corresponded to the land occupied by the Açu Port infrastructure. The annual land use and cover data, expressed in hectares and categorized into classes such as forest, farming, and urban areas (industrialization), were linearly interpolated to produce a monthly time series compatible with the temporal resolution of the MODIS datasets used in this study.

- **River discharge and precipitation**

Monthly river discharge data (in $m^3 \cdot s^{-1}$) for the Paraíba do Sul River were downloaded from the HIDROWEB platform, which is maintained by the Brazilian National Water Agency (Agência Nacional de Águas- ANA) and provides consistent hydrological time series for major river systems in Brazil (https://www.snirh.gov.br/hidroweb/mapa (accessed on 1 January 2025), station name, 21.6453°S, 41.7522°W). Although this station is situated inland, it was the only one available that provided continuous data covering the complete study period (2002-2022).

Monthly precipitation estimates were downloaded from NASA's Integrated Multi-satellitE Retrievals for GPM (IMERG) product (https://gpm.nasa.gov/data/directory (accessed on 1 January 2025)), which provides global precipitation data with a spatial resolution of 0.1° and a temporal frequency of 30 minutes, available from 2000 to the present. Precipitation data for the entire Brazilian territory were extracted, and a regional average was computed over the study area using a 5×5 pixel window centered on the red box shown in Figure 1. This process resulted in a monthly precipitation time series (in $mm \cdot month^{-1}$), which was used to evaluate the influence of rainfall on hydrological variability within the area of interest.

- **Currents and winds**

We used data from the Global Total Surface Currents product provided by the Copernicus GlobCurrent service (https://data.marine.copernicus.eu/product/MULTIOBS_GLO_PHY_MYNRT_015_003/ (accessed on 1 January 2025)), to analyze surface circulation in the study area. This dataset combines satellite altimetry and gravimetry (GOCE project), along with in situ observations (Rio et al., 2014). It offers consistent estimates of total surface currents, as well as their geostrophic and Ekman components, at the surface and a depth of 15 meters. The product has a spatial resolution of 1/4° (~25 km at the equator).

Wind data were obtained from the Cross-Calibrated Multi-Platform (CCMP) version 3.0 product (Mears et al., 2022), available from Remote Sensing Systems (https://www.remss.com/measurements/ccmp/ (accessed on 1 January 2025)). The CCMP v3.0 dataset provides high-resolution, gap-free, global wind vector fields at a spatial resolution of 1/4° based on satellite microwave observations blended with numerical weather prediction model outputs.

- **Significant wave height and wave period**

Significant wave height (SWH) and mean wave period (MWP) were obtained from the ERA5 monthly reanalysis (Hersbach et al., 2020), produced by the European Centre for Medium-Range Weather Forecasts (ECMWF). The dataset has a spatial resolution of 0.25° × 0.25°, covers the global ocean from 1979 to the present, and is available through the Copernicus Climate Data Store (https://cds.climate.copernicus.eu (accessed on 1 September 2025)). Wave power ($W \cdot m^{-1}$) was estimated using the finite-depth formulation, expressed as:

$$\boldsymbol{P = \frac{1}{8}\rho g H_s^2 C_g} \quad \textbf{(3.7)}$$

Where $\boldsymbol{C_g}$ is the group velocity derived from the linear dispersion relation, **Hs** is the significant wave height (m), $\boldsymbol{\rho}$ the water density (1025 kg m^{-3}), and **g** the gravitational acceleration (9.81 m s^{-2}). This parameter combines wave height and period into a single measure of wave energy, providing a physically meaningful proxy for wave-driven processes in coastal environments (Siegle and Costa, 2017; Negri and Malavasi, 2018).

3.2.4. Statistical analysis

3.2.4.1. Statistical indicators

The performance of the SPM bio-optical algorithms was evaluated using the following statistical metrics: Root Mean Square Deviation (RMSD), Median Absolute Percentage Difference (MAPD Median Ratio), slope, Coefficient of Determination (R^2), and Median Ratio (MR). These metrics were calculated by comparing model-derived and in-situ concentrations of SPM.

$$\boldsymbol{RMSD = \sqrt{\sum_{i=1}^{N} \frac{\left[log_{10}(X_i^{mod}) - log_{10}(X_i^{obs})\right]^2}{N}}} \quad \textbf{(3.8)}$$

$$\boldsymbol{MAPD = median\left[\frac{\left|log_{10}\left(X_i^{mod}\right) - log_{10}(X_i^{obs})\right|}{log_{10}\left(X_i^{obs}\right)}\right] \times 100} \quad \textbf{(3.9)}$$

$$\boldsymbol{MR = median\left(\frac{X_i^{mod}}{X_i^{obs}}\right)} \quad \textbf{(3.10)}$$

where X_i^{mod} and X_i^{mod} are the SPM in situ and model-derived concentrations, respectively.

3.2.4.2. Time series decomposition method

Monthly SPM composites were generated using daily MODIS OC-SMART data from July 2002 to December 2022. To investigate the temporal variability and long-term changes in water quality in the study area, the resulting monthly time series and the monthly data on wind, currents, river discharge, and precipitation were analyzed using the Census X11 decomposition method and the seasonal Mann-Kendall trend test.

The Census X11 method (Pezzulli et al., 2005) is widely used in ocean color studies (Cardoso Dos Santos et al., 2025; Vantrepotte and Mélin, 2011; Loisel et al., 2014; Keerthi et al., 2022) and was employed here to decompose each variable's time series *X(t)* into three additive components: a seasonal signal *S(t)*, an interannual component *T(t)*, and an irregular component *I(t)*, such that:

$$\boldsymbol{X(t) = S(t) + T(t) + I(t)} \quad \textbf{(3.11)}$$

This decomposition was performed on a pixel-by-pixel basis across the study area. This method employs an iterative application of bandpass filters and explicitly allows for interannual variability in the seasonal cycle. This makes it particularly well-suited to describing non-stationary seasonal dynamics in coastal waters (Vantrepotte and Mélin, 2011). The trend-cycle component from the X11 decomposition has been shown to effectively capture non-linear trajectories in ocean color records (Vantrepotte and Mélin, 2011), providing valuable insights into the multi-annual evolution of water quality indicators in response to environmental and anthropogenic pressures.

Interannual variability in SPM was assessed using standardized fields, obtained by dividing each SPM map by its respective long-term mean. This standardization reduces the effect of differences in absolute concentrations between pixels and emphasizes relative temporal fluctuations. This allows interannual variability to be detected independently of spatial concentration gradients.

To complement the decomposition analysis, the non-parametric seasonal Mann-Kendall test (Hirsch, Slack and Smith, 1982) was applied to each time series to detect monotonic trends, with statistical significance evaluated at the probability $p < 0.05$ level. The magnitude of the detected trends was estimated using the seasonal Sen's slope estimator (Sen, 1968) and expressed as a rate of change (RC) in percent per year.

3.3. Results

3.3.1. A combined bio-optical model for SPM estimation based on OWTs

A combined model was developed to estimate SPM concentrations by blending two existing bio-optical algorithms, based on the 5 OWTs classification performed on the in situ data set. This followed the method described in Section 2.2.2. This approach was adopted to account for the optical complexity of coastal environments, where a wide range of water types is typically encountered (Mélin and Vantrepotte, 2015). The Supplementary Material (Figure A.1) illustrates this by showing the spatial distribution of the most frequently occurring OWT class at each pixel over the study area, highlighting that the five classes adequately capture the optical diversity of the region. The two SPM inversion models selected for blending were chosen based on a comparative analysis of twelve SPM algorithms applied to optically diverse coastal waters (Subirade et al., 2024). This study, which focused on the application of the GLORIA in situ dataset to the Sentinel-3 Ocean and Land Colour Instrument (OLCI), revealed that the formulations proposed by Novoa et al. (2017) and Jiang et al. (2021) demonstrated the best overall performance. However, these models rely on spectral bands that are not available in MODIS data, specifically, the 620 nm band used by Jiang et al. (Jiang et al., 2021), and the 856 nm band used by Novoa et al. (2017). To address this limitation, alternative algorithms with reliable performance using the available MODIS bands were selected. Subirade et al. (2024) reported that the Siswanto et al. (2011) algorithm performs best in clear waters, particularly for SPM concentrations between 1 and 10 $mg \cdot L^{-1}$. Additionally, Han et al. (2016) model, in both their visible-only and NIR-inclusive versions, demonstrated consistent performance across a range of conditions and were thus suitable for use with MODIS OC-SMART bands.

These two algorithms were therefore tuned and adapted to the MODIS OC-SMART spectral bands and to the coastal OWTs. The coefficients for the Siswanto et al. (2011) algorithm were recalibrated using in situ data corresponding to OWT classes 1 to 3, representing oligotrophic to mesotrophic waters. For OWT classes 4 and 5, which correspond to turbid waters, we applied the NIR-based approach from Han et al. (2016). This approach performs

well in high-SPM conditions due to the strong relationship between NIR reflectance and suspended particle backscattering (Doxaran et al., 2002; Nechad et al., 2010).

The adapted version of the Siswanto et al. (2011) algorithm ($R^2 = 0.66$, N =185) for MODIS OC-SMART ($\boldsymbol{SPM_S}$) is expressed as follows:

$$\boldsymbol{log_{10}\, SPM_S = 0.7752 + 15.994\left(R_{rs}(547) + R_{rs}(667)\right) - 0.7103\left(\frac{R_{rs}(488)}{R_{rs}(547)}\right)} \quad \textbf{(3.12)}$$

The NIR-based model from Han et al. (2016) has been adapted for use with MODIS OC-SMART ($\boldsymbol{SPM_{NIR}}$) and uses water-leaving reflectance at 748 nm ($R^2 = 0.79$, N = 304). It is given by the following formula based on previous work from Nechad et al. (2010):

$$\boldsymbol{SPM_{NIR} = \frac{2181.029 \times R_w(748)}{1 - \frac{R_w(748)}{0.3852}}} \quad \textbf{(3.13)}$$

where: $\boldsymbol{R_w(748) = \pi R_{rs}(748)}$.

The final SPM estimate is obtained by combining the two models using the OWTs probabilities as described in section 3.2.2.2:

$$\boldsymbol{SPM = \frac{W_1 SPM_S + W_2 SPM_{NIR}}{W_1 + W_2}} \quad \textbf{(3.14)}$$

where $\boldsymbol{W_1 = p_{OWT_1} + p_{OWT_2} + p_{OWT_3}}$, and $\boldsymbol{W_2 = p_{OWT_4} + p_{OWT_5}}$, each belonging probabilities to **OWT₁** to **OWT₅**, being computed from the equation (5). The combined model was validated using both in situ and satellite-derived R_{rs} (λ) data.

Figure 3.4 shows the results of validating the combined model (Siswanto et al., 2011; Han et al., 2016) using in situ (Figure 3.4a) and OC-SMART satellite-derived reflectance data (Figure 3.4b). The model shows a strong correlation between the estimated and measured SPM values in the in situ dataset ($R^2 = 0.80$, slope = 0.94), with relatively low error metrics (RMSD = 0.28, MAPD = 18.91%). These results confirm the robustness of the combined approach across a wide range of optical water types, particularly in turbid conditions (OWT 4 and 5).

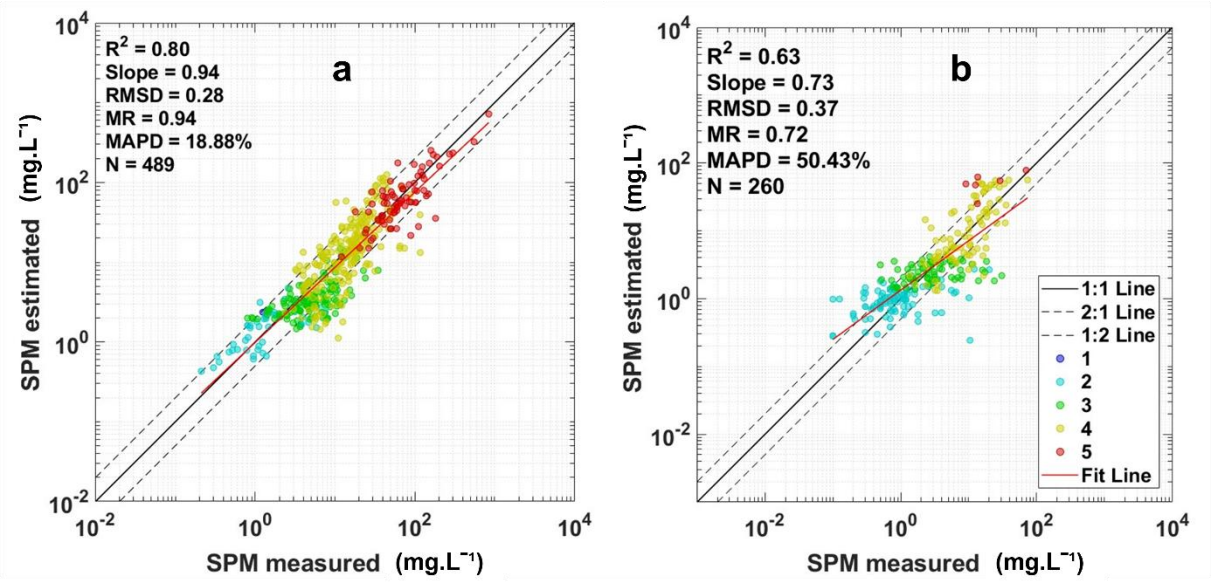

Figure 3.4. Validation of the new inversion algorithm for estimating SPM from R_{rs} (λ): Siswanto et al. (Siswanto et al., 2011)and Han et al. (Han et al., 2016) combination based on optical water types (OWT 1-3 and 4-5, respectively). (a) in situ validation, (b) satellite matchup validation (MODIS - OC-SMART).

Satellite-based validation using OC-SMART shows slightly lower performance ($R^2 = 0.63$, slope = 0.73), with greater dispersion (MAPD = 50.43%). This degradation is expected due to the additional uncertainties associated with atmospheric correction and satellite-derived reflectance. Nevertheless, the model still provides a reasonable estimate of SPM concentrations in coastal waters, demonstrating its potential for large-scale monitoring.

This new combined model was then applied to 20 years of MODIS OC-SMART data (2002–2022) in order to estimate the dynamics of SPM in Brazilian coastal waters over the last two decades.

3.3.2. Spatio-temporal dynamics of SPM

3.3.2.1. SPM seasonal variation

The seasonal distribution of SPM in the study area is illustrated by monthly average maps derived from MODIS-Aqua data processed with OC-SMART (1 km resolution, 2002-2022). Figure 3.5 shows the average SPM concentrations in the austral winter (e.g. July) and summer (e.g. December) months. Overall, SPM concentrations are higher during the austral winter, with elevated levels extending farther offshore than in summer. Near the coast, higher concentrations are likely due to enhanced resuspension processes. In both seasons, the highest concentrations are consistently observed near the coast, decreasing towards the open sea. Coefficient of variation (CV) maps (Figures 3.5c-d) show relatively low temporal variability across most of

the shelf domain (CV < 40%), which further indicates persistent seasonal patterns over the 20-year period.

The discharge of the Paraíba do Sul River shows no significant correlation with SPM dynamics within the APIC at Point A (Figure 3.5) assessed using spearman correlation (r), ($r = -0.2$, $p<0.05$, $N = 246$). Moderately elevated concentrations are observed near the river mouth (≥ 10 mg. L⁻1; Figure 3.5a–b), likely due to localized inputs. However, the overall contribution is minimal as the flow of the river is heavily regulated to supply urban areas with water, generate hydroelectric power, and support agriculture, despite being one of Brazil's largest rivers (Lämmle et al., 2022; Ioris, 2008; Cavalcanti and Marques, 2016; de Oliveira et al., 2023). Consequently, sediment transport from land to sea via the river is substantially reduced.

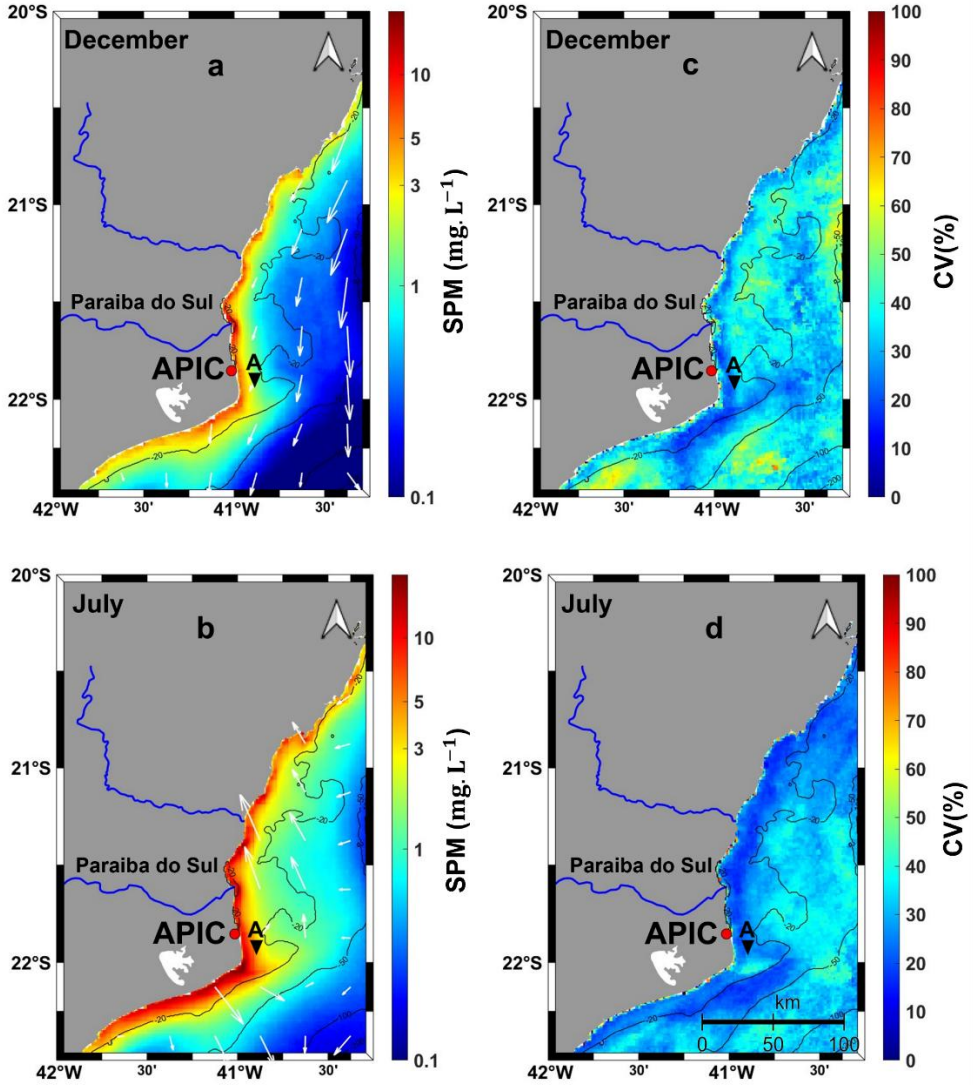

Figure 3.5. (a, b) Satellite-derived monthly mean surface suspended particulate matter (SPM) concentrations (mg. L⁻¹) from MODIS OC-SMART (2002-2022) illustrating SPM distribution during (a) austral summer (e.g. December) and (b) austral winter (e.g. July). (c, d) Coefficient of variation (%) of SPM concentrations during (c) austral summer (December) and (d) austral winter (July). White arrows represent current circulation during (a) austral summer (December 2019) and (b) austral winter (July 2019).

The X11 seasonal variation of SPM (Figure 3.6) appears to be positively correlated with the X11 seasonal variation of the meridional (V) component of surface currents and wind within the APIC. Higher SPM concentrations coincide with positive values of the V component, indicating enhanced northward transport during periods of elevated SPM.

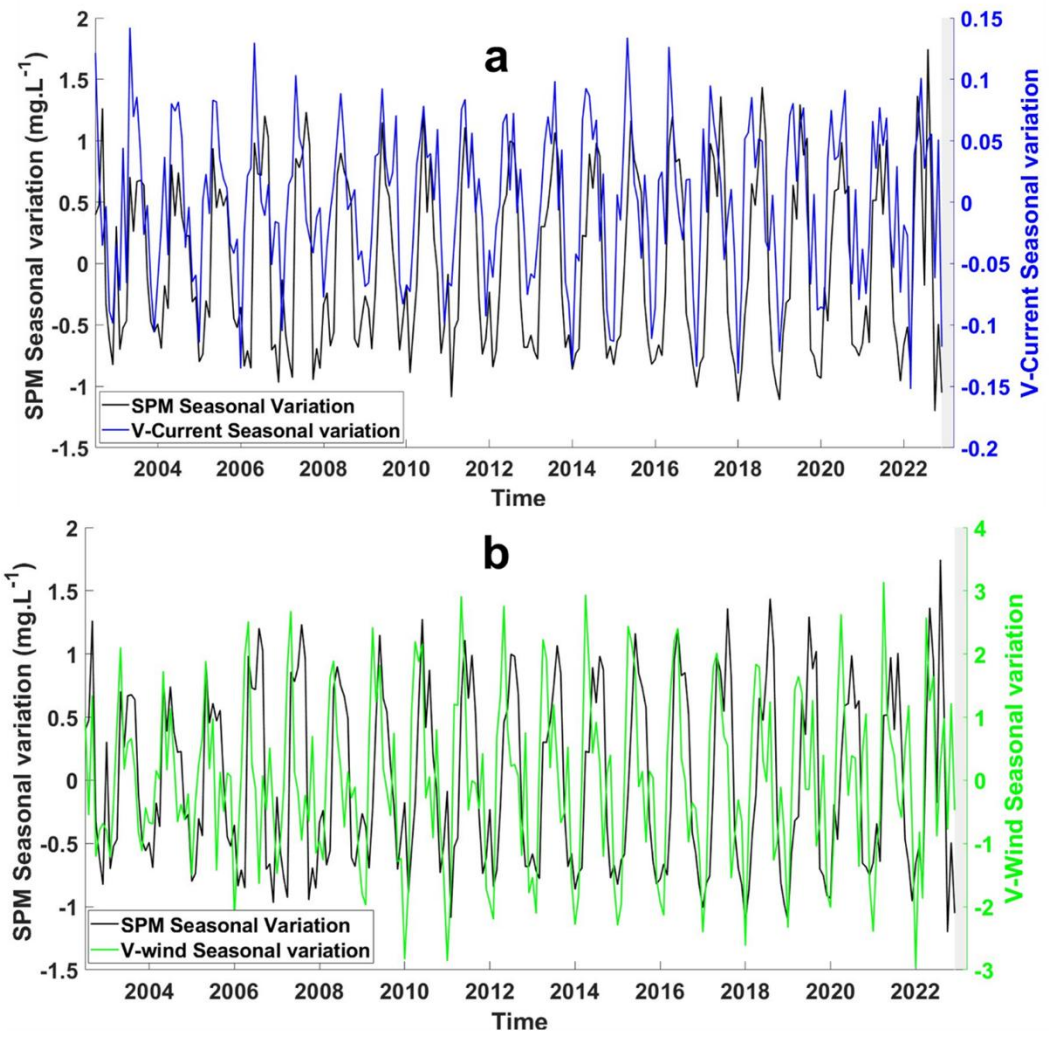

Figure 3.6. (a) Time series of Seasonal variation (X11 outputs) of SPM (black), meridional current (blue), (b) Time series of Seasonal variation (X11 outputs) of SPM and meridional wind (green) extracted at Point A, located offshore (20 m depth) the Açu Port (Figure 3.5a).

However, the correlation between SPM seasonality and seasonal variation of the meridional wind component ($r = 0.43$, $p<0.001$, $N = 246$) was weaker than with the meridional component of surface currents ($r = 0.65$, $p<0.001$, $N = 246$), highlighting the dominant role of current-driven transport relative to direct wind forcing. The seasonal component of wave power also shows a strong positive correlation with the seasonal variation of SPM ($r = 0.70$, $p < 0.001$, $N = 246$; Figure A.2), indicating that wave-induced resuspension contributes substantially to the observed seasonal signal.

In contrast, the zonal (U) component exerts little influence on SPM variability. There was no correlation found between SPM seasonality and the zonal current component ($r = –0.1$, $p>0.1$, $N = 246$), which indicates that east–west advection does not contribute to SPM transport in the APIC. Similarly, the zonal wind component showed only a moderate correlation with SPM ($r = 0.37$, $p<0.05$, $N = 246$), Correlation maps of seasonal SPM with the seasonal components of currents and winds (see Supplementary Material, Figure A.3) confirm these patterns spatially. The maps highlight a robust and coherent positive correlation between SPM and the meridional current across the APIC, supporting the dominance of northward transport processes.

In addition, the seasonal component of precipitation, extracted using the X11 method exhibits a clear seasonal pattern and shows a negative correlation with the seasonal component of SPM at point A, which is located next to the APIC ($r = –0.64$, $p<0.05$, $N = 246$) (see Supplementary Material, Figure A.4). This inverse relationship suggests a dilution effect associated with increased rainfall.

3.3.2.2. SPM interannual variability

Figure 3.7 shows the annual average of monotonic trends in SPM observed from MODIS data gathered across the study area between 2002 and 2022.

Figure 3.7 displays the significant monotonic trends ($p < 0.05$) observed from the analysis of 20 years of monthly SPM data from MODIS (in $\%.year^{-1}$). The most pronounced and persistent increases were located immediately offshore of the APIC, with hotspots extending along the 20-50 m isobaths to the south and southeast of the port area. In this area, SPM increased by 20-60% between 2002 and 2022. By contrast, the mouth of Paraíba do Sul River showed a slight decrease in SPM (~10%) over the 20-year period, with only a few pixels in front of the river exhibiting a restricted but significant downward trend, which is consistent with previous studies (Ovalle et al., 2013; Lämmle et al., 2022).

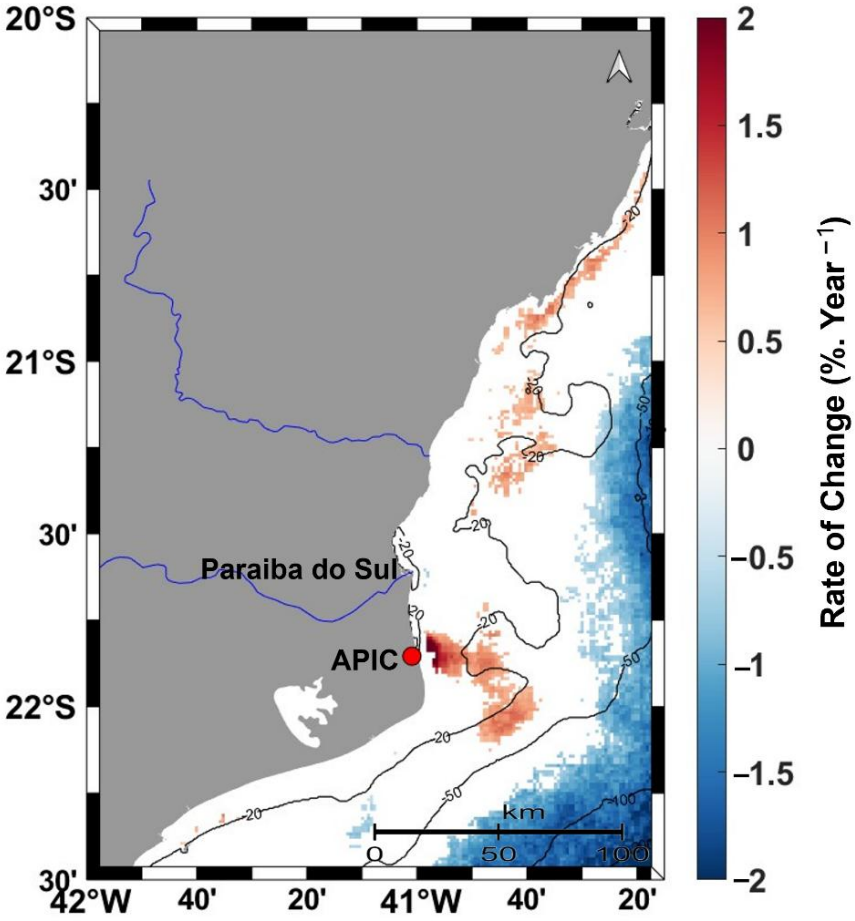

Figure 3.7. Temporal Rate of Change (RC) in SPM between 2002-2022 within the study area, showing only statistically significant changes ($p < 0.05$).

Decreasing SPM patterns were observed offshore in oceanic water (bathymetry > 50 m), which is probably related to oceanic processes that are beyond the scope of this study. The significant increase in SPM from 2002 to 2022 observed in front of the Açu Port area (Figure 3.7) is detailed in Figure 3.8a. Figures 3.8b and 3.8c show the corresponding time series: Figure 3.8b represents the raw SPM, while Figure 3.8c shows the standardized interannual variation derived from the X11 decomposition. Both figures are averaged over the area in Figure 3.8a where a significant increase was detected ($RC > 0$, $p < 0.05$, $N = 246$).

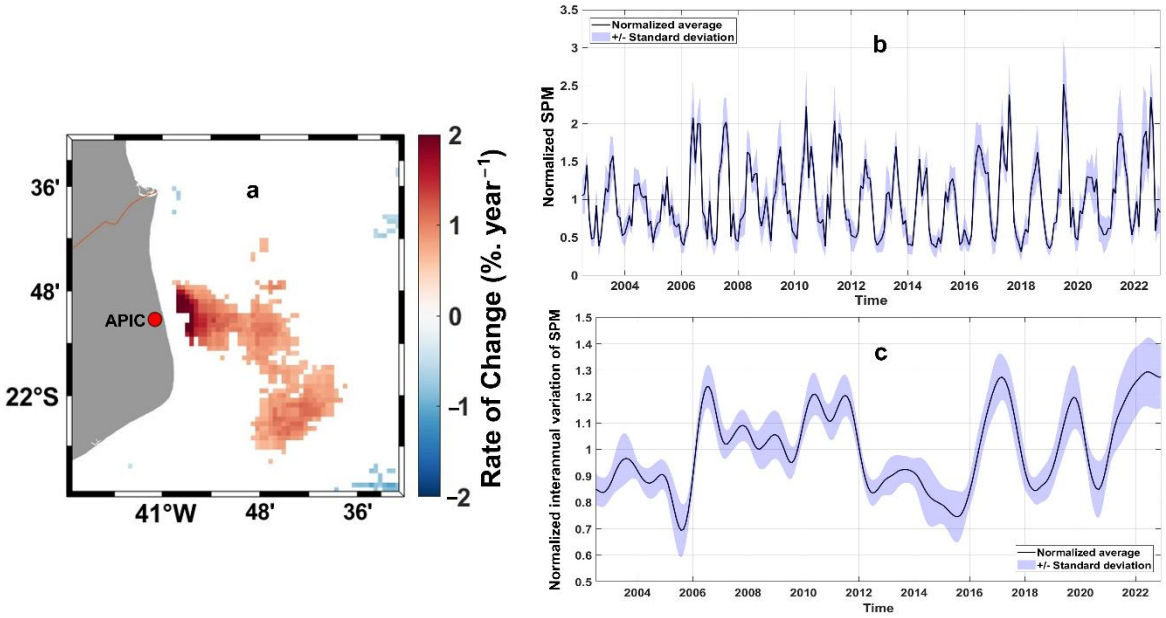

Figure 3.8. (a) Map showing the spatial extent of the surface area used for extracting the time series. (b)Time series of the raw SPM (c) and Census X11 interannual term from 2002 to 2022, both (b and c) averaged over the area within the Açu Port where the RC is positive (RC > 0) and statistically significant ($p < 0.05$, N = 246).

To evaluate whether the increasing SPM trend detected near the APIC could be influenced by uncertainties in the satellite retrievals, a Monte Carlo error-propagation analysis was performed (the distribution of simulated trends is shown in Supplementary Materials, Figure A.5). Retrieval errors were first quantified using the MAPD value (50.4%) computed from the matchup dataset by comparing in situ and satellite-derived SPM values. Based on this error metric, 1000 perturbed monthly SPM series were generated by adding random noise to the original time series (Nguyen et al., 2024; Tran et al., 2025). The noise level was defined by a normal distribution with a mean of 0 and an effective standard deviation (σ_{eff}).

$$\sigma_{eff} = MAPD/\sqrt{N_{eff}} \quad (3.15)$$

where N_{eff} is the effective number of independent observations contributing to each monthly value (National Research Council, 2011). In this case, N_{eff} was set to 30, corresponding approximately to one independent observation per day. For each simulation, the Seasonal Mann–Kendall test and Sen's slope were recomputed, yielding 1000 estimates of the long-term RC.

Near the APIC hotspot (Figure 3.8a), SPM increased by 20‑60% between 2002 and 2022, while the spatially averaged RC reached 0.82%. year^{-1} (~+16% over 20 years). The Monte Carlo ensemble produced a mean RC of 0.80%. year^{-1}, which is nearly identical to the original estimate (bias = −0.02%. year^{-1}), with a 95% confidence interval of 0.67–0.94%. year^{-1}. The

perturbed trends showed a mean absolute relative error of 7.2%, and all simulated Sen slopes remained positive. These results demonstrate that realistic retrieval uncertainties cannot reverse the trend and only marginally affect the magnitude of the observed long-term increase in SPM near the APIC.

The spatial correlation map between the interannual variation of SPM across the entire study area and the reference time series extracted from the Açu Port region (where statistically significant increases in SPM were observed) (Figure 3.9a) reveals a coherent spatial pattern over a larger spatial area. High correlation values ($r > 0.8$, $p<0.001$, $N = 246$) are concentrated near the APIC area, indicating that SPM dynamics in this zone closely follow those observed at the port. Further north, the correlation gradually decreases but remains positive, suggesting that SPM variability in northern coastal waters may be influenced by similar drivers. This spatial continuity implies a possible northward propagation of SPM-related changes, which may be linked to hydrodynamic processes such as coastal currents or wind-driven transport. This could indicate that the influence of APIC-related activities extends beyond the immediate vicinity of the port. Indeed, trend analyses suggest a slight increase of SPM towards this northern area (Figure 3.9b), although this is not statistically significant.

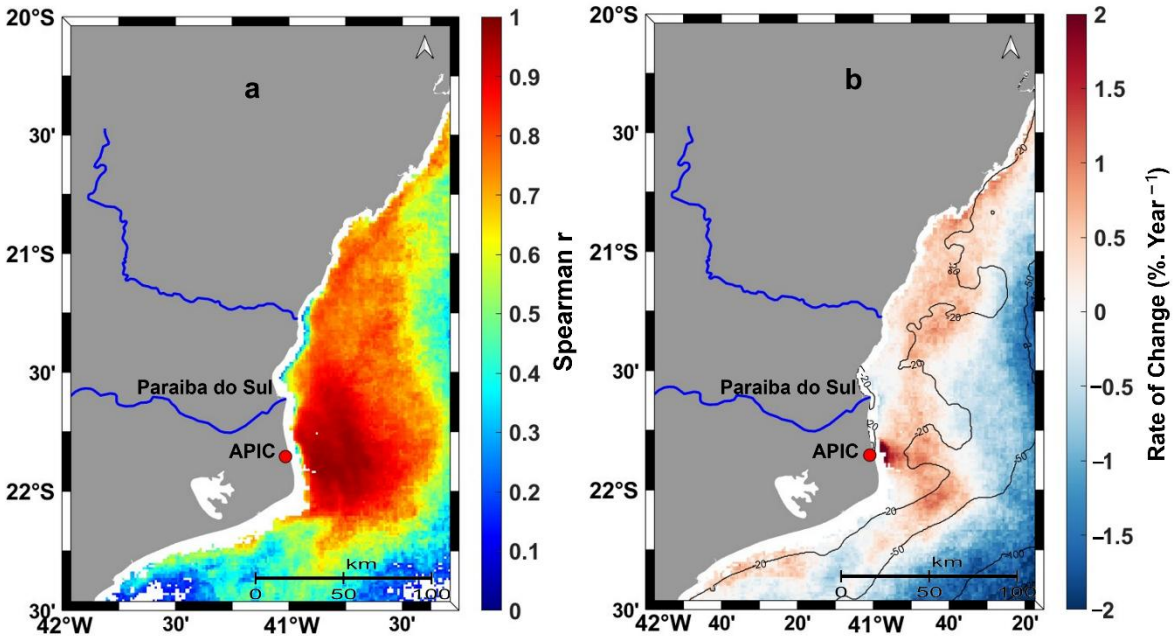

Figure 3.9. (a) Correlation map ($p < 0.05$, $N = 246$) between the interannual variation of SPM in the entire study area and the referenced time series of interannual variation extracted from the Açu Port region exhibiting significant SPM increase shown in Figure 8c. (b) RC of SPM including both significant and non-significant variations.

3.3.3. Evolution of the environmental conditions

3.3.3.1. Land use and cover

The land cover and use maps for 2002 and 2022 (Figure 3.10), derived from the MapBiomas platform, illustrate the profound transformation of the coastal landscape following the construction of the APIC, from late 2006/early 2007 to 2014. Before the development of the port in 2002, the area was characterized by natural features such as beach dunes, herbaceous-shrub vegetation, and forest patches, interspersed with small farming zones. The region exhibited minimal urban occupation, with water bodies limited to natural lagoons and river channels (Figure 3.10a). By contrast, the 2022 map reveals extensive changes in land cover, driven by the expansion of industrial and urban infrastructure associated with the APIC (Figure 3.10b). This transformation includes the construction of artificial water bodies, storage areas, access roads, and industrial facilities. Concurrently, natural landscapes such as dunes and herbaceous vegetation have partially given way to industrial land use and urban development.

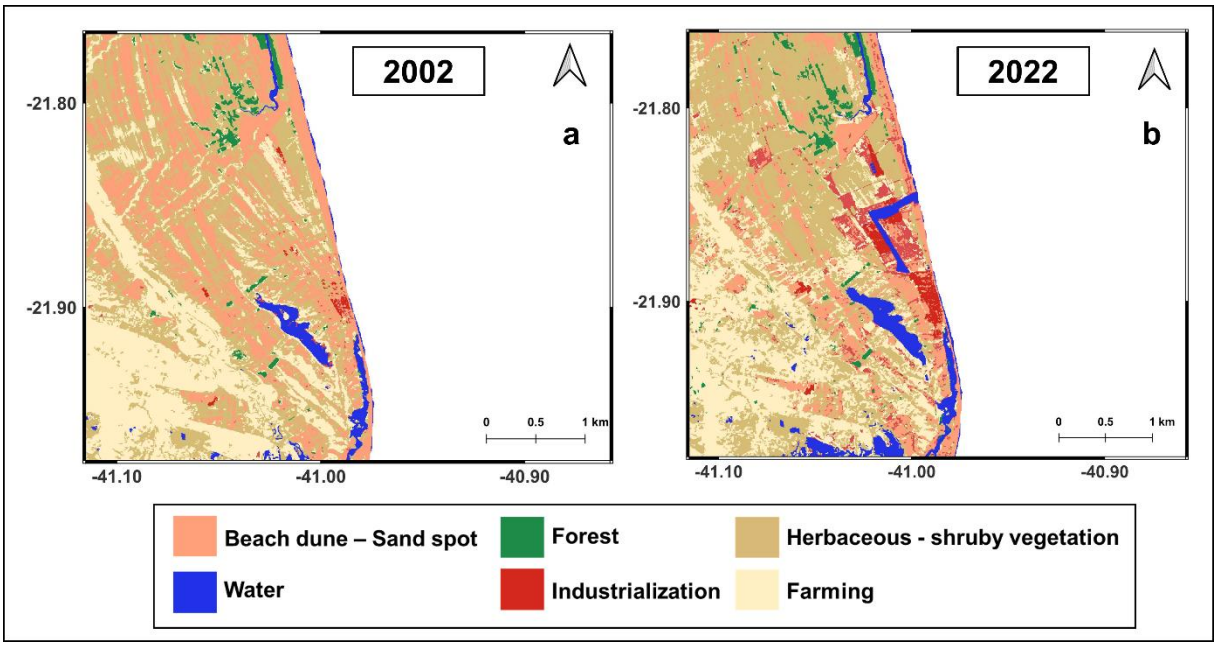

Figure 3.10. Land use and land cover maps for the years 2002 and 2022 within the Açu Port (MapBiomas)). (a) 2002 land cover map, (b) 2022 land cover map.

3.3.3.2. Combined impact of industrialization and environmental forcings on the regional SPM dynamics

Analysis of SPM interannual variation in relation to APIC's industrial development reveals three distinct phases: pre-port, construction and operational (Figure 3.11).

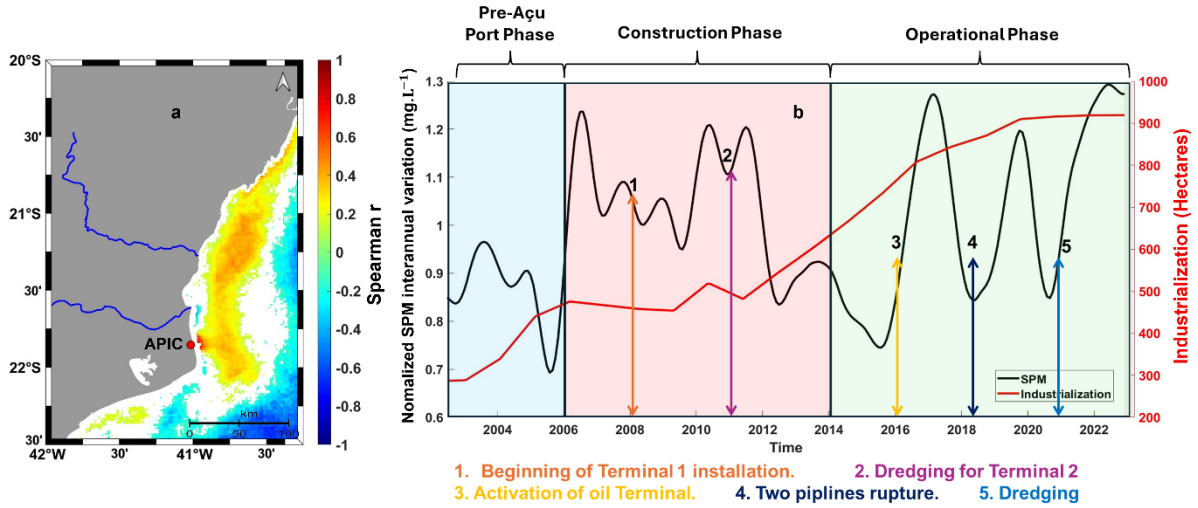

Figure 3.11. Impact of industrialization (Açu) on the SPM variation. (a) Correlation map between industrialization and SPM interannual variation between 2002 and 2022. (b) Time series of the interannual variation of SPM (black) and the industrialization growth (red).

A clear connection can be observed between port activity and SPM dynamics (Figure 3.11b), which can be summarized as follows:

- **2002 - 2006, Pre-Açu Port Phase:** industrial activity in São João da Barra was minimal, with around 300 hectares of industrialized land. SPM levels remained relatively stable and low, reflecting limited anthropogenic disturbance.
- **2006 - 2014, Construction Phase:** significant dredging activities began as port infrastructure took shape. The installation of Terminal 1 (T1) began in 2008 and involved around 20 million m³ of dredged material. This was followed by the construction of a 3 km bridge and a breakwater. In 2011, dredging for Terminal 2 (T2) commenced, totaling ~65 million m³ of sediments (Porto do Açu, 2021). Despite a moderate increase in the industrial area (to ~500 hectares by 2012), SPM levels showed marked increase in interannual variability starting in 2007, likely due to sediment resuspension and coastal disturbance. Elevated SPM levels persisted throughout this phase, peaking between 2008 and 2012.
- **2014 - 2015, Early Operational Phase:** industrialization accelerated, with the industrialized area expanding from ~500 hectares in 2012 to over 900 hectares by 2022, representing nearly 40% of the municipality (Vilani et al., 2021). SPM levels decreased slightly between 2014 and 2015, possibly due to a reduction in dredging intensity and the stabilization of port infrastructure.
- **2016, Intensification of Operations:** SPM concentrations increased again, corresponding to the activation of the T-OIL terminal and the onset of intense traffic

from Very Large Crude Carriers (VLCCs) (Porto do Açu, 2016). In the same year, the T1 deepening permitting process introduced the Adaptive Dredging Plan, combining dredging operations with spatial zoning to enhance sediment management. The works were scheduled over 15 months (Porto do Açu, 2021).

- **2018, Pipeline Ruptures:** according to Technical Report 21 282-301 (Ministério Público do Estado do Rio de Janeiro, 2021), two pipeline ruptures occurred in March 2018, leading to a temporary suspension of operations. A significant drop in SPM levels was observed that year, likely linked to the rupture events. When operations resumed in December 2018, SPM levels remained below those of 2016 levels but began to rise alongside the increase in industrial activity.
- **2021 - 2022, Maintenance Dredging and Peak SPM:** SPM levels rose again, coinciding with large volumes of sediment deposition totaling 676,000 m³ at T1 (88% fluid mud) and 938,300 m³ at T2 (76% fluid mud). This period also saw the implementation of maintenance dredging and sediment management strategies to mitigate siltation, particularly during periods of heavy rainfall, which were identified as key drivers of erosion and sediment transport based on monitoring data collected between January 2021 and October 2022 (Lima et al., 2024).

Figure 3.11a shows the spatial correlation between the interannual variation of SPM and the progression of industrialization in the Açu region. The strongest positive correlations are observed in the waters adjacent to the Açu Port, suggesting that industrial activities have significantly impacted sediment dynamics in the immediate vicinity of the port. Notably, the influence predominantly extends towards the north, as evidenced by a clear northward gradient of high correlation values. This pattern suggests that sediment transport processes favor the northward dispersion of suspended material, amplifying the industrial impact in this direction. This is also indicated by the correlation between the SPM X11 time series in the area (showing a significant increase in front of the Açu Port) and the SPM interannual pattern in the northern part of this coastal domain (Figure 3.9a), as well as by the presence of a slight increase in SPM over the 2002–2022 time period in the corresponding area (Figure 3.9b).

To explain the regional interannual dynamics of SPM, we compared the Census X11 interannual components of SPM, wind, currents, and waves. Monotonic trend analysis revealed no significant long-term trends in the wind components or wave power within the study area ($p > 0.05$), while the currents showed a few patchy and contradictory trends that were not aligned

with the significant increase in SPM. This indicates that the observed rise in SPM cannot be explained by persistent changes in natural hydrodynamic regimes.

Correlation analysis of the X11 interannual component of SPM and hydrodynamic drivers reveals a distinct asymmetry in the potential impact of currents, winds, and waves (Figure 3.12). Currents have little effect: neither the meridional (V) nor the zonal (U) com-ponents are significantly correlated with SPM at the interannual scale between 2002 and 2022 near the port (point A, Figure 3.12a, b), while correlations in the northern area are weak, patchy, and inconsistent across space.

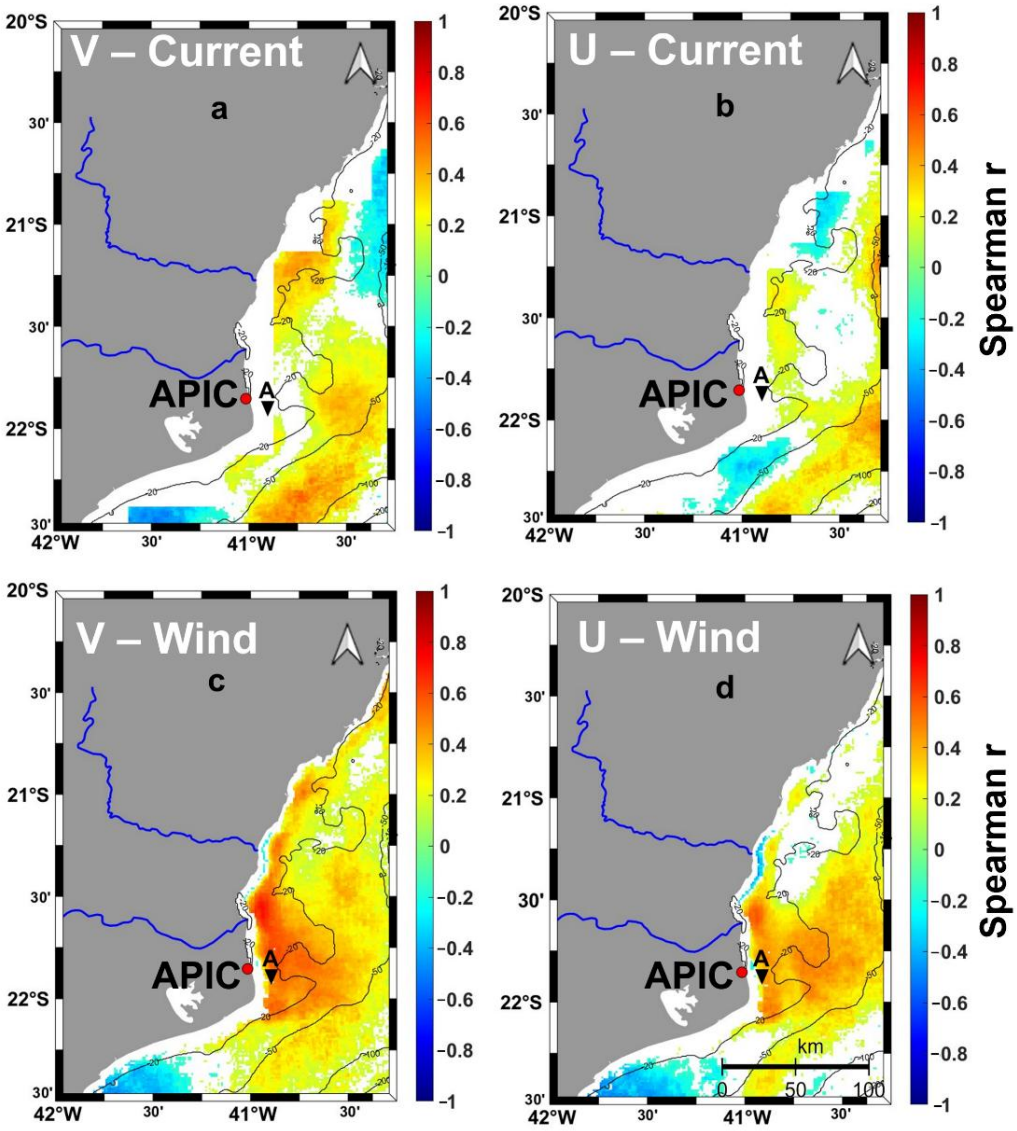

Figure 3.12. Correlation maps between interannual components of SPM, wind and current. (a) correlation map between the interannual component of SPM and meridional current (V). (b) correlation map between the interannual component of SPM and zonal current (U). (c) correlation map between the interannual component of SPM and meridional wind (V). (d) correlation map between the interannual component of SPM and zonal wind (U). Only significant correlations ($p < 0.05$, $N = 246$) are shown.

In contrast, winds exhibit stronger interannual correlations with SPM, particularly in shallow waters (< 20 m). The meridional (V) wind component is especially influential (Figure 3.12c), which is consistent with the recurrent northward dispersion of turbid waters ($r > 0.5$, $p < 0.001$, $N = 246$). This indicates that enhanced SPM concentrations are consistently associated with northward coastal transport at the interannual scale. The zonal (U) wind component (Figure 3.12d) also plays a role, exhibiting moderate positive correlation offshore of the APIC ($r > 0.4$, $p < 0.001$, $N = 246$).

The interannual component of wave power also shows a moderate but significant correlation with SPM variability ($r = 0.30$, $P<0.05$, $N = 246$) Figure A.6).

The role of the meridional components of winds and current is further illustrated by the time series at Point A (Figure 3.13). The V-current fluctuates around zero, with weak interannual signals; however, peaks in SPM often coincide with periods of northward flow in the raw signal, indicating their seasonal influence. In contrast, the V-wind shows a much stronger correspondence with SPM variability: northerly winds consistently align with elevated SPM levels, confirming their role in modulating and transporting sediments northward. Occasional lags between wind or current (1 to 2 months) changes and SPM peaks suggest sediment remobilization or delayed transport, as observed in other coastal systems (Dogliotti et al., 2016; Mazzini et al., 2025).

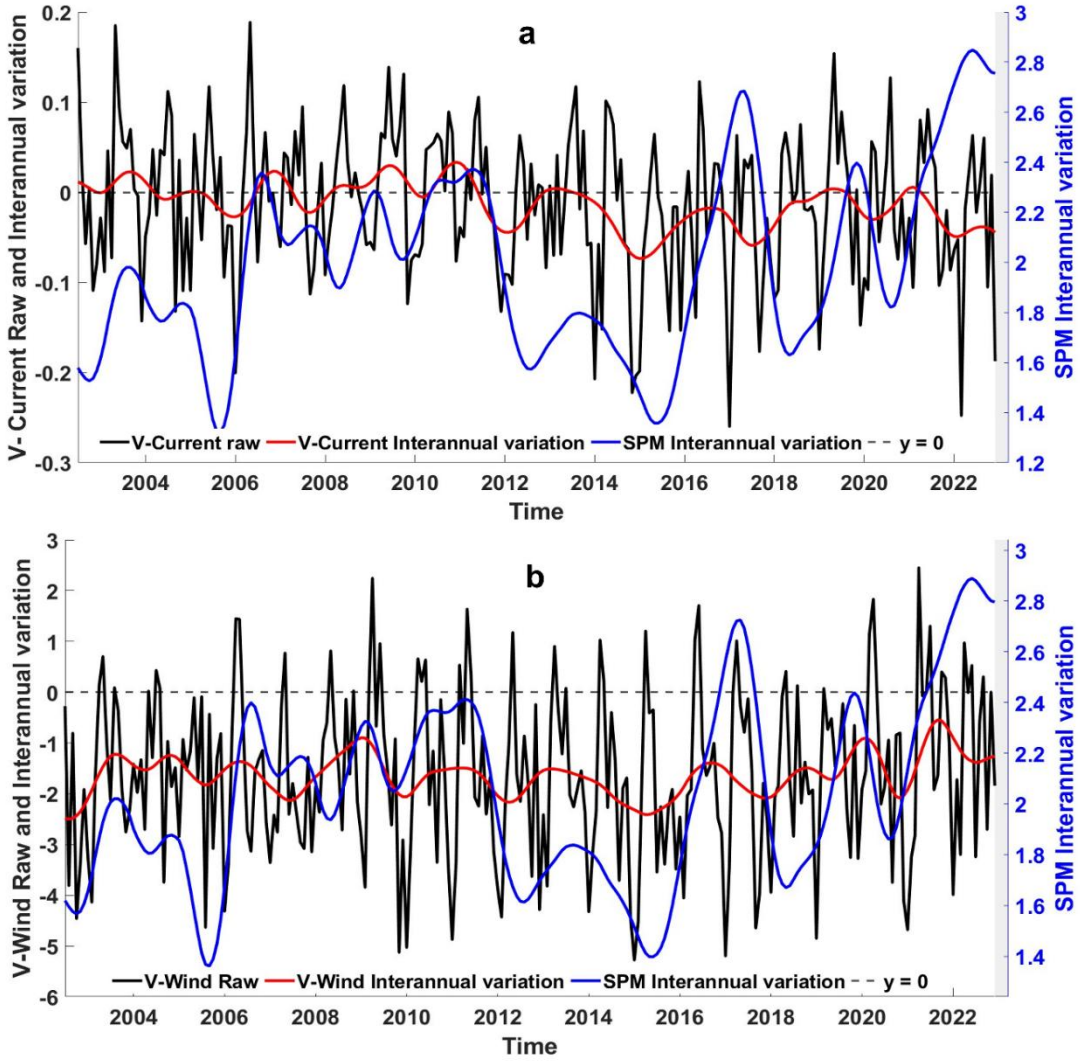

Figure 3.13. (a) Time series of the interannual variation of SPM (black) and interannual variation of V current (red) at point A parallel to the APIC. (b) Time series of the interannual variation of SPM (black) and interannual variation of V wind (red) at point A parallel to the APIC (bathy = 20 m).

3.4. Discussion

3.4.1. A combined bio-optical model for SPM estimation based on OWTs

A new combined bio-optical model has been developed for the application of MODIS in a case study of the Açu Port area. A key advantage of this method is its OWT-based structure (Vantrepotte et al., 2012; Carvalho et al, 2014), which has been trained using the GLORIA marine coastal dataset. This allows the model to be applied reliably even in regions lacking in situ data, provided that the optical conditions match those of the training OWTs. The performance of the combined model is consistent with values typically reported for SPM retrievals in coastal waters. In situ validation (Figure 3.4a) falls within the upper range of what

has been achieved in previous algorithm evaluations using multispectral sensors (R^2 = 0.80; MAPD ≈ 19%). Similar levels of agreement have been reported for SPM retrievals in turbid environments, with R^2 typically ranging from 0.70 to 0.85 (e.g., (Novoa et al., 2017; Jiang et al., 2021; Han et al., 2016)). These results indicate that the OWT-based combination performs reliably within its intended optical domain.

The reduced performance of satellite matchups (Figure 3.4b; R^2 = 0.63; MAPD ≈ 50%) is consistent with previous studies, which suggest that atmospheric correction and sensor-specific limitations generally result in weaker correlations than those obtained through direct in situ reflectance. Several studies report R^2 values between 0.50 and 0.70, as well as relative errors often exceeding 40%, for MODIS and OLCI in coastal and estuarine waters (Nechad et al., 2010; Han et al., 2016; Subirade et al., 2024). Such degradation is typical in highly dynamic regions with strong turbidity gradients and complex particulate assemblages. In this context, the performance achieved here remains within the expected range for regional-scale applications. Overall, the results demonstrate that combining two adapted SPM formulations through OWT probabilities improves the robustness of the algorithm while maintaining accuracy that is comparable to, or better than values reported for similar coastal environments. This approach is therefore suitable for analyzing long-term SPM dynamics from MODIS OC-SMART.

In this study, we used the GLORIA dataset (Lehmann et al., 2023) because it provides broad optical coverage representative of coastal and shelf waters, consistent with the conditions observed around the Açu Port region (Figure A.1). The recently published data BRAZA (Maciel et al., 2025), covering mostly inland waters, might complement the GLORIA data set and further enable the development of SPM inversion model adapted to applications along the land-sea continuum and will represent the objective of future studies.

3.4.2. Spatio-temporal dynamics of SPM

The spatio-temporal patterns of SPM revealed by MODIS-Aqua and the Census X11 decomposition indicate that seasonal hydrodynamics, interannual variability, and human activities jointly control suspended sediment dynamics in the APIC region. Seasonal analyses show systematically higher SPM concentrations during austral winter, with enhanced offshore extension and a clear northward gradient along the coast, whereas interannual analyses highlight a marked long-term increase in SPM immediately offshore of the Açu Port, particularly after the onset of port construction. Together, these observations point to a system where natural forcing defines the short-term variability while anthropogenic pressures

progressively reshape the long-term baseline. These changes occur in the context of profound land-use transformation and rapid industrial development along the northern coast of Rio de Janeiro.

The circulation in the study area is influenced by both mesoscale and coastal processes. At the mesoscale, the region is affected by the southward flow of the Brazil Current (BC), which transports warm surface waters along the southeastern coast of Brazil (Castro and Miranda, 1998; Brandini et al., 2018). Seasonal reversals may occur during the austral winter (Figure 3.5), when coastal currents can flow northward (Scheel et al., 2023). On the inner shelf, circulation is mainly wind-driven: NE winds promote south-eastward flow, while southerly winds associated with cold fronts can reverse this pattern (Cassar and Neves, 1993). The alternating wave climate generates longshore sediment transport in opposite directions depending on the season, a process long recognized as key in shaping coastal plains in southeastern Brazil (Dominguez et al., 1983; Bastos and Silva, 2000). These hydrodynamic regimes provide the physical framework within which SPM is mobilized, redistributed, and exported.

3.4.2.1. Seasonal variation of SPM and environmental forcings

The moderate correlation between the seasonal variation of SPM and seasonal variation of V wind (Figure 3.6b) compared to the good correlation of SPM with V current (Figure 3.6a), suggests that wind forcing primarily acts as a trigger, while the effective seasonal redistribution of suspended material is controlled by the dynamics of surface currents (Qiao et al., 2016; Lopez-Gamundi et al., 2024). Similar delayed responses have been documented, where wind-induced perturbations require time to evolve into established circulation patterns through mesoscale instabilities (Kobashi and Kawamura, 2002). Thus, the weaker wind–SPM relationship compared to the stronger current-SPM relationship is consistent with a temporal lag between wind variability and SPM seasonality, as illustrated in the climatological averages of wind, current, and SPM shown in the Supplementary Material (Figure A.6). This lagged response underscores the importance of cumulative hydrodynamic adjustments rather than instantaneous forcing.

This northward transport coincides with periods of elevated SPM concentrations within the coastal domain, as illustrated in Figure 3.5b, and likely contributes to the broader dispersion of suspended material observed primarily northward along the coast during the winter months, possibly due to resuspension processes and riverine inputs. Coastal winds predominantly blow from the northeast but tend to shift towards the south, southeast, and southwest in austral

autumn and winter (Dereczynski et al., 2019; Lämmle and Bulhões, 2019; Lämmle et al., 2022). This further promotes northward coastal circulation through Ekman transport, influencing nearshore current patterns and sediment dynamics. The seasonal alignment between enhanced meridional circulation and elevated SPM thus suggests a strong coupling between hydrodynamic forcing and sediment redistribution (Green and Coco, 2014).

The good correlation of seasonal SPM with seasonal variation of wave power (Figure A.2) highlights the role of surface waves in enhancing sediment resuspension (Green and Coco, 2014; Siegle and Costa, 2017; Li et al., 2020), particularly during periods of increased wave energy in austral winter (Castro et al., 2025). In contrast to wind, which primarily acts as a trigger for circulation variability, waves directly mobilize bottom sediments in the coastal and inner-shelf domains. This resuspension elevates nearshore SPM concentrations, which can be subsequently redistributed by northward coastal currents, reinforcing the seasonal pattern of higher wintertime SPM levels. This two-step mechanism wave-driven resuspension followed by current-driven transport is consistent with sediment dynamics observed in other energetic coastal systems (Green and Coco, 2014; Qiao et al., 2016; Liu et al., 2018).

The limited correlation of seasonal SPM with seasonal variation of zonal wind and currents (Figure A.3b-d) suggests that it plays a limited role in modulating SPM dynamics compared to the dominant effect of meridional processes. By contrast, the relationship with the meridional wind is more fragmented and restricted to specific sectors, which is consistent with its weaker and more indirect influence. In contrast, correlations with the zonal current are spatially incoherent and close to zero across most of the region, which reinforces the negligible role of east-west advection. The zonal wind displays slightly more structured patterns than the zonal current, but its influence remains weak compared to that of the meridional processes. Overall, the correlation maps (Figure A.3) indicate that SPM seasonality in the APIC is primarily governed by northward transport.

The seasonal variability of precipitation is negatively correlated with SPM seasonality within the APIC (Figure A.4). This relationship is likely to be driven by a dilution effect: increased rainfall reduces concentrations of particles in surface waters by increasing the input of fresh water and limiting the resuspension of sediment (Rose and Karwan, 2021). Such dilution effects have also been described in coastal systems where enhanced rainfall reduces suspended sediment concentrations by increasing freshwater input and stabilizing the water column(Ovalle et al., 2013; Dogliotti et al., 2016; Rose and Karwan, 2021).

3.4.2.2. Interplay between port development and environmental forcing in shaping SPM interannual variability

The long-term MODIS analysis, based on the seasonal Mann-Kendall test and Sen's slope estimator, reveals a marked and spatially coherent increase (20 - 60%) in SPM in the vicinity of the APIC (Figure 3.7). The concentration of significant positive trends around the APIC indicates that the increase in SPM is limited to the port-influenced coastal area, rather than affecting the wider region. Such a pattern is typical of areas where maritime infrastructure alters hydrodynamics, enhances resuspension, and increases sediment availability (Wang and Andutta, 2013; Prumm and Iglesias, 2016; Guarnieri et al., 2021). In contrast, the lack of comparable positive trends near the Paraíba do Sul River suggests that changes in fluvial supply are not the main driver.

The nonlinear interannual modulation of SPM reveals a clear shift in the sediment regime of the APIC region. SPM concentrations were at their lowest before the onset of port construction in late 2006 / early 2007. After this period, a gradual increase is observed, accompanied by pronounced interannual fluctuations (Figure 3.8c). These variations likely reflect the combined influence of seasonal dynamics and external factors such as water circulation, wind patterns, and, importantly, the intensification of port-related activities and operations.

The spatial correlation analysis (Figure 3.9a) reinforces this interpretation by revealing that the interannual SPM signal observed near the APIC is not entirely confined to the port area. High correlations extend northward along the coast, suggesting that part of the variability detected at the port propagates beyond its immediate influence zone. This pattern is consistent with northward-moving coastal circulation and wind-driven transport, which can redistribute suspended material along the shoreline. Although the northern trends are weaker and not statistically significant (Figure 3.9b), the coherent spatial structure indicates that APIC-related changes may affect adjacent coastal waters through alongshore sediment transport.

These results point to a port-driven alteration of coastal sediment dynamics, which is further supported by land-use and land-cover changes (Figure 3.10). The transition from a predominantly natural system to a highly industrialized landscape (Hora et al., 2021; Lima et al., 2024) highlights the magnitude of human-induced disturbance and supports the observed trends in coastal water quality parameters, including the increase in SPM near the port area. The spatial expansion of industrial structures, artificial water bodies, and dredged zones is consistent with rising sediment availability and altered local hydrodynamics (Johnston, 1981; Yan and Li, 2023).

Overall, the temporal alignment between industrial growth, major dredging activities, and changes in SPM levels suggests a strong anthropogenic influence (Figure 3.11b). The progressive industrialization of São João da Barra, particularly the intensification of port operations since 2016 appears to have played a major role in shaping SPM dynamics. These patterns emphasize the need for long-term sediment management and environmental monitoring as industrial activities expand.

In addition, the spatial correlation of SPM interannual variation with the industrialization timeline (Figure 3.11a) further indicates that the influence of the APIC is not strictly local but tends to extend northward. The northward gradient of high correlation values aligns with the alongshore transport pattern identified earlier (Figure 3.9), suggesting that port-related disturbances are progressively transferred to adjacent coastal waters through sediment pathways oriented in this direction.

Climate-related impacts do not provide a convincing explanation for the observed SPM increase. Scheel et al. (Scheel et al., 2023) underscore the importance of incorporating local information in climate change assessments for ports, and their analyses indicate that the Açu Port is expected to remain relatively resilient to sea-level rise and wave condition changes before 2070. No significant sea-level driven impacts are projected before this timeframe, and wave conditions should remain largely stable. The main projected change concerns wind speed, with potential increases of up to 10% after 2070, which may influence sediment transport in the longer term. However, these projections lie outside the temporal scope of the present analysis.

The long-term increase in SPM offshore of the APIC, including its northward and eastward extension, therefore cannot be attributed to interannual fluctuations in currents (Figure 3.12a-b). As shown previously, the influence of currents is mainly seasonal, with short-term changes in the meridional component occasionally contributing to episodic northward sediment export. The absence of significant long-term trends in the current components confirms their limited capacity to drive persistent SPM increases.

In contrast, winds emerge as an important driver of sediment redistribution, transporting suspended material both alongshore and offshore (Fettweis et al., 2010). Although wind components do not exhibit significant long-term trends, their interannual fluctuations correlate strongly with SPM variability in shallow waters (Figure 3.12c-d), especially for the meridional (V) component. This pattern is consistent with the recurrent northward dispersion of suspended sediments observed throughout the study area.

Wave power also contributes to modulating SPM concentrations. While it shows no monotonic long-term trend, its year-to-year fluctuations coincide with SPM peaks (Figure A.7),

reflecting the capacity of waves to resuspend bottom sediments and increase their availability for advection (Green and Coco, 2014; Li et al., 2020). This mechanism is particularly evident near the port area (Point A, Figure 3.12), where interannual SPM maxima align with episodes of increased wave energy. However, the weaker correlation between waves and SPM, compared to winds, suggests that waves primarily enhance sediment resuspension rather than drive long-term increases.

Given the absence of significant long-term trends in winds, waves, and currents, the persistent rise in SPM offshore of the APIC cannot be explained by natural hydrodynamic forcing alone. It most likely reflects the intensification of industrial and port activities, which increase sediment availability within the system. In this context, winds modulate the direction and efficiency of sediment transport, whereas waves amplify resuspension processes, together sustaining interannual variability and promoting the northward dispersal of suspended sediments (Van den Eynde and Fettweis, 2006; Fettweis et al., 2010, 2016).

Similar patterns have been documented in other major port-affected systems. In the Yangtze River estuary, Fan et al. (Fan et al., 2023) showed that dredging activities resuspend large quantities of bottom material that can be transported far beyond the dredging zone, increasing SPM concentrations in adjacent regions. The authors also report that shipping activities disturb surface sediments and modify the spatial distribution of SPM, while large engineering structures alter sediment pathways and produce persistent changes in estuarine sediment regimes. These mechanisms closely mirror the increase and northward redistribution of SPM observed near the Açu Port, indicating that port development in dynamic coastal environments tends to produce long-lasting and spatially coherent modifications in sediment availability and transport.

Beyond these drivers, sea surface height (SSH) has shown an increasing trend in the study area over the past two decades (8 to 9 cm in 20 years, corresponding to approximately 4 mm $year^{-1}$; Figure A.8). This rate is consistent with the global mean sea level rise derived from satellite altimetry, which has accelerated to about 4 mm $year^{-1}$ in recent decades (Hamlington et al., 2024; Shariot-Ullah, 2024). Along the Brazilian coast, including our study region, sea level rise occurs at variable rates depending on local oceanographic and climatic conditions (Alfredini and Arasaki, 2018; Toste et al., 2024; Daniel et al., 2025; Ferreira et al., 2025). Rising SSH may influence shoreline stability and intensify erosion processes, thereby increasing sediment availability for resuspension and transport (Ogston and Field, 2010; Passeri et al., 2015; Zarillo, 2023). While our dataset does not allow us to fully assess this mechanism, it is plausible that long-term SSH changes could exacerbate the impacts of industrial activities on

regional SPM dynamics. Confirming this hypothesis will require longer observational records and targeted analyses explicitly linking SSH variability to coastal erosion and sediment fluxes.

3.4.3. Limitations and Perspectives for Multi-Scale Monitoring

This study has clearly demonstrated the potential of long-lasting ocean color time series (here MODIS 1 km resolution data) for characterizing SPM variability in a complex and industrialized coastal environment although limitations for describing the most nearshore domain due to reduced spatial resolution. The 20-year MODIS record (2002-2022) captured the evolution of SPM both before the installation of the Açu Port and throughout its subsequent construction and operational phases, allowing the identification of clear seasonal patterns, interannual fluctuations, and a significant long-term increase coinciding with the intensification of industrial activities. Through the combination of MODIS monthly composites with the Census X-11 decomposition, the seasonal Mann-Kendall test, and Sen's slope estimator, the sensor proved capable of resolving coherent and persistent changes in sediment dynamics at regional scale. While its moderate spatial resolution does not allow the identification of fine-scale dredging plumes or small disposal features, the results show that MODIS provides robust information on broad-scale coastal processes and long-term environmental evolution. The reliability of these long-term patterns is further supported by the use of OC-SMART for atmospheric correction. Its multilayer neural-network architecture and enhanced cloud-screening capabilities (Fan et al., 2021) ensure stable, spatially consistent $R_{rs}(\lambda)$ retrievals in this turbid, optically complex region. In addition, OC-SMART has recently been validated for MODIS-Aqua coastal applications (Tran et al., 2025), providing additional confidence in the consistency of the 20-year SPM time series.

This study illustrates the impact of the Açu Port installation on surface SPM dynamics for the first time using a 20-year ocean-color time series. The available information on port activities consists mainly of qualitative descriptions of construction phases, dredging episodes, and operational milestones, with no quantitative records of dredged volumes or sediment fluxes associated with pipelines. This limits the ability to attribute precise magnitudes to the observed changes. In addition, no operational hydro-sedimentary model exists for the region, preventing a full three-dimensional assessment of sediment transport pathways. Despite these constraints, the long-term MODIS analysis provides an initial regional diagnosis that establishes the baseline necessary for future quantitative modeling and process-based studies.

Future work could benefit from complementing this approach with higher-resolution sensors such as the Sentinel-2 Multispectral Instrument (MSI) or the Landsat-8/9 Operational

Land Imager (OLI), in order to better resolve nearshore structures and localized sediment patterns. A multi-scale framework combining the temporal continuity of MODIS (the only long-lasting mono-sensor time series able to depict the pre and post port phases) with the spatial detail of high-resolution missions (able to describe specific events and the nearshore domain) would further enhance the monitoring of rapidly evolving coastal systems.

3.5. Conclusions

This study presents a comprehensive satellite-based approach to quantifying long-term changes in coastal sediment dynamics, focusing on the impact of industrial port infrastructure. A new SPM retrieval model was developed by combining two optimized bio-optical algorithms based on OWTs to ensure accurate performance across a wide range of coastal optical conditions for MODIS applications. Validation using both in situ and satellite data confirmed the reliability of this approach, particularly in turbid environments, where the accuracy of conventional models is often reduced.

When applied to 20 years (2002-2022) of MODIS-Aqua imagery, the model revealed significant spatial and temporal variations in SPM concentrations along the northern coast of Rio de Janeiro state. The most significant and statistically robust increases occurred near the APIC, with trends reaching 60% in two decades. These increases coincided with major phases of industrial development, including large-scale dredging and port expansion, indicating a significant anthropogenic influence. Natural processes also modulate SPM dynamics: currents exert a strong seasonal influence by driving the plume northward, winds show significant correlations with SPM at the interannual scale, and waves enhance sediment resuspension in coastal and inner-shelf domains, amplifying short- to interannual-scale variability. However, since no long-term increase was detected in either wind intensity or wave power, their role remains limited to modulation rather than driving the persistent rise in SPM. Together, winds and waves continue to redistribute suspended material and sustain the observed northward and eastward sediment dispersion, but industrialization remains the dominant driver of the long-term increase in SPM near the APIC.

The amount of sediment that needs to be dredged in the APIC is closely linked to SPM concentrations, which are subject to tidal, meteorological, and climatological variability. In addition to these natural drivers, anthropogenic activities such as dredging, shipping, and sediment disposal can modify the distribution of SPM by enhancing the processes of dispersal, resuspension, and buffering (Smith and Friedrichs, 2011; Decrop et al., 2015; Van Maren et al.,

2015; Fettweis et al., 2016). Elevated SPM levels in adjacent coastal waters have significant implications for water quality and the functioning of ecosystems. Sediment particles carry trace metals and hydrophobic organic contaminants (Turner and Millward, 2002), and also contribute to nutrient inputs (Shaikh et al., 2021). While SPM can stimulate primary production, excessive enrichment increases the risk of eutrophication, oxygen depletion, and fish mortality (Ménesguen and Lacroix, 2018; Le Moal et al., 2019). Furthermore, high turbidity reduces light penetration, thereby altering phytoplankton bloom dynamics and affecting higher trophic levels (Loisel et al., 2014). These results demonstrate that long-term increases in SPM offshore of the APIC are primarily linked to a port-driven supply of sediment, while natural circulation patterns regulate its redistribution and transport. This interplay between anthropogenic pressures and hydrodynamic modulation emphasizes the importance of both sediment management and ecological monitoring in preserving coastal ecosystems amid expanding industrial activity.

Satellite ocean color remote sensing has become an indispensable tool for monitoring SPM dynamics and assessing water quality in complex and impacted coastal zones. Long-term datasets from optical sensors such as MODIS provide extensive spatial coverage and historical depth, enabling the consistent detection of environmental trends over time and across space. The methodological framework applied here, which integrates atmospheric correction, OWT-based algorithm fusion, and statistical time-series analysis, offers a robust, scalable, and transferable strategy for identifying human-induced changes in coastal systems. AS well as supporting environmental assessments and constraining hydro-sedimentary models, these tools enhance our ability to distinguish anthropogenic signals from natural variability. Although this approach has been demonstrated for the Brazilian coast, and particularly the heavily industrialized Açu Port region, it can be used as a valuable template for similar applications in other coastal areas undergoing rapid industrialization and facing sediment management challenges.

Nonetheless, several limitations must be acknowledged. The progressive degradation of the MODIS-Aqua sensor since 2022 has affected the continuity and reliability of the time series. While multi-sensor datasets such as GlobColour and OC-CCI offer extended coverage, their lower reliability in optically complex nearshore waters constrains their utility. Furthermore, validation efforts are hindered by the limited availability and spatial representativeness of in situ measurements, particularly during key periods of industrial change. Future work should prioritize the integration of higher-resolution sensors such as Sentinel2- MSI or data from the recently launched hyperspectral NASA mission Plankton, Aerosol, Cloud, Ocean Ecosystem (PACE), which promise improved retrieval accuracy in coastal zones.

CHAPTER 4: IMPACTS OF DEFORESTATION AND PASTURE EXPANSION ON SUSPENDED PARTICULATE MATTER AND CHLOROPHYLL-A IN THE COASTAL WATERS OF MARANHÃO, NORTHERN BRAZIL, DERIVED FROM 20 YEARS OF MODIS OBSERVATIONS (2002–2022)

4.1. Introduction

Coastal ecosystems are key interfaces between land and sea, where physical, chemical, and biological processes interact over various spatial and temporal scales. They provide essential ecological and economic functions that support human societies (Economidou, 1982). However, these environments are increasingly threatened by both natural dynamics and human activities (Lotze et al., 2006; Halpern et al., 2008)). In recent decades, pressures such as deforestation, agriculture, urbanization, and dam construction have intensified, leading to habitat loss, changes in sediment delivery, and water quality degradation (Burke et al., 2001; Barbier et al., 2011; Barragán and de Andrés, 2015; Marchesiello et al., 2019). Such pressures modify sediment and nutrient fluxes from land to sea, affecting the physical and biogeochemical balance of coastal environments (Nixon, 1998; Cloern, 2001; Bianchi, Allison and Cai, 2014). These transformations are further intensified by climate modulation, which influences hydrological regimes, temperature, and the frequency of extreme events, thereby exacerbating the cumulative effects of anthropogenic pressures on coastal ecosystems (Duarte et al., 2020; IPCC, 2023).

The Brazilian coastline holds major ecological, social, and economic importance but remains highly vulnerable to both natural processes and human activities (Nicolodi and Petermann, 2010; Bernardes et al., 2012). Changes in land use and land cover have profoundly affected the quality of coastal waters by intensifying sediment and nutrient runoff and introducing various pollutants (Foley et al., 2005; Zhang et al., 2020; Salah Salah et al., 2025). Deforestation promotes soil erosion and enhances fluvial sediment transport, while the expansion of agriculture and urban settlements has increased the discharge of effluents rich in organic and inorganic compounds from both natural and artificial sources (Bernardes et al., 2012).

Among the variables most sensitive to these disturbances, suspended particulate matter (SPM) and chlorophyll-a (Chl-a) play a key role in assessing coastal water quality. SPM

regulates water transparency and light availability and acts as a major vector for the transport of nutrients and contaminants (Miller and Cruise, 1995; Velegrakis et al., 1997; Kroon et al., 2012). Its concentration and composition are strongly influenced by land-use and land-cover changes, which alter soil erosion rates, sediment mobilization, and the efficiency of sediment transfer from catchments to river networks and ultimately to coastal waters (Bainbridge et al., 2024). Chl-a is commonly used to characterize phytoplankton biomass and variability in coastal waters and responds to changes in nutrient loads as well as to variations in light conditions, hydrodynamic forcing, and particulate dynamics, including sediment resuspension, advection, and episodic bloom development (Kasprzak et al., 2008; Wang and Convertino, 2023). Understanding how terrestrial processes affecting land-sea fluxes, such as deforestation, influence these variables is therefore essential for evaluating the ecological status of coastal ecosystems and for developing adapted and sustainable coastal management strategies (Cloern et al., 2016; Bidlack et al., 2021).

In this context, satellite ocean color remote sensing (OCR) provides the opportunity to monitor multidecadal evolution of Chl-a and SPM over large spatial and temporal scales, particularly valuable in regions where long-term and spatially extensive in situ observations are lacking, as is the case for most Brazilian coastal waters. However, reliable satellite retrievals in optically complex and highly turbid coastal environments require bio-optical algorithms specifically adapted to such conditions (Loisel et al., 2013; Mélin and Vantrepotte, 2015; Groom et al., 2019). The application of ocean optical water types (OWTs) represents an effective strategy, as it enables the use of water-type-specific algorithms and improves retrieval accuracy under diverse optical conditions (Vantrepotte et al., 2012; Carvalho et al., 2014; Salah Salah et al., 2025; Tran et al., 2025).

The Moderate Resolution Imaging Spectroradiometer (MODIS) onboard the Aqua satellite (1 km spatial resolution) provides the longest continuous record of ocean color observations, spanning more than two decades. By contrast, GlobColour (4km) and the Ocean Color Climate Change Initiative (OC-CCI, 1km) datasets offer global coverage but remain less reliable in optically complex coastal waters, especially due to the coarser resolution of GlobColour (Cardoso Dos Santos et al., 2025). In addition, the lack of near-infrared (NIR) bands in these products remains a major limitation, as NIR information is essential for accurate retrieval of Chl-a and SPM in optically complex environments.

This study focuses on the western coast of Maranhão State, northern Brazil, within the Amazonian Equatorial Coast and specifically aims to evaluate the influence of regional deforestation and pasture expansion on the biogeochemical dynamics of Chl-a and SPM in

coastal waters using long-term MODIS satellite observations. The Amazon biome in Brazil covers about 4.2 million km², extending across nine federative states, including Maranhão. Historically, approximately 110.4 thousand km² of Maranhão was part of the Amazon biome, but around 75% of this forest cover has been cleared, mainly to accommodate agriculture and cattle ranching (Celentano et al., 2017; Silva Junior et al., 2020). This deforestation process has long been politically justified by the pursuit of "economic development," yet its social, economic, and environmental consequences remain largely negative and have intensified social inequality and environmental degradation (Celentano et al., 2012, 2017; Silva Junior et al., 2020).

The main objective of this work is to assess the impact of land-use and land-cover changes in Maranhão State on the biogeochemical quality of its coastal waters over the last 20 years time period (2002-2022). For this purpose, 1km 20-year time series (2002-2022) of MODIS data were processed using the Ocean Color - Simultaneous Marine and Aerosol Retrieval Tool (OC-SMART) atmospheric correction (Fan et al., 2021) to generate the remote sensing reflectance while Chl-a and SPM data were generated across the entire study area using up to date OWT based bio-optical models (Salah Salah et al., 2025; Tran et al., 2025).

The resulting Chl-a and SPM time series were analyzed using the seasonal Mann-Kendall test and the Census X-11 decomposition method (Pezzulli et al., 2005; Vantrepotte and Mélin, 2011) to detect monotonic trends over 2002-2022 and to characterize temporal variability at multiple scales (seasonal and interannual). Generalized Additive Models (GAMs) were also applied to disentangle the relative contributions of natural and anthropogenic drivers to long-term Chl-a and SPM dynamics in Maranhão coastal waters. GAMs offer a flexible statistical framework to identify and quantify non-linear relationships between environmental variables and biogeochemical responses and have been widely used in ocean color and coastal ecosystem studies (Hastie and Tibshirani, 1986; Wood, 2017; He et al., 2019; Weihao et al., 2021). Finally, the spatiotemporal patterns of Chl-a and SPM were interpreted in relation to the main natural and anthropogenic drivers of the region, including river discharge, hydrodynamic processes, wind regime, and land-use and land-cover dynamics.

4.2. Materials and Methods

4.2.1. Study area

The study area is located on the western coast of Maranhão State, northern Brazil, between Turiaçu Bay (~1.65°S, 45.4°W) and São Marcos Bay (~2.50°S, 44.3°W), within the Amazonian Equatorial Coast (Vargas Borges et al., 2016; Celentano et al., 2017; Silva Junior et al., 2020)

(Figure 4.1). This region is marked by ria estuaries, high turbidity, and complex fluvio-estuarine dynamics (Muehe, 2006; Barbosa Martins et al., 2015). The hydrography is dominated by the Turiaçu, Mearim, Pindaré, and Grajaú rivers. The Mearim represents the largest basin of the Maranhão state (~99,059 km²), with the Pindaré River, one of its main tributaries, draining approximately 40,400 km² (Costa et al., 2011; Lefèvre et al., 2017; Limeira-Filho et al., 2023).

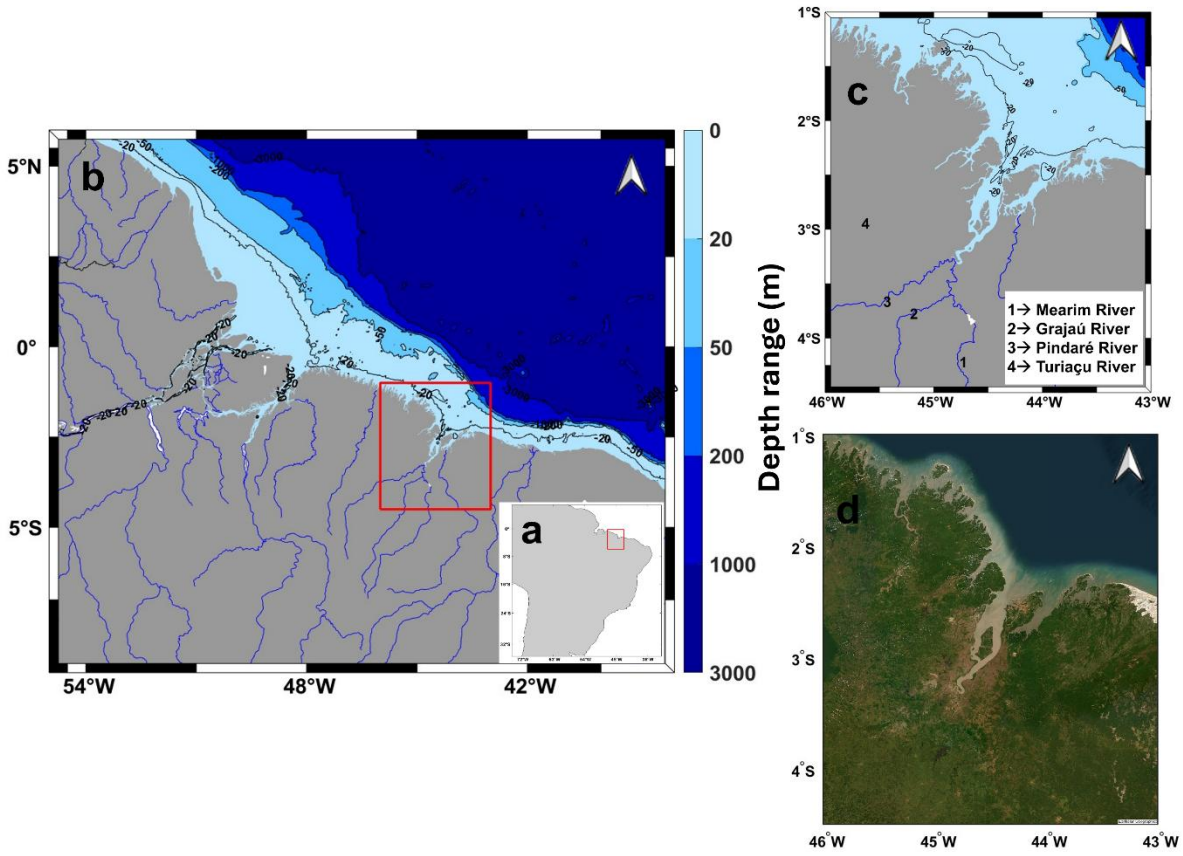

Figure 4.1. Study area location. (a) Maranhão State. (b) Northern Brazilian coastal region with the red box highlighting western Maranhão. (c) Detailed view of the study area and main rivers. (d) True-color image of the study area from Google Satellite imagery.

These systems play a major role in freshwater and sediment inputs to the adjacent coastal zone. The region has a typical equatorial climate, with a marked rainy season from December to May and a dry season from June to November (Xavier et al., 2021). Coastal circulation is driven by the seasonal migration of the Intertropical Convergence Zone (ITCZ) and by the influence of the North Brazil Current (NBC), a strong western boundary current that intensifies between July and August under strengthened southeasterly trade winds and weakens during April–May when these winds relax (Johns et al., 1998; Lefèvre et al., 2017). Land use in Maranhão is strongly influenced by livestock farming, which has contributed to deforestation and significant land-cover changes (Celentano et al., 2017). At the same time, the region hosts

some of Brazil's most preserved and structurally complex mangrove ecosystems, extending along most of the littoral domain (Hayashi et al., 2019).

4.2.2. Ocean Color Satellite data

From 2002 to 2022, MODIS-Aqua Level 1 (L1) imagery at 1 km spatial resolution was acquired from NASA's Ocean Biology Processing Group (OBPG) at the Goddard Space Flight Center (https://oceandata.sci.gsfc.nasa.gov/MODIS-Aqua/). MODIS-Aqua provides the longest continuous ocean color record from a single platform, supporting consistent long-term monitoring of coastal waters. Atmospheric correction was performed with the OC-SMART algorithm (Fan et al., 2021). OC-SMART integrates multilayer neural networks with radiative transfer simulations from the AccuRT coupled atmosphere-²ocean model to retrieve remote sensing reflectance ($R_{rs}(\lambda)$). Validation studies have shown that OC-SMART performs comparably to, and in some coastal and turbid environments better than other approaches such as Polymer, ACOLITE, and C2RCC, with reported improvements depending on water type and optical conditions (Bui et al., 2022; Pachniak et al., 2023). It is particularly effective in turbid waters due to its advanced cloud screening and reduced sensitivity to sunglint and cloud-edge contamination (Fan et al., 2021). OC-SMART has proven effective for coastal applications using MODIS-Aqua imagery, as shown by Tran et al. (2025). This finding is consistent with results from the IOCCG (2025) evaluation, which assessed atmospheric correction algorithms for MODIS using global in situ and synthetic datasets and highlighted the robust performance of OC-SMART across a range of optical conditions.

Brazilian coastal waters, and especially those along Maranhão state, are characterized by strong optical heterogeneity resulting from riverine discharges, seasonal precipitation, and variable biogeochemical conditions (Lefèvre et al., 2017). This variability produces distinct OWTs, with multiple classes often coexisting in the same region ranging from very clear (OWT 17) to very turbid environments (e.g. OWT 1 and 2) (Figure 4.2). Recognizing this complexity is essential, as it underscores the need to use bio-optical algorithms developed for coastal waters and grounded in OWT classifications, which are particularly effective in improving the estimation of biogeochemical variables in optically complex environments (Vantrepotte et al., 2012; Carvalho et al., 2014; Salah Salah et al., 2025; Tran et al., 2025). In this study a focus on the coastal waters of the Maranhão state (bathymetry < 50) (Figure 2b).

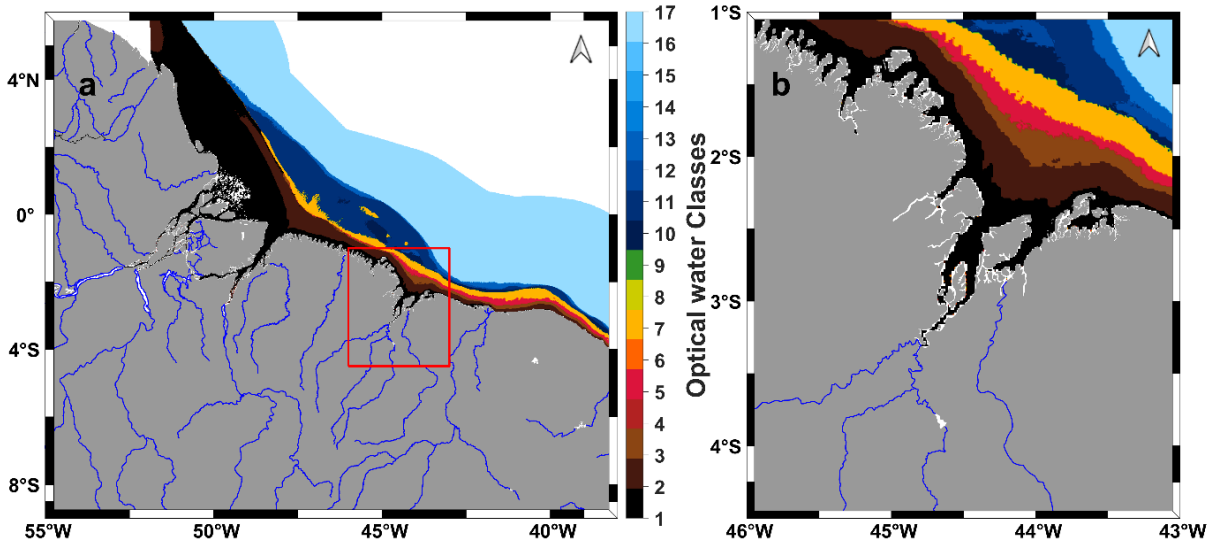

Figure 4.2. Dominant Optical Water Types distribution over the MODIS 2002-2022 time period (17 classes; Mélin and Vantrepotte, 2015, Jorge et al., 2021). (a) OWT distribution along the northern Brazilian coast. (b) in the study area on the western coast of Maranhão State.

4.2.3. Bio-optical models for SPM and Chl-a estimation

Daily MODIS-Aqua reflectance data spanning the period 2002-2022 were processed using existing bio-optical algorithms developed for global coastal waters and adapted to optically complex environments, covering the water types present in the study area; the resulting Chl-a and SPM estimates were subsequently aggregated into monthly products for further analyses.

4.2.3.1. Chl-a model CONNECT

To estimate Chl-a concentrations, the CONNECT model was employed (Tran et al., 2025). This neural network-based algorithm, developed for MODIS applications from a comprehensive worldwide distributed data set (N = 3750), is designed to handle varying optical water conditions. This model integrates two distinct neural networks: one utilizes the blue, green, and red spectral bands for clear waters, while the other incorporates blue, green, red, and near-infrared (NIR) bands for turbid waters. The selection between these networks is guided by the classification of OWTs, ensuring accurate Chl-a retrievals across diverse coastal environments.

4.2.3.2. SPM bio-optical model

To derive SPM concentrations, we employed the OWT-based bio-optical model recently proposed for global coastal environments (Salah Salah et al., 2025). The model relies on the integration of two complementary algorithms: Siswanto et al. (2011) for oligotrophic to mesotrophic waters, and Han et al. (2016) for turbid to highly turbid conditions. Both

algorithms were recalibrated for MODIS-Aqua spectral bands, and their outputs were merged using an OWT probability-weighted procedure, ensuring robust retrievals under the optically heterogeneous conditions typical of the Maranhão coastal zone.

4.2.4. Ancillary data

To complement the satellite observations and improve the interpretation of biogeochemical variability, several ancillary data sources were considered in the analysis, addressing land-sea interactions through river discharge, atmospheric forcing (precipitation and winds), oceanic circulation (currents), and land use and land cover.

- **River discharge**

River discharge records were sourced from the HIDROWEB database maintained by the Brazilian National Water Agency (ANA) (https://www.snirh.gov.br/hidroweb/mapa (accessed on 1 January 2025)). Four river systems were considered, the Mearim, Pindaré, Grajaú, and Turiaçu rivers as they represent the principal hydrological inputs to the study region (Dos Santos Cerqueira et al., 2009; Limeira-Filho et al., 2023). For each river, data were extracted from specific monitoring stations located at Mearim (4.2194° S, 44.7653° W), Pindaré (3.6597° S, 45.4661° W), Grajaú (3.7722° S, 45.2181° W), and Turiaçu (2.9442° S, 45.6672° W). Monthly discharge values ($m^3. s^{-1}$) were used in the analysis.

- **Precipitation**

Precipitation was characterized using NASA's IMERG (Integrated Multi-satellite Retrievals for GPM) product (https://gpm.nasa.gov/data/directory (accessed on 1 January 2025)), which provides rainfall estimates at 0.1° spatial and 30-minute temporal resolution since 2000. Monthly totals ($mm \cdot month^{-1}$) were averaged over the area covering the river discharge stations to generate a regional precipitation index, used to evaluate rainfall impacts on hydrological dynamics.

- **Surface current**

Surface currents were assessed through the Copernicus GlobCurrent dataset (https://data.marine.copernicus.eu/product/MULTIOBS_GLO_PHY_MYNRT_015_003/ (accessed on 1 January 2025)), which merges satellite altimetry and gravimetry (GOCE mission) with in situ measurements (Rio et al., 2014). The product provides total surface

currents and their geostrophic and Ekman components at both the surface and 15 m depth, with a spatial resolution of 1/4° (~25 km at the Equator).

- **Winds**

Wind forcing was analyzed using the Cross-Calibrated Multi-Platform (CCMP) version 3.0 dataset (Mears et al., 2022), distributed by Remote Sensing Systems (https://www.remss.com/measurements/ccmp/ (accessed on 1 January 2025)). CCMP v3.0 combines satellite microwave observations with numerical weather prediction outputs to deliver consistent, gap-free global wind vector fields at 1/4° resolution.

- **Land cover and land use**

Land cover and use information was obtained from the MapBiomas Project (https://brasil.mapbiomas.org/en/ (accessed on 1 January 2025)), which provides annual land cover and use classifications for Brazil from 1985 to present. For this study, the focus was on Maranhão State, particularly its Amazonian sector where deforestation pressure is most intense (Celentano et al., 2017; Silva Junior et al., 2020). The selected area was defined to encompass the main river basins draining into the coastal zone of Maranhão, namely the Mearim, Turiaçu, and Pindaré systems (Limeira-Filho et al., 2023). These basins represent the dominant sources of freshwater, sediments, and terrestrially derived organic matter to the adjacent coastal waters and are therefore key drivers of coastal biogeochemical variability (Bianchi, Allison and Cai, 2014; Cloern et al., 2016). In addition, they have experienced significant land use and land cover changes over recent decades, particularly linked to deforestation, agricultural expansion, and pasture development, which have been shown to alter riverine sediment and nutrient exports in the region (Celentano et al., 2017; Silva Junior et al., 2020). The spatial extent (in hectares) of land use categories including agriculture, mangroves, forest, urban zones, farming, and pastures was extracted and linearly interpolated to generate monthly time series consistent with the temporal resolution of the Chl-a and SPM products.

4.2.5. Statistical analysis

4.2.5.1. Time series decomposition method and trend analysis

Monthly composites of SPM and Chl-spanning July 2002 to December 2022 together with monthly time series of wind, currents, river discharge, and precipitation were analyzed using the Census X-11 decomposition method and the seasonal Mann-Kendall test to investigate seasonal cycles and interannual variability of water quality. The coefficient of variation (CV)

was also calculated for each pixel as the ratio of the standard deviation to the mean of the monthly time series and expressed as a percentage (%).

The Census X-11 approach (Pezzulli et al., 2005), widely used in ocean color applications (e.g. (Vantrepotte and Mélin, 2011; Loisel et al., 2014; Keerthi et al., 2022; Cardoso Dos Santos et al., 2025), decomposes each time series $X(t)$ into three additive components: a seasonal cycle $S(t)$, an interannual component $T(t)$, and an irregular signal $I(t)$, such as:

$$\mathbf{X(t) = S(t) + T(t) + I(t)} \quad \textbf{(4.1)}$$

The decomposition was applied on a pixel-by-pixel basis across the study region. Because the method iteratively applies bandpass filters and accounts for changes in the seasonal cycle through time, it is particularly suitable for describing non-stationary seasonal and interannual dynamics in coastal waters (Vantrepotte and Mélin, 2011).

To ensure comparability between spatially heterogeneous pixels and to minimize biases related to differences in magnitude, both Chl-a and SPM time series were standardized. The standardization was applied on a pixel-by-pixel basis by dividing each pixel value by its temporal mean over the study period. This approach emphasizes relative temporal variations rather than absolute concentrations, allowing a consistent analysis of spatial and interannual patterns (Vantrepotte and Mélin, 2011).

Finally, monotonic variations were assessed with the non-parametric seasonal Mann-Kendall test (Hirsch et al., 1982), applied to each time series with significance evaluated at $p < 0.05$. The rate of change (RC) was estimated using the seasonal Sen's slope estimator (Sen, 1968) and expressed as percent per year.

4.2.5.2. Generalized Additive Model Analysis

To assess the relative impact of land use and hydrological variability on the 20-year biogeochemical evolution of Maranhão coastal waters, Generalized Additive Models (GAMs) were computed. GAMs are non-parametric regression models that allow for flexible modeling of non-linear relationships between a response variable and multiple explanatory variables (Hastie and Tibshirani, 1986). They extend the Generalized Linear Model (GLM) by replacing linear terms with smooth functions, enabling the data to determine the shape of the relationship (Weihao et al., 2021). This makes GAM particularly suitable for biogeochemical data, where predictor-response relationships are often complex and non-linear. In this study, GAM was used to analyze the influence of land cover (pasture), river discharge, currents and winds on the temporal variability of Chl-a and SPM concentrations.

The formulation of the GAM used in this study is:

$$\mathbf{Y_i = \beta_0 + f_1(Pasture_i) + f_2(Discharge_i) + f_3(Winds_i) + f_4(Currents_i) + \varepsilon_i} \quad \textbf{(4.2)}$$

where Y_i is the expected SPM or Chl-a value, β_0 the intercept, f_1- f_4 smooth functions fitted to the explanatory variables (here pasture, river discharge, winds and currents), and ε_i the residual error term accounting for unexplained variability.

Models were fitted in R using the "mgcv" package (Wood, 2017). Smoothing parameters were estimated with restricted maximum likelihood (REML), and model quality was assessed through adjusted R^2, deviance explained and residual diagnostics (Pya and Wood, 2015).

The contribution of each predictor was evaluated using the estimated degrees of freedom (edf), F-statistics, and p-values. An edf close to 1 indicates an approximately linear relationship, whereas higher values reflect increasing non-linearity. GAMs were used to explore the combined and potentially non-linear effects of the explanatory variables on water quality and to assess the role of land-river-coast interactions in shaping biogeochemical variability.

4.3. Results

4.3.1. Chl-a and SPM climatological distribution

From 2002 to 2022, Chl-a concentrations ranged from 0.1 to 20.0 mg. m^{-3} (P5-P95 = 0.13-4.72 mg. m^{-3}; mean = 1.21 mg. m^{-3}), with slightly higher values during the rainy season (Figure 4.3a; mean = 1.30 mg. m^{-3}) than in the dry season (Figure 4.3b; mean = 1.13 mg. m^{-3}), reflecting increased riverine input and mixing. These ranges are consistent with in situ data for Maranhão coastal waters, such as 0.5-8.5 mg. m^{-3} reported by Carvalho et al. (2016), 0.3-10 mg. m^{-3} by Castro et al. (2018) and Cavalcanti-Lima et al. (2023), and up to 16 mg. m^{-3} in nearshore turbid waters (Pardal et al., 2011). The satellite-derived P5-P95 range (0.1-5 mg. m^{-3}) thus fits well within published limits, confirming the reliability of the CONNECT-based Chl-a product.

Satellite-derived SPM concentrations ranged from 0.1 to 145.8 mg. L^{-1} (P5-P95 = 0.13-9.53 mg. L^{-1}), with climatological means of 4.35 mg. L^{-1} (rainy, Figure 4.3e) and 4.49 mg. L^{-1} (dry, Figure 4.3f). These are lower than highly turbid estuarine values (33.6 ± 5.0 mg. L^{-1} in the rainy and 103.4 ± 35.5 mg. L^{-1} in the dry season; (Santos et al., 2023)), but consistent with the broader coastal gradient reported by Castro et al. (2018), who observed 0.4-163 mg. L^{-1} (mean 23.4 and 48.7 mg. L^{-1} in rainy and dry seasons, respectively). The lower satellite means reflect the broad spatial coverage of the study area (Figure 2), which spans highly turbid

coastal/estuarine waters (OWT classes 1-8) as well as clearer oceanic waters (classes 9-17). This heterogeneous optical domain results in averaged SPM concentrations that are lower than those reported for purely estuarine sites (Santos et al., 2023).

Overall, both OWT-based algorithms reproduce realistic magnitudes and seasonal contrasts of Chl-a and SPM along the Maranhão coast, in good agreement with available field data, supporting their suitability for long-term coastal monitoring.

The seasonal climatological distribution of Chl-a and SPM shows a clear spatial and seasonal contrast between the rainy (December-May) and dry (June-November) seasons along the Amazonian Equatorial Coast of Maranhão (Figure 4.3). During the rainy season, mean Chl-a and SPM concentrations are higher near estuarine and deltaic regions. This coastal accumulation reflects the strong influence of river discharge, land runoff, and sediment resuspension under highly turbid conditions, which enhance both particulate matter and phytoplankton biomass nearshore (Hoover and Mackenzie, 2009; Chen et al., 2018).

In contrast, during the dry season, concentrations generally decrease across the shelf, with the strongest decline observed seaward of the inner shelf (i.e., beyond the ~20-50 m isobaths), where clearer waters dominate. Reduced freshwater input and increased marine forcing over mid- to outer-shelf depths promote particle dispersion and dilution, resulting in lower SPM values (Uncles et al., 2000; Deng et al., 2023; Liu et al., 2023).

Chl-a remains locally elevated in shallow, turbid waters where resuspension continues to supply nutrients and light remains limiting but sufficient for growth (Llames et al., 2009, p. 2010; Porter and Sanford, 2010). The seasonal coefficient of variation (CV) highlights stronger seasonal variability in coastal and estuarine regions, indicating that these environments are the most responsive to hydrological fluctuations. Conversely, the outer shelf exhibits lower variability, reflecting a more stable marine regime throughout the year (Doxaran et al., 2009; Loisel et al., 2014).

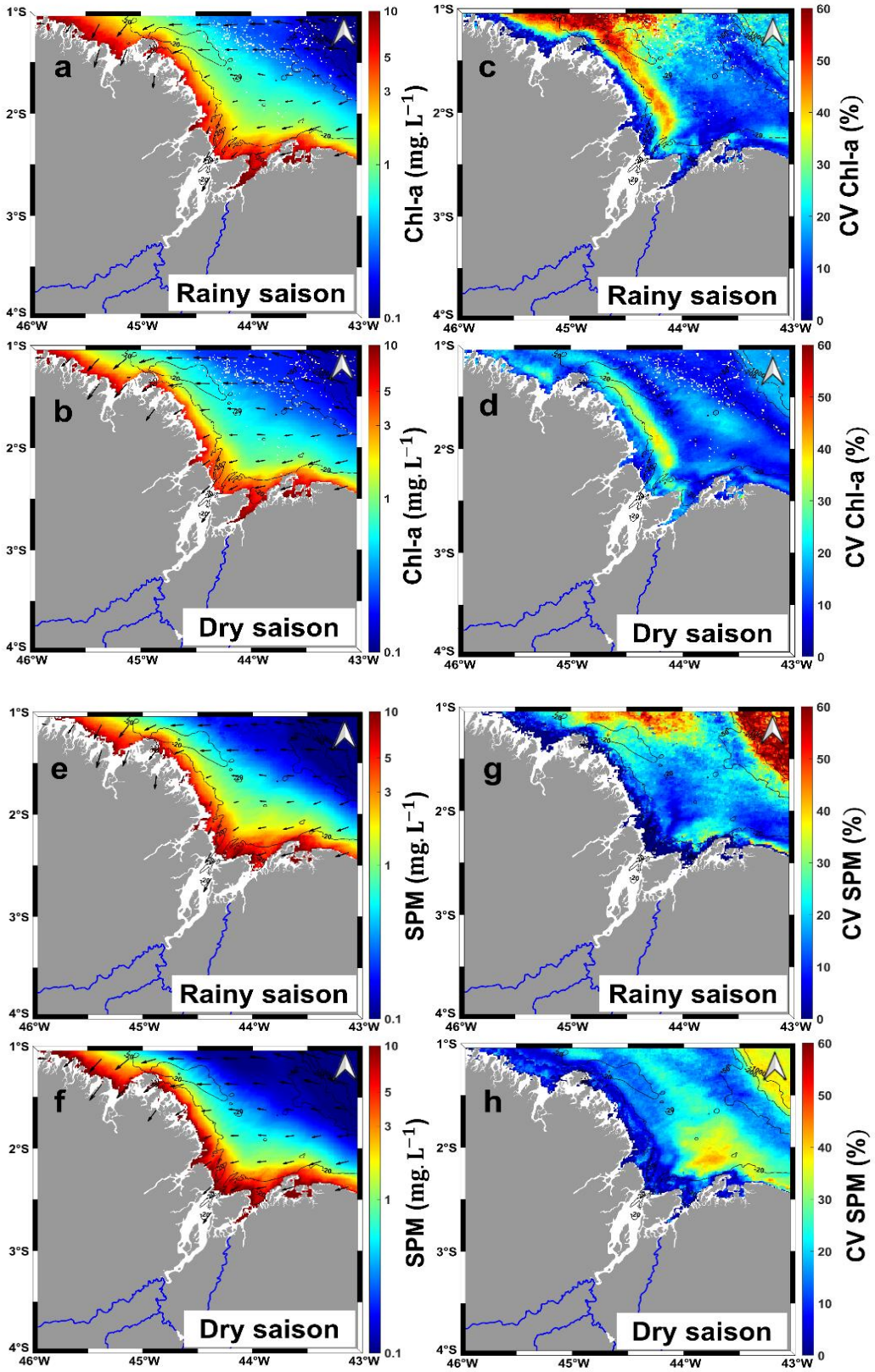

Figure 4.3. Seasonal average (2002-2022) of Chl-a (a-d) and SPM (e-h) during the rainy season (December-May) and dry season (June–November) for the western coast of Maranhão State(a-b) Mean Chl-a for the rainy and dry seasons; (c-d) Chl-a coefficient of variation for the rainy and dry seasons; (e-f) Mean SPM for the rainy and dry seasons; (g-h) SPM coefficient of variation for the rainy and dry seasons. Dominant surface currents indicated by black arrows.

While the mean spatial distributions of Chl-a and SPM are broadly comparable, their CV patterns differ markedly in near-coastal areas. This discrepancy may reflect differences in the dominant controlling processes: Chl-a variability is likely more sensitive to seasonal changes in river discharge, nutrient availability, and light conditions (Cloern, 1996; Guillaud et al., 2008), whereas SPM concentrations are largely governed by physical processes such as tidal resuspension and continuous sediment supply, which may persist throughout the year (Postma, 1961; Fettweis et al., 2016). As a result, biologically driven Chl-a can exhibit stronger seasonal contrasts than SPM, despite similar mean spatial patterns. These contrasting CVs suggest a partial decoupling between biological production and sediment dynamics in highly turbid coastal waters (Gohin et al., 2005)

The mean surface circulation over 2002-2022 reveals a persistent northwestward flow along the Maranhão coast, consistent with the large-scale pathway of the North Brazil Current (NBC) that dominates the offshore circulation in the western tropical Atlantic (Johns et al., 1998; Aguiar et al., 2022; Dimoune et al., 2023). In both the rainy and dry seasons (Figure 4.3), the flow remains predominantly northwestward and aligned with the coastline. During the rainy season, currents intensify and become more coherent, forming a continuous alongshore jet extending from São Marcos Bay to Turiaçu Bay. Localized onshore deviations and recirculation features develop near the embayments, particularly around 1.5° S and 45.5° W, where the flow partially turns landward and forms weak retention zones that may promote the return of coastal waters and suspended material toward the coast before rejoining the dominant northwestward current. In the dry season, the circulation weakens and becomes more diffuse, exhibiting a broader but less energetic northwestward pattern across the shelf. Such circulation patterns likely contribute to the coastal trapping of suspended matter and phytoplankton, explaining the nearshore maxima and enhanced spatial variability of Chl-a and SPM observed in Figure 4.3.

4.3.2. Chl-a and SPM general variability patterns

The temporal variability of Chl-a and SPM during the MODIS 2002-2022 time period is illustrated through the Census X11 decomposition outputs (Figure 4.4), which provide the relative importance of the seasonal, interannual, and irregular components in the total variance of the time series. Figures 4.4a and 4.4e show the overall coefficient of variation (CV, %) of Chl-a and SPM, respectively. Globally, coastal waters exhibit moderate variability, reaching up to ~50 % in some nearshore regions, while offshore areas display higher heterogeneity, likely influenced by oceanic processes.

The seasonal component represents the dominant contribution to total variance for both variables (Figures 4.4b and 4.4f). For Chl-a, the seasonal contribution generally exceeds 60 % over most of the coastal and inner-shelf areas and locally reaches values above 70 %. Similarly, SPM shows strong seasonal dominance, with seasonal contributions typically ranging between 60 and 80 % along the coast and in river-influenced zones.

The interannual component (Figures 4.4c and 4.4g) contributes a smaller but spatially structured fraction of the total variance. For Chl-a, interannual contributions are generally below 20 % over large portions of the study area but locally exceed 25 % near the coastline. In contrast, SPM exhibits higher interannual contributions, reaching approximately 20-30 % in coastal and estuarine-influenced regions.

The irregular component (Figures 4.4d and 4.4h) accounts for the lowest share of total variance for both Chl-a and SPM. Irregular contributions generally remain below 15-20 %, with localized maxima along the complex coastal geometry and near estuarine outlets.

Overall, this study emphasizes the dominant role of seasonal and interannual dynamics in controlling biogeochemical variability along the Maranhão coastal zone. The irregular variation is beyond the scope of the current work.

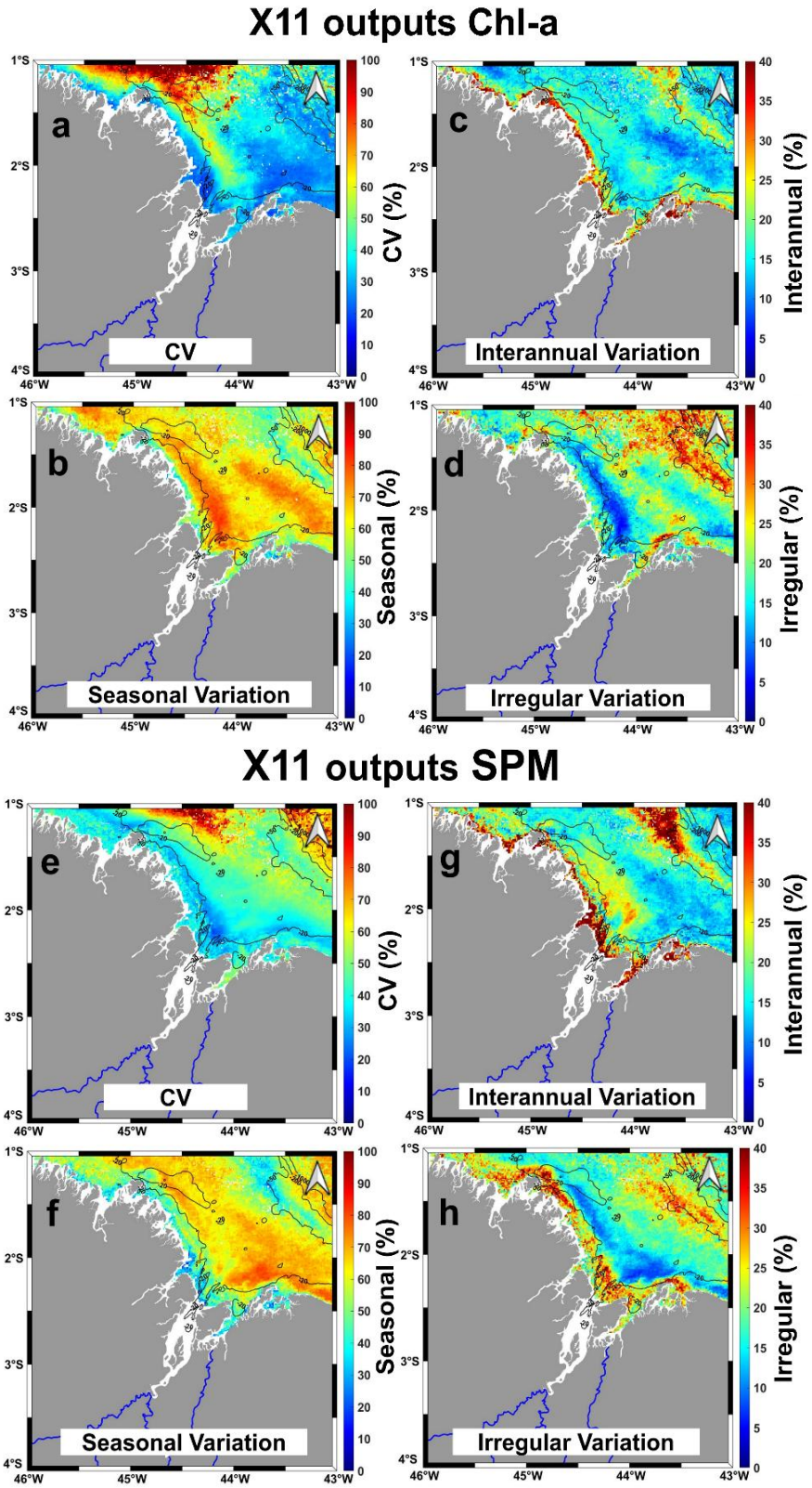

Figure 4.4. Relative contributions (%) of seasonal, interannual, and irregular components derived from Census X-11 decomposition (2002 - 2022) to the total variance of Chl-a (a–d) and SPM (e–h) along the western coast of Maranhão State: (a) Chl-a coefficient of variation (%); (b) seasonal contribution to Chl-a total variance (%); (c) interannual contribution to Chl-a total variance (%); (d) irregular contribution to Chl-a total variance (%); (e) SPM coefficient of variation (%); (f) seasonal contribution to SPM total variance (%); (g) interannual contribution to SPM total variance (%); (h) irregular contribution to SPM total variance (%).

4.3.3. Seasonal Variation of Chl-a and SPM and environmental factors

The analysis first focused on seasonal variations only, using the seasonal components extracted from the Census X-11 decomposition of the Chl-a and SPM time series and compared with the seasonal components of river discharge, precipitation, winds, and currents.

4.3.3.1. River discharge and precipitation

The western coast of Maranhão State is characterized by the presence of several river systems, among which the Turiaçu, Mearim, Grajaú, and the Pindaré (Figure 4.1) are the most influential. These rivers play a major role in delivering freshwater and sediments to the coastal zone, strongly shaping its biogeochemical and hydrodynamic characteristics (Costa et al., 2011; Lefèvre et al., 2017; Limeira-Filho et al., 2023). The seasonal variations of these river systems are generally correlated (Spearman correlation: $r > 0.7$, $p<.0.01$, $N = 246$), reflecting the regional rainfall regime that drives synchronized hydrological responses across the basin. In this study, particular attention is given to the Pindaré River, one of the main tributaries in the region, which represents a key contributor to the observed variability within the study area (Limeira-Filho et al., 2023).

The seasonal variations of the Pindaré discharge and precipitation are presented in Figure 4.5. A strong and significant Spearman correlation is observed between the two variables ($r = 0.77$, $p < 0.001$, $N = 246$), indicating a precipitation-driven seasonal hydrological response.

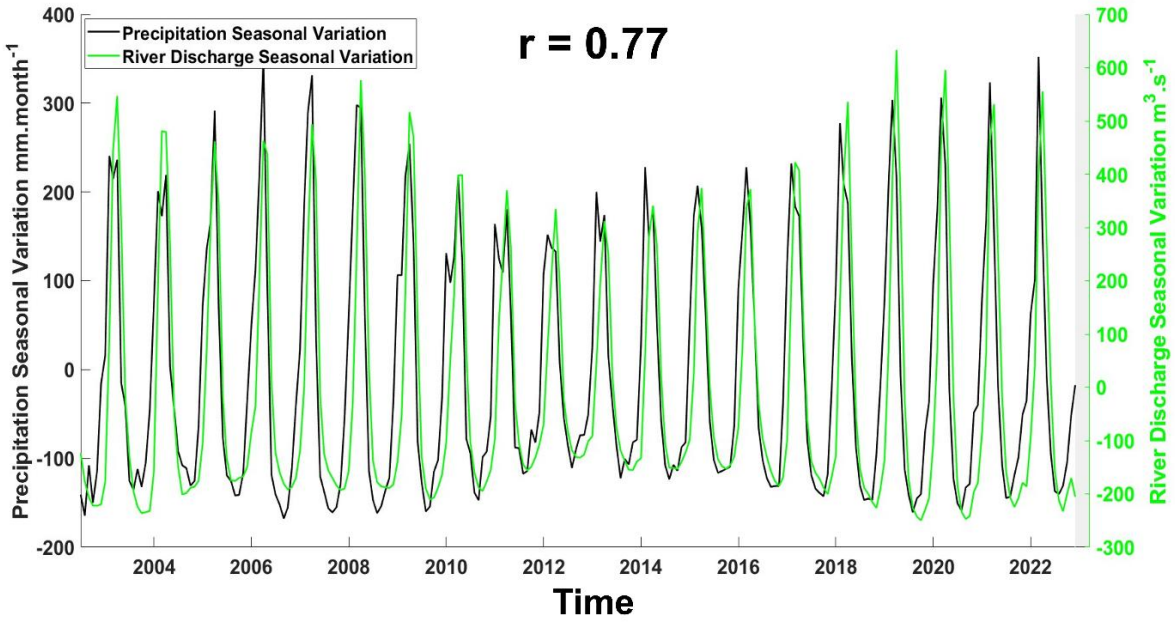

Figure 4.5. Time series of the seasonal variation (Census X-11 outputs) of the Pindaré River (Figure 4.1) discharge and the mean precipitation over the study area (2002–2022).

Beyond this overall synchronicity, a slight temporal shift can be observed between the seasonal extrema of precipitation and river discharge. In most years, precipitation maxima and minima tend to precede those of river discharge by approximately one month, although this lag is not always sharply defined. Such a delay is consistent with the expected hydrological response time of the watershed, reflecting the integration of rainfall through soil infiltration, groundwater storage, and surface runoff before contributing to river flow (Beven, 2012). This behaviour suggests that, while precipitation is the primary driver of seasonal discharge variability, basin-scale storage and transfer processes modulate the timing of discharge extrema (Moussa, Voltz and Andrieux, 2002; Dingman, 2015)

The spatial correlations between the seasonal variation of the Pindaré River discharge and the seasonal variations of Chl-a and SPM are shown in Figures 4.6a and 4.6b, respectively. The strongest correlations are observed along the inner shelf, particularly near the river mouths and estuarine areas, where the influence of freshwater input is most pronounced. Correlation patterns are also stronger toward the north and northwest of the river mouth, whereas they rapidly weaken eastward, consistent with the dominant west-northwestward coastal transport that limits the downstream influence of riverine inputs in the eastern direction. This spatial asymmetry highlights the strong coupling between hydrological variability and biogeochemical responses along the main transport pathway of the coastal circulation.

The time series extracted at point A (Figures 4.6c-d) further confirm the tight relationship between the seasonal variation of river discharge and the seasonal variations of Chl-a ($r = 0.86$, $p < 0.001$, $N = 246$) and SPM ($r = 0.79$, $p < 0.001$, $N = 246$). Both parameters exhibit synchronous peaks, with higher concentrations occurring during the rainy season when the river discharge is at its maximum. This reflects the combined effects of enhanced nutrient supply and increased suspended matter transport associated with intensified runoff. During the dry season, reduced discharge results in lower sediment and nutrient input, leading to decreased Chl-a and SPM concentrations in the coastal domain.

Overall, the strong correlation between regional river discharge (here illustrated using the Pindaré river) and both Chl-a and SPM underscores the dominant role of fluvial forcing and precipitation in shaping the seasonal biogeochemical dynamics of the study area.

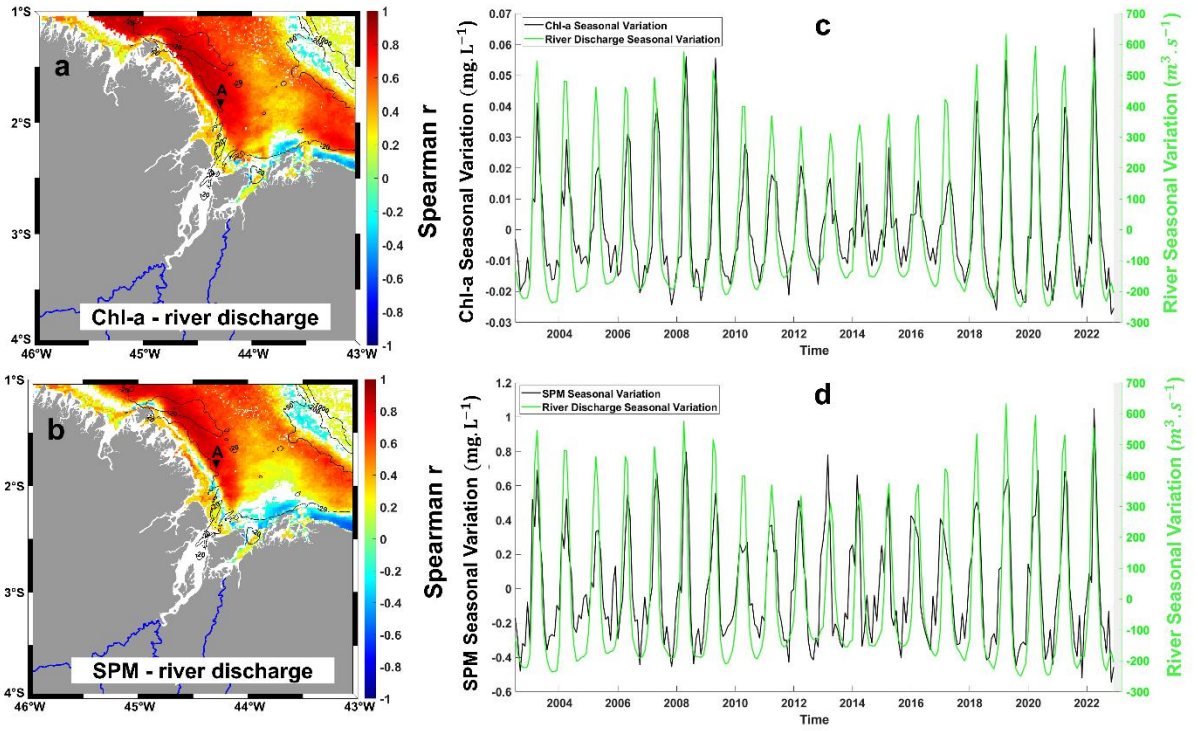

Figure 4.6. Correlation between the seasonal variation (Census X-11 outputs) of river discharge and Chl-a and SPM over the western coast of Maranhão State: (a-b) spatial correlation maps between the seasonal variation of Chl-a and SPM and the seasonal variation of river discharge; (c-d) time series of the seasonal variation of Chl-a and SPM extracted at point A with the seasonal variation of river discharge (2002–2022).

4.3.3.2. Currents and winds

The correlation maps between the seasonal variations of Chl-a and SPM and the seasonal variations of the zonal (U) components of wind and surface currents (Figure 4.7a-4.7d) show predominantly positive Spearman correlations along the coastal and inner-shelf regions, with the strongest values observed near the shoreline and river-influenced areas. These spatial patterns indicate that east-to-west transport driven by trade winds and surface currents enhances the advection of fluvial and coastal materials along the Maranhão coast.

The spatial correlations are supported by temporal relationships derived from the seasonal components of the time series extracted at point A (Figure 4.7). Significant positive correlations are found between the seasonal variation of the U-wind component and Chl-a seasonal variability ($r = 0.66$, $p < 0.001$, $N = 246$; Figure A.9a), as well as between the seasonal variation of U-wind and SPM seasonal variability ($r = 0.74$, $p < 0.001$, $N = 246$; Figure A.9b). Similarly, the seasonal zonal current component is significantly correlated with both Chl-a ($r = 0.50$, $p < 0.001$, $N = 246$; Figure A.10a) and SPM ($r = 0.46$, $p < 0.001$, $N = 246$; Figure A.10b) at the seasonal scale.

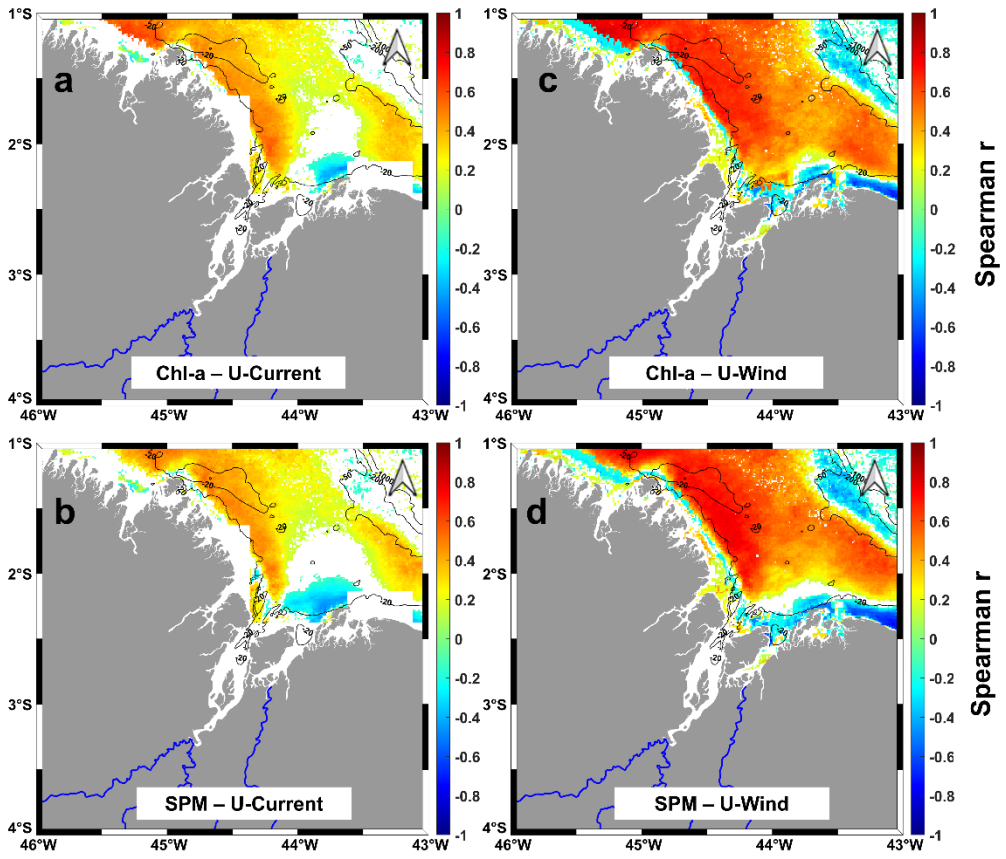

Figure 4.7. Correlation maps between the seasonal variation (Census X-11 outputs) of Chl-a and SPM and the seasonal variation of the zonal component of current and wind (U-current, U-wind) over the western coast of Maranhão State: (a) correlation between Chl-a and U-current; (b) correlation between SPM and U-current; (c) correlation between Chl-a and U-wind; (d) correlation between SPM and U-wind.

The correlations between the seasonal variations of Chl-a and SPM and the seasonal variation of the meridional component of the surface current (V-current; Figures 4.8a-b) are generally weak and spatially heterogeneous across the western Maranhão coast. Most of the study area is characterized by low and non-significant Spearman correlation coefficients ($|r| < 0.2$, $p \geq 0.05$, $N = 246$), as indicated by the extensive white regions. Where significant correlations occur, they remain patchy and of limited magnitude ($|r| < 0.3$), indicating that the seasonal V-current does not play a dominant role in controlling the seasonal variability of Chl-a and SPM.

In contrast, the correlation maps between the seasonal variations of Chl-a and SPM and the seasonal variation of the meridional wind component (V-wind; Figures 4.8c–d) exhibit a distinct and spatially coherent coastal–offshore structure. Along the immediate coastal zone, significant positive correlations are observed ($r = 0.3$ to 0.6, $p < 0.05$, $N = 246$), indicating that seasonal maxima in Chl-a and SPM tend to occur during periods of enhanced seasonal V-wind. Conversely, over the inner and mid-shelf, correlations are predominantly negative and statistically significant ($r = -0.3$ to -0.7, $p < 0.05$, $N = 246$), showing that offshore seasonal

peaks in Chl-a and SPM coincide with periods of weakened seasonal V-wind. This pattern results in a narrow nearshore band of positive correlations and a broader offshore region of negative correlations, aligned with the coastline.

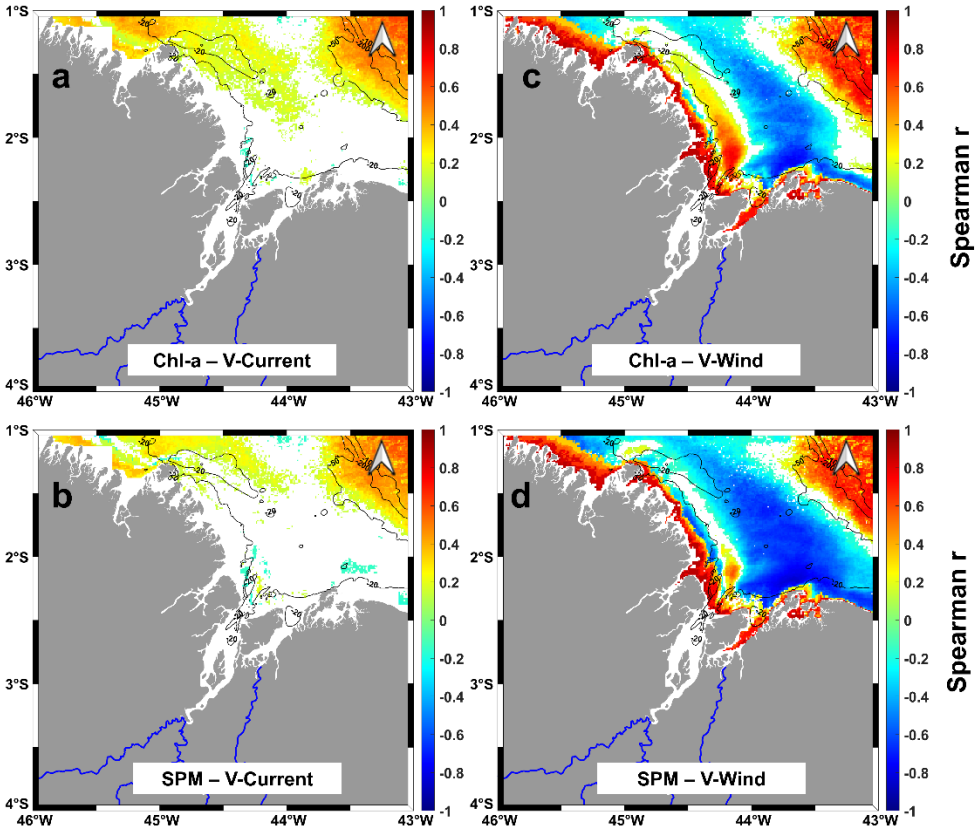

Figure 4.8. Correlation maps between the seasonal variation (Census X-11 outputs) of Chl-a and SPM and the seasonal variation of the meridional component of current and wind (V-current, V-wind) over the western coast of Maranhão State: (a) correlation between Chl-a and V-current; (b) correlation between SPM and V-current; (c) correlation between Chl-a and V-wind; (d) correlation between SPM and V-wind.

4.3.4. Interannual variation of Chl-a and SPM:

4.3.4.1. Trend Analysis

The trend analysis of Chl-a and SPM between 2002 and 2022 revealed a significant increase ($p < 0.01$, $N = 246$) of approximately 30% and 50%, respectively (Figure 4.9a, b). Figures 4.9a and 4.9b show the spatial distribution of the rate of change (RC, %. year^{-1}) for Chl-a and SPM derived from 20 years of monthly data over the western coast of Maranhão State. The focus of this study is on coastal waters shallower than 50 m, before the shelf break, as the offshore variability lies beyond the scope of this work. In this coastal region, both SPM and Chl-a show significant increasing trends.

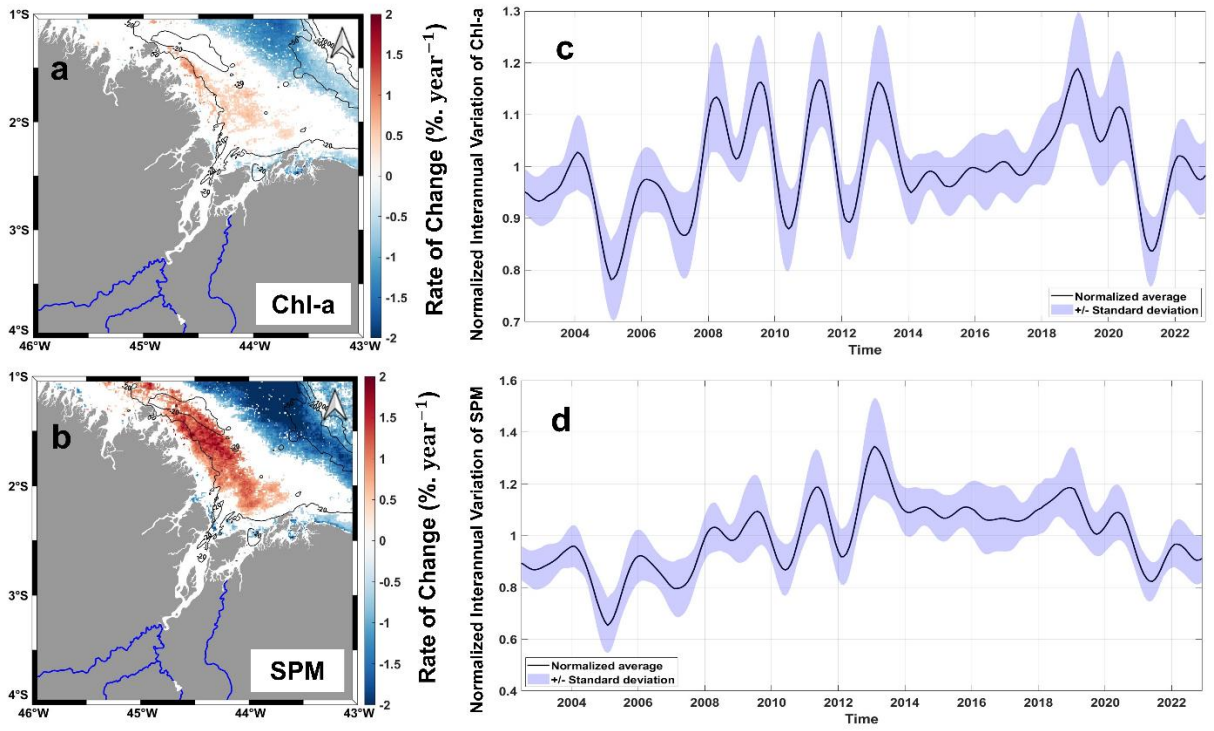

Figure 4.9. Rate of change (RC) of Chl-a and SPM between 2002–2022 over the western coast of Maranhão State: (a) RC of Chl-a; (b) RC of SPM, showing only statistically significant changes ($p < 0.05$); (c) Time series of Census X-11 interannual variation of Chl-a; (d) Standardized time series of Census X-11 interannual variation of SPM, both averaged over the areas with positive and statistically significant RC ($RC > 0$, $p < 0.05$, $N = 246$).

Figures 4.9c and 4.9d illustrate the standardized interannual variations of Chl-a and SPM, respectively, from 2002 to 2022. The black lines represent the standardized averages, while the shaded areas indicate the standard deviations around the zonal mean. Both series display strong interannual variability, with alternating peaks and declines roughly every 2-4 years. Around 2012 and 2019, both parameters reached their highest values. After 2020, Chl-a shows a noticeable decline, whereas SPM exhibits a more moderate decrease and remains close to its long-term mean toward 2021-2022. Despite these fluctuations, the long-term trend indicates an overall increase over the two decades. A key difference between the two parameters emerges after 2014: SPM values remain relatively elevated until the end of the study period, with only a slight decline toward 2022, whereas Chl-a follows a similar interannual pattern but exhibits a more pronounced decrease after mid-2020.

4.3.4.2. Anthropogenic treats (land use and land cover)

To better understand the observed increase in Chl-a and SPM concentrations, land use and land cover data were analyzed to identify potential anthropogenic drivers in Maranhão State. The land cover maps derived from the MapBiomas platform show a marked transformation of the landscape between 2002 (Figure 4.10a) and 2022 (Figure 4.10b). During this period,

extensive deforestation occurred, with large forested areas being progressively replaced by pastures mainly dedicated to livestock farming activities.

Quantitative analysis of land cover changes based on a comparison of surface areas in 2002 and 2022 (Figure A.11) indicates that mangrove coverage remained relatively stable over the study period, exhibiting only minor variations compared to the pronounced decrease in forested areas and the substantial expansion of pastures. Urban areas, mainly concentrated around São Luís, show a measurable increase between 2002 and 2022; however, this increase remains limited in terms of total surface area when compared to the magnitude of forest loss and pasture expansion. Overall, these results suggest that pasture expansion represents the dominant anthropogenic land-based pressure potentially affecting terrestrial inputs to the coastal zone.

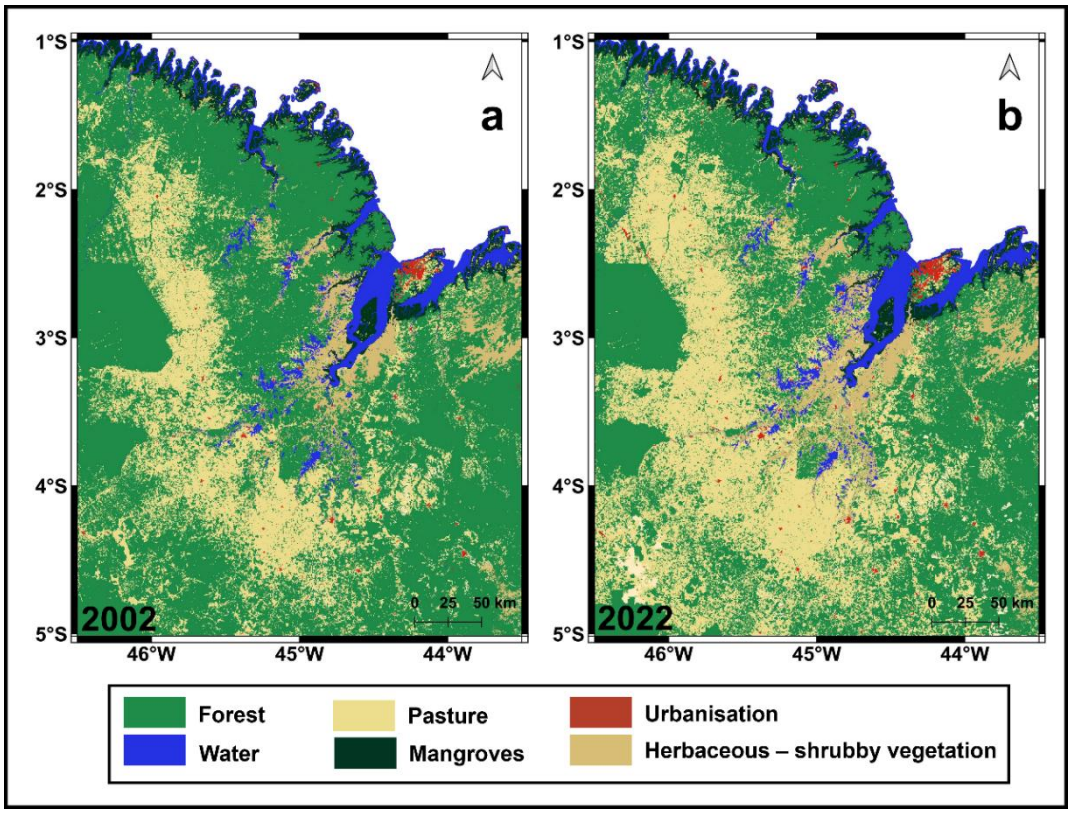

Figure 4.10. Land use and land cover maps for 2002 and 2022 within the study area (MapBiomas): (a) land cover map for 2002; (b) land cover map for 2022.

Spatial correlation maps between pasture expansion and the interannual variations of Chl-a and SPM (Figures 4.11a-b) reveal predominantly positive and statistically significant Spearman correlations across the western coast of the study area. The strongest correlations are observed along the coastal and nearshore zones, with correlation coefficients generally ranging between $r = 0.4$ and 0.7 ($p < 0.05$, $N = 246$), particularly in areas influenced by river discharges. Offshore regions exhibit weaker and often non-significant correlations ($r < 0.2$), as indicated by the masked areas. This spatial coherence suggests that regions experiencing the most

pronounced pasture expansion are also those showing enhanced interannual variability of Chl-a and SPM.

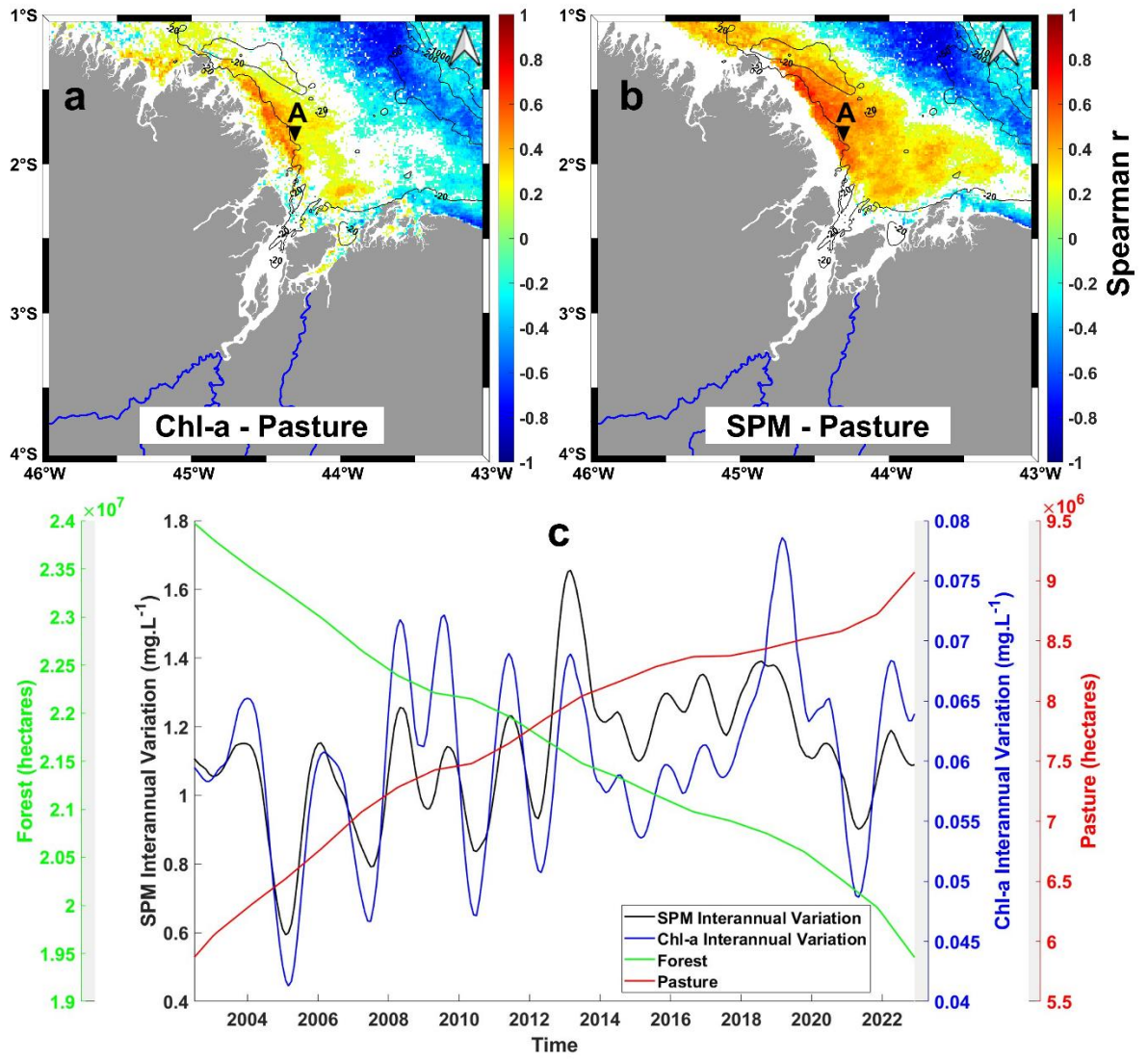

Figure 4.11. Correlation between land use and the interannual variation of Chl-a and SPM over the western coast of Maranhão State: (a) correlation map between the interannual variation of Chl-a and pasture; (b) correlation map between the interannual variation of SPM and pasture; (c) time series of the interannual variation of Chl-a (blue) and SPM (black) extracted at point A together with forest (green) and pasture (red) areas from 2002 to 2022.

The temporal relationship between land use change and coastal biogeochemical variability is further illustrated in Figure 4.11c using time series extracted at point A (Figure 4.11). A significant positive correlation is observed between pasture surface area and the interannual variation of SPM ($r = 0.48$, $p < 0.001$, $N = 246$), indicating that increasing pasture extent is associated with enhanced interannual variability of suspended particulate matter. A weaker but still significant relationship is found between pasture surface area and the interannual variation of Chl-a ($r = 0.30$, $p < 0.001$, $N = 246$), suggesting a more indirect or modulated response of phytoplankton biomass to pasture expansion.

4.3.4.3. Interannual Variation of Chl-a/SPM

Along the western coast of Maranhão, the Chl-a:SPM ratio exhibits a significant negative trend between 2002 and 2022 ($p < 0.05$, $N = 246$), with the strongest decreases concentrated over the inner shelf where terrigenous inputs and hydrodynamic forcing dominate (Figure 4.12a). This decline reflects the combined effect of increasing SPM (+50 %) and a weaker but still positive rise in Chl- a (+30 %). Together, these patterns indicate that particulate inputs derived from land-use change particularly deforestation and the expansion of pasturelands have increased more rapidly than phytoplankton biomass over the last two decades. Similar results have been documented in other tropical margins where erosion and runoff enhance sediment export and strengthen light limitation in coastal waters (Carvalho et al., 2016; Castro et al., 2018; Viana et al., 2023).

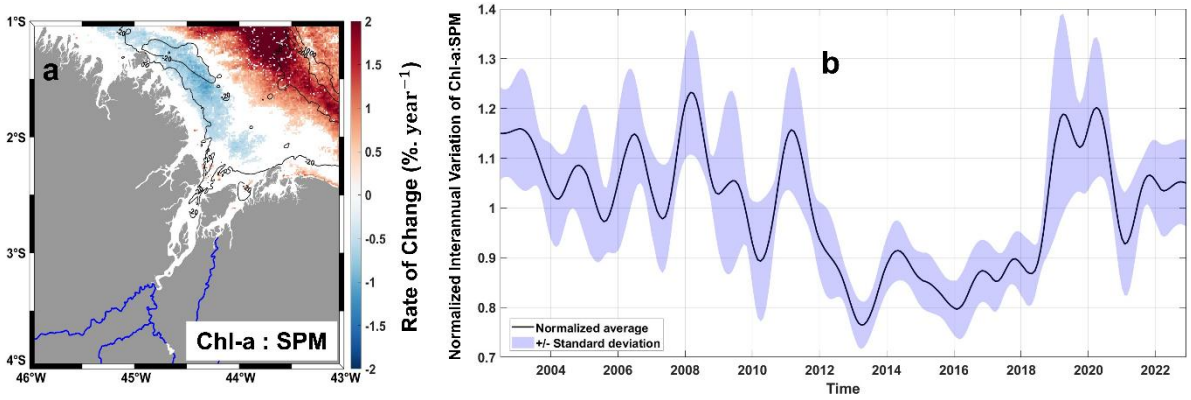

Figure 4.12. RC of the Chl-a:SPM ratio between 2002–2022 over the western coast of Maranhão State: (a) RC of the Chl-a:SPM ratio, showing only statistically significant changes ($p < 0.05$); (b) time series of the Census X-11 interannual variation of the Chl-a:SPM ratio from 2002 to 2022, averaged over areas where RC is negative and statistically significant ($RC < 0$, $p < 0.05$).

The interannual evolution of the standardized Chl-a/SPM ratio (Figure 4.12b) reveals three distinct phases over the study period. From 2002 to approximately 2011, the ratio shows a marked decrease, reflecting a phase dominated by enhanced particulate inputs relative to phytoplankton biomass. This period coincides with intense land-use change and strong riverine forcing, characterized by pronounced interannual variability in both precipitation and river discharge, which favored sediment export to the coastal zone.

Between 2011 and 2016, the ratio stabilizes at lower values, indicating a transitional phase during which the relative contributions of Chl-a and SPM remain more balanced, consistent with a period of reduced interannual variability in hydrological forcing.

After 2016, the ratio increases despite a decline in SPM, while Chl-a remains relatively elevated. This divergence occurs during a phase marked by renewed hydrological variability, as reflected by coherent interannual fluctuations in precipitation and river discharge (Figure

A.12), which are significantly correlated ($r = 0.50$, $p < 0.001$, $N = 246$). Together, these patterns highlight contrasted responses of particulate matter and phytoplankton biomass to changing land-river-coastal dynamics during the most recent years of the record.

4.3.5. Relative importance of climate and human pressures on interannual Variation of Chl-a and SPM

To further confirm the relative contribution of anthropogenic forcing and environmental drivers on the evolution of coastal biogeochemical dynamics, we applied a GAM to Chl-a and SPM interannual variations using a set of environmental predictors that potentially affect water composition and transport processes. These predictors include interannual variation of river discharge, interannual variation of zonal and meridional components of surface currents and winds (U-current, V-current, U-wind, V-wind), and pasture surface area.

Although both river discharge and precipitation data were available, only river discharge was included in the models to avoid multicollinearity, as these variables were strongly correlated ($r > 0.7$, $p < 0.001$, $N = 246$). Among the four rivers influencing the region, the Pindaré River was selected as the representative hydrological input due to its greater importance within the Mearim Basin and its strong correlation with the others ($r > 0.7$, $p < 0.001$, $N = 246$).

For the interannual component of Chl-a, the GAM achieved an adjusted R^2 of 0.99 and explained 99.4 % of the deviance, indicating an excellent model fit. The pasture surface was by far the most influential variable, with an F-statistic of 255 and a relative contribution of 73.9 % (Table A.1). River discharge interannual variation contributed 12.1 %, while the interannual variation of the meridional current (V-current) explained 9.6 % of the variance (Table A.1). The remaining variables (winds and U-current) contributed less than 3 %, suggesting a minor role in controlling the long-term variability of Chl-a. These results indicate that increases in pasture area play a major role in shaping Chl-a interannual dynamics, exceeding the contribution of physical oceanic variability.

For the interannual component of SPM, the GAM showed a similarly strong performance (adjusted $R^2 = 0.99$, deviance explained = 99.8 %). Once again, pasture surface dominated the model, with an F-statistic of 958 and a contribution of 89.4 % (Table A.2), confirming its leading influence on SPM concentration. The interannual variation of the meridional current (V-current, 3.9 %, Table A.2) and river discharge (2.6 %, Table A.2)) provided secondary contributions, while the wind and zonal current components together accounted for less than 5 % of the variance.

Notably, river discharge, winds, and surface currents do not exhibit any monotonic trend over the study period ($p>0.05$). Their lack of long-term change indicates that these physical drivers cannot explain the sustained increases observed in Chl-a and SPM. Instead, they primarily modulate the interannual variability around the rising trajectory, while the upward trends themselves are more closely associated with pasture expansion.

To isolate the contribution of natural drivers to interannual variability, the effect of pasture expansion was first removed from the Chl-a and SPM time series. This was achieved by fitting a GAM in which interannual variations of Chl-a (or SPM) were explained solely by pasture surface area. The pasture-related component was then estimated from the model predictions and subtracted from the original time series, yielding detrended series in which the influence of pasture expansion was excluded.

These detrended time series were subsequently used as response variables in new GAMs to assess the residual influence of hydrodynamic and atmospheric drivers. The models included interannual variations in river discharge, and the zonal and meridional components of winds and surface currents (U-wind, V-wind, U-current, and V-current), while the pasture variable was intentionally excluded.

After detrending, the models showed a substantial reduction in explanatory power, as expected following the removal of the dominant anthropogenic signal. For SPM, the GAM achieved an adjusted R^2 of 0.13 and explained 15.7 % of the deviance, while for Chl-a the adjusted R^2 decreased to 0.09 with 10.6 % of the deviance explained. Despite this reduced performance, both models remained statistically significant, with river discharge emerging as the main explanatory variable of the remaining interannual variability ($p < 0.001$). In contrast, the zonal and meridional components of winds and surface currents were not statistically significant ($p > 0.1$), indicating that these physical drivers exert only a secondary modulation on interannual variability once the long-term anthropogenic forcing is removed.

The partial effect plots for river discharge (Figure 4.13) illustrate the isolated effect of discharge on Chl-a and SPM, after accounting for the influence of the other predictors in the GAM. Consistent with the modeling framework described in the Materials and Methods section, the estimated degrees of freedom (edf) for river discharge are clearly greater than 1 for both Chl-a (edf = 3.32) and SPM (edf = 4.61), indicating that the relationship between discharge and these variables is markedly non-linear rather than approximately linear. At low to moderate discharge values, concentrations increase rapidly, indicating that higher river flow enhances the transport of suspended sediments and nutrients to coastal waters. This positive phase reflects the intensification of fluvial inputs during high-flow conditions.

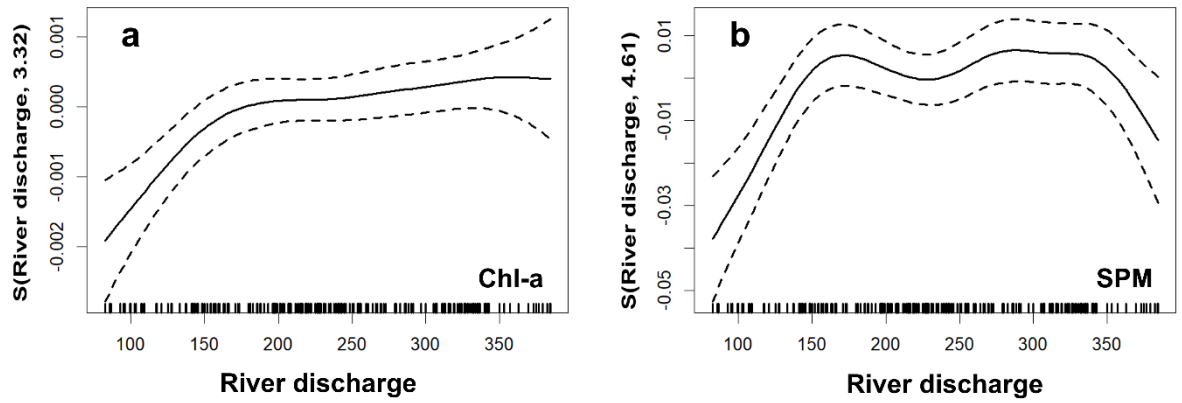

Figure 4.13. Partial effects of river discharge on Chl-a and SPM obtained from the GAM analysis: (a) smooth function of river discharge for Chl-a; (b) smooth function of river discharge for SPM.

For SPM, the relationship with river discharge shows a clear saturation plateau, indicating that once catchments and floodplains become saturated and land-flushing is maximized, additional increases in discharge do not lead to higher suspended particle concentrations. At the highest discharge values, the curve slightly declines, which may indicate enhanced offshore exports, likely due to dilution and sediment dispersion or settling of material. For Chl-a, the response also shows an initial increase followed by a stabilization at higher discharges, suggesting that phytoplankton biomass benefits from increased fluvial inputs up to a saturation point, beyond which other factors (such as nutrient limitation, turbidity and light reduction, or changes in source waters) likely prevent further increases.

Finally, these detrended models confirm that once the anthropogenic effect of pasture is removed, river discharge becomes the dominant natural control of interannual variability in SPM and Chl-a, while other oceanic and atmospheric factors play only a minor supporting role.

4.4. Discussion

4.4.1. Chl-a and SPM general patterns

The seasonal component (Figures 4.4b and 4.4f) dominates the overall variability for both Chl-a and SPM, reflecting the strong influence of regional hydrodynamics. This pattern is closely linked to the seasonal cycle of river discharge and precipitation, which modulates the input of nutrients and suspended matter into the coastal zone (Choudhury and Pal, 2010; Delgado et al., 2015; Shampa et al., 2024). Moreover, wind-driven mixing and coastal currents contribute to the redistribution of particulate and phytoplankton material, enhancing the seasonal signal across the shelf (Lentz and Fewings, 2012; Chen et al., 2020; Ferronato et al., 2023).

Beyond this dominant seasonal forcing, the interannual component (Figures 4.4c and 4.4g) reveals variability exceeding 20 % near the Maranhão coast, more pronounced for SPM. This longer-term variability indicates that, in addition to recurrent hydrological cycles, the system responds to large-scale climatic influences and long-term hydrological variations, including changes in rainfall regimes, river discharge, and possibly the cumulative impact of anthropogenic pressures on the coastal system (Loisel et al., 2014; Gensac et al., 2016; Bortolin et al., 2022).

Superimposed on both the seasonal and interannual signals, the irregular (residual) component (Figures 4.4d and 4.4h) corresponds to short-term, non-cyclic variations associated with transient events such as storms, episodic river floods, or abrupt changes in circulation (Loisel et al., 2014; van der Hout et al., 2017; Prend et al., 2022). These irregular modulations are particularly evident along the complex coastline, where local hydrodynamic processes amplify spatial variability.

4.4.2. Chl-a and SPM seasonal variability (2002-2022)

Precipitation exerts primary control on river discharge (Figure 4.5), directly influencing the magnitude and timing of sediment and nutrient fluxes entering the coastal waters (Ludwig and Probst, 1998; Lohrenz et al., 2008; Richardson et al., 2025). As a result, the combined effect of riverine inputs and rainfall determines the seasonal patterns of Chl-a and SPM concentrations observed along the coast (Sullivan et al., 2001; Frigstad et al., 2020).

Consistently, the seasonal variability in precipitation and river discharge plays a crucial role in controlling the seasonal dynamics of Chl-a and SPM (Figure 4.6), as increased runoff during the rainy season enhances nutrient and sediment inputs, stimulating phytoplankton growth and elevating suspended particulate concentrations in coastal waters (Sigleo and Frick, 2007; Fong, Gaynus and Carpenter, 2020).

The observed correlation between seasonal variation of river discharge and seasonal variation of Chl-a and SPM (Figure 4.6) is therefore consistent with previous studies in tropical coastal systems, showing that river discharge and precipitation are major drivers of seasonal biogeochemical variability (e.g., Hamilton, 2010; Molleri, Novo and Kampel, 2010; Borges and Abril, 2011; Miguel, 2018; Shi and Wang, 2024). Enhanced freshwater inflow not only stimulates phytoplankton growth through nutrient enrichment but also increases light attenuation due to higher sediment loads, leading to complex and spatially variable responses (Medeiros et al., 2013; Zang et al., 2020; Pires et al., 2024). These river-driven effects are further modulated along the Maranhão coast by coastal currents and wind-driven mixing, which

redistribute suspended and particulate material across the shelf (Carvalho et al., 2016; Castro et al., 2018).

In this context, the western coast of Maranhão, located within the Gulf of Maranhão, is exposed to a persistent trade-wind regime, with near-surface winds blowing predominantly from the east to northeast for most of the year, modulated by the seasonal migration of the Intertropical Convergence Zone and by local sea-land breeze cycles near the coast (Planchon et al., 2004; Alvares et al., 2013; Assireu et al., 2022; Pimenta et al., 2023). This shallow, macrotidal shelf experiences energetic hydrodynamics, where trade-wind forcing combined with strong tidal currents enhances coastal circulation, vertical mixing, and sediment resuspension, redistributing suspended and particulate material across the shelf (Castro et al., 2018; dos Santos et al., 2020; Gomes et al., 2021; Aguiar et al., 2022). Under such conditions, both wind stress and surface circulation play crucial roles in the transport and dispersion of riverine inputs, influencing the spatial and temporal variability of biogeochemical properties such as Chl-a and SPM (Carvalho et al., 2016).

The spatial and temporal correlations between seasonal variation of Chl-a and SPM and seasonal variation of the zonal component of wind and currents (Figure 4.7) further highlight the role of westward wind-driven and current-driven transport in redistributing suspended sediments and nutrients across the inner shelf, thereby supporting enhanced turbidity and phytoplankton biomass in nearshore waters. These patterns are consistent with the dominance of northeasterly trade winds and associated westward surface circulation along the Maranhão coast (Castro et al., 2018; Assireu et al., 2022; Pimenta et al., 2023).

This zonal dominance is coherent with the regional circulation, which is characterized by a persistent northwestward alongshore flow associated with the North Brazil Current, leaving the meridional component weak and highly variable (Aguiar et al., 2022; Dimoune et al., 2023). In this macrotidal system, tidal currents and the dominant alongshore jet play the main role in material transport, while cross-shore flow remains limited (Castro et al., 2018; Gomes et al., 2021).

Because winds along the Maranhão coast are predominantly easterly to northeasterly throughout the year, the seasonal cycle of V-wind primarily reflects the seasonal modulation of the southward component embedded within these trade winds. Periods of higher V-wind values correspond to a relative weakening of the southward wind stress, whereas lower values correspond to its seasonal strengthening. This modulation is dynamically relevant because it affects the balance between alongshore wind forcing, coastal setup, and cross-shelf Ekman transport on the northern Brazilian shelf, consistent with classical descriptions of wind-driven

offshore transport and plume detachment (García Berdeal, Hickey and Kawase, 2002; Hickey et al., 2005; Burla et al., 2010) and with regional analyses showing that meridional wind stress modulates cross-shelf divergence and plume spreading in northern Brazil (Nikiema et al., 2007; Coles et al., 2013; Osadchiev et al., 2020).

The positive correlations of Chl-a and SPM with V-wind at seasonal scale (Figure 4.8), observed along the coast, indicate that the seasonal increase in Chl-a and SPM coincides with periods in which the southward component of the trade-wind field is seasonally reduced, favouring coastal convergence and the retention of plume and suspended material. Conversely, the negative correlations offshore imply that the seasonal enhancement of offshore Chl-a and SPM occurs when the southward wind stress intensifies, promoting cross-shelf divergence and the seaward export of buoyant and particulate coastal waters. This coastal–offshore dipole is consistent with the expected seasonal adjustments of wind-driven Ekman dynamics on tropical shelves and with the sensitivity of coastal plumes to the seasonal modulation of alongshore wind stress (García Berdeal, Hickey and Kawase, 2002; Hickey et al., 2005; Nikiema, Devenon and Baklouti, 2007; Burla et al., 2010; Coles et al., 2013; Osadchiev, Silvestrova and Myslenkov, 2020).

Overall, these correlations demonstrate that the seasonal variability of Chl-a and SPM in the Maranhão coastal zone is not solely controlled by fluvial input but also by the combined influence of atmospheric and hydrodynamic forcing. The zonal wind component enhances the westward advection and nearshore accumulation of suspended and biogenic material, while the meridional wind component modulates the cross-shelf structure and spreading of the river plume. Together, these wind-driven processes shape the seasonal patterns of sediment resuspension and phytoplankton biomass along the western coast of Maranhão.

4.4.3. Interannual variability of Chl-a and SPM driven by anthropogenic and environmental factors

The conversion of forests to pasturelands is a well-known driver of soil degradation and erosion, which increases sediment transport to rivers and coastal systems (e.g., Neill et al., 2006; Latawiec et al., 2014; Sattler et al., 2018). Runoff from pasture areas carries higher sediment loads that ultimately reach estuarine and coastal waters, leading to an increase in SPM concentrations (Le Gall et al., 2017; Viana et al., 2023). This enhanced land-derived input can also increase both particulate and dissolved nutrient fluxes, stimulating primary productivity and contributing to the observed rise in Chl-a levels (Latawiec et al., 2014; Silva et al., 2019). In this context, the intensification of livestock and pasture expansion in the Maranhão region

(Figure 4.10) appears to be a key factor driving the long-term increase in both SPM and Chl-a concentrations in coastal waters.

Consistent with this interpretation, the long-term increase in Chl-a and SPM observed between 2002 and 2022 (Figure 4.9) is closely linked to the expansion of pasturelands and deforestation in the study area. The strong spatial and temporal correlations (Figure 4.11) between pasture growth, deforestation, and water constituents highlight the increasing influence of land-use change on coastal biogeochemical dynamics. Similar relationships have been reported in other tropical systems where deforestation and agricultural conversion enhance soil erosion, nutrient export, and suspended sediment loads (Neill et al., 2006; Figueiredo et al., 2010; Nóbrega et al., 2018; Tanaka, Minggat and Roseli, 2021; Narayanan, Cohen and Gardner, 2024). These terrestrial alterations modify the quantity and composition of materials reaching estuaries, promoting higher turbidity and phytoplankton biomass (Figueiredo et al., 2010; Tanaka, Minggat and Roseli, 2021).

The GAM analysis further quantifies this influence and confirms the preponderant role of pasture, which explained more than two-thirds of the interannual variability in both Chl-a and SPM. This dominant contribution reveals a strong anthropogenic control on coastal water composition. The increase in particulate matter and organic carbon derived from soil erosion and runoff likely enhanced nutrient availability, stimulating phytoplankton growth (Granéli, Carlsson and Legrand, 1999; Thomas et al., 2004; Tanaka, Minggat and Roseli, 2021). However, this same process also increases light attenuation, potentially reducing photosynthetic efficiency in turbid nearshore waters (Cloern, 2001; Jassby et al., 2002; Domingues et al., 2011) . The resulting coupling between SPM and Chl-a therefore reflects a balance between nutrient enrichment and optical limitation, a pattern typical of productive but degraded tropical estuarine systems (Lins et al., 2018; Silva et al., 2019).

To further resolve this balance, the Chl-a:SPM ratio was computed to better characterize the relationship between phytoplankton biomass and suspended particles in this highly dynamic coastal system. This ratio is commonly used to evaluate how changes in suspended matter influence light availability and phytoplankton development in turbid coastal waters (Irigoien and Castel, 1997; Stramski et al., 2004; Loisel et al., 2006; Tran et al., 2023). In the study area, SPM and Chl-a have both increased over the past two decades, but SPM shows a much stronger rise, largely driven by enhanced sediment delivery from river discharge and by land-use change, particularly deforestation linked to pasture expansion. Higher SPM reduces light penetration and modifies underwater irradiance, limiting the capacity of phytoplankton to fully respond to nutrient enrichment (Cloern, 2001; Doxaran et al., 2009; Domingues et al., 2011; Loisel et al.,

2014). The Chl-a:SPM ratio therefore provides a relevant indicator of whether the increase in suspended particles outpaces the increase in phytoplankton biomass and of how terrigenous inputs affect coastal water conditions.

Consistently, because SPM strongly attenuates underwater light, elevated sediment loads limited the capacity of phytoplankton to respond proportionally to nutrient enrichment supplied by runoff (Granéli et al., 1999; Jassby et al., 2002; Kang et al., 2020). Although Chl-a increased over the study period, it rose much more slowly than SPM. As a result, phytoplankton biomass represented a progressively smaller fraction of the suspended material, leading to a sustained decrease in the Chl-a:SPM ratio.

Despite this long-term decline, the increase in the Chl-a:SPM ratio after 2015 (Figure 4.12) indicates a partial recovery of phytoplankton relative to suspended sediments. This pattern reflects the progressive stabilization of sediment inputs following the earlier phase of intense erosion linked to rapid deforestation and pasture expansion (Walling, 1999; Liébault et al., 2005; Wu et al., 2023). As sediment-source areas become depleted, the rise in SPM slows and water clarity improves, allowing phytoplankton to respond more efficiently when nutrient availability remains high. Interannual variability in rainfall, runoff, and fluvial transport further modulates both nutrient delivery and fine-sediment dynamics, periodically enhancing light availability in a system primarily limited by turbidity. These combined processes explain the recent rise in the ratio despite continued increases in both SPM and Chl-a. Additional influences such as tidal mixing, internal recycling, and shifts in optical water types may also contribute to this behavior.

When isolating anthropogenic effects, the detrended GAMs show that river discharge emerges as the dominant natural driver of residual interannual variability. This confirms that, in the absence of strong anthropogenic pressure, hydrological variability controls much of the interannual behavior of coastal biogeochemistry. Similar findings have been observed in the Amazon and other equatorial estuaries, where discharge variations modulate sediment export, nutrient delivery, and coastal productivity (Hu et al., 2004; Araujo et al., 2014; Kang et al., 2020). The nonlinear responses observed here, characterized by an increase followed by saturation or a slight decline at high discharges, suggest that moderate flows enhance sediment and nutrient inputs. At very high discharge levels, the system may approach hydrological saturation of catchments and floodplains, such that additional water primarily results in dilution, offshore export, or enhanced sediment settling, rather than further increases in river borne material delivery (Merseburger et al., 2005; Weigelhofer, 2017; Dalu et al., 2019).

By contrast, the limited influence of winds and currents implies that oceanic and atmospheric processes mainly modulate the transport and dispersion of materials, especially at the seasonal scale, rather than drive long-term biogeochemical trends, as documented on other highly turbid tropical margins where local hydrology and land-use changes exert stronger control than marine forcings (Tanaka et al., 2021).

Overall, these results demonstrate that the combined effects of land-use change and hydrological variability govern the long-term evolution of coastal water quality in this region. The dominance of the pasture signal underscores the growing vulnerability of tropical coastal ecosystems to terrestrial disturbances. Continued agricultural expansion and forest loss are likely to amplify sediment and nutrient fluxes, altering the balance between turbidity and productivity, with cascading consequences for carbon cycling and fisheries (Neill et al., 2006; Latawiec et al., 2014; Sattler et al., 2018). These saturation patterns further highlight the need for integrated models that explicitly couple watershed hydrology and coastal hydrodynamics to better resolve the nonlinear response of SPM and Chl-a to extreme discharge events.

4.5. Conclusion

This study shows that two decades of MODIS-Aqua satellite data, combined with land-use information and statistical modeling, provide a coherent picture of how deforestation and pasture expansion are reshaping coastal waters along the western Maranhão coast.

Between 2002 and 2022, both Chl-a and SPM increased significantly in coastal waters shallower than 50 m, by about 30 % and 50 %, respectively. Census X-11 decomposition and trend analysis indicate that these changes are not random fluctuations but represent robust, long-term shifts superimposed on strong seasonal and interannual variability. The seasonal signal is largely controlled by precipitation and river discharge, which govern the timing and magnitude of sediment and nutrient delivery to the coast, while winds and currents redistribute fluvial plumes along and across the shelf.

Linking these changes to land dynamics shows a clear anthropogenic imprint. MapBiomas data reveal a strong conversion of forest to pasture in Maranhão's Amazonian sector, and spatial–temporal correlations show that the regions with the strongest increases in Chl-a and SPM tend to coincide with those where the influence of pasture expansion is most pronounced. GAM results confirm this link: pasture area is the dominant predictor of interannual variability, explaining most of the variance in both Chl-a and SPM, whereas river discharge and hydrodynamic variables play secondary roles and do not exhibit long-term trends. When the

pasture signal is removed, river discharge emerges as the main natural driver, indicating that, in the absence of strong land-use change, hydrology would control most of the residual interannual variability.

The analysis of the Chl-a:SPM ratio provides an integrated view of the long-term evolution of coastal water quality by explicitly accounting for the relative changes between phytoplankton biomass and suspended particulate matter. The marked decline of the ratio over the inner shelf indicates that the increase in SPM has outpaced that of Chl-a, reflecting a shift toward more turbid conditions where light limitation constrains phytoplankton development despite sustained nutrient inputs. The increase observed after 2015 suggests a partial stabilization of sediment inputs and a modest improvement in light availability, allowing a more efficient phytoplankton response. However, this recovery does not reverse the long-term trajectory of the system, which remains strongly controlled by terrigenous inputs. These results highlight the need to assess coastal water quality through combined indicators that capture both absolute trends and the relative evolution of key biogeochemical variables.

A central result of this work is the demonstration that long-term MODIS-Aqua observations, processed with OC-SMART and OWT-based bio-optical algorithms, are essential to detect and attribute the observed changes in coastal biogeochemistry. In a region where in situ measurements are sparse, the 1 km, 20-year MODIS record was crucial to (i) resolve seasonal and interannual variability, (ii) identify coherent spatial patterns along the coast, and (iii) link coastal trends to both land-use trajectories and environmental forcing. The integration of MODIS with MapBiomas land-cover data, hydrological information (river discharge and precipitation), and atmospheric-oceanic drivers (winds and currents), combined with advanced stati-river-coast interactions in tropical margins.

Maintaining long, consistent satellite time series is therefore critical for coastal studies, where biogeochemical variability occurs over decadal scales. The progressive degradation of the MODIS-Aqua sensor and its expected mission end threaten the continuity of such analyses. Although multi-sensor products such as GlobColour and OC-CCI provide extended temporal coverage, they are not yet fully operational in optically complex coastal waters, where uncertainties remain high. Ensuring continuity through the deployment and long-term operation of new sensors specifically suited for coastal environments is thus essential to sustain the monitoring of coastal water quality and land-river-coast interactions.

From a management perspective, the results highlight that coastal water quality in western Maranhão is now strongly conditioned by terrestrial practices. Continued pasture expansion and forest loss will likely intensify sediment and nutrient fluxes, reinforce turbidity and alter the

balance between productivity and light limitation. Effective mitigation therefore requires coordinated policies that integrate watershed management, control of deforestation, and coastal conservation, using satellite-based indicators such as Chl-a, SPM, and the Chl-a:SPM ratio as operational tools for long-term monitoring.

CHAPTER 5: GENERAL DISCUSSION

5.1. Synthesis of the main findings

This PhD thesis provides a comprehensive assessment of the spatiotemporal variability and long-term evolution of coastal biogeochemical properties along the Brazilian margin over the 2002-2022 period, based on satellite ocean color observations. By combining a consistent MODIS-Aqua dataset processed with the OC-SMART atmospheric correction, OWT-based bio-optical models, and robust time-series analysis methods, this work addresses key limitations associated with monitoring optically complex coastal environments.

At the national scale, the results reveal a pronounced spatial heterogeneity in the distribution and temporal evolution of Chl-a, SPM, and POC. Coastal systems exhibit contrasted trajectories, ranging from relatively stable regions to areas characterized by strong variability or significant long-term changes. These patterns highlight the coexistence of multiple forcing mechanisms acting at different spatial and temporal scales, including hydroclimatic variability, riverine inputs, and anthropogenic pressures.

The identification of coastal hotspots of change further emphasizes the non-uniform nature of biogeochemical evolution along the Brazilian coast. While some regions display stable or weakly varying conditions, others exhibit significant increasing or decreasing trends, reflecting localized environmental perturbations. These findings are consistent with previous studies highlighting the strong regional variability of coastal ecosystems and the influence of both natural and human-driven processes (Ciotti et al., 2010; Bernardes et al., 2012; Brandini et al., 2018).

At the regional scale, the two case studies provide complementary insights into the drivers of coastal biogeochemical variability. In southeastern Brazil, the analysis demonstrates a clear and spatially localized increase in SPM associated with the development of the Açu Port Industrial Complex, suggesting a dominant anthropogenic control linked to dredging and port expansion activities. In contrast, along the Amazonian Equatorial Coast of Maranhão, long-term increases in SPM and Chl-a are closely related to land-use changes, particularly deforestation and pasture expansion, highlighting the indirect but pervasive influence of watershed-scale human activities on coastal systems.

5.2. Relative roles of natural forcing and anthropogenic pressures

One of the central objectives of this thesis was to disentangle the respective contributions of natural forcing and anthropogenic pressures to the observed variability in coastal biogeochemical properties. The results demonstrate that these drivers operate simultaneously and interact across multiple scales, making attribution inherently complex.

At seasonal timescales, variability is primarily driven by hydroclimatic forcing, including river discharge, precipitation, wind patterns, and ocean circulation. These processes control the transport of sediments, nutrients, and organic matter from land to sea, as well as mixing and stratification within the coastal ocean (Milliman et al., 2008; Ward et al., 2017). The strong seasonal signals observed in both case studies confirm the dominant role of natural forcing in shaping short-term variability.

At interannual to decadal timescales, however, anthropogenic pressures emerge as key drivers of long-term trends. The results show that human activities can induce persistent and spatially coherent changes in coastal biogeochemical properties, either directly, as in the case of port development, or indirectly through land-use changes affecting riverine inputs. These findings are consistent with global assessments indicating that coastal ecosystems are increasingly influenced by cumulative anthropogenic impacts, including deforestation, agriculture, urbanization, and infrastructure development (Halpern et al., 2015; IPCC, 2022).

Importantly, the interaction between natural and anthropogenic drivers appears to be non-linear. In several regions, climate variability may amplify or modulate the effects of human pressures, while anthropogenic changes in land use can alter the sensitivity of coastal systems to hydroclimatic forcing. This interplay complicates the attribution of observed trends and highlights the need for integrated approaches combining long-term observations and process-based analyses (Doney et al., 2012; Regnier et al., 2013).

5.3. Methodological contributions and implications

This thesis demonstrates the value of an integrated methodological framework for monitoring coastal biogeochemical variability in optically complex environments. The use of MODIS-Aqua as a single-sensor dataset ensures temporal consistency over more than two decades, avoiding potential biases associated with multi-sensor merging approaches, which have been shown to affect trend detection in coastal waters (Mélin, 2016; Yu et al., 2023).

The application of the OC-SMART atmospheric correction represents a key methodological improvement, particularly in turbid coastal environments where standard atmospheric

correction schemes often fail (Fan et al., 2021). In addition, the development and implementation of OWT-based bio-optical models provide a flexible and robust approach to account for the strong optical heterogeneity of coastal waters. By combining and weighting algorithms according to optical conditions, this approach improves the accuracy and spatial consistency of retrieved biogeochemical products, as previously demonstrated in coastal and inland waters (Moore et al., 2014; Spyrakos et al., 2018).

The integration of advanced time-series analysis methods, including Census X-11 decomposition, seasonal Mann–Kendall tests, and generalized additive models (GAMs), further strengthens the robustness of the results. These methods allow the separation of seasonal, interannual, and long-term components, and provide a rigorous framework for trend detection and interpretation in highly variable environments (Hastie and Tibshirani, 1986; Vantrepotte and Mélin, 2011; Wood, 2017).

Overall, the methodological framework developed in this thesis offers a transferable approach for long-term monitoring of coastal water quality, with potential applications in other optically complex regions worldwide.

5.4. Limitations and uncertainties

Despite these advances, several limitations must be acknowledged. First, satellite ocean color observations are restricted to the near-surface layer and do not provide direct information on vertical structure or subsurface processes. As a result, the derived products represent surface conditions and may not fully capture the complexity of coastal biogeochemical dynamics (IOCCG, 2000; Kirk, 1994).

Second, uncertainties associated with atmospheric correction and bio-optical inversion remain significant, particularly in highly turbid waters where multiple optically active constituents contribute to the observed signal. Although the use of OC-SMART and OWT-based models reduces these uncertainties, residual errors may still affect the magnitude and spatial distribution of retrieved variables (Dierssen, 2010; Mobley et al., 2016).

Third, the spatial resolution of MODIS-Aqua (1 km) limits the detection of fine-scale coastal features, such as narrow estuaries, small river plumes, and localized anthropogenic impacts. Higher-resolution sensors, such as Sentinel-3 OLCI, may provide complementary information, although their shorter temporal coverage limits their use for long-term trend analysis.

Finally, the scarcity and uneven distribution of in situ observations constrain the validation and calibration of satellite-derived products. While the integration of available datasets partially

addresses this limitation, the development of sustained in situ monitoring networks remains essential for improving the reliability of satellite-based assessments (Muller-Karger et al., 2018).

5.5. Implications for coastal monitoring and management

The results of this thesis have important implications for coastal monitoring and environmental management. By providing a consistent and spatially extensive assessment of biogeochemical variability over two decades, this work contributes to a better understanding of the functioning and evolution of Brazilian coastal ecosystems.

The identification of coastal hotspots of change and the quantification of long-term trends offer valuable information for environmental monitoring programs and policy-making. In particular, the ability to detect and attribute anthropogenic impacts at regional scales highlights the potential of satellite ocean color observations as a tool for supporting evidence-based coastal management strategies.

More broadly, this study underscores the importance of integrating satellite observations, in situ measurements, and land-use data to address the complex interactions between terrestrial and marine systems. Such integrated approaches are essential for assessing the impacts of global change on coastal environments and for developing sustainable management practices in the face of increasing anthropogenic pressures.

5.6. Concluding remarks

This general discussion highlights that coastal biogeochemical variability along the Brazilian margin results from a complex interplay between natural forcing and anthropogenic pressures, operating across multiple spatial and temporal scales. While hydroclimatic processes dominate short-term variability, human activities emerge as key drivers of long-term changes in several regions.

By combining long-term satellite observations with advanced bio-optical modeling and statistical analysis, this thesis provides a robust framework for monitoring and interpreting coastal biogeochemical dynamics in optically complex environments. The results emphasize the critical role of sustained observations in improving our understanding of coastal systems and supporting effective environmental management in a context of rapid global change.

GENERAL CONCLUSION

This PhD thesis investigated the spatiotemporal variability and long-term evolution of coastal biogeochemical dynamics along the Brazilian margin using satellite ocean color observations. By combining more than two decades of MODIS-Aqua (1 km, 2002-2022) data with advanced atmospheric correction (OC-SMART), OWT-based bio-optical approaches, and robust statistical analyses (Census X-11 decomposition, seasonal Mann-Kendall trend test, and GAMs), this work provides a coherent assessment of coastal water quality dynamics across a wide range of environmental and anthropogenic contexts. Through a combination of large-scale analyses and targeted regional case studies, the thesis addresses methodological, observational, and process-oriented challenges associated with monitoring optically complex coastal waters.

In response to the first scientific question, this thesis demonstrates that the reliable monitoring of Chl-a, SPM, and POC dynamics in optically complex coastal waters requires both adapted satellite products and flexible bio-optical modeling strategies. The long-term consistency, spatial resolution, and spectral configuration of MODIS-Aqua (1 km), when processed using the OC-SMART atmospheric correction, make it particularly suitable for trend analysis in Brazilian coastal environments, providing more spatially complete and robust products than alternative multi-sensor datasets such as GlobColour and OC-CCI in highly turbid waters.

Beyond sensor selection, this work highlights the limitations of single-algorithm approaches in coastal environments characterized by strong optical heterogeneity. To address this challenge, dedicated retrieval algorithms for SPM (Salah Salah et al., 2025) and POC were developed during this PhD. These algorithms are based on an OWT framework that combines and weights existing bio-optical models according to their performance within specific optical regimes. This approach enables robust and spatially consistent retrievals across the land-sea continuum, from highly turbid river-influenced waters to clearer offshore conditions. These results directly address the methodological objective of this thesis by demonstrating that OWT-based algorithm selection is an effective and necessary strategy for improving satellite-derived biogeochemical products in optically complex coastal systems.

In response to the second scientific question, the analysis of MODIS-Aqua time series from 2002 to 2022 reveals pronounced spatial heterogeneity in the evolution of Brazilian coastal water quality and allows the identification of contrasted coastal hotspots of change at the national scale. Coastal waters exhibit distinct temporal trajectories reflecting the combined

influence of regional hydroclimatic variability, riverine inputs, and localized human pressures. Long-term trend analyses indicate significant changes in Chl-a, SPM, and POC concentrations in several regions, with marked differences between river-dominated systems, industrialized coastal sectors, and more oceanic environments.

Coastal regions influenced by strong terrestrial inputs display pronounced seasonal cycles and high interannual variability in particulate and biogeochemical properties, closely linked to river discharge, precipitation, and land–sea fluxes. In contrast, industrialized and urbanized coastal zones show distinct long-term evolutions in particulate matter and Chl-a that cannot be explained by climatic variability alone. At the national scale, while seasonal and interannual variability dominate many regions, the spatial coherence of long-term trends reveals sustained modifications of coastal biogeochemical conditions over the last two decades. These results provide the first spatially consistent, satellite-based assessment of long-term biogeochemical changes along the Brazilian margin.

The third scientific question of this thesis explicitly concerns the relative importance of anthropogenic pressures and climatic forcing in driving long-term coastal biogeochemical changes, and it is addressed through the combination of national-scale analyses and two contrasted regional case studies. By integrating trend analyses, seasonal decomposition, and GAMs, this work disentangles the respective roles of natural and human-induced drivers of coastal biogeochemical variability. The results demonstrate that climatic forcing, particularly through river discharge variability and large-scale climate oscillations, exerts a strong control on seasonal and interannual variability across much of the Brazilian coast.

However, the regional case studies provide clear and contrasted evidence that anthropogenic pressures dominate the long-term trajectories of coastal biogeochemical properties in specific settings. In southeastern Brazil, the Açu Port Industrial Complex constitutes a clear example of industrial and port development significantly modifying suspended sediment dynamics over the 2002-2022 period. The strong and spatially localized increase in SPM observed in the vicinity of the port is temporally consistent with dredging activities, port expansion, and sediment disposal operations, while regional hydrodynamics primarily control sediment dispersion. This case study demonstrates that long-term satellite observations can isolate and quantify anthropogenic signals superimposed on natural hydrodynamic variability.

Along the Amazonian Equatorial Coast of Maranhão, long-term increases in SPM and Chl-a are closely associated with land-use changes, particularly deforestation and pasture expansion within river basins draining into the coastal zone. While seasonal variability remains controlled by precipitation and river discharge, the absence of significant long-term trends in hydrological forcing, combined with the strong statistical link between pasture expansion and particulate matter concentrations, indicates a dominant anthropogenic control on the observed long-term biogeochemical changes. This case study highlights how land-use changes can progressively alter coastal turbidity and phytoplankton dynamics, intensifying light limitation and modifying ecosystem functioning.

Overall, this thesis makes three major contributions. First, it establishes the relevance of an integrated methodological framework combining long-term satellite observations, OWT-based bio-optical modeling, and advanced statistical analyses for monitoring coastal biogeochemical dynamics in optically complex waters. Second, it delivers the first comprehensive and spatially coherent assessment of long-term changes in Brazilian coastal water quality at the national scale, identifying regions of stability, variability, and rapid change. Third, through two contrasted and process-oriented case studies, it demonstrates that anthropogenic pressures such as industrial development in southeastern Brazil and land-use change in northern Brazil, play a dominant role in driving long-term coastal biogeochemical alterations, thereby directly addressing the core scientific objectives stated in the introduction and reinforcing the relevance of satellite-based observations for environmental assessment and coastal management.

By integrating methodological developments with process-oriented analyses, this work advances the understanding of coastal biogeochemical functioning along the Brazilian margin and provides a scientifically robust basis for evaluating human and environmental impacts on coastal water quality.

PERSPECTIVES

The results presented in this thesis highlight several perspectives for advancing the monitoring and understanding of coastal biogeochemical dynamics in optically complex environments, particularly along the Brazilian margin.

- **Extension and continuity of satellite time series**

A first major perspective concerns the extension of long-term satellite ocean color time series. While MODIS-Aqua provides an exceptional and internally consistent dataset spanning more than two decades, its eventual termination planned for 2026 will create a critical gap for climate-scale studies. Moreover, NASA currently recommends not using MODIS-Aqua ocean color data for scientific analyses beyond 2022 due to progressive sensor degradation, which may affect radiometric stability.

In this context, it becomes necessary to evaluate the potential impact of sensor ageing on the trends observed over the 2002-2022 period, in order to assess the robustness of the detected long-term biogeochemical changes and to distinguish instrumental effects from genuine environmental signals.

Current multi-sensor products such as OC-CCI and GlobColour represent a necessary pathway to ensure temporal continuity. However, their limitations in optically complex coastal waters, particularly the absence of near-infrared bands and their reduced performance in highly turbid environments, remain a major challenge. Improving multi-sensor harmonization strategies and adapting atmospheric correction and bio-optical approaches to coastal conditions will therefore be essential to build long and consistent time series suitable for the detection of long-term biogeochemical trends.

- **Coupling medium spatial resolution satellite observations with high spatial resolution data**

Another key perspective lies in the integration of moderate resolution ocean color products with high spatial resolution satellite observations. Coastal processes often occur at spatial scales that are not fully resolved by sensors such as MODIS Aqua, particularly in nearshore zones, estuaries, and areas affected by localized anthropogenic activities. The combined use of sensors such as Sentinel 3 OLCI for ocean color continuity, Sentinel 2 MSI and Landsat missions for high spatial resolution observations, would allow a more detailed characterization of coastal processes. Such multiscale approaches would improve the detection of fine spatial gradients,

enhance the monitoring of coastal hotspots, and better resolve the influence of localized forcing mechanisms.

- **Integration with hydrological, hydrodynamic, and sediment transport models**

The interpretation of satellite derived biogeochemical variability would strongly benefit from tighter coupling with numerical models describing land ocean exchanges. Hydrodynamic and sediment transport models are particularly relevant for industrialized coastal regions such as the Açu Port area, where sediment redistribution is strongly controlled by circulation patterns and port infrastructure. In northern Brazil, particularly along the Amazonian Equatorial Coast of Maranhão, the results suggest potential buffering effects and non-linear relationships between precipitation, land flushing, and coastal particulate inputs, highlighting the need for hydrological modeling to better understand these land-sea transfer processes. The coupling between hydrological, hydrodynamic, and ocean biogeochemical models would enable a more mechanistic understanding of matter transfers from the continent to the ocean and improve the attribution of observed changes to specific forcing processes.

- **Towards integrated multivariable coastal biogeochemical budgets**

While this thesis focused on key particulate and phytoplankton related variables, a major perspective is the development of integrated coastal biogeochemical budgets that simultaneously consider dissolved, particulate, and phytoplankton compartments. Such an approach would allow the assessment of the relative responses of these compartments to different anthropogenic and climatic forcings. For instance, land use changes related to agriculture may preferentially affect particulate or dissolved matter, whereas other anthropogenic pressures may primarily impact phytoplankton dynamics. Integrated multivariable analyses would therefore provide a more comprehensive understanding of how different forcing mechanisms redistribute matter within coastal systems.

- **Implications for coastal carbon fluxes and three-dimensional perspectives**

An ultimate perspective concerns the role of coastal waters in regional carbon cycling. Understanding how anthropogenic and climatic forcings affect not only surface concentrations but also carbon stocks and fluxes require moving beyond two-dimensional surface observations. The development and coupling of three-dimensional models capable of representing carbon stocks, vertical redistribution, and the export of carbon from coastal waters toward the open ocean would be a critical step toward quantifying the contribution of coastal systems to the marine carbon cycle and their response to ongoing environmental

REFERENCES

Ab'Sáber, A.N., 2003. Os domínios de natureza no Brasil: potencialidades paisagísticas. Atelie Editorial.

Ab'Sáber, A.N., Holmquist, C., 2001. Litoral do Brasil. Metalivros, São Paulo, SP, Brasil.

Aguiar, A.L., Marta-Almeida, M., Cruz, L.O., Pereira, J., Cirano, M., 2022. Forcing mechanisms of the circulation on the Brazilian Equatorial Shelf. Continental Shelf Research 247, 104811. https://doi.org/10.1016/j.csr.2022.104811

Aguiar, V.M. de C., Neto, J.A.B., Rangel, C.M., 2011. Eutrophication and hypoxia in four streams discharging in Guanabara Bay, RJ, Brazil, a case study. Marine Pollution Bulletin 62, 1915–1919. https://doi.org/10.1016/j.marpolbul.2011.04.035

Alfredini, P., Arasaki, E., 2018. Estimation and Impacts of Sea Level Rise in Santos Port and Adjacent Areas (Brazil). TransNav 12, 739–744. https://doi.org/10.12716/1001.12.04.13

Allen, J.G., Siegel, D.A., Nelson, N.B., Halewood, S., 2020. Controls on ocean color spectra observed during the North Atlantic Aerosols and Marine Ecosystems Study (NAAMES). Frontiers in Marine Science 7, 567007. https://doi.org/10.3389/fmars.2020.567007

Alvares, C.A., Stape, J.L., Sentelhas, P.C., Gonçalves, J. de M., Sparovek, G., 2013. Köppen's climate classification map for Brazil. Meteorologische zeitschrift 22, 711–728.

Alvera-Azcárate, A., Van der Zande, D., Barth, A., Dille, A., Massant, J., Beckers, J.-M., 2025. Generation of super-resolution gap-free ocean colour satellite products using data-interpolating empirical orthogonal functions (DINEOF). Ocean Science 21, 787–805. https://doi.org/10.5194/os-21-787-2025

Amorim, J.P.M., Silveira, I.C.A. da, Borges-Silva, M., Souza-Neto, P.W.M., Bernardo, P.S., Dottori, M., Belo, W.C., Martins, R.P., Biló, T.C., 2024. The Brazil current cyclonic meandering and shelf-slope water exchanges at 27°S–31°S. Deep Sea Research Part I: Oceanographic Research Papers 206, 104276. https://doi.org/10.1016/j.dsr.2024.104276

Anderson, D.M., Glibert, P.M., Burkholder, J.M., 2002. Harmful algal blooms and eutrophication: Nutrient sources, composition, and consequences. Estuaries 25, 704–726. https://doi.org/10.1007/BF02804901

Andutta, F.P., Wang, X.H., Li, L., Williams, D., 2014. Hydrodynamics and Sediment Transport in a Macro-tidal Estuary: Darwin Harbour, Australia, in: Wolanski, E. (Ed.), Estuaries of Australia in 2050 and Beyond. Springer Netherlands, Dordrecht, pp. 111–129. https://doi.org/10.1007/978-94-007-7019-5_7

Araujo, M., Noriega, C., Hounsou-gbo, G.A., Veleda, D., Araujo, J., Bruto, L., Feitosa, F., Flores-Montes, M., Lefèvre, N., Melo, P., Otsuka, A., Travassos, K., Schwamborn, R., Neumann-Leitão, S., 2017. A Synoptic Assessment of the Amazon River-Ocean Continuum during Boreal Autumn: From Physics to Plankton Communities and Carbon Flux. Front. Microbiol. 8. https://doi.org/10.3389/fmicb.2017.01358

Araujo, M., Noriega, C., LefÃ¨vre, N., 2014. Nutrients and carbon fluxes in the estuaries of major rivers flowing into the tropical Atlantic. Front. Mar. Sci. 1. https://doi.org/10.3389/fmars.2014.00010

Arnaud, B., DE SAINT LEGER Emmanuel, KOCH-LARROUY Ariane, 2021. AMAZOMIX 2021 cruise,Antea R/V. https://doi.org/10.17600/18001364

Assireu, A.T., Pimenta, F.M., de Freitas, R.M., Saavedra, O.R., Neto, F.L.A., Júnior, A.R.T., Oliveira, C.B.M., Lopes, D.C.P., de Lima, S.L., Veras, R.B.S., Saraiva, N.P., Marcondes, L.G.P., Oliveira, D.Q., 2022. EOSOLAR Project: Assessment of Wind Resources of a Coastal Equatorial Region of Brazil—Overview and Preliminary Results. Energies 15, 2319. https://doi.org/10.3390/en15072319

Bainbridge, Z.T., Olley, J.M., Lewis, S.E., Stevens, T., Smithers, S.G., 2024. Tracing sources of inorganic suspended particulate matter in the Great Barrier Reef lagoon, Australia. Sci Rep 14, 15651. https://doi.org/10.1038/s41598-024-66561-5

Barbier, E.B., Hacker, S.D., Kennedy, C., Koch, E.W., Stier, A.C., Silliman, B.R., 2011. The value of estuarine and coastal ecosystem services. Ecological Monographs 81, 169–193. https://doi.org/10.1890/10-1510.1

Barbosa Martins, A.P., Silva Nunes, J.L., Da Silva Filho, E., Manir Feitosa, L., Nunes E Silva, L.P., Da Silva De Almeida, Z., 2015. Sexual dimorphism of sharks from the amazonian equatorial coast. Univ. Sci. 20, 297. https://doi.org/10.11144/Javeriana.SC20-3.sdos

Barragán, J.M., de Andrés, M., 2015. Analysis and trends of the world's coastal cities and agglomerations. Ocean & Coastal Management 114, 11–20. https://doi.org/10.1016/j.ocecoaman.2015.06.004

Barrón, C., Duarte, C.M., 2015. Dissolved organic carbon pools and export from the coastal ocean. Global Biogeochemical Cycles 29, 1725–1738. https://doi.org/10.1002/2014GB005056

Bastos, A.C., Silva, C.G., 2000. Caracterização morfodinâmica do litoral Norte Fluminense, RJ, Brasil. Rev. Bras. Oceanogr. 48, 41–60. https://doi.org/10.1590/S1413-77392000000100004

Bauer, J.E., Cai, W.-J., Raymond, P.A., Bianchi, T.S., Hopkinson, C.S., Regnier, P.A.G., 2013. The changing carbon cycle of the coastal ocean. Nature 504, 61–70. https://doi.org/10.1038/nature12857

Behrenfeld, M.J., Boss, E., Siegel, D.A., Shea, D.M., 2005. Carbon-based ocean productivity and phytoplankton physiology from space. Global Biogeochemical Cycles 19. https://doi.org/10.1029/2004GB002299

Beltrán-Abaunza, J.M., Kratzer, S., Brockmann, C., 2014. Evaluation of MERIS products from Baltic Sea coastal waters rich in CDOM. Ocean Science 10, 377–396. https://doi.org/10.5194/os-10-377-2014

Bernardes, M., Knoppers, B., Rezende, C., Souza, W., Ovalle, A., 2012. Land-sea interface features of four estuaries on the South America Atlantic coast. Braz. J. Biol. 72, 761–774. https://doi.org/10.1590/S1519-69842012000400011

Beusen, A.H.W., Dekkers, A.L.M., Bouwman, A.F., Ludwig, W., Harrison, J., 2005. Estimation of global river transport of sediments and associated particulate C, N, and P. Global Biogeochemical Cycles 19. https://doi.org/10.1029/2005GB002453

Beven, K., 2012. Evolution of Rainfall–Runoff Models: Survival of the Fittest?, in: Rainfall-Runoff Modelling. John Wiley & Sons, Ltd, pp. 25–50. https://doi.org/10.1002/9781119951001.ch2

Bianchi, T.S., Allison, M.A., Cai, W.-J. (Eds.), 2014. Biogeochemical dynamics at major river-coastal interfaces: linkages with global change. Cambridge University Press, New York, NY.

Bidlack, A.L., Bisbing, S.M., Buma, B.J., Diefenderfer, H.L., Fellman, J.B., Floyd, W.C., Giesbrecht, I., Lally, A., Lertzman, K.P., Perakis, S.S., Butman, D.E., D'Amore, D.V., Fleming, S.W., Hood, E.W., Hunt, B.P.V., Kiffney, P.M., McNicol, G., Menounos, B., Tank, S.E., 2021. Climate-Mediated Changes to Linked Terrestrial and Marine Ecosystems across the Northeast Pacific Coastal Temperate Rainforest Margin. BioScience 71, 581–595. https://doi.org/10.1093/biosci/biaa171

Bierman, P., Lewis, M., Ostendorf, B., Tanner, J., 2011. A review of methods for analysing spatial and temporal patterns in coastal water quality. Ecological Indicators, Spatial information and indicators for sustainable management of natural resources 11, 103–114. https://doi.org/10.1016/j.ecolind.2009.11.001

Bishop, C.M., 1993. Novelty Detection and Neural Network Validation, in: Gielen, S., Kappen, B. (Eds.), ICANN '93. Springer, London, pp. 789–794. https://doi.org/10.1007/978-1-4471-2063-6_225

Bissett, P., Arnone, R.A., Davis, C.O., Dickey, T.D., Dye, D., Kohler, D.D.R., Gould, R.W., 2004. From Meters to Kilometers: A look at ocean-color scales of variability, spatial coherence, and the need for fine-scale remote sensing in coastal ocean optics. Oceanography 17, 32–43.

Bitencourt, R., Filho, E.T.A., Chagas, A. das, Hora, H. da, Reis, T.B., 2017. A estruturação e a dinamização do cluster portuário do Açu: uma abordagem prospectiva. Petróleo Royalties e Região 14.

Blair, N.E., Aller, R.C., 2012. The Fate of Terrestrial Organic Carbon in the Marine Environment. Annual Review of Marine Science 4, 401–423. https://doi.org/10.1146/annurev-marine-120709-142717

Blondeau-Patissier, D., Gower, J.F.R., Dekker, A.G., Phinn, S.R., Brando, V.E., 2014. A review of ocean color remote sensing methods and statistical techniques for the detection, mapping and analysis of phytoplankton blooms in coastal and open oceans. Progress in Oceanography 123, 123–144. https://doi.org/10.1016/j.pocean.2013.12.008

Bonelli, A.G., Vantrepotte, V., Jorge, D.S.F., Demaria, J., Jamet, C., Dessailly, D., Mangin, A., Fanton d'Andon, O., Kwiatkowska, E., Loisel, H., 2021. Colored dissolved organic matter absorption at global scale

from ocean color radiometry observation: Spatio-temporal variability and contribution to the absorption budget. Remote Sensing of Environment 265, 112637. https://doi.org/10.1016/j.rse.2021.112637

BOPP, L., LEGENDRE, L., MONFRAY, P., 2002. La pompe à carbone va-t-elle se gripper? Recherche (Paris 1970) 48–51.

Borges, A., Abril, G., 2011. 5.04 - Carbon Dioxide and Methane Dynamics in Estuaries. Academic Press, Waltham, United States - Massachusetts. https://doi.org/10.1016/B978-0-12-374711-2.00504-0

Bortolin, E.C., Távora, J., Fernandes, E.H.L., 2022. Long-Term Variability on Suspended Particulate Matter Loads From the Tributaries of the World's Largest Choked Lagoon. Front. Mar. Sci. 9. https://doi.org/10.3389/fmars.2022.836739

Bowers, D.G., Binding, C.E., 2006. The optical properties of mineral suspended particles: A review and synthesis. Estuarine, Coastal and Shelf Science 67, 219–230. https://doi.org/10.1016/j.ecss.2005.11.010

Brandini, F.P., Tura, P.M., Santos, P.P.G.M., 2018. Ecosystem responses to biogeochemical fronts in the South Brazil Bight. Progress in Oceanography 164, 52–62. https://doi.org/10.1016/j.pocean.2018.04.012

Breiman, L., 2001. Random Forests. Machine Learning 45, 5–32. https://doi.org/10.1023/A:1010933404324

Breitburg, D., Levin, L., Oschlies, A., Grégoire, M., Chavez, F., Conley, D., Garcon, V., Gilbert, D., Gutiérrez, D., Isensee, K., Jacinto, G., Limburg, K., Montes, I., Naqvi, S.W.A., Pitcher, G., Rabalais, N., Roman, M., Rose, K., Seibel, B., Zhang, J., 2018. Declining oxygen in the global ocean and coastal waters. Science (New York, N.Y.) 359. https://doi.org/10.1126/science.aam7240

Brito, A.C., Garrido-Amador, P., Gameiro, C., Nogueira, M., Moita, M.T., Cabrita, M.T., 2020. Integrating In Situ and Ocean Color Data to Evaluate Ecological Quality under the Water Framework Directive. Water 12. https://doi.org/10.3390/w12123443

Bui, Q.-T., Jamet, C., Vantrepotte, V., Mériaux, X., Cauvin, A., Mograne, M.A., 2022. Evaluation of Sentinel-2/MSI Atmospheric Correction Algorithms over Two Contrasted French Coastal Waters. Remote Sensing 14, 1099. https://doi.org/10.3390/rs14051099

Bulleri, F., Chapman, M.G., 2010. The introduction of coastal infrastructure as a driver of change in marine environments. Journal of Applied Ecology 47, 26–35. https://doi.org/10.1111/j.1365-2664.2009.01751.x

Burke, L.M., 2001. Pilot analysis of global ecosystems: coastal ecosystems. World Resources Institute, Washington, DC.

Burla, M., Baptista, A.M., Zhang, Y., Frolov, S., 2010. Seasonal and interannual variability of the Columbia River plume: A perspective enabled by multiyear simulation databases. Journal of Geophysical Research: Oceans 115. https://doi.org/10.1029/2008JC004964

Burnett, W.C., Bokuniewicz, H., Huettel, M., Moore, W.S., Taniguchi, M., 2003. Groundwater and pore water inputs to the coastal zone. Biogeochemistry 66, 3–33. https://doi.org/10.1023/B:BIOG.0000006066.21240.53

Burone, L., Franco-Fraguas, P., Carranza, A., Calliari, D., Mahiques, M.M. de, Gómez, M., Marin, Y., Gutiérrez, O., Ortega, L., 2021. Physical Drivers and Dominant Oceanographic Processes on the Uruguayan Margin (Southwestern Atlantic): A Review and a Conceptual Model. Journal of Marine Science and Engineering 9. https://doi.org/10.3390/jmse9030304

Cael, B.B., Bisson, K., Boss, E., Dutkiewicz, S., Henson, S., 2023. Global climate-change trends detected in indicators of ocean ecology. Nature 619, 551–554. https://doi.org/10.1038/s41586-023-06321-z

Capotondi, A., Rodrigues, R.R., Sen Gupta, A., Benthuysen, J.A., Deser, C., Frölicher, T.L., Lovenduski, N.S., Amaya, D.J., Le Grix, N., Xu, T., Hermes, J., Holbrook, N.J., Martinez-Villalobos, C., Masina, S., Roxy, M.K., Schaeffer, A., Schlegel, R.W., Smith, K.E., Wang, C., 2024. A global overview of marine heatwaves in a changing climate. Commun Earth Environ 5, 701. https://doi.org/10.1038/s43247-024-01806-9

Cardoso Dos Santos, J.F., 2025. Spatiotemporal dynamics of satellite-derived chlorophyll-a along the Brazilian continental margin: case studies from the southeastern region. INPE, Brazil.

Cardoso Dos Santos, J.F., Kampel, M., Vantrepotte, V., 2025. Spatiotemporal variability of chlorophyll-a concentration in the South Brazil Bight using 25 years of multi-sensor orbital data (1998–2022). Front. Remote Sens. 6, 1544375. https://doi.org/10.3389/frsen.2025.1544375

Cardoso Dos Santos, J., 2013. Algoritmos bio-ópticos e variabilidade da biomassa fitoplanctônica na pluma do rio Amazonas.

Carvalho, M., Ciotti, A.M., Gianesella, S.M.F., Corrêa, F.M.P.S., Perinotto, R.R.C., 2014. Bio-Optical Properties of the Inner Continental Shelf off Santos Estuarine System, Southeastern Brazil, and their Implications for Ocean Color Algorithm Performance. Braz. j. oceanogr. 62, 71–87. https://doi.org/10.1590/S1679-87592014044506202

Carvalho, R.C.Q., Cutrim, M.V.J., Eschrique, S.A., Azevedo-Cutrim, A.C.G., Moreira, E.G., Silveira, P.C.A., Coêlho, J.M., 2016. Microphytoplankton composition, chlorophyll-a concentration and environmental variables of the Maranhão Continental Shelf, Northern Brazil. Latin American Journal of Aquatic Research 44, 256–266. https://doi.org/10.3856/vol44-issue2-fulltext-7

Cassar, J.C.M., Neves, C.F., 1993. Application of Coastal Transport Roses to the North Fluminense Coast. Revista Brasileira de Engenharia – Caderno de Recursos Hídricos 11, 81–106.

Castelo, W.F.L., Martins, M.V.A., de Lima Ferreira, P.A., Figueira, R., da Costa, C.F., da Fonseca, L.B., Bergamashi, S., Pereira, E., Terroso, D., Pinto, A.F.S., Simon, M.B., Socorro, O.A.A., Frontalini, F., da Silva, L.C., Rocha, F., Geraldes, M., Guerra, J.V., 2021. Long-term eutrophication and contamination of the central area of Sepetiba Bay (SW Brazil). Environ Monit Assess 193, 100. https://doi.org/10.1007/s10661-021-08861-1

Castro, A.L.C., Eschrique, S.A., Silveira, P.C.A., Azevedo, J.W.J., Ferreira, H.R.S., Soares, L.S., Monteles, J.S., Araujo, M.C., Nunes, J.L., Silva, M.H.L., 2018. Physicochemical properties and distribution of nutrients on the inner continental shelf adjacent to the Gulf of Maranhão (Brazil) in the Equatorial Atlantic. Applied Ecology and Environmental Research 16, 4829–4847.

Castro, B., Brandini, F., Pires-Vanin, A., Miranda, L., 2006. Multidisciplinary Oceanographic Processes On the Western Atlantic Continental Shelf Between 4N and 34S. The Sea 14, 259–293.

Castro, B.M. de, Miranda, L.B. de, 1998. Hydrographic properties in the São Sebastião Channel: daily variations observed in March 1980. Rev. Bras. Oceanogr. 46, 111–123. https://doi.org/10.1590/S1413-77391998000200002

Castro, J.W.A., Junior, W.C.G., Fernandes, D., Cabral, C.L., 2025. Impacts of climate change on coastal erosion and marine flooding in Rio de Janeiro city, Brazil.

CAUWET, G., 2002. DOM in the coastal zone. Biogeochemistry of marine dissolved organic matter.

Cavalcanti, B.S., Marques, G.G., 2016. Recursos hídricos e gestão de conflitos. A bacia hidrográfica do rio Paraíba do Sul a partir da crise hídrica de 2014-2015. Revista Portuguesa e Brasileira de Gestão 15, 4–16.

Cavalcanti-Lima, L.F., Cutrim, M.V.J., Feitosa, F.A. do N., Flores-Montes, M. de J., Dias, F.J.S., Sá, A.K.D. dos S., Santos, T.P., da Cruz, Q.S., Lourenço, C.B., 2023. Effects of climate, spatial and hydrological processes on shaping phytoplankton community structure and β-diversity in an estuary-ocean continuum (Amazon continental shelf, Brazil). Journal of Sea Research 193, 102384. https://doi.org/10.1016/j.seares.2023.102384

Cazzaniga, I., Bresciani, M., Colombo, R., Della Bella, V., Padula, R., Giardino, C., 2019. A comparison of Sentinel-3-OLCI and Sentinel-2-MSI-derived Chlorophyll-a maps for two large Italian lakes. Remote Sensing Letters 10, 978–987. https://doi.org/10.1080/2150704X.2019.1634298

Celentano, D., Rousseau, G.X., Muniz, F.H., Varga, I. van D., Martinez, C., Carneiro, M.S., Miranda, M.V.C., Barros, M.N.R., Freitas, L., Narvaes, I. da S., Adami, M., Gomes, A.R., Rodrigues, J.C., Martins, M.B., 2017. Towards zero deforestation and forest restoration in the Amazon region of Maranhão state, Brazil. Land Use Policy 68, 692–698. https://doi.org/10.1016/j.landusepol.2017.07.041

Celentano, D., Sills, E., Sales, M., Veríssimo, A., 2012. Welfare Outcomes and the Advance of the Deforestation Frontier in the Brazilian Amazon. World Development 40, 850–864. https://doi.org/10.1016/j.worlddev.2011.09.002

CEMBRA, 2019. CEMBRA 2019 O Brasil e o mar no século XXI - Baixar pdf de Doceru.com. Doceru.com. URL https://doceru.com/doc/1c1enen (accessed on 01-01-2026).

Chen, M., Pattiaratchi, C.B., Ghadouani, A., Hanson, C., 2020. Influence of Storm Events on Chlorophyll Distribution Along the Oligotrophic Continental Shelf Off South-Western Australia. Front. Mar. Sci. 7. https://doi.org/10.3389/fmars.2020.00287

Chen, N., Krom, M.D., Wu, Y., Yu, D., Hong, H., 2018. Storm induced estuarine turbidity maxima and controls on nutrient fluxes across river-estuary-coast continuum. Science of The Total Environment 628–629, 1108–1120. https://doi.org/10.1016/j.scitotenv.2018.02.060

Choudhury, A.K., Pal, R., 2010. Phytoplankton and nutrient dynamics of shallow coastal stations at Bay of Bengal, Eastern Indian coast. Aquat Ecol 44, 55–71. https://doi.org/10.1007/s10452-009-9252-9

Ciotti, Á.M., Garcia, C.A.E., Jorge, D.S.F., 2010. Variabilidade temporal e meridional de estimativas de Satélite da concentração de clorofila superficial na plataforma continental brasileira.

Cloern, J.E., 1996. Phytoplankton bloom dynamics in coastal ecosystems: A review with some general lessons from sustained investigation of San Francisco Bay, California. Reviews of Geophysics 34, 127–168. https://doi.org/10.1029/96RG00986

Cloern, J.E., 2001. Our evolving conceptual model of the coastal eutrophication problem. Marine Ecology Progress Series 210, 223–253. https://doi.org/10.3354/meps210223

Cloern, J.E., Abreu, P.C., Carstensen, J., Chauvaud, L., Elmgren, R., Grall, J., Greening, H., Johansson, J.O.R., Kahru, M., Sherwood, E.T., Xu, J., Yin, K., 2016. Human activities and climate variability drive fast-paced change across the world's estuarine–coastal ecosystems. Global Change Biology 22, 513–529. https://doi.org/10.1111/gcb.13059

Cloern, J.E., Foster, S.Q., Kleckner, A.E., 2014. Phytoplankton primary production in the world's estuarine-coastal ecosystems. Biogeosciences 11, 2477–2501. https://doi.org/10.5194/bg-11-2477-2014

Cloern, J.E., Jassby, A.D., 2012. Drivers of change in estuarine-coastal ecosystems: Discoveries from four decades of study in San Francisco Bay. Reviews of Geophysics 50. https://doi.org/10.1029/2012RG000397

Coles, V.J., Brooks, M.T., Hopkins, J., Stukel, M.R., Yager, P.L., Hood, R.R., 2013. The pathways and properties of the Amazon River Plume in the tropical North Atlantic Ocean. Journal of Geophysical Research: Oceans 118, 6894–6913. https://doi.org/10.1002/2013JC008981

Costa, K.S., Bezerra, V.L.A., Costa, H. de O., Sousa, C.J. da S., 2011. Estudo da potencialidade hídrica da Amazônia maranhense através do comportamento de vazões. Amazônia maranhense: diversidade e conservação. Belém: MPEG 71–89.

Costanza, R., de Groot, R., Sutton, P., van der Ploeg, S., Anderson, S.J., Kubiszewski, I., Farber, S., Turner, R.K., 2014. Changes in the global value of ecosystem services. Global Environmental Change 26, 152–158. https://doi.org/10.1016/j.gloenvcha.2014.04.002

Cotovicz, L.C., Knoppers, B.A., Deirmendjian, L., Abril, G., 2019. Sources and sinks of dissolved inorganic carbon in an urban tropical coastal bay revealed by δ13C-DIC signals. Estuarine, Coastal and Shelf Science 220, 185–195. https://doi.org/10.1016/j.ecss.2019.02.048

Cotovicz, L.C., Knoppers, B.A., Régis, C.R., Tremmel, D., Costa-Santos, S., Abril, G., 2021. Eutrophication overcoming carbonate precipitation in a tropical hypersaline coastal lagoon acting as a CO2 sink (Araruama Lagoon, SE Brazil). Biogeochemistry 156, 231–254. https://doi.org/10.1007/s10533-021-00842-3

Cotovicz Jr., L.C., Knoppers, B.A., Brandini, N., Costa Santos, S.J., Abril, G., 2015. A strong CO2 sink enhanced by eutrophication in a tropical coastal embayment (Guanabara Bay, Rio de Janeiro, Brazil). Biogeosciences 12, 6125–6146. https://doi.org/10.5194/bg-12-6125-2015

Cotovicz, L.C., Knoppers, B.A., Brandini, N., Poirier, D., Costa Santos, S.J., Cordeiro, R.C., Abril, G., 2018. Predominance of phytoplankton-derived dissolved and particulate organic carbon in a highly eutrophic tropical coastal embayment (Guanabara Bay, Rio de Janeiro, Brazil). Biogeochemistry 137, 1–14. https://doi.org/10.1007/s10533-017-0405-y

Cotovicz, L.C., Vidal, L.O., De Rezende, C.E., Bernardes, M.C., Knoppers, B.A., Sobrinho, R.L., Cardoso, R.P., Muniz, M., Dos Anjos, R.M., Biehler, A., Abril, G., 2020. Carbon dioxide sources and sinks in the delta of the Paraíba do Sul River (Southeastern Brazil) modulated by carbonate thermodynamics, gas exchange and

ecosystem metabolism during estuarine mixing. Marine Chemistry 226, 103869. https://doi.org/10.1016/j.marchem.2020.103869

Coutinho, P.N., 1995. Levantamento do estado da arte da pesquisa dos recursos vivos marinhos do Brasil. Programa REVIZEE. Brasilia: Ministé rio do Meio Ambiente, dos Recursos Hıdricos e da Amazônia Legal.

Crossland, C.J., Baird, D., Ducrotoy, J.-P., Lindeboom, H., Buddemeier, R.W., Dennison, W.C., Maxwell, B.A., Smith, S.V., Swaney, D.P., 2005. The Coastal Zone a Domain of Global Interactions, in: Crossland, C.J., Kremer, H.H., Lindeboom, H.J., Marshall Crossland, J.I., Le Tissier, M.D.A. (Eds.), Coastal Fluxes in the Anthropocene: The Land-Ocean Interactions in the Coastal Zone Project of the International Geosphere-Biosphere Programme. Springer, Berlin, Heidelberg, pp. 1–37. https://doi.org/10.1007/3-540-27851-6_1

Cunha, C. de L. da N., Rosman, P.C.C., Ferreira, A.P., Carlos do Nascimento Monteiro, T., 2006. Hydrodynamics and water quality models applied to Sepetiba Bay. Continental Shelf Research 26, 1940–1953. https://doi.org/10.1016/j.csr.2006.06.010

D'Alimonte, D., Melin, F., Zibordi, G., Berthon, J.-F., 2003. Use of the novelty detection technique to identify the range of applicability of empirical ocean color algorithms. IEEE Transactions on Geoscience and Remote Sensing 41, 2833–2843. https://doi.org/10.1109/TGRS.2003.818020

Da Silva, D.R., Mansur, K.L., Borghi, L., 2018. Evaluation of the scientific value of Lagoa Salgada (Rio de Janeiro, Brazil): characterization as geological heritage, threats and strategies for geoconservation. JGSB 1, 69–80. https://doi.org/10.29396/jgsb.2018.v1.n2.2

Da Silva, E.F.F., Novo, E.M.L.D.M., Lobo, F.D.L., Barbosa, C.C.F., Noernberg, M.A., Rotta, L.H.D.S., Cairo, C.T., Maciel, D.A., Flores Júnior, R., 2021. Optical water types found in Brazilian waters. Limnology 22, 57–68. https://doi.org/10.1007/s10201-020-00633-z

da Silva, R.M., Santos, C.A.G., Moreira, M., Corte-Real, J., Silva, V.C.L., Medeiros, I.C., 2015. Rainfall and river flow trends using Mann–Kendall and Sen's slope estimator statistical tests in the Cobres River basin. Nat Hazards 77, 1205–1221. https://doi.org/10.1007/s11069-015-1644-7

da Silveira, I.C.A., Napolitano, D.C., Farias, I.U., 2020. Water Masses and Oceanic Circulation of the Brazilian Continental Margin and Adjacent Abyssal Plain, in: Sumida, P.Y.G., Bernardino, A.F., De Léo, F.C. (Eds.), Brazilian Deep-Sea Biodiversity. Springer International Publishing, Cham, pp. 7–36. https://doi.org/10.1007/978-3-030-53222-2_2

Dagum, E.B., 1983. Spectral properties of the concurrent and forecasting seasonal linear filters of the X-11-ARIMA method. Canadian Journal of Statistics 11, 73–90. https://doi.org/10.2307/3314713

Dagum, E.B., 2010. Time series modeling and decomposition. Statistica 70, 433–457. https://doi.org/10.6092/issn.1973-2201/3597

Dai, A., Qian, T., Trenberth, K.E., Milliman, J.D., 2009. Changes in Continental Freshwater Discharge from 1948 to 2004. Journal of Climate 22, 2773–2792. https://doi.org/10.1175/2008JCLI2592.1

Dai, M., Zhao, Y., Chai, F., Chen, M., Chen, N., Chen, Y., Cheng, D., Gan, J., Guan, D., Hong, Y., Huang, J., Lee, Y., Leung, K., Lim, P.E., Lin, S., Lin, X., Liu, X., Liu, Z., Luo, Y.-W., Zhang, Z., 2023. Persistent eutrophication and hypoxia in the coastal ocean. Cambridge Prisms: Coastal Futures 1, 1–71. https://doi.org/10.1017/cft.2023.7

Dalu, T., Wasserman, R.J., Magoro, M.L., Froneman, P.W., Weyl, O.L.F., 2019. River nutrient water and sediment measurements inform on nutrient retention, with implications for eutrophication. Sci Total Environ 684, 296–302. https://doi.org/10.1016/j.scitotenv.2019.05.167

Daniel, E., Harari, J., Camargo, R., Soares, S., Mascagnia, M.L., Filho, A.F.H.F., 2025. Sea Level Variation on the Brazilian Coast from the Perspective of Climate Change. https://doi.org/10.2139/ssrn.5127601

De Andrés, M., Barragán, J.M., Scherer, M., 2018. Urban centres and coastal zone definition: Which area should we manage? Land Use Policy 71, 121–128. https://doi.org/10.1016/j.landusepol.2017.11.038

De Oliveira, D.M., Carvalho, V.S.B., da Silva, B.C., Reboita, M.S., de Campos, B., 2023. Hydrological and Precipitation Extremes and Trends over the Paraiba do Sul River Basin, Brazil. Climate 11, 138. https://doi.org/10.3390/cli11070138

De Souza, M.M., Mathis, M., Mayer, B., Noernberg, M.A., Pohlmann, T., 2020. Possible impacts of anthropogenic climate change to the upwelling in the South Brazil Bight. Clim Dyn 55, 651–664. https://doi.org/10.1007/s00382-020-05289-0

De'ath, G., Fabricius, K.E., 2000. Classification and Regression Trees: A Powerful yet Simple Technique for Ecological Data Analysis. Ecology 81, 3178–3192. https://doi.org/10.1890/0012-9658(2000)081%255B3178:CARTAP%255D2.0.CO;2

Decrop, B., De Mulder, T., Toorman, E., Sas, M., 2015. Large-eddy simulations of turbidity plumes in crossflow. European Journal of Mechanics - B/Fluids 53, 68–84. https://doi.org/10.1016/j.euromechflu.2015.03.013

Delgado, A.L., Loisel, H., Jamet, C., Vantrepotte, V., Perillo, G.M.E., Piccolo, M.C., 2015. Seasonal and Inter-Annual Analysis of Chlorophyll-a and Inherent Optical Properties from Satellite Observations in the Inner and Mid-Shelves of the South of Buenos Aires Province (Argentina). Remote Sensing 7, 11821–11847. https://doi.org/10.3390/rs70911821

Deng, L., Hu, S., Chen, S., Zeng, X., Wang, Z., Xu, Z., Liu, S., 2023. Vertical distribution of suspended particulate matter and its response to river discharge and seawater intrusion: a case study in the Pearl River Estuary during the 2020 dry season. Front. Mar. Sci. 10. https://doi.org/10.3389/fmars.2023.1239649

Dereczynski, C.P., Lopes, Í.R., Carvalho, N.O., Silva, M.G.A.J., Grossmann, K.S., Martins, R.P., 2019. Climatology of Espírito Santo and the Northern Campos Basin, Offshore Southeast Brazil. Anuário IGEO UFRJ 42, 386–401. https://doi.org/10.11137/2019_1_386_401

Dhillon, G.S., Inamdar, S., 2014. Storm event patterns of particulate organic carbon (POC) for large storms and differences with dissolved organic carbon (DOC). Biogeochemistry 118, 61–81. https://doi.org/10.1007/s10533-013-9905-6

Dierssen, H.M., 2010. Perspectives on empirical approaches for ocean color remote sensing of chlorophyll in a changing climate. Proceedings of the National Academy of Sciences 107, 17073–17078. https://doi.org/10.1073/pnas.0913800107

Dimoune, D.M., Birol, F., Hernandez, F., Léger, F., Araujo, M., 2023. Revisiting the tropical Atlantic western boundary circulation from a 25-year time series of satellite altimetry data. Ocean Science 19, 251–268. https://doi.org/10.5194/os-19-251-2023

Dingman, S.L., 2015. Physical Hydrology: Third Edition. Waveland Press.

Ditty, J.M., Rezende, C.E., 2014. Unjust and unsustainable: A case study of the Açu port industrial complex. Marine Policy 45, 82–88. https://doi.org/10.1016/j.marpol.2013.11.018

Dogliotti, A.I., Ruddick, K., Guerrero, R., 2016. Seasonal and inter-annual turbidity variability in the Río de la Plata from 15 years of MODIS: El Niño dilution effect. Estuarine, Coastal and Shelf Science 182, 27–39. https://doi.org/10.1016/j.ecss.2016.09.013

Domingues, R.B., Anselmo, T.P., Barbosa, A.B., Sommer, U., Galvão, H.M., 2011. Light as a driver of phytoplankton growth and production in the freshwater tidal zone of a turbid estuary. Estuarine, Coastal and Shelf Science 91, 526–535. https://doi.org/10.1016/j.ecss.2010.12.008

Dominguez, J.M.L., 2009. The Coastal Zone of Brazil, in: Dillenburg, S.R., Hesp, P.A. (Eds.), Geology and Geomorphology of Holocene Coastal Barriers of Brazil. Springer, Berlin, Heidelberg, pp. 17–51. https://doi.org/10.1007/978-3-540-44771-9_2

Dominguez, J.M.L., Bittencourt, A.C.S.P., Martin, L., 1983. The role of longshore drift of sandy sediments in the construction of coastal plains associated with the mouths of the São Francisco (SE/AL), Jequitinhonha (BA), Doce (ES) and Paraíba do Sul (RJ) rivers. Brazilian Journal of Geosciences 13, 98–105.

Doney, S.C., 2010. The Growing Human Footprint on Coastal and Open-Ocean Biogeochemistry. Science 328, 1512–1516. https://doi.org/10.1126/science.1185198

Doney, S.C., Ruckelshaus, M., Duffy, J.E., Barry, J.P., Chan, F., English, C.A., Galindo, H.M., Grebmeier, J.M., Hollowed, A.B., Knowlton, N., Polovina, J., Rabalais, N.N., Sydeman, W.J., Talley, L.D., 2012. Climate Change Impacts on Marine Ecosystems. Annual Review of Marine Science 4, 11–37. https://doi.org/10.1146/annurev-marine-041911-111611

Donker, J.J.A., De Swart, H.E., 2013. Effects of bottom slope, flocculation and hindered settling on the coupled dynamics of currents and suspended sediment in highly turbid estuaries, a simple model. Ocean Dynamics 63, 311–327. https://doi.org/10.1007/s10236-013-0593-5

dos Santos, V.H.M., da Silva Dias, F.J., Torres, A.R., Soares, R.A., Terto, L.C., de Castro, A.C.L., Santos, R.L., Cutrim, M.V.J., 2020. Hydrodynamics and suspended particulate matter retention in macrotidal estuaries located in Amazonia-semiarid interface (Northeastern-Brazil). International Journal of Sediment Research 35, 417–429. https://doi.org/10.1016/j.ijsrc.2020.03.004

Doxaran, D., Froidefond, J.-M., Castaing, P., Babin, M., 2009. Dynamics of the turbidity maximum zone in a macrotidal estuary (the Gironde, France): Observations from field and MODIS satellite data. Estuarine, Coastal and Shelf Science 81, 321–332. https://doi.org/10.1016/j.ecss.2008.11.013

Doxaran, D., Froidefond, J.-M., Lavender, S., Castaing, P., 2002. Spectral signature of highly turbid waters: Application with SPOT data to quantify suspended particulate matter concentrations. Remote Sensing of Environment 81, 149–161. https://doi.org/10.1016/S0034-4257(01)00341-8

Doxaran, D., Lamquin, N., Park, Y.-J., Mazeran, C., Ryu, J.-H., Wang, M., Poteau, A., 2014. Retrieval of the seawater reflectance for suspended solids monitoring in the East China Sea using MODIS, MERIS and GOCI satellite data. Remote Sensing of Environment, Liege Colloquium Special Issue: Remote sensing of ocean colour, temperature and salinity 146, 36–48. https://doi.org/10.1016/j.rse.2013.06.020

Druffel, E.R.M., Williams, P.M., Bauer, J.E., Ertel, J.R., 1992. Cycling of dissolved and particulate organic matter in the open ocean. Journal of Geophysical Research: Oceans 97, 15639–15659. https://doi.org/10.1029/92JC01511

Duarte, C.M., 2014. Global change and the future ocean: a grand challenge for marine sciences. Front. Mar. Sci. 1. https://doi.org/10.3389/fmars.2014.00063

Dutkiewicz, S., Hickman, A.E., Jahn, O., Henson, S., Beaulieu, C., Monier, E., 2019. Ocean colour signature of climate change. Nat Commun 10, 578. https://doi.org/10.1038/s41467-019-08457-x

Eberhard, A., Campos, A., Turra, A., Prates, A., Lobo, A., Queiroz, A., Silva, A., Pedrosa, B., Ferreira, B., Domit, C., Oliveira, C., Rezende, C., Marques, C., Seixas, C., Santos, D., Vila Nova, D., Herbst, D., Crist, D., Coelho, E., Sriram, T., 2016. Brazilian Future Ocean Panel (PainelMar): Strategic Document. https://doi.org/10.13140/RG.2.2.16119.01449

Economidou, E., 1982. The ecological value of coastal ecosystems. Ekistics 49, 98–101.

Ekau, W., Knoppers, B., 1999. An introduction to the pelagic system of the Northeast and East Brazilian shelf.

Eleveld, M.A., Ruescas, A.B., Hommersom, A., Moore, T.S., Peters, S.W.M., Brockmann, C., 2017. An Optical Classification Tool for Global Lake Waters. Remote Sensing 9. https://doi.org/10.3390/rs9050420

Erbas, T., Marques, A., Abril, G., 2021. A CO2 sink in a tropical coastal lagoon impacted by cultural eutrophication and upwelling. Estuarine, Coastal and Shelf Science 263, 107633. https://doi.org/10.1016/j.ecss.2021.107633

Fan, J., Yang, J., Cheng, F., Zhang, S., 2023. The Source, Distribution, and Environmental Effects of Suspended Particulate Matter in the Yangtze River System. Water 15, 3429. https://doi.org/10.3390/w15193429

Fan, Y., Li, W., Chen, N., Ahn, J.-H., Park, Y.-J., Kratzer, S., Schroeder, T., Ishizaka, J., Chang, R., Stamnes, K., 2021. OC-SMART: A machine learning based data analysis platform for satellite ocean color sensors. Remote Sensing of Environment 253, 112236. https://doi.org/10.1016/j.rse.2020.112236

Farias, G. B.; Ternon, J.-F.; Hillion, S.; Melo, P. A. M. de C.; Carré, C.; Molinero, J.-C.; Baurand, F.; Grelet, J.; Chaigneau, A.; Costa Da Silva, A.; Devasa, J.; Roubaud, F.; Bertrand, A (2015). Phytoplankton pigment data collected during the ABRACOS 1 and 2 surveys performed along the northeast Brazilian continental shelf, slope and open ocean. [S. l.]: SEANOE. DOI 10.17882/95171. Available at: https://www.seanoe.org/data/00840/95171/. Accessed on: 24 Jul. 2025.

Ferrari, J.J.C., 1995. Pollution and environmental degradation, in: Integrated Coastal Zone Management in Eastern Africa Including the Island States. Coastal Management Center, pp. 63–84.

Ferreira, L., and Hitchcock, D.B., 2009. A Comparison of Hierarchical Methods for Clustering Functional Data. Communications in Statistics - Simulation and Computation 38, 1925–1949. https://doi.org/10.1080/03610910903168603

Ferreira, V.L.D., Pereira, E.S., Souza De Mello, L.P., Silva, R.A.G., Dias, F.F., 2025. Analysis of Coastal Environmental Vulnerabilities in the Municipality of Niterói, Rio de Janeiro, Brazil, in the Face of Sea Level Rise Projections. Coasts 5, 11. https://doi.org/10.3390/coasts5010011

Ferronato, C., Berden, G., Rivarossa, M., Guinder, V.A., 2023. Wind-driven currents and water masses shape spring phytoplankton distribution and composition in hydrologically complex, productive shelf waters. Limnology and Oceanography 68, 2195–2210. https://doi.org/10.1002/lno.12413

Fettweis, M., Baeye, M., Cardoso, C., Dujardin, A., Lauwaert, B., Van den Eynde, D., Van Hoestenberghe, T., Vanlede, J., Van Poucke, L., Velez, C., Martens, C., 2016. The impact of disposal of fine-grained sediments from maintenance dredging works on SPM concentration and fluid mud in and outside the harbor of Zeebrugge. Ocean Dynamics 66, 1497–1516. https://doi.org/10.1007/s10236-016-0996-1

Fettweis, M., Francken, F., Van den Eynde, D., Verwaest, T., Janssens, J., Van Lancker, V., 2010. Storm influence on SPM concentrations in a coastal turbidity maximum area with high anthropogenic impact (southern North Sea). Continental Shelf Research 30, 1417–1427. https://doi.org/10.1016/j.csr.2010.05.001

Figueiredo, R.O., Markewitz, D., Davidson, E.A., Schuler, A.E., dos S. Watrin, O., de Souza Silva, P., 2010. Land-use effects on the chemical attributes of low-order streams in the eastern Amazon. Journal of Geophysical Research: Biogeosciences 115. https://doi.org/10.1029/2009JG001200

Fistarol, G.O., Coutinho, F.H., Moreira, A.P.B., Venas, T., Cánovas, A., de Paula, S.E.M., Coutinho, R., de Moura, R.L., Valentin, J.L., Tenenbaum, D.R., Paranhos, R., do Valle, R. de A.B., Vicente, A.C.P., Amado Filho, G.M., Pereira, R.C., Kruger, R., Rezende, C.E., Thompson, C.C., Salomon, P.S., Thompson, F.L., 2015. Environmental and Sanitary Conditions of Guanabara Bay, Rio de Janeiro. Front. Microbiol. 6. https://doi.org/10.3389/fmicb.2015.01232

Foley, J.A., DeFries, R., Asner, G.P., Barford, C., Bonan, G., Carpenter, S.R., Chapin, F.S., Coe, M.T., Daily, G.C., Gibbs, H.K., Helkowski, J.H., Holloway, T., Howard, E.A., Kucharik, C.J., Monfreda, C., Patz, J.A., Prentice, I.C., Ramankutty, N., Snyder, P.K., 2005. Global Consequences of Land Use. Science 309, 570–574. https://doi.org/10.1126/science.1111772

Fong, C.R., Gaynus, C.J., Carpenter, R.C., 2020. Extreme rainfall events pulse substantial nutrients and sediments from terrestrial to nearshore coastal communities: a case study from French Polynesia. Sci Rep 10, 2955. https://doi.org/10.1038/s41598-020-59807-5

Franz, B.A., Bailey, S.W., Werdell, P.J., McClain, C.R., 2007. Sensor-independent approach to the vicarious calibration of satellite ocean color radiometry. Appl. Opt., AO 46, 5068–5082. https://doi.org/10.1364/AO.46.005068

Frascari, F., Frignani, M., Guerzoni, S., Ravaioli, M., 1988. Sediments and Pollution in the Northern Adriatic Seaa. Annals of the New York Academy of Sciences 534, 1000–1020. https://doi.org/10.1111/j.1749-6632.1988.tb30191.x

Freire, K., Aragão, J.A., Araújo, A., da Silva, A., Bispo, M., Velasco, G., Carneiro, M., Gonçalves, F., Keunecke, K., Mendonça, J., Moro, P., Motta, F.S., Olavo, G., Pezzuto, P., Aguiar dos Santos, R., Trindade-Santos, I., Vasconcelos, J., Vianna, M., Divovich, E., 2014. Revisiting Brazilian Catch Data for Brazilian Marine Waters (1950-2010). Fisheries Centre Working Paper Series Working Paper #2014-23, 1–41.

Frigstad, H., Kaste, Ø., Deininger, A., Kvalsund, K., Christensen, G., Bellerby, R.G.J., Sørensen, K., Norli, M., King, A.L., 2020. Influence of Riverine Input on Norwegian Coastal Systems. Front. Mar. Sci. 7. https://doi.org/10.3389/fmars.2020.00332

Gadotti, A.P., Souza, C., Serique, C., Ribeiro, C., Mota, I., Lerina, P., 2025. Challenges and Regulatory Strategies for Green Hydrogen in the Port of Açu.

Gallego, G., Cuevas, C., Mohedano, R., García, N., 2013. On the Mahalanobis Distance Classification Criterion for Multidimensional Normal Distributions. IEEE Trans. Signal Process. 61, 4387–4396. https://doi.org/10.1109/TSP.2013.2269047

Gao, Y., Baisch, P., Mirlean, N., Rodrigues Da Silva Júnior, F.M., Van Larebeke, N., Baeyens, W., Leermakers, M., 2018. Arsenic speciation in fish and shellfish from the North Sea (Southern bight) and Açu Port area (Brazil) and health risks related to seafood consumption. Chemosphere 191, 89–96. https://doi.org/10.1016/j.chemosphere.2017.10.031

García Berdeal, I., Hickey, B.M., Kawase, M., 2002. Influence of wind stress and ambient flow on a high discharge river plume. Journal of Geophysical Research: Oceans 107, 13-1-13–24. https://doi.org/10.1029/2001JC000932

Garcia, C., Cunha, G., Pereira, E., Wally, M., Copertino, M., Moller, O., Fetter-Filho, A., Sobral, F., Noernberg, M., Ciotti, A., Krieger, S., Bellini, C., Cirano, M., Bucair, N., Dix, F., 2016. The Brazilian Coastal Monitoring System (SiMCosta) for Climate Studies.

Garnesson, P., Mangin, A., Fanton d'Andon, O., Demaria, J., Bretagnon, M., 2019. The CMEMS GlobColour chlorophyll a product based on satellite observation: multi-sensor merging and flagging strategies. Ocean Science 15, 819–830. https://doi.org/10.5194/os-15-819-2019

Gattuso, J.-P., Frankignoulle, M., Wollast, R., 1998. CARBON AND CARBONATE METABOLISM IN COASTAL AQUATIC ECOSYSTEMS. Annual Review of Ecology, Evolution, and Systematics 29, 405–434. https://doi.org/10.1146/annurev.ecolsys.29.1.405

Gensac, E., Martinez, J.-M., Vantrepotte, V., Anthony, E.J., 2016. Seasonal and inter-annual dynamics of suspended sediment at the mouth of the Amazon river: The role of continental and oceanic forcing, and implications for coastal geomorphology and mud bank formation. Continental Shelf Research 118, 49–62. https://doi.org/10.1016/j.csr.2016.02.009

Geider, R. J., MacIntyre, H. L., & Kana, T. M. (1997). Dynamic model of phytoplankton growth and acclimation: responses of the balanced growth rate and the chlorophyll a: carbon ratio to light, nutrient-limitation and temperature. *Marine Ecology Progress Series*, *148*, 187-200.

Giglio, V.J., Pinheiro, H.T., Bender, M.G., Bonaldo, R.M., Costa-Lotufo, L.V., Ferreira, C.E.L., Floeter, S.R., Freire, A., Gasparini, J.L., Joyeux, J.-C., Krajewski, J.P., Lindner, A., Longo, G.O., Lotufo, T.M.C., Loyola, R., Luiz, O.J., Macieira, R.M., Magris, R.A., Mello, T.J., Quimbayo, J.P., Rocha, L.A., Segal, B., Teixeira, J.B., Vila-Nova, D.A., Vilar, C.C., Zilberberg, C., Francini-Filho, R.B., 2018. Large and remote marine protected areas in the South Atlantic Ocean are flawed and raise concerns: Comments on Soares and Lucas (2018). Marine Policy 96, 13–17. https://doi.org/10.1016/j.marpol.2018.07.017

Giordani, P., Hammond, D.E., Berelson, W.M., Montanari, G., Poletti, R., Milandri, A., Frignani, M., Langone, L., Ravaioli, M., Rovatti, G., Rabbi, E., 1992. Benthic fluxes and nutrient budgets for sediments in the Northern Adriatic Sea: burial and recycling efficiencies, in: Marine Coastal Eutrophication. Elsevier, pp. 251–275. https://doi.org/10.1016/B978-0-444-89990-3.50025-0

Gohin, F., Loyer, S., Lunven, M., Labry, C., Froidefond, J.-M., Delmas, D., Huret, M., Herbland, A., 2005. Satellite-derived parameters for biological modelling in coastal waters: Illustration over the eastern continental shelf of the Bay of Biscay. Remote Sensing of Environment 95, 29–46. https://doi.org/10.1016/j.rse.2004.11.007

Gomes, V.J.C., Asp, N.E., Siegle, E., Gomes, J.D., Silva, A.M.M., Ogston, A.S., Nittrouer, C.A., 2021. Suspended-Sediment Distribution Patterns in Tide-Dominated Estuaries on the Eastern Amazon Coast: Geomorphic Controls of Turbidity-Maxima Formation. Water 13, 1568. https://doi.org/10.3390/w13111568

Gonçalves, L.R., Gerhardinger, L.C., Polette, M., Turra, A., Gonçalves, L.R., Gerhardinger, L.C., Polette, M., Turra, A., 2021. An Endless Endeavor: The Evolution and Challenges of Multi-Level Coastal Governance in the Global South. Sustainability 13. https://doi.org/10.3390/su131810413

Gonzalez-Silvera, A., Santamaria-del-Angel, E., Garcia, V.M.T., Garcia, C.A.E., Millán-Nuñez, R., Muller-Karger, F., 2004. Biogeographical regions of the tropical and subtropical Atlantic Ocean off South America: classification based on pigment (CZCS) and chlorophyll-a (SeaWiFS) variability. Continental Shelf Research 24, 983–1000. https://doi.org/10.1016/j.csr.2004.03.002

Gonçalves-Araujo, R., Röttgers, R., Haraguchi, L., Brandini, F.P., 2019. Hydrography-Driven Variability of Optically Active Constituents of Water in the South Brazilian Bight: Biogeochemical Implications. Front. Mar. Sci. 6. https://doi.org/10.3389/fmars.2019.00716

Gordon, H.R., Brown, O.B., Evans, R.H., Brown, J.W., Smith, R.C., Baker, K.S., Clark, D.K., 1988. A semianalytic radiance model of ocean color. Journal of Geophysical Research: Atmospheres 93, 10909–10924. https://doi.org/10.1029/JD093iD09p10909

Gordon, H.R., Wang, M., 1994. Retrieval of water-leaving radiance and aerosol optical thickness over the oceans with SeaWiFS: a preliminary algorithm. Appl. Opt., AO 33, 443–452. https://doi.org/10.1364/AO.33.000443

Gordon, H. R., & Morel, A. Y. (1983). Remote Assessment of Ocean Color for Interpretation of Satellite Visible Imagery: A Review. In Lect. Notes Coastal Estuarine Stud. (Vol. 4).

Granéli, E., Carlsson, P., Legrand, C., 1999. The role of C, N and P in dissolved and particulate organic matter as a nutrient source for phytoplankton growth, including toxic species. Aquatic Ecology 33, 17–27. https://doi.org/10.1023/A:1009925515059

Green, M.O., Coco, G., 2014. Review of wave-driven sediment resuspension and transport in estuaries: WAVE-DRIVEN SEDIMENT TRANSPORT. Rev. Geophys. 52, 77–117. https://doi.org/10.1002/2013RG000437

Gregg, W.W., Rousseaux, C.S., Franz, B.A., 2017. Global trends in ocean phytoplankton: a new assessment using revised ocean colour data. Remote Sensing Letters 8, 1102–1111. https://doi.org/10.1080/2150704X.2017.1354263

Gregg, W.W., Woodward, R.H., 1998. Improvements in coverage frequency of ocean color: combining data from SeaWiFS and MODIS. IEEE Transactions on Geoscience and Remote Sensing 36, 1350–1353. https://doi.org/10.1109/36.701084

Groom, S., Sathyendranath, S., Ban, Y., Bernard, S., Brewin, R., Brotas, V., Brockmann, C., Chauhan, P., Choi, J., Chuprin, A., Ciavatta, S., Cipollini, P., Donlon, C., Franz, B., He, X., Hirata, T., Jackson, T., Kampel, M., Krasemann, H., Lavender, S., Pardo-Martinez, S., Mélin, F., Platt, T., Santoleri, R., Skakala, J., Schaeffer, B., Smith, M., Steinmetz, F., Valente, A., Wang, M., 2019. Satellite Ocean Colour: Current Status and Future Perspective. Front. Mar. Sci. 6. https://doi.org/10.3389/fmars.2019.00485

Guarnieri, A., Saremi, S., Pedroncini, A., Jensen, J.H., Torretta, S., Vaccari, M., Vincenzi, C., 2021. Effects of marine traffic on sediment erosion and accumulation in ports: a new model-based methodology. Ocean Science 17, 411–430. https://doi.org/10.5194/os-17-411-2021

Guillaud, J.-F., Aminot, A., Delmas, D., Gohin, F., Lunven, M., Labry, C., Herbland, A., 2008. Seasonal variation of riverine nutrient inputs in the northern Bay of Biscay (France), and patterns of marine phytoplankton response. Journal of Marine Systems, Oceanography of the Bay of Biscay 72, 309–319. https://doi.org/10.1016/j.jmarsys.2007.03.010

Gurlin, D., Gitelson, A.A., Moses, W.J., 2011. Remote estimation of chl-a concentration in turbid productive waters Return to a simple two-band NIR-red model? Remote Sensing of Environment 115, 3479–3490. https://doi.org/10.1016/j.rse.2011.08.011

Håkanson, L., Gyllenhammar, A., Brolin, A., 2004. A dynamic compartment model to predict sedimentation and suspended particulate matter in coastal areas. Ecological Modelling 175, 353–384. https://doi.org/10.1016/j.ecolmodel.2003.09.036

Halpern, B.S., Frazier, M., Potapenko, J., Casey, K.S., Koenig, K., Longo, C., Lowndes, J.S., Rockwood, R.C., Selig, E.R., Selkoe, K.A., Walbridge, S., 2015. Spatial and temporal changes in cumulative human impacts on the world's ocean. Nat Commun 6, 7615. https://doi.org/10.1038/ncomms8615

Halpern, B.S., Walbridge, S., Selkoe, K.A., Kappel, C.V., Micheli, F., D'Agrosa, C., Bruno, J.F., Casey, K.S., Ebert, C., Fox, H.E., Fujita, R., Heinemann, D., Lenihan, H.S., Madin, E.M.P., Perry, M.T., Selig, E.R., Spalding, M., Steneck, R., Watson, R., 2008. A Global Map of Human Impact on Marine Ecosystems. Science 319, 948–952. https://doi.org/10.1126/science.1149345

Hamilton, S., 2010. Biogeochemical implications of climate change for tropical rivers and floodplains. Hydrobiologia 657, 19–35. https://doi.org/10.1007/s10750-009-0086-1

Hamlington, B.D., Bellas-Manley, A., Willis, J.K., Fournier, S., Vinogradova, N., Nerem, R.S., Piecuch, C.G., Thompson, P.R., Kopp, R., 2024. The rate of global sea level rise doubled during the past three decades. Commun Earth Environ 5, 601. https://doi.org/10.1038/s43247-024-01761-5

Hammond, M.L., Beaulieu, C., Henson, S.A., Sahu, S.K., 2020. Regional surface chlorophyll trends and uncertainties in the global ocean. Sci Rep 10, 15273. https://doi.org/10.1038/s41598-020-72073-9

Han, B., Loisel, H., Vantrepotte, V., Mériaux, X., Bryère, P., Ouillon, S., Dessailly, D., Xing, Q., Zhu, J., 2016. Development of a Semi-Analytical Algorithm for the Retrieval of Suspended Particulate Matter from Remote Sensing over Clear to Very Turbid Waters. Remote Sensing 8, 211. https://doi.org/10.3390/rs8030211

Hansell, D.A., Carlson, C.A., 1998. Deep-ocean gradients in the concentration of dissolved organic carbon. Nature 395, 263–266. https://doi.org/10.1038/26200

Hansell, D.A., Carlson, C.A., 2014. Biogeochemistry of Marine Dissolved Organic Matter. Academic Press.

Hastie, T., Tibshirani, R., 1986. Generalized Additive Models. Statistical Science 1, 297–310. https://doi.org/10.1214/ss/1177013604

He, Z., Huo, S., Ma, C., Zhang, H., An, D., Xi, B., Xu, Q., Xia, X., Wu, F., 2019. The Contributions of Climate Changes and Human Activities to Long-Term Variations in Lake Sediments Based on Results from Generalized Additive Models. Water Resour Manage 33, 1069–1085. https://doi.org/10.1007/s11269-018-2167-2

Hengl, T., Nussbaum, M., Wright, M.N., Heuvelink, G.B.M., Gräler, B., 2018. Random forest as a generic framework for predictive modeling of spatial and spatio-temporal variables. PeerJ 6, e5518. https://doi.org/10.7717/peerj.5518

Henson, S.A., Beaulieu, C., Lampitt, R., 2016. Observing climate change trends in ocean biogeochemistry: when and where. Glob Chang Biol 22, 1561–1571. https://doi.org/10.1111/gcb.13152

Henson, S.A., Cole, H.S., Hopkins, J., Martin, A.P., Yool, A., 2018. Detection of climate change-driven trends in phytoplankton phenology. Global Change Biology 24, e101–e111. https://doi.org/10.1111/gcb.13886

Henson, S.A., Sarmiento, J.L., Dunne, J.P., Bopp, L., Lima, I., Doney, S.C., John, J., Beaulieu, C., 2010. Detection of anthropogenic climate change in satellite records of ocean chlorophyll and productivity. Biogeosciences 7, 621–640. https://doi.org/10.5194/bg-7-621-2010

Hersbach, H., Bell, B., Berrisford, P., Hirahara, S., Horányi, A., Muñoz-Sabater, J., Nicolas, J., Peubey, C., Radu, R., Schepers, D., Simmons, A., Soci, C., Abdalla, S., Abellan, X., Balsamo, G., Bechtold, P., Biavati, G., Bidlot, J., Bonavita, M., De Chiara, G., Dahlgren, P., Dee, D., Diamantakis, M., Dragani, R., Flemming, J., Forbes, R., Fuentes, M., Geer, A., Haimberger, L., Healy, S., Hogan, R.J., Hólm, E., Janisková, M., Keeley, S., Laloyaux, P., Lopez, P., Lupu, C., Radnoti, G., de Rosnay, P., Rozum, I., Vamborg, F., Villaume, S., Thépaut, J.-N., 2020. The ERA5 global reanalysis. Quarterly Journal of the Royal Meteorological Society 146, 1999–2049. https://doi.org/10.1002/qj.3803

Hickey, B., Geier, S., Kachel, N., MacFadyen, A., 2005. A bi-directional river plume: The Columbia in summer. Continental Shelf Research 25, 1631–1656. https://doi.org/10.1016/j.csr.2005.04.010

Hirsch, R.M., Slack, J.R., 1984. A Nonparametric Trend Test for Seasonal Data With Serial Dependence. Water Resources Research 20, 727–732. https://doi.org/10.1029/WR020i006p00727

Hirsch, R.M., Slack, J.R., Smith, R.A., 1982. Techniques of trend analysis for monthly water quality data. Water Resources Research 18, 107–121. https://doi.org/10.1029/WR018i001p00107

Hobday, A.J., Alexander, L.V., Perkins, S.E., Smale, D., Straub, S., Oliver, E.C.J., Benthuysen, J.A., Burrows, M.T., Donat, M.G., Feng, M., Holbrook, N.J., Moore, P.J., Scannell, H.A., Sen Gupta, A., Wernberg, T., 2016. A hierarchical approach to defining marine heatwaves. Progress in Oceanography 141, 227–238. https://doi.org/10.1016/j.pocean.2015.12.014

Hoover, D.J., Mackenzie, F.T., 2009. Fluvial Fluxes of Water, Suspended Particulate Matter, and Nutrients and Potential Impacts on Tropical Coastal Water Biogeochemistry: Oahu, Hawai‘i. Aquat Geochem 15, 547–570. https://doi.org/10.1007/s10498-009-9067-2

Hora, A.L.B.D., Lima, F.D.S., Hora, H.R.M.D., Silva Neto, R.E., 2021. port digitalization and its aspects in acu port, in northern rio de janeiro - Brazil, in: Anais Do(a) Encontro Nacional de Modelagem Computacional e Encontro de Ciência e Tecnologia de Materiais. Presented at the Encontro nacional de modelagem computacional e encontro de ciência e tecnologia de materiais, Even3, Evento Online. https://doi.org/10.29327/154013.24-20

Hu, C., Lee, Z., Franz, B., 2012. Chlorophyll aalgorithms for oligotrophic oceans: A novel approach based on three-band reflectance difference. Journal of Geophysical Research: Oceans 117. https://doi.org/10.1029/2011JC007395

Hu, C., Montgomery, E.T., Schmitt, R.W., Muller-Karger, F.E., 2004. The dispersal of the Amazon and Orinoco River water in the tropical Atlantic and Caribbean Sea: Observation from space and S-PALACE floats. Deep Sea Research Part II: Topical Studies in Oceanography, Views of Ocean Processes from the Sea-viewing Wide Field-of-view Sensor (SeaWiFS) Mission: Volume 2 51, 1151–1171. https://doi.org/10.1016/j.dsr2.2004.04.001

Intergovernmental Panel On Climate Change (IPCC), 2022. The Ocean and Cryosphere in a Changing Climate: Special Report of the Intergovernmental Panel on Climate Change, 1st ed. Cambridge University Press. https://doi.org/10.1017/9781009157964

IOCCG, 1999. Status and plans for satellite ocean-colour missions: considerations for complementary missions.

IOCCG, 2000. Remote sensing of ocean colour in coastal, and other optically-complex, waters.

IOCCG, 2007. Ocean-Colour Data Merging.

IOCCG, 2025. Evaluation of Atmospheric Correction Algorithms over Turbid Waters; Jamet, C., Balasubramanian, S.V., Eds.; IOCCG Report Series, No. 21; International Ocean Colour Coordinating Group: Dartmouth, NS, Canada; in press.

IOCCG, 2010. IMIS | MarineInfo. Reports and Monographs of the International Ocean-Colour Coordinating Group (IOCCG).

Ioris, A.A.R., 2008. Os limites políticos de uma reforma incompleta: a implementação da lei dos recursos hídricos na Bacia do Paraíba do Sul. Revista Brasileira de Estudos Urbanos e Regionais 10, 61–61. https://doi.org/10.22296/2317-1529.2008v10n1p61

Irigoien, X., Castel, J., 1997. Light Limitation and Distribution of Chlorophyll Pigments in a Highly Turbid Estuary: the Gironde (SW France). Estuarine, Coastal and Shelf Science 44, 507–517. https://doi.org/10.1006/ecss.1996.0132

Jackson, T., Sathyendranath, S., Mélin, F., 2017. An improved optical classification scheme for the Ocean Colour Essential Climate Variable and its applications. Remote Sensing of Environment, Earth Observation of Essential Climate Variables 203, 152–161. https://doi.org/10.1016/j.rse.2017.03.036

Jassby, A.D., Cloern, J.E., Cole, B.E., 2002. Annual primary production: Patterns and mechanisms of change in a nutrient-rich tidal ecosystem. Limnology & Oceanography 47, 698–712. https://doi.org/10.4319/lo.2002.47.3.0698

Jiang, D., Matsushita, B., Pahlevan, N., Gurlin, D., Lehmann, M.K., Fichot, C.G., Schalles, J., Loisel, H., Binding, C., Zhang, Y., Alikas, K., Kangro, K., Uusõue, M., Ondrusek, M., Greb, S., Moses, W.J., Lohrenz, S., O'Donnell, D., 2021. Remotely estimating total suspended solids concentration in clear to extremely turbid waters using a novel semi-analytical method. Remote Sensing of Environment 258, 112386. https://doi.org/10.1016/j.rse.2021.112386

Johns, W.E., Lee, T.N., Beardsley, R.C., Candela, J., Limeburner, R., Castro, B., 1998. Annual Cycle and Variability of the North Brazil Current. Journal of Physical Oceanography 28, 103–128. https://doi.org/10.1175/1520-0485(1998).

Johnston, S.A., 1981. Estuarine dredge and fill activities: A review of impacts. Environmental Management 5, 427–440. https://doi.org/10.1007/BF01866820

Kampel, M., Cortivo, F.D., Valério, L., Freitas, L.B., Rudorff, N.M., 2019. Caracterização sazonal de campos superficiais estimados por sensoriamento remoto na bacia de Sergipe-Alagoas (SE-AL), in: Ambiente Pelágico Da Bacia de Sergipe-Alagoas. Editora Universidade Federal de Sergipe, São Cristóvão, Brasil, pp. 179–221.

Kampel, M., 2003. Estimativa da produção primária e biomassa fitoplanctônica através de sensoriamento remoto da cor do oceano e dados in situ na Costa Sudeste Brasileira (Doutorado em Oceanografia Biológica). Universidade de São Paulo, São Paulo. https://doi.org/10.11606/T.21.2003.tde-29042004-165724

Kang, Y., Kang, Y.-H., Kim, J.-K., Kang, H.Y., Kang, C.-K., 2020. Year-to-year variation in phytoplankton biomass in an anthropogenically polluted and complex estuary: A novel paradigm for river discharge influence. Marine Pollution Bulletin 161, 111756. https://doi.org/10.1016/j.marpolbul.2020.111756

Kasprzak, P., Padisák, J., Koschel, R., Krienitz, L., Gervais, F., 2008. Chlorophyll a concentration across a trophic gradient of lakes: An estimator of phytoplankton biomass? Limnologica, Integrating approaches in limnological research: from basic to applied and from empirical to theoretical 38, 327–338. https://doi.org/10.1016/j.limno.2008.07.002

Keerthi, M.G., Prend, C.J., Aumont, O., Lévy, M., 2022. Annual variations in phytoplankton biomass driven by small-scale physical processes. Nat. Geosci. 15, 1027–1033. https://doi.org/10.1038/s41561-022-01057-3

Kerr, R., da Cunha, L.C., Kikuchi, R.K.P., Horta, P.A., Ito, R.G., Müller, M.N., Orselli, I.B.M., Lencina-Avila, J.M., de Orte, M.R., Sordo, L., Pinheiro, B.R., Bonou, F.K., Schubert, N., Bergstrom, E., Copertino, M.S., 2016. The Western South Atlantic Ocean in a High-CO2 World: Current Measurement Capabilities and Perspectives. Environ Manage 57, 740–752. https://doi.org/10.1007/s00267-015-0630-x

Kineke, G.C., Sternberg, R.W., Trowbridge, J.H., Geyer, W.R., 1996. Fluid-mud processes on the Amazon continental shelf. Continental Shelf Research 16, 667–696. https://doi.org/10.1016/0278-4343(95)00050-X

Kirk, J.T.O., 1994. Light and Photosynthesis in Aquatic Ecosystems. Cambridge University Press.

Knoppers, B., Kjerfve, B., 1999. Coastal Lagoons of Southeastern Brazil: Physical and Biogeochemical Characteristics, in: Perillo, G.M.E., Piccolo, M.C., Pino-Quivira, M. (Eds.), Estuaries of South America: Their Geomorphology and Dynamics. Springer, Berlin, Heidelberg, pp. 35–66. https://doi.org/10.1007/978-3-642-60131-6_3

Knoppers, B., Medeiros, P.R.P., de Souza, W.F.L., Jennerjahn, T., 2006. The São Francisco Estuary, Brazil, in: Wangersky, P.J. (Ed.), Estuaries. Springer, Berlin, Heidelberg, pp. 51–70. https://doi.org/10.1007/698_5_026

Kobashi, F., Kawamura, H., 2002. Seasonal variation and instability nature of the North Pacific Subtropical Countercurrent and the Hawaiian Lee Countercurrent. Journal of Geophysical Research: Oceans 107, 6-1-6–18. https://doi.org/10.1029/2001JC001225

Kroon, F.J., Kuhnert, P.M., Henderson, B.L., Wilkinson, S.N., Kinsey-Henderson, A., Abbott, B., Brodie, J.E., Turner, R.D.R., 2012. River loads of suspended solids, nitrogen, phosphorus and herbicides delivered to the Great Barrier Reef lagoon. Marine Pollution Bulletin 65, 167–181. https://doi.org/10.1016/j.marpolbul.2011.10.018

Kutner, D.S., Bowman, J.S., Saldanha-Corrêa, F.M.P., Chuqui, M.G., Tura, P.M., Moreira, D.L., Brandini, F.P., Signori, C.N., 2023. Inorganic carbon assimilation by planktonic community in Santos Basin, Southwestern Atlantic Ocean. Ocean Coast. Res. 71, e23006. https://doi.org/10.1590/2675-2824071.22085dsk

Kwiatkowska, E.J., Fargion, G.S., 2003. Merger of ocean color data from multiple satellite missions within the SIMBIOS project, in: Ocean Remote Sensing and Applications. Presented at the Ocean Remote Sensing and Applications, SPIE, pp. 168–182. https://doi.org/10.1117/12.466833

Lämmle, L., Bulhões, E.M.R., 2019. Impactos de obras costeiras na linha de costa: O Caso do Porto do Açu, Município de São João da Barra, RJ. Boletim do Observatório Ambiental Alberto Ribeiro Lamego 13, 131–152. https://doi.org/10.19180/2177-4560.v13n12019p131-152

Lämmle, L., Perez Filho, A., Donadio, C., Arienzo, M., Ferrara, L., Santos, C.D.J., Souza, A.O., 2022. Anthropogenic Pressure on Hydrographic Basin and Coastal Erosion in the Delta of Paraíba do Sul River, Southeast Brazil. JMSE 10, 1585. https://doi.org/10.3390/jmse10111585

Latawiec, A.E., Strassburg, B.B.N., Valentim, J.F., Ramos, F., Alves-Pinto, H.N., 2014. Intensification of cattle ranching production systems: socioeconomic and environmental synergies and risks in Brazil. Animal 8, 1255–1263. https://doi.org/10.1017/S1751731114001566

Lavigne, H., Van der Zande, D., Ruddick, K., Cardoso Dos Santos, J.F., Gohin, F., Brotas, V., Kratzer, S., 2021. Quality-control tests for OC4, OC5 and NIR-red satellite chlorophyll-a algorithms applied to coastal waters. Remote Sensing of Environment 255, 112237. https://doi.org/10.1016/j.rse.2020.112237

Le Gall, M., Evrard, O., Dapoigny, A., Tiecher, T., Zafar, M., Minella, J.P.G., Laceby, J.P., Ayrault, S., 2017. Tracing Sediment Sources in a Subtropical Agricultural Catchment of Southern Brazil Cultivated With Conventional and Conservation Farming Practices. Land Degradation & Development 28, 1426–1436. https://doi.org/10.1002/ldr.2662

Le Moal, M., Gascuel-Odoux, C., Ménesguen, A., Souchon, Y., Étrillard, C., Levain, A., Moatar, F., Pannard, A., Souchu, P., Lefebvre, A., Pinay, G., 2019. Eutrophication: A new wine in an old bottle? Sci Total Environ 651, 1–11. https://doi.org/10.1016/j.scitotenv.2018.09.139

Le, C., Lehrter, J.C., Hu, C., MacIntyre, H., Beck, M.W., 2017. Satellite observation of particulate organic carbon dynamics on the Louisiana continental shelf. Journal of Geophysical Research: Oceans 122, 555–569. https://doi.org/10.1002/2016JC012275

Lee, Z., Carder, K.L., Arnone, R.A., 2002. Deriving inherent optical properties from water color: a multiband quasi-analytical algorithm for optically deep waters. Appl. Opt., AO 41, 5755–5772. https://doi.org/10.1364/AO.41.005755

Lefèvre, N., da Silva Dias, F.J., de Torres, A.R., Noriega, C., Araujo, M., de Castro, A.C.L., Rocha, C., Jiang, S., Ibánhez, J.S.P., 2017. A source of CO2 to the atmosphere throughout the year in the Maranhense continental shelf (2°30'S, Brazil). Continental Shelf Research 141, 38–50. https://doi.org/10.1016/j.csr.2017.05.004

Lehmann, M.K., Gurlin, D., Pahlevan, N., Alikas, K., Conroy, T., Anstee, J., Balasubramanian, S.V., Barbosa, C.C.F., Binding, C., Bracher, A., Bresciani, M., Burtner, A., Cao, Z., Dekker, A.G., Di Vittorio, C., Drayson, N., Errera, R.M., Fernandez, V., Ficek, D., Fichot, C.G., Gege, P., Giardino, C., Gitelson, A.A., Greb, S.R., Henderson, H., Higa, H., Rahaghi, A.I., Jamet, C., Jiang, D., Jordan, T., Kangro, K., Kravitz, J.A., Kristoffersen, A.S., Kudela, R., Li, L., Ligi, M., Loisel, H., Lohrenz, S., Ma, R., Maciel, D.A., Malthus, T.J., Matsushita, B., Matthews, M., Minaudo, C., Mishra, D.R., Mishra, S., Moore, T., Moses, W.J., Nguyễn, H., Novo, E.M.L.M., Novoa, S., Odermatt, D., O'Donnell, D.M., Olmanson, L.G., Ondrusek, M., Oppelt, N., Ouillon, S., Pereira Filho, W., Plattner, S., Verdú, A.R., Salem, S.I., Schalles, J.F., Simis, S.G.H., Siswanto, E., Smith, B., Somlai-Schweiger, I., Soppa, M.A., Spyrakos, E., Tessin, E., van der Woerd, H.J., Vander Woude, A., Vandermeulen, R.A., Vantrepotte, V., Wernand, M.R., Werther, M., Young, K., Yue, L., 2023. GLORIA - A globally representative hyperspectral in situ dataset for optical sensing of water quality. Sci Data 10, 100. https://doi.org/10.1038/s41597-023-01973-y

Lentz, S.J., Fewings, M.R., 2012. The Wind- and Wave-Driven Inner-Shelf Circulation. Annual Review of Marine Science 4, 317–343. https://doi.org/10.1146/annurev-marine-120709-142745

Levin, L.A., Liu, K.-K., Emeis, K.-C., Breitburg, D.L., Cloern, J., Deutsch, C., Giani, M., Goffart, A., Hofmann, E.E., Lachkar, Z., Limburg, K., Liu, S.-M., Montes, E., Naqvi, W., Ragueneau, O., Rabouille, C., Sarkar, S.K., Swaney, D.P., Wassman, P., Wishner, K.F., 2015. Comparative biogeochemistry ecosystem human interactions on dynamic continental margins. Journal of Marine Systems 141, 3–17. https://doi.org/10.1016/j.jmarsys.2014.04.016

Li, B., Jia, Y., Liu, J.P., Liu, X., Wang, Z., 2020. Effect of Wave, Current, and Lutocline on Sediment Resuspension in Yellow River Delta-Front. Water 12, 845. https://doi.org/10.3390/w12030845

Li, Q., Jiang, L., Chen, Y., Tang, J., Gao, S., 2023. Absorption-based algorithm for satellite estimating the particulate organic carbon concentration in the global surface ocean. Front. Mar. Sci. 9. https://doi.org/10.3389/fmars.2022.1048893

Liébault, F., Gomez, B., Page, M., Marden, M., Peacock, D., Richard, D., Trotter, C.M., 2005. Land-use change, sediment production and channel response in upland regions. River Research and Applications 21, 739–756. https://doi.org/10.1002/rra.880

Lima, L. dos S., Rosman, P.C.C., Carneiro, J.C., Lima, L. dos S., Rosman, P.C.C., Carneiro, J.C., 2024. Integrated Modeling of Hydrosedimentological Processes for Port Resilience and Environmental Assessment for Decision-Making: Case Study of the Paraíba do Sul River, Brazil, in: Hydrology - Current Research and Future Directions. IntechOpen. https://doi.org/10.5772/intechopen.1004881

Limeira-Filho, D., Moraes, P.S.S., Almeida, M.S., Silva, A.C.C., Silva, J.L.N., Farias-Rodrigues, L., Teixeira, B.R.S., Anjos, J.V.X., Birindelli, J.L.O., Barros, M.C., Fraga, E.C., 2023. Fish diversity in the rivers that drain the Baixada Maranhense and the Mearim basin in northeastern Brazil. Braz. J. Biol. 83, e273525. https://doi.org/10.1590/1519-6984.273525

Lins, R.C., Martinez, J.-M., Motta Marques, D.D., Cirilo, J.A., Medeiros, P.R.P., Fragoso Júnior, C.R., 2018. A Multivariate Analysis Framework to Detect Key Environmental Factors Affecting Spatiotemporal Variability of Chlorophyll-a in a Tropical Productive Estuarine-Lagoon System. Remote Sensing 10, 853. https://doi.org/10.3390/rs10060853

Liu, J., Qiu, Z., Feng, J., Wong, K.P., Tsou, J.Y., Wang, Y., Zhang, Y., 2023. Monitoring Total Suspended Solids and Chlorophyll-a Concentrations in Turbid Waters: A Case Study of the Pearl River Estuary and Coast Using Machine Learning. Remote Sensing 15, 5559. https://doi.org/10.3390/rs15235559

Liu, S.D., Qiao, L.L., Li, G.X., Shi, J.H., Huang, L.L., Yao, Z.G., Gao, F., Wang, Z., Min, J.X., 2018. Variation in the Current Shear Front and Its Potential Effect on Sediment Transport Over the Inner Shelf of the East China Sea in Winter. Journal of Geophysical Research: Oceans 123, 8264–8283. https://doi.org/10.1029/2018JC014241

Llames, M.E., Lagomarsino, L., Diovisalvi, N., Fermani, P., Torremorell, A.M., Perez, G., Unrein, F., Bustingorry, J., Escaray, R., Ferraro, M., Zagarese, H.E., 2009. The effects of light availability in shallow, turbid waters: a mesocosm study. J Plankton Res 31, 1517–1529. https://doi.org/10.1093/plankt/fbp086

Lohrenz, S.E., Fahnenstiel, G.L., Schofield, O., Millie, D.F., 2008. Coastal Sediment Dynamics and River Discharge as Key Factors Influencing: Coastal Ecosystem Productivity in Southeastern Lake Michigan. Oceanography 21, 60–69.

Loisel, H., Duforêt-Gaurier, L., Tran, T.K., Schaffer Ferreira Jorge, D., Steinmetz, F., Mangin, A., Bretagnon, M., Hembise Fanton d'Andon, O., 2023. Characterization of the organic vs. inorganic fraction of suspended particulate matter in coastal waters based on ocean color radiometry remote sensing. State of the Planet 1-osr7, 1–12. https://doi.org/10.5194/sp-1-osr7-11-2023

Loisel, H., Mangin, A., Vantrepotte, V., Dessailly, D., Ngoc Dinh, D., Garnesson, P., Ouillon, S., Lefebvre, J.-P., Mériaux, X., Minh Phan, T., 2014. Variability of suspended particulate matter concentration in coastal waters under the Mekong's influence from ocean color (MERIS) remote sensing over the last decade. Remote Sensing of Environment 150, 218–230. https://doi.org/10.1016/j.rse.2014.05.006

Loisel, H., Nicolas, J.-M., Deschamps, P.-Y., Frouin, R., 2002. Seasonal and inter-annual variability of particulate organic matter in the global ocean. Geophysical Research Letters 29, 49-1-49–4. https://doi.org/10.1029/2002GL015948

Loisel, H., Nicolas, J.-M., Sciandra, A., Stramski, D., Poteau, A., 2006. Spectral dependency of optical backscattering by marine particles from satellite remote sensing of the global ocean. Journal of Geophysical Research: Oceans 111. https://doi.org/10.1029/2005JC003367

Loisel, H., Vantrepotte, V., Dessailly, D., Mériaux, X., 2014. Assessment of the colored dissolved organic matter in coastal waters from ocean color remote sensing. Opt. Express, OE 22, 13109–13124. https://doi.org/10.1364/OE.22.013109

Loisel, H., Vantrepotte, V., Jamet, C., NgocDat, D., Loisel, H., Vantrepotte, V., Jamet, C., NgocDat, D., 2013. Challenges and New Advances in Ocean Color Remote Sensing of Coastal Waters, in: Topics in Oceanography. IntechOpen. https://doi.org/10.5772/56414

Loisel, H., Vantrepotte, V., Ouillon, S., Ngoc, D.D., Herrmann, M., Tran, V., Mériaux, X., Dessailly, D., Jamet, C., Duhaut, T., Nguyen, H.H., Van Nguyen, T., 2017. Assessment and analysis of the chlorophyll-a concentration variability over the Vietnamese coastal waters from the MERIS ocean color sensor (2002–2012). Remote Sensing of Environment 190, 217–232. https://doi.org/10.1016/j.rse.2016.12.016

Longhurst, A., Sathyendranath, S., Platt, T., Caverhill, C., 1995. An estimate of global primary production in the ocean from satellite radiometer data. J Plankton Res 17, 1245–1271. https://doi.org/10.1093/plankt/17.6.1245

Lopez-Gamundi, C., Barnes, B.B., Bakker, A.C., Harris, P. (Mitch), Eberli, G.P., Purkis, S.J., 2024. Spatial, seasonal and climatic drivers of suspended sediment atop Great Bahama Bank. Sedimentology 71, 769–792. https://doi.org/10.1111/sed.13151

Lotze, H.K., Lenihan, H.S., Bourque, B.J., Bradbury, R.H., Cooke, R.G., Kay, M.C., Kidwell, S.M., Kirby, M.X., Peterson, C.H., Jackson, J.B.C., 2006. Depletion, Degradation, and Recovery Potential of Estuaries and Coastal Seas. Science 312, 1806–1809. https://doi.org/10.1126/science.1128035

Lubac, B., Loisel, H., Guiselin, N., Astoreca, R., Felipe Artigas, L., Mériaux, X., 2008. Hyperspectral and multispectral ocean color inversions to detect Phaeocystis globosa blooms in coastal waters. Journal of Geophysical Research: Oceans 113. https://doi.org/10.1029/2007JC004451

Ludwig, W., Probst, J.-L., 1998. River sediment discharge to the oceans; present-day controls and global budgets. American Journal of Science 298, 265–295.

Luisetti, T., Turner, R.K., Jickells, T., Andrews, J., Elliott, M., Schaafsma, M., Beaumont, N., Malcolm, S., Burdon, D., Adams, C., Watts, W., 2014. Coastal Zone Ecosystem Services: From science to values and decision making; a case study. Science of The Total Environment 493, 682–693. https://doi.org/10.1016/j.scitotenv.2014.05.099

Magris, R.A., Costa, M.D.P., Ferreira, C.E.L., Vilar, C.C., Joyeux, J.-C., Creed, J.C., Copertino, M.S., Horta, P.A., Sumida, P.Y.G., Francini-Filho, R.B., Floeter, S.R., 2021. A blueprint for securing Brazil's marine biodiversity and supporting the achievement of global conservation goals. Diversity and Distributions 27, 198–215. https://doi.org/10.1111/ddi.13183

Majid, A., Ikhsan, N., Hassan, Z., 2025. Utility of satellite imagery in estimating coastal marine water attributes. Continental Shelf Research 292, 105509. https://doi.org/10.1016/j.csr.2025.105509

Mann, H.B., 1945. Nonparametric Tests Against Trend. Econometrica 13, 245–259. https://doi.org/10.2307/1907187

Marchesiello, P., Nguyen, N.M., Gratiot, N., Loisel, H., Anthony, E.J., Dinh, C.S., Nguyen, T., Almar, R., Kestenare, E., 2019. Erosion of the coastal Mekong delta: Assessing natural against man induced processes. Continental Shelf Research 181, 72–89. https://doi.org/10.1016/j.csr.2019.05.004

Marcos, M., Wöppelmann, G., Matthews, A., Ponte, R.M., Birol, F., Ardhuin, F., Coco, G., Santamaría-Gómez, A., Ballu, V., Testut, L., Chambers, D., Stopa, J.E., 2019. Coastal Sea Level and Related Fields from Existing Observing Systems. Surv Geophys 40, 1293–1317. https://doi.org/10.1007/s10712-019-09513-3

Maritorena, S., d'Andon, O.H.F., Mangin, A., Siegel, D.A., 2010. Merged satellite ocean color data products using a bio-optical model: Characteristics, benefits and issues. Remote Sensing of Environment 114, 1791–1804. https://doi.org/10.1016/j.rse.2010.04.002

Marques, A., Martins, I.S., Kastner, T., Plutzar, C., Theurl, M.C., Eisenmenger, N., Huijbregts, M.A.J., Wood, R., Stadler, K., Bruckner, M., Canelas, J., Hilbers, J.P., Tukker, A., Erb, K., Pereira, H.M., 2019. Increasing impacts of land use on biodiversity and carbon sequestration driven by population and economic growth. Nat Ecol Evol 3, 628–637. https://doi.org/10.1038/s41559-019-0824-3

Mazzini, P.L.F., Pianca, C., Pareja-Roman, L.F., Cole, K.L., Walter, R.K., Castelao, R.M., Hunter, E.J., Chant, R.J., 2025. Spatio-temporal variability of San Francisco Bay Plume from space. Front. Mar. Sci. 12. https://doi.org/10.3389/fmars.2025.1588441

McClain, C.R., 2009. A Decade of Satellite Ocean Color Observations*. Annual Review of Marine Science 1, 19–42. https://doi.org/10.1146/annurev.marine.010908.163650

Mears, C., Lee, T., Ricciardulli, L., Wang, X., Wentz, F., 2022. Improving the Accuracy of the Cross-Calibrated Multi-Platform (CCMP) Ocean Vector Winds. Remote Sensing 14, 4230. https://doi.org/10.3390/rs14174230

Medeiros, L.E., Magnago, R. de O., Fisch, G., Marciotto, E.R., 2013. Observational Study of the Surface Layer at an Ocean–Land Transition Region. Journal of Aerospace Technology and Management 5, 449–458.

Mélin, F., 2016. Impact of inter-mission differences and drifts on chlorophyll-a trend estimates. International Journal of Remote Sensing 37, 2233–2251. https://doi.org/10.1080/01431161.2016.1168949

Mélin, F., Vantrepotte, V., 2015. How optically diverse is the coastal ocean? Remote Sensing of Environment 160, 235–251. https://doi.org/10.1016/j.rse.2015.01.023

Mélin, F., Vantrepotte, V., Chuprin, A., Grant, M., Jackson, T., Sathyendranath, S., 2017. Assessing the fitness-for-purpose of satellite multi-mission ocean color climate data records: A protocol applied to OC-CCI chlorophyll-a data. Remote Sensing of Environment, Earth Observation of Essential Climate Variables 203, 139–151. https://doi.org/10.1016/j.rse.2017.03.039

Mélin, F., Vantrepotte, V., Clerici, M., D'Alimonte, D., Zibordi, G., Berthon, J.-F., Canuti, E., 2011. Multi-sensor satellite time series of optical properties and chlorophyll-a concentration in the Adriatic Sea. Progress in Oceanography 91, 229–244. https://doi.org/10.1016/j.pocean.2010.12.001

Mélin, F., Zibordi, G., 2007. Optically based technique for producing merged spectra of water-leaving radiances from ocean color remote sensing. Appl. Opt., AO 46, 3856–3869. https://doi.org/10.1364/AO.46.003856

Melo, E.R., Brandini, N., Medeiros, P.R.P., Silva, R., Cavalcante, G., 2020. Nutrients Load Estimation in a Regulated Streamflow Estuary: The São Francisco Estuary (NE/Brazil). Rev. bras. meteorol. 35, 803–811. https://doi.org/10.1590/0102-7786355000007

Ménesguen, A., Lacroix, G., 2018. Modelling the marine eutrophication: A review. Sci Total Environ 636, 339–354. https://doi.org/10.1016/j.scitotenv.2018.04.183

Merseburger, G.C., Martí, E., Sabater, F., 2005. Net changes in nutrient concentrations below a point source input in two streams draining catchments with contrasting land uses. Science of The Total Environment 347, 217–229. https://doi.org/10.1016/j.scitotenv.2004.12.022

Miguel, L.L.A.J., 2018. Study on seasonal hydrology and biogeochemical variability in a tropical estuarine system, Central Mozambique Coast, Africa. Marine Pollution Bulletin 131, 674–692. https://doi.org/10.1016/j.marpolbul.2018.04.071

Mikelsons, K., Wang, M., Jiang, L., Bouali, M., 2014. Destriping algorithm for improved satellite-derived ocean color product imagery. Opt. Express, OE 22, 28058–28070. https://doi.org/10.1364/OE.22.028058

Millennium Ecosystem Assessment, 2005. Ecosystems and human well-being: wetlands and water synthesis : a report of the Millennium Ecosystem Assessment. World Resources Institute, Washington, DC.

Miller, R.L., Cruise, J.F., 1995. Effects of suspended sediments on coral growth: Evidence from remote sensing and hydrologic modeling. Remote Sensing of Environment 53, 177–187. https://doi.org/10.1016/0034-4257(95)00081-B

Miller, R.L., McKee, B.A., 2004. Using MODIS Terra 250 m imagery to map concentrations of total suspended matter in coastal waters. Remote Sensing of Environment 93, 259–266. https://doi.org/10.1016/j.rse.2004.07.012

Milliman, J., Farnsworth, K., Jones, P., Xu, K., Smith, L., 2008. Climatic and anthropogenic factors affecting river discharge to the global ocean, 1951-2000. Global and Planetary Change 62, 187–194. https://doi.org/10.1016/j.gloplacha.2008.03.001

Ministério Público do Estado do Rio de Janeiro, 2021. Avaliação Técnica das condições de Integridade e de Gestão de Riscos do Mineroduto do Sistema Minas-Rio—Etapa 2: Parecer Técnico Final; Technical Report 21 282-301; Ministério Público do Estado do Rio de Janeiro: Rio de Janeiro, Brazil. Available online: https://brasil.angloamerican.com/pt-pt (accessed on 10 October 2025).

Miranda, F. a. V., Moser, G. a. O., Lima, D.T., Machado, W.T.V., Brandini, N., Fernandes, A.M., Costa, L.V.M., Amaral, M.F., Oliveira, G.B., Abril, G.Y., 2024. Phytoplankton Diversity Across a Coastal Urbanization and Eutrophication Gradient: The Sepetiba Bay—Ilha Grande Bay Continuum in Rio de Janeiro. Marine Ecology 45, e12838. https://doi.org/10.1111/maec.12838

Mobley, C.D., 1999. Estimation of the remote-sensing reflectance from above-surface measurements. Appl. Opt., AO 38, 7442–7455. https://doi.org/10.1364/AO.38.007442

Mobley, C.D., Stramski, D., Bissett, W.P., Boss, E., 2004. Optical Modeling of Ocean Waters: Is the Case 1 - Case 2 Classification Still Useful? Oceanography 17, 60–67.

Mobley, C.D., Werdell, J., Franz, B., Ahmad, Z., Bailey, S., 2016. Atmospheric Correction for Satellite Ocean Color Radiometry (No. GSFC-E-DAA-TN35509).

Molinier, M., Guyot, J.-L., Guimaraes, V., Oliveira, E. de, 1993. Hydrologie du bassin de l'Amazone.

Molisani, M.M., Marins, R.V., Machado, W., Paraquetti, H.H.M., Bidone, E.D., Lacerda, L.D., 2004. Environmental changes in Sepetiba Bay, SE Brazil. Reg Environ Change 4, 17–27. https://doi.org/10.1007/s10113-003-0060-9

Molleri, G.S.F., Novo, E.M.L. de M., Kampel, M., 2010. Space-time variability of the Amazon River plume based on satellite ocean color. Continental Shelf Research 30, 342–352. https://doi.org/10.1016/j.csr.2009.11.015

Moore, T.S., Campbell, J.W., Dowell, M.D., 2009. A class-based approach to characterizing and mapping the uncertainty of the MODIS ocean chlorophyll product. Remote Sensing of Environment 113, 2424–2430. https://doi.org/10.1016/j.rse.2009.07.016

Moore, T.S., Campbell, J.W., Feng, H., 2001. A fuzzy logic classification scheme for selecting and blending satellite ocean color algorithms. IEEE Transactions on Geoscience and Remote Sensing 39, 1764–1776. https://doi.org/10.1109/36.942555

Moore, T.S., Dowell, M.D., Bradt, S., Ruiz Verdu, A., 2014. An optical water type framework for selecting and blending retrievals from bio-optical algorithms in lakes and coastal waters. Remote Sensing of Environment 143, 97–111. https://doi.org/10.1016/j.rse.2013.11.021

Morel, A., 1988. Optical modeling of the upper ocean in relation to its biogenous matter content (case I waters). Journal of Geophysical Research: Oceans 93, 10749–10768. https://doi.org/10.1029/JC093iC09p10749

Morel, A., Prieur, L., 1977. Analysis of variations in ocean color. Limnology and Oceanography 22, 709–722. https://doi.org/10.4319/lo.1977.22.4.0709

Mourão, F.V., de Sousa, A.C.S.R., da Luz Mendes, R.M., Castro, K.M., da Silva, A.C., El-Robrini, M., de Oliveira Salomão, U., Pereira, J.A.R., de Lourdes Souza Santos, M., 2020. Water quality and eutrophication in the Curuçá estuary in northern Brazil. Regional Studies in Marine Science 39, 101450. https://doi.org/10.1016/j.rsma.2020.101450

Moussa, R., Voltz, M., Andrieux, P., 2002. Effects of the spatial organization of agricultural management on the hydrological behaviour of a farmed catchment during flood events. Hydrological Processes 16, 393–412. https://doi.org/10.1002/hyp.333

Mouw, C.B., Greb, S., Aurin, D., DiGiacomo, P.M., Lee, Z., Twardowski, M., Binding, C., Hu, C., Ma, R., Moore, T., Moses, W., Craig, S.E., 2015. Aquatic color radiometry remote sensing of coastal and inland waters: Challenges and recommendations for future satellite missions. Remote Sensing of Environment 160, 15–30. https://doi.org/10.1016/j.rse.2015.02.001

Muehe, D., 2006. Erosão e progradação do litoral brasileiro. Ministério do Meio Ambiente : PGGM-Programa de Geologia e Geofísica Marinha, Brasília, DF.

Muller-Karger, F.E., Hestir, E., Ade, C., Turpie, K., Roberts, D.A., Siegel, D., Miller, R.J., Humm, D., Izenberg, N., Keller, M., Morgan, F., Frouin, R., Dekker, A.G., Gardner, R., Goodman, J., Schaeffer, B., Franz, B.A., Pahlevan, N., Mannino, A.G., Concha, J.A., Ackleson, S.G., Cavanaugh, K.C., Romanou, A., Tzortziou, M., Boss, E.S., Pavlick, R., Freeman, A., Rousseaux, C.S., Dunne, J., Long, M.C., Klein, E., McKinley, G.A., Goes, J., Letelier, R., Kavanaugh, M., Roffer, M., Bracher, A., Arrigo, K.R., Dierssen, H., Zhang, X., Davis, F.W., Best, B., Guralnick, R., Moisan, J., Sosik, H.M., Kudela, R., Mouw, C.B., Barnard, A.H., Palacios, S., Roesler, C., Drakou, E.G., Appeltans, W., Jetz, W., 2018. Satellite sensor requirements for monitoring essential biodiversity variables of coastal ecosystems. Ecological Applications 28, 749–760. https://doi.org/10.1002/eap.1682

Narayanan, A., Cohen, S., Gardner, J.R., 2024. Riverine sediment response to deforestation in the Amazon basin. Earth Surface Dynamics 12, 581–599. https://doi.org/10.5194/esurf-12-581-2024

Nechad, B., Ruddick, K.G., Park, Y., 2010. Calibration and validation of a generic multisensor algorithm for mapping of total suspended matter in turbid waters. Remote Sensing of Environment 114, 854–866. https://doi.org/10.1016/j.rse.2009.11.022

Negri, M., Malavasi, S., 2018. Wave Energy Harnessing in Shallow Water through Oscillating Bodies. Energies 11, 2730. https://doi.org/10.3390/en11102730

Neill, C., Piccolo, M.C., Cerri, C.C., Steudler, P.A., Melillo, J.M., 2006. Soil Solution Nitrogen Losses During Clearing of Lowland Amazon Forest for Pasture. Plant Soil 281, 233–245. https://doi.org/10.1007/s11104-005-4435-1

Neumann, B., Vafeidis, A.T., Zimmermann, J., Nicholls, R.J., 2015. Future Coastal Population Growth and Exposure to Sea-Level Rise and Coastal Flooding - A Global Assessment. PLOS ONE 10, e0118571. https://doi.org/10.1371/journal.pone.0118571

Nicolodi, J.L., Petermann, R.M., 2010. Potential vulnerability of the Brazilian coastal zone in its environmental, social, and technological aspects.

Nikiema, O., Devenon, J.-L., Baklouti, M., 2007. Numerical modeling of the Amazon River plume. Continental Shelf Research 27, 873–899. https://doi.org/10.1016/j.csr.2006.12.004

Nixon, S.W., 1998. Enriching the sea to death. Scientific American 9, 48–53.

Nóbrega, R.L.B., Guzha, A.C., Lamparter, G., Amorim, R.S.S., Couto, E.G., Hughes, H.J., Jungkunst, H.F., Gerold, G., 2018. Impacts of land-use and land-cover change on stream hydrochemistry in the Cerrado and Amazon biomes. Science of The Total Environment 635, 259–274. https://doi.org/10.1016/j.scitotenv.2018.03.356

Novoa, S., Doxaran, D., Ody, A., Vanhellemont, Q., Lafon, V., Lubac, B., Gernez, P., 2017. Atmospheric Corrections and Multi-Conditional Algorithm for Multi-Sensor Remote Sensing of Suspended Particulate Matter in Low-to-High Turbidity Levels Coastal Waters. Remote Sensing 9, 61. https://doi.org/10.3390/rs9010061

O'Reilly, J.E., Maritorena, S., Mitchell, B.G., Siegel, D.A., Carder, K.L., Garver, S.A., Kahru, M., McClain, C., 1998. Ocean color chlorophyll algorithms for SeaWiFS. Journal of Geophysical Research: Oceans 103, 24937–24953. https://doi.org/10.1029/98JC02160

Odermatt, D., Gitelson, A., Brando, V.E., Schaepman, M., 2012. Review of constituent retrieval in optically deep and complex waters from satellite imagery. Remote Sensing of Environment 118, 116–126. https://doi.org/10.1016/j.rse.2011.11.013

Ody, A., Doxaran, D., Vanhellemont, Q., Nechad, B., Novoa, S., Many, G., Bourrin, F., Verney, R., Pairaud, I., Gentili, B., Ody, A., Doxaran, D., Vanhellemont, Q., Nechad, B., Novoa, S., Many, G., Bourrin, F., Verney, R., Pairaud, I., Gentili, B., 2016. Potential of High Spatial and Temporal Ocean Color Satellite Data to Study the Dynamics of Suspended Particles in a Micro-Tidal River Plume. Remote Sensing 8. https://doi.org/10.3390/rs8030245

Ogston, A.S., Field, M.E., 2010. Predictions of Turbidity Due to Enhanced Sediment Resuspension Resulting from Sea-Level Rise on a Fringing Coral Reef: Evidence from Molokai, Hawaii. Journal of Coastal Research 26, 1027–1037.

Oliveira, E.N.D., Knoppers, B.A., Lorenzzetti, J.A., Medeiros, P.R.P., Carneiro, M.E., Souza, W.F.L.D., 2012. A satellite view of riverine turbidity plumes on the NE-E Brazilian coastal zone. Braz. j. oceanogr. 60, 283–298. https://doi.org/10.1590/S1679-87592012000300002

Oliveira, E.N., Fernandes, A.M., Kampel, M., Cordeiro, R.C., Brandini, N., Vinzon, S.B., Grassi, R.M., Pinto, F.N., Fillipo, A.M., Paranhos, R., 2016. Assessment of remotely sensed chlorophyll-a concentration in Guanabara Bay, Brazil. JARS 10, 026003. https://doi.org/10.1117/1.JRS.10.026003

Orpin, A.R., Ridd, P.V., Thomas, S., Anthony, K.R.N., Marshall, P., Oliver, J., 2004. Natural turbidity variability and weather forecasts in risk management of anthropogenic sediment discharge near sensitive environments. Marine Pollution Bulletin 49, 602–612. https://doi.org/10.1016/j.marpolbul.2004.03.020

Osadchiev, A., Silvestrova, K., Myslenkov, S., 2020. Wind-Driven Coastal Upwelling near Large River Deltas in the Laptev and East-Siberian Seas. Remote Sensing 12, 844. https://doi.org/10.3390/rs12050844

Ovalle, A.R.C., Silva, C.F., Rezende, C.E., Gatts, C.E.N., Suzuki, M.S., Figueiredo, R.O., 2013. Long-term trends in hydrochemistry in the Paraíba do Sul River, southeastern Brazil. Journal of Hydrology 481, 191–203. https://doi.org/10.1016/j.jhydrol.2012.12.036

Pachniak, E., Fan, Y., Li, W., Stamnes, K., 2023. Quantifying Uncertainties in OC-SMART Ocean Color Retrievals: A Bayesian Inversion Algorithm. Algorithms 16, 301. https://doi.org/10.3390/a16060301

Paerl, H.W., 2006. Assessing and managing nutrient-enhanced eutrophication in estuarine and coastal waters: Interactive effects of human and climatic perturbations. Ecological Engineering, Advances in coastal habitat restoration in the northern Gulf of Mexico 26, 40–54. https://doi.org/10.1016/j.ecoleng.2005.09.006

Pahlevan, N., Sarkar, S., Franz, B.A., 2016. Uncertainties in coastal ocean color products: Impacts of spatial sampling. Remote Sensing of Environment 181, 14–26. https://doi.org/10.1016/j.rse.2016.03.022

Pardal, E.C., Pereira, L.C.C., de O. Guimarães, D., Oliveira, S.M.O., Trindade, W.N., da Costa, R.M., 2011. Influence of oceanographic conditions on the spatial and temporal distribution of chlorophyll-a in the coastal waters of the Brazilian Amazon region (São Luís-MA). Journal of Coastal Research 421–424.

Passeri, D.L., Hagen, S.C., Medeiros, S.C., Bilskie, M.V., Alizad, K., Wang, D., 2015. The dynamic effects of sea level rise on low-gradient coastal landscapes: A review. Earth's Future 3, 159–181. https://doi.org/10.1002/2015EF000298

Pauly, D., Christensen, V., 1995. Primary production required to sustain global fisheries. Nature 374, 255–257. https://doi.org/10.1038/374255a0

Pauthenet, E., Martinez, E., Gorgues, T., Roussillon, J., Drumetz, L., Fablet, R., Roux, M., 2024. Contrasted Trends in Chlorophyll-a Satellite Products. Geophysical Research Letters 51, e2024GL108916. https://doi.org/10.1029/2024GL108916

Pedlowski, M.A., 2013. When the State Becomes the Land Grabber: Violence and Dispossession in the Name of 'Development' in Brazil. lag 12, 91–111. https://doi.org/10.1353/lag.2013.0045

Pereira, O.N.A., Rodrigues, M.A. da C., Dias, J.M.A., 2018. An approach to the contribution of anthropogenic actions for the araruama lagoonal system (se brazil) geomorphological evolution / uma abordagem sobre a influência antropogênica na evolução geomorfológica do sistema lagunar de araruama (SE, Brasil). Journal of Sedimentary Environments 108–120. https://doi.org/10.12957/jse.2018.35533

Pezzulli, S., Stephenson, D.B., Hannachi, A., 2005. The Variability of Seasonality. Journal of Climate 18, 71–88. https://doi.org/10.1175/JCLI-3256.1

Pimenta, F.M., Saavedra, O.R., Oliveira, D.Q., Assireu, A.T., Torres Júnior, A.R., de Freitas, R.M., Neto, F.L.A., Lopes, D.C.P., Oliveira, C.B.M., de Lima, S.L., Neto, J.C. de O., Veras, R.B.S., 2023. Characterization of Wind Resources of the East Coast of Maranhão, Brazil. Energies 16, 5555. https://doi.org/10.3390/en16145555

Piola, A.R., Matano, R.P., Palma, E.D., Möller Jr., O.O., Campos, E.J.D., 2005. The influence of the Plata River discharge on the western South Atlantic shelf. Geophysical Research Letters 32. https://doi.org/10.1029/2004GL021638

Pires, P.V.B., Sousa, E.B.D., Gomes, A.L., Cunha, C.J.S., Tavares, V.B.D.C., Pinheiro, S.C.C., Carneiro, B.S., Melo, N.F. a. C.D., 2024. Effect of seasonality and estuarine waters on the phytoplankton of the Guamá River (Belém, Amazon, Brazil). An. Acad. Bras. Ciênc. 96, e20220413. https://doi.org/10.1590/0001-3765202420220413

Planchon, O., Dubreuil, V., Damato, F., Gouéry, P., Decaux, S., 2004. Recherche sur les types de temps associes aux brises de mer: Une méthode d'analyse par téledetection. Norois 191, 59–74. https://doi.org/10.4000/norois.1027

Pontes Da Silva Júnior, J.L., Pedlowski, M.A., 2022. Percepção de agricultores familiares sobre os impactos socioambientais causados pelo Porto do Açu em São João da Barra-RJ. SN 34. https://doi.org/10.14393/SN-v34-2022-63123

Porter, E.T., Sanford, L.P., 2010. Effect of tidal resuspension on benthic–pelagic coupling in an experimental ecosystem study. Marine Ecology Progress Series 413, 33–53. https://doi.org/10.3354/meps08709

Porto do Açu, 2016. T-OIL Terminal Operations; Porto do Açu: São João da Barra, Brazil. Available online: https://portodo acu.com.br/ (accessed on 10 October 2025).

Porto do Açu, 2021. Protocolo Padrão para Dragagens de Manutenção; Porto do Açu: São João da Barra, Brazil. Available online: https://esg.portodoacu.com.br/pt/ (accessed on 10 October 2025).

Postma, H., 1961. Transport and accumulation of suspended matter in the Dutch Wadden Sea. Netherlands Journal of Sea Research 1, 148–190. https://doi.org/10.1016/0077-7579(61)90004-7

Pottier, C., Garcon, V., Larnicol, G., Sudre, J., Schaeffer, P., Le Traon, P.-Y., 2006. Merging SeaWiFS and MODIS/Aqua Ocean Color Data in North and Equatorial Atlantic Using Weighted Averaging and Objective Analysis. IEEE Transactions on Geoscience and Remote Sensing 44, 3436–3451. https://doi.org/10.1109/TGRS.2006.878441

Prado, H.M., Schlindwein, M.N., Murrieta, R.S.S., Nascimento Júnior, D.R. do, Souza, E.P. de, Cunha-Lignon, M., Mahiques, M.M. de, Giannini, P.C.F., Contente, R.F., 2019. O canal do valo grande no complexo estuarino cananéia-iguape (SP, Brasil): história ambiental, ecologia e perspectivas futuras. ambient. soc. 22, e01822. https://doi.org/10.1590/1809-4422asoc0182r2vu19L4TD

Prend, C.J., Keerthi, M.G., Lévy, M., Aumont, O., Gille, S.T., Talley, L.D., 2022. Sub-Seasonal Forcing Drives Year-To-Year Variations of Southern Ocean Primary Productivity. Global Biogeochemical Cycles 36, e2022GB007329. https://doi.org/10.1029/2022GB007329

Prieur, L., Sathyendranath, S., 1981. An optical classification of coastal and oceanic waters based on the specific spectral absorption curves of phytoplankton pigments, dissolved organic matter, and other particulate materials. Limnology and Oceanography 26, 671–689. https://doi.org/10.4319/lo.1981.26.4.0671

Prumm, M., Iglesias, G., 2016. Impacts of port development on estuarine morphodynamics: Ribadeo (Spain). Ocean & Coastal Management 130, 58–72. https://doi.org/10.1016/j.ocecoaman.2016.05.003

Qiao, L., Zhong, Y., Wang, N., Zhao, K., Huang, L., Wang, Z., 2016. Seasonal transportation and deposition of the suspended sediments in the Bohai Sea and Yellow Sea and the related mechanisms. Ocean Dynamics 66, 751–766. https://doi.org/10.1007/s10236-016-0950-2

Racault, M.-F., Sathyendranath, S., Brewin, R.J.W., Raitsos, D.E., Jackson, T., Platt, T., 2017. Impact of El Niño Variability on Oceanic Phytoplankton. Front. Mar. Sci. 4. https://doi.org/10.3389/fmars.2017.00133

Ramesh, R., Chen, Z., Cummins, V., Day, J., D'Elia, C., Dennison, B., Forbes, D.L., Glaeser, B., Glaser, M., Glavovic, B., Kremer, H., Lange, M., Larsen, J.N., Le Tissier, M., Newton, A., Pelling, M., Purvaja, R., Wolanski, E., 2015. Land-Ocean Interactions in the Coastal Zone: Past, present & future. Anthropocene 12, 85–98. https://doi.org/10.1016/j.ancene.2016.01.005

Ramessur, R., 2002. Anthropogenic-driven changes with focus on the coastal zone of Mauritius, south-western Indian Ocean. Reg Environ Change 3, 99–106. https://doi.org/10.1007/s10113-002-0045-0

Regnier, P., Friedlingstein, P., Ciais, P., Mackenzie, F.T., Gruber, N., Janssens, I.A., Laruelle, G.G., Lauerwald, R., Luyssaert, S., Andersson, A.J., Arndt, S., Arnosti, C., Borges, A.V., Dale, A.W., Gallego-Sala, A., Goddéris, Y., Goossens, N., Hartmann, J., Heinze, C., Ilyina, T., Joos, F., LaRowe, D.E., Leifeld, J., Meysman, F.J.R., Munhoven, G., Raymond, P.A., Spahni, R., Suntharalingam, P., Thullner, M., 2013. Anthropogenic perturbation of the carbon fluxes from land to ocean. Nature Geosci 6, 597–607. https://doi.org/10.1038/ngeo1830

Richardson, C.M., Peucker-Ehrenbrink, B., Wyatt, S., Bourbonnais, A., Hatje, V., Frey, C., Sanders, T., Varela, D.E., Paytan, A., 2025. Effects of climate change on river and groundwater nutrient inputs to the coastal ocean. Commun Earth Environ 6, 761. https://doi.org/10.1038/s43247-025-02594-6

Rio, M.-H., Mulet, S., Picot, N., 2014. Beyond GOCE for the ocean circulation estimate: Synergetic use of altimetry, gravimetry, and in situ data provides new insight into geostrophic and Ekman currents. Geophysical Research Letters 41, 8918–8925. https://doi.org/10.1002/2014GL061773

Rodrigues, R.R., Lorenzzetti, J.A., 2001. A numerical study of the effects of bottom topography and coastline geometry on the Southeast Brazilian coastal upwelling. Continental Shelf Research 21, 371–394. https://doi.org/10.1016/S0278-4343(00)00094-7

Rose, L.A., Karwan, D.L., 2021. Stormflow concentration–discharge dynamics of suspended sediment and dissolved phosphorus in an agricultural watershed. Hydrological Processes 35, e14455. https://doi.org/10.1002/hyp.14455

Ruddick, K.G., De Cauwer, V., Park, Y.-J., Moore, G., 2006. Seaborne measurements of near infrared water-leaving reflectance: The similarity spectrum for turbid waters. Limnology and Oceanography 51, 1167–1179. https://doi.org/10.4319/lo.2006.51.2.1167

Ruddick, K.G., Ovidio, F., Rijkeboer, M., 2000. Atmospheric correction of SeaWiFS imagery for turbid coastal and inland waters. Appl. Opt., AO 39, 897–912. https://doi.org/10.1364/AO.39.000897

Rudorff, N., Kampel, M., Rezende, C., 2011. Spectral mapping of the Paraíba do Sul River plume (Brazil) using multitemporal Landsat images. Journal of Applied Remote Sensing 5, 053550–1. https://doi.org/10.1117/1.3630220

Salah Salah, I., Vantrepotte, V., Cardoso dos Santos, J.F., Tran, M.D., Jorge, D.S.F., Kampel, M., Loisel, H., 2025. Impact of Industrialization on the Evolution of Suspended Particulate Matter from MODIS Data (2002–2022): Case Study of Açu Port, Brazil. Remote Sensing 17, 4020. https://doi.org/10.3390/rs17244020

Sánchez, E., Colmenarejo, M.F., Vicente, J., Rubio, A., García, M.G., Travieso, L., Borja, R., 2007. Use of the water quality index and dissolved oxygen deficit as simple indicators of watersheds pollution. Ecological Indicators 7, 315–328. https://doi.org/10.1016/j.ecolind.2006.02.005

Santer, R., Schmechtig, C., 2000. Adjacency effects on water surfaces: primary scattering approximation and sensitivity study. Appl. Opt., AO 39, 361–375. https://doi.org/10.1364/AO.39.000361

Santos, C.A.G., Brasil Neto, R.M., Passos, J.S. de A., da Silva, R.M., 2017. Drought assessment using a TRMM-derived standardized precipitation index for the upper São Francisco River basin, Brazil. Environ Monit Assess 189, 250. https://doi.org/10.1007/s10661-017-5948-9

Santos, V.H.M. dos, Dias, F.J. da S., Dottori, M., Torres, A.R., Santos, R.L., Soares, R. de A., Ribeiro, J.C.M., Serejo, J.H.F., Lima, H.P., Azevedo, I.H.R., 2023. Investigation of physical properties and suspended particulate matter discharge in a macrotidal estuary at the Amazon-semiarid transition zone. Regional Studies in Marine Science 67, 103194. https://doi.org/10.1016/j.rsma.2023.103194

Sathyendranath, S., Brewin, R.J.W., Brockmann, C., Brotas, V., Calton, B., Chuprin, A., Cipollini, P., Couto, A.B., Dingle, J., Doerffer, R., Donlon, C., Dowell, M., Farman, A., Grant, M., Groom, S., Horseman, A., Jackson, T., Krasemann, H., Lavender, S., Martinez-Vicente, V., Mazeran, C., Mélin, F., Moore, T.S., Müller, D., Regner, P., Roy, S., Steele, C.J., Steinmetz, F., Swinton, J., Taberner, M., Thompson, A., Valente, A., Zühlke, M., Brando, V.E., Feng, H., Feldman, G., Franz, B.A., Frouin, R., Gould, R.W., Hooker, S.B., Kahru, M., Kratzer, S., Mitchell, B.G., Muller-Karger, F.E., Sosik, H.M., Voss, K.J., Werdell, J., Platt, T., 2019. An Ocean-Colour Time Series for Use in Climate Studies: The Experience of the Ocean-Colour Climate Change Initiative (OC-CCI). Sensors 19, 4285. https://doi.org/10.3390/s19194285

Sathyendranath, S., Brewin, R.J.W., Jackson, T., Mélin, F., Platt, T., 2017. Ocean-colour products for climate-change studies: What are their ideal characteristics? Remote Sensing of Environment, Earth Observation of Essential Climate Variables 203, 125–138. https://doi.org/10.1016/j.rse.2017.04.017

Sattler, D., Seliger, R., Nehren, U., de Torres, F.N., da Silva, A.S., Raedig, C., Hissa, H.R., Heinrich, J., 2018. Pasture Degradation in Southeast Brazil: Status, Drivers and Options for Sustainable Land Use Under Climate Change, in: Leal Filho, W., Esteves de Freitas, L. (Eds.), Climate Change Adaptation in Latin America: Managing Vulnerability, Fostering Resilience. Springer International Publishing, Cham, pp. 3–17. https://doi.org/10.1007/978-3-319-56946-8_1

Saulquin, B., Fablet, R., Mangin, A., Mercier, G., Antoine, D., Fanton d'Andon, O., 2013. Detection of linear trends in multisensor time series in the presence of autocorrelated noise: Application to the chlorophyll-a SeaWiFS and MERIS data sets and extrapolation to the incoming Sentinel 3-OLCI mission. Journal of Geophysical Research: Oceans 118, 3752–3763. https://doi.org/10.1002/jgrc.20264

Scheel, F., de Jong, M.P.C.; Dobrochinski, J.P.H., de Boer, W.P., Carneiro, J.C., 2023. The Importance of Using Local Information in Climate Change Impact Assessments for Ports. In Proceedings of the PIANC COPEDEC X Conference, Manila, Philippines, 91 - 3 October.

Schroeder, T., Brando, V., Blondeau, D., Clementson, L., Anstee, J., Thapar, N., King, E.,2015. Remote sensing methods to map and monitor the condition of coastal habitats and other surrogates for biodiversity.

Sen, P.K., 1968. Estimates of the Regression Coefficient Based on Kendall's Tau. Journal of the American Statistical Association 63, 1379–1389. https://doi.org/10.1080/01621459.1968.10480934

Shahidul Islam, Md., Tanaka, M., 2004. Impacts of pollution on coastal and marine ecosystems including coastal and marine fisheries and approach for management: a review and synthesis. Marine Pollution Bulletin 48, 624–649. https://doi.org/10.1016/j.marpolbul.2003.12.004

Shaikh, S.M.S., Tagde, J.P., Singh, P.R., Dutta, S., Sangolkar, L.N., Kumar, M.S., 2021. Impact of Port and harbour activities on plankton distribution and dynamics: A multivariate approach. Marine Pollution Bulletin 165, 112105. https://doi.org/10.1016/j.marpolbul.2021.112105

Shampa, Mosa.T.A., Ahmed, Md.K., Chowdhury, K.M.A., Islam, Md.A., Hasan, M., Rahman, M.S., Islam, Md.S., 2024. Spatial and seasonal variability of chlorophyll-a, total suspended matter, and colored dissolved organic matter in the Sundarban mangrove forest using earth observation and field data. Heliyon 10, e38789. https://doi.org/10.1016/j.heliyon.2024.e38789

Shariot-Ullah, Md., 2024. Sea-level rise and sustainable shore protection strategies in the low-lying delta: A case study of Bangladesh. Regional Studies in Marine Science 71, 103424. https://doi.org/10.1016/j.rsma.2024.103424

Shi, W., Wang, M., 2024. Monitoring the Amazon River plume from satellite observations. GIScience & Remote Sensing 61, 2416725. https://doi.org/10.1080/15481603.2024.2416725

Shiskin, J., Young, A.H., Musgrave, J.C., 1965. The X-11 Variant of the Census Method II Seasonal Adjustment Program. U.S. Government Printing Office.

Siegel, D.A., Behrenfeld, M.J., Maritorena, S., McClain, C.R., Antoine, D., Bailey, S.W., Bontempi, P.S., Boss, E.S., Dierssen, H.M., Doney, S.C., Eplee, R.E., Evans, R.H., Feldman, G.C., Fields, E., Franz, B.A., Kuring, N.A., Mengelt, C., Nelson, N.B., Patt, F.S., Robinson, W.D., Sarmiento, J.L., Swan, C.M., Werdell, P.J., Westberry, T.K., Wilding, J.G., Yoder, J.A., 2013. Regional to global assessments of phytoplankton dynamics from the SeaWiFS mission. Remote Sensing of Environment 135, 77–91. https://doi.org/10.1016/j.rse.2013.03.025

Siegle, E., Costa, M.B., 2017. Nearshore Wave Power Increase on Reef-Shaped Coasts Due to Sea-Level Rise. Earth's Future 5, 1054–1065. https://doi.org/10.1002/2017EF000624

Sigleo, A.C., Frick, W.E., 2007. Seasonal variations in river discharge and nutrient export to a Northeastern Pacific estuary. Estuarine, Coastal and Shelf Science 73, 368–378. https://doi.org/10.1016/j.ecss.2007.01.015

Silva Junior, C.H.L., Celentano, D., Rousseau, G.X., De Moura, E.G., Varga, I.V.D., Martinez, C., Martins, M.B., 2020. Amazon forest on the edge of collapse in the Maranhão State, Brazil. Land Use Policy 97, 104806. https://doi.org/10.1016/j.landusepol.2020.104806

Silva, L.M. da, Feitosa, F.A. do N., Montes, M. de J.F., Otsuka, A.Y., Saldanha-Corrêa, F., Noriega, C., 2019. Phytoplankton Productivity and Hydrology in an Impacted Estuarine Complex in Northeastern Brazil. Open Journal of Ecology 9, 458–477. https://doi.org/10.4236/oje.2019.910030

Silva, M.S., Guedes, C.C.F., Silva, G.A.M. da, Ribeiro, G.P., 2021. Active mechanisms controlling morphodynamics of a coastal barrier: Ilha Comprida, Brazil. Ocean Coast. Res. 69, e21004. https://doi.org/10.1590/2675-2824069.20-338mss

Simão, R., Távora, J., Salama, M.S., Fernandes, E., Simão, R., Távora, J., Salama, M.S., Fernandes, E., 2024. Optimizing Optical Coastal Remote-Sensing Products: Recommendations for Regional Algorithm Calibration. Remote Sensing 16. https://doi.org/10.3390/rs16091497

Siswanto, E., Tang, J., Yamaguchi, H., Ahn, Y.-H., Ishizaka, J., Yoo, S., Kim, S.-W., Kiyomoto, Y., Yamada, K., Chiang, C., Kawamura, H., 2011. Empirical ocean-color algorithms to retrieve chlorophyll-a, total suspended matter, and colored dissolved organic matter absorption coefficient in the Yellow and East China Seas. J Oceanogr 67, 627–650. https://doi.org/10.1007/s10872-011-0062-z

Small, C., Nicholls, R.J., 2003. A Global Analysis of Human Settlement in Coastal Zones. Journal of Coastal Research 19, 584–599.

Smith, S.J., Friedrichs, C.T., 2011. Size and settling velocities of cohesive flocs and suspended sediment aggregates in a trailing suction hopper dredge plume. Continental Shelf Research 31, S50–S63. https://doi.org/10.1016/j.csr.2010.04.002

Soares, M.O., Bezerra, L.E.A., Copertino, M., Lopes, B.D., Barros, K.V. de S., Rocha-Barreira, C.A., Maia, R.C., Beloto, N., Cotovicz, L.C., 2022. Blue Carbon Ecosystems in Brazil: Overview and an Urgent Call for Conservation and Restoration. Front. Mar. Sci. 9. https://doi.org/10.3389/fmars.2022.797411

Souza, J.C.M., Shimbo, J.Z., Rosa, M.R., Parente, L.L., Alencar, A.A., Rudorff, B.F.T., Hasenack, H., Matsumoto, M., Ferreira, L.G., Souza-Filho, P.W.M., Oliveira, S.W. de, Rocha, W.F., Fonseca, A.V., Marques, C.B., Diniz, C.G., Costa, D., Monteiro, D., Rosa, E.R., Vélez-Martin, E., Weber, E.J., Lenti, F.E.B., Paternost, F.F., Pareyn, F.G.C., Siqueira, J.V., Viera, J.L., Neto, L.C.F., Saraiva, M.M., Sales, M.H., Salgado, M.P.G., Vasconcelos, R., Galano, S., Mesquita, V.V., Azevedo, 2020. Reconstructing Three Decades of Land Use and Land Cover Changes in Brazilian Biomes with Landsat Archive and Earth Engine. Remote Sensing 12. https://doi.org/10.3390/rs12172735

Souza, M.F.L., Kjerfve, B., Knoppers, B., Landim de Souza, W.F., Damasceno, R.N., 2003. Nutrient budgets and trophic state in a hypersaline coastal lagoon: Lagoa de Araruama, Brazil. Estuarine, Coastal and Shelf Science 57, 843–858. https://doi.org/10.1016/S0272-7714(02)00415-8

Spalding, M.D., Fox, H.E., Allen, G.R., Davidson, N., Ferdaña, Z.A., Finlayson, M., Halpern, B.S., Jorge, M.A., Lombana, A., Lourie, S.A., Martin, K.D., McManus, E., Molnar, J., Recchia, C.A., Robertson, J., 2007. Marine Ecoregions of the World: A Bioregionalization of Coastal and Shelf Areas. BioScience 57, 573–583. https://doi.org/10.1641/B570707

Spyrakos, E., O'Donnell, R., Hunter, P.D., Miller, C., Scott, M., Simis, S.G.H., Neil, C., Barbosa, C.C.F., Binding, C.E., Bradt, S., Bresciani, M., Dall'Olmo, G., Giardino, C., Gitelson, A.A., Kutser, T., Li, L., Matsushita, B., Martinez-Vicente, V., Matthews, M.W., Ogashawara, I., Ruiz-Verdú, A., Schalles, J.F., Tebbs, E., Zhang, Y., Tyler, A.N., 2018. Optical types of inland and coastal waters. Limnology and Oceanography 63, 846–870. https://doi.org/10.1002/lno.10674

Stedmon, C.A., Markager, S., Kaas, H., 2000. Optical Properties and Signatures of Chromophoric Dissolved Organic Matter (CDOM) in Danish Coastal Waters. Estuarine, Coastal and Shelf Science 51, 267–278. https://doi.org/10.1006/ecss.2000.0645

Steinmetz, F., Deschamps, P.-Y., Ramon, D., 2011. Atmospheric correction in presence of sun glint: application to MERIS. Opt. Express, OE 19, 9783–9800. https://doi.org/10.1364/OE.19.009783

Stramski, D., Boss, E., Bogucki, D., Voss, K.J., 2004. The role of seawater constituents in light backscattering in the ocean. Progress in Oceanography 61, 27–56. https://doi.org/10.1016/j.pocean.2004.07.001

Subirade, C., Jamet, C., Tran, M.D., Vantrepotte, V., Han, B., 2024. Evaluation of twelve algorithms to estimate suspended particulate matter from OLCI over contrasted coastal waters. Opt. Express, OE 32, 45719–45744. https://doi.org/10.1364/OE.529712

Sullivan Sealey, K., Bustamante, G., 1999. Setting geographic priorities for marine conservation in Latin America and the Caribbean. Arlington, VA: The Nature Conservancy.

Sullivan, B.E., Prahl, F.G., Small, L.F., Covert, P.A., 2001. Seasonality of phytoplankton production in the Columbia River: A natural or anthropogenic pattern? Geochimica et Cosmochimica Acta 65, 1125–1139. https://doi.org/10.1016/S0016-7037(00)00565-2

Swift, D. J., Stanley, D. J, Swift, D. J. P., 1976. Collected Reprints. U.S. Department of Commerce, National Oceanic and Atmospheric Administration, Environmental Research Laboratories.

Syvitski, J.P.M., Vörösmarty, C.J., Kettner, A.J., Green, P., 2005. Impact of Humans on the Flux of Terrestrial Sediment to the Global Coastal Ocean. Science 308, 376–380. https://doi.org/10.1126/science.1109454

Tanaka, Y., Minggat, E., Roseli, W., 2021. The impact of tropical land-use change on downstream riverine and estuarine water properties and biogeochemical cycles: a review. Ecological Processes 10, 40. https://doi.org/10.1186/s13717-021-00315-3

Tavora, J., Boss, E., Doxaran, D., Hill, P., Tavora, J., Boss, E., Doxaran, D., Hill, P., 2020. An Algorithm to Estimate Suspended Particulate Matter Concentrations and Associated Uncertainties from Remote Sensing Reflectance in Coastal Environments. Remote Sensing 12. https://doi.org/10.3390/rs12132172

Thomas, S.M., Neill, C., Deegan, L.A., Krusche, A.V., Ballester, V.M., Victoria, R.L., 2004. Influences of land use and stream size on particulate and dissolved materials in a small Amazonian stream network. Biogeochemistry 68, 135–151. https://doi.org/10.1023/B:BIOG.0000025734.66083.b7

Tilstone, G.H., Pardo, S., Simis, S.G.H., Qin, P., Selmes, N., Dessailly, D., Kwiatkowska, E., 2021. Consistency between Satellite Ocean Colour Products under High Coloured Dissolved Organic Matter Absorption in the Baltic Sea. Remote Sensing 14. https://doi.org/10.3390/rs14010089

Toste, R., Vasconcelos, A., Assad, L.P.D.F., Landau, L., 2024. Dynamically downscaled coastal flooding in Brazil's Guanabara Bay under a future climate change scenario. Nat Hazards 120, 7845–7869. https://doi.org/10.1007/s11069-024-06556-7

Tran, M.D., Vantrepotte, V., El Hourany, R., Jorge, D.S.F., Kampel, M., Cardoso dos Santos, J.F., Oliveira, E.N., Paranhos, R., Jamet, C., 2025. Combination of neural network models for estimating Chlorophyll-a over turbid and clear waters (CONNECT). Front. Remote Sens. 6. https://doi.org/10.3389/frsen.2025.1570827

Tran, M.D., Vantrepotte, V., Loisel, H., Oliveira, E.N., Tran, K.T., Jorge, D., Mériaux, X., Paranhos, R., 2023. Band Ratios Combination for Estimating Chlorophyll-a from Sentinel-2 and Sentinel-3 in Coastal Waters. Remote Sensing 15, 1653. https://doi.org/10.3390/rs15061653

Tran, T.K., Duforêt-Gaurier, L., Vantrepotte, V., Jorge, D.S.F., Mériaux, X., Cauvin, A., d'Andon, O.F., Loisel, H., Tran, T.K., Duforêt-Gaurier, L., Vantrepotte, V., Jorge, D.S.F., Mériaux, X., Cauvin, A., d'Andon, O.F., Loisel, H., 2019. Deriving Particulate Organic Carbon in Coastal Waters from Remote Sensing: Inter-

Comparison Exercise and Development of a Maximum Band-Ratio Approach. Remote Sensing 11. https://doi.org/10.3390/rs11232849

Turner, A., Millward, G.E., 2002. Suspended Particles: Their Role in Estuarine Biogeochemical Cycles. Estuarine, Coastal and Shelf Science 55, 857–883. https://doi.org/10.1006/ecss.2002.1033

Uncles, R.J., Bloomer, N.J., Frickers, P.E., Griffiths, M.L., Harris, C., Howland, R.J., Morris, A.W., Plummer, D.H., Tappin, A.D., 2000. Seasonal variability of salinity, temperature, turbidity and suspended chlorophyll in the Tweed Estuary. Sci Total Environ 251–252, 115–124. https://doi.org/10.1016/s0048-9697(00)00405-8

Valerio, A. de M., Kampel, M., Vantrepotte, V., Ward, N.D., Sawakuchi, H.O., Less, D.F.D.S., Neu, V., Cunha, A., Richey, J., 2018. Using CDOM optical properties for estimating DOC concentrations and pCO2 in the Lower Amazon River. Opt. Express, OE 26, A657–A677. https://doi.org/10.1364/OE.26.00A657

Van den Eynde, D., Fettweis, M., 2006. Modelling of Fine-Grained Sediment Transport and Dredging Material Dumpings at the Belgian Continental Shelf. Journal of Coastal Research 1564–1569.

van der Hout, C.M., Witbaard, R., Bergman, M.J.N., Duineveld, G.C.A., Rozemeijer, M.J.C., Gerkema, T., 2017. The dynamics of suspended particulate matter (SPM) and chlorophyll-a from intratidal to annual time scales in a coastal turbidity maximum. Journal of Sea Research, SI: North Sea Coastal System 127, 105–118. https://doi.org/10.1016/j.seares.2017.04.011

Van Maren, D.S., Van Kessel, T., Cronin, K., Sittoni, L., 2015. The impact of channel deepening and dredging on estuarine sediment concentration. Continental Shelf Research 95, 1–14. https://doi.org/10.1016/j.csr.2014.12.010

Vantrepotte, V., Loisel, H., Dessailly, D., Mériaux, X., 2012. Optical classification of contrasted coastal waters. Remote Sensing of Environment 123, 306–323. https://doi.org/10.1016/j.rse.2012.03.004

Vantrepotte, V., Mélin, F., 2009. Temporal variability of 10-year global SeaWiFS time-series of phytoplankton chlorophyll a concentration. ICES J Mar Sci 66, 1547–1556. https://doi.org/10.1093/icesjms/fsp107

Vantrepotte, V., Mélin, F., 2011. Inter-annual variations in the SeaWiFS global chlorophyll a concentration (1997–2007). Deep Sea Research Part I: Oceanographic Research Papers 58, 429–441. https://doi.org/10.1016/j.dsr.2011.02.003

Vargas Borges, H., Carvalho, A., Ii, Mendes, Oliveira, A., Ii, Miranda, Harada, A., Ii, H., Paraense, M., Goeldi, E., Belém, M., 2016. Mapping the scientific output of the Costal Studies Program (PEC) of the Museu Paraense Emílio Goeldi, Belém, Pará, Brazil, as a contribution to coastal ecosystem services Mapeamento da produção científica do Programa de Estudos Costeiros (PEC) do Museu Paraense Emílio Goeldi, Belém, Pará, Brasil, visando serviços de ecossistemas marinhos e costeiros. Boletim do Museu Paraense Emílio Goeldi. Ciências Naturais 183–190.

Velegrakis, A.F., Gao, S., Lafite, R., Dupont, J.P., Huault, M.F., Nash, L.A., Collins, M.B., 1997. Resuspension and advection processes affecting suspended particulate matter concentrations in the central English Channel. Journal of Sea Research 38, 17–34. https://doi.org/10.1016/S1385-1101(97)00041-5

Viana, J.F. de S., Montenegro, S.M.G.L., Srinivasan, R., Santos, C.A.G., Mishra, M., Kalumba, A.M., da Silva, R.M., 2023. Land Use and Land Cover Trends and Their Impact on Streamflow and Sediment Yield in a Humid Basin of Brazil's Atlantic Forest Biome. Diversity 15, 1220. https://doi.org/10.3390/d15121220

Vilani, R.M., Cruz, J.L.V.D., Pedlowski, M.A., 2021. Salty Port: Environmental Conflicts Resulting from the Açu Port, Rio de Janeiro state, Brazil. Ambient. soc. 24, e01901. https://doi.org/10.1590/1809-4422asoc20200190r1vu2021l5ao

Walling, D.E., 1999. Linking land use, erosion and sediment yields in river basins. Hydrobiologia 410, 223–240. https://doi.org/10.1023/A:1003825813091

Wang, F., Shao, W., Yu, H., Kan, G., He, X., Zhang, D., Ren, M., Wang, G., 2020. Re-evaluation of the Power of the Mann-Kendall Test for Detecting Monotonic Trends in Hydrometeorological Time Series. Front. Earth Sci. 8. https://doi.org/10.3389/feart.2020.00014

Wang, H., Convertino, M., 2023. Algal bloom ties: Systemic biogeochemical stress and Chlorophyll-a shift forecasting. Ecological Indicators 154, 110760. https://doi.org/10.1016/j.ecolind.2023.110760

Wang, M., Shi, W., 2007. The NIR-SWIR combined atmospheric correction approach for MODIS ocean color data processing. Opt. Express, OE 15, 15722–15733. https://doi.org/10.1364/OE.15.015722

Wang, N., Qiao, L., Li, G., Zhong, Y., Song, D., Ding, D., Gao, F., Ji, F., 2019. Numerical Study on Seasonal Transportation of the Suspended Sediments in the Modern Yellow River Mouth Effected by the Artificial Water and Sediment Regulation. J. Ocean Univ. China 18, 20–30. https://doi.org/10.1007/s11802-019-3646-7

Wang, X.H., Andutta, F.P., 2013. Sediment Transport Dynamics in Ports, Estuaries and. Sediment Transport: Processes and Their Modelling Applications 1.

Ward Jr., J.H., 1963. Hierarchical Grouping to Optimize an Objective Function. Journal of the American Statistical Association 58, 236–244. https://doi.org/10.1080/01621459.1963.10500845

Ward, N.D., Bianchi, T.S., Medeiros, P.M., Seidel, M., Richey, J.E., Keil, R.G., Sawakuchi, H.O., 2017. Where Carbon Goes When Water Flows: Carbon Cycling across the Aquatic Continuum. Front. Mar. Sci. 4. https://doi.org/10.3389/fmars.2017.00007

Weigelhofer, G., 2017. The potential of agricultural headwater streams to retain soluble reactive phosphorus. Hydrobiologia 793, 149–160. https://doi.org/10.1007/s10750-016-2789-4

Weihao, Y., Hua, W., Yubao, X.I.A., Yichuan, Z., Yanqing, D., Yuanyuan, L.I., Xinyue, Z., 2021. Relationship of Chlorophyll A and Water Quality Factors in Poyang Lake Based on GAM Model. Ecology and Environment 30, 1716. https://doi.org/10.16258/j.cnki.1674-5906.2021.08.018

Werdell, P.J., Bailey, S.W., Franz, B.A., Harding, L.W., Feldman, G.C., McClain, C.R., 2009. Regional and seasonal variability of chlorophyll-a in Chesapeake Bay as observed by SeaWiFS and MODIS-Aqua. Remote Sensing of Environment 113, 1319–1330. https://doi.org/10.1016/j.rse.2009.02.012

Werdell, P.J., McKinna, L.I.W., Boss, E., Ackleson, S.G., Craig, S.E., Gregg, W.W., Lee, Z., Maritorena, S., Roesler, C.S., Rousseaux, C.S., Stramski, D., Sullivan, J.M., Twardowski, M.S., Tzortziou, M., Zhang, X., 2018. An overview of approaches and challenges for retrieving marine inherent optical properties from ocean color remote sensing. Progress in Oceanography 160, 186–212. https://doi.org/10.1016/j.pocean.2018.01.001

Willey, J.D., Kieber, R.J., Eyman, M.S., Avery Jr., G.B., 2000. Rainwater dissolved organic carbon: Concentrations and global flux. Global Biogeochemical Cycles 14, 139–148. https://doi.org/10.1029/1999GB900036

Wood, S.N., 2017. Generalized Additive Models: An Introduction with R, Second Edition, 2nd ed. Chapman and Hall/CRC, New York. https://doi.org/10.1201/9781315370279

Wu, X., Feng, X., Fu, B., Yin, S., He, C., 2023. Managing erosion and deposition to stabilize a silt-laden river. Science of The Total Environment 881, 163444. https://doi.org/10.1016/j.scitotenv.2023.163444

Xavier, A.C.F., Rudke, A.P., Serrão, E.A. de O., Terassi, P.M. de B., Pontes, P.R.M., 2021. Evaluation of Satellite-Derived Products for the Daily Average and Extreme Rainfall in the Mearim River Drainage Basin (Maranhão, Brazil). Remote Sensing 13. https://doi.org/10.3390/rs13214393

Yan, J., Li, F., 2023. Effects of sediment dredging on freshwater system: a comprehensive review. Environ Sci Pollut Res 30, 119612–119626. https://doi.org/10.1007/s11356-023-30851-8

Yu, S., Bai, Y., He, X., Gong, F., Li, T., 2023. A new merged dataset of global ocean chlorophyll-a concentration for better trend detection. Front. Mar. Sci. 10. https://doi.org/10.3389/fmars.2023.1051619

Yudhistira, M.H., Karimah, I.D., Maghfira, N.R., 2022. The effect of port development on coastal water quality: Evidence of eutrophication states in Indonesia. Ecological Economics 196, 107415. https://doi.org/10.1016/j.ecolecon.2022.107415

Zang, Z., Xue, Z.G., Xu, K., Bentley, S.J., Chen, Q., D'Sa, E.J., Zhang, L., Ou, Y., 2020. The role of sediment-induced light attenuation on primary production during Hurricane Gustav (2008). Biogeosciences 17, 5043–5055. https://doi.org/10.5194/bg-17-5043-2020

Zarillo, G.A., 2023. Inter-annual sea level change and transgression along a barrier Island coast. Front. Environ. Sci. 11, 1107458. https://doi.org/10.3389/fenvs.2023.1107458

Zhang, H., Meng, C., Wang, Yujie, Wang, Yunqi, Li, M., 2020. Comprehensive evaluation of the effects of climate change and land use and land cover change variables on runoff and sediment discharge. Science of The Total Environment 702, 134401. https://doi.org/10.1016/j.scitotenv.2019.134401

Zhang, M., Tang, J., Dong, Q., Song, Q., Ding, J., 2010. Retrieval of total suspended matter concentration in the Yellow and East China Seas from MODIS imagery. Remote Sensing of Environment 114, 392–403. https://doi.org/10.1016/j.rse.2009.09.016

Zibordi, G., Berthon, J.-F., Mélin, F., D'Alimonte, D., Kaitala, S., 2009. Validation of satellite ocean color primary products at optically complex coastal sites: Northern Adriatic Sea, Northern Baltic Proper and Gulf of Finland. Remote Sensing of Environment 113, 2574–2591. https://doi.org/10.1016/j.rse.2009.07.013

ANNEX

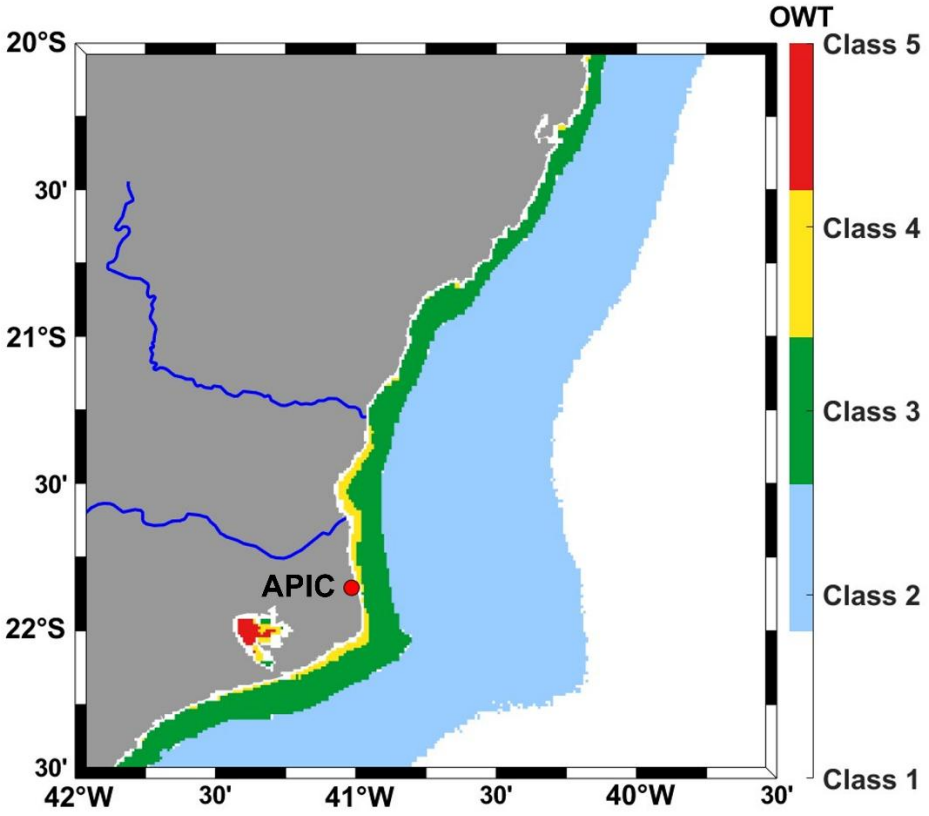

Figure A.1. Map representing the maximum occurrence of OWT for each pixel within the study area observed from the monthly MODIS-Aqua (1km) data from 2002-2022.

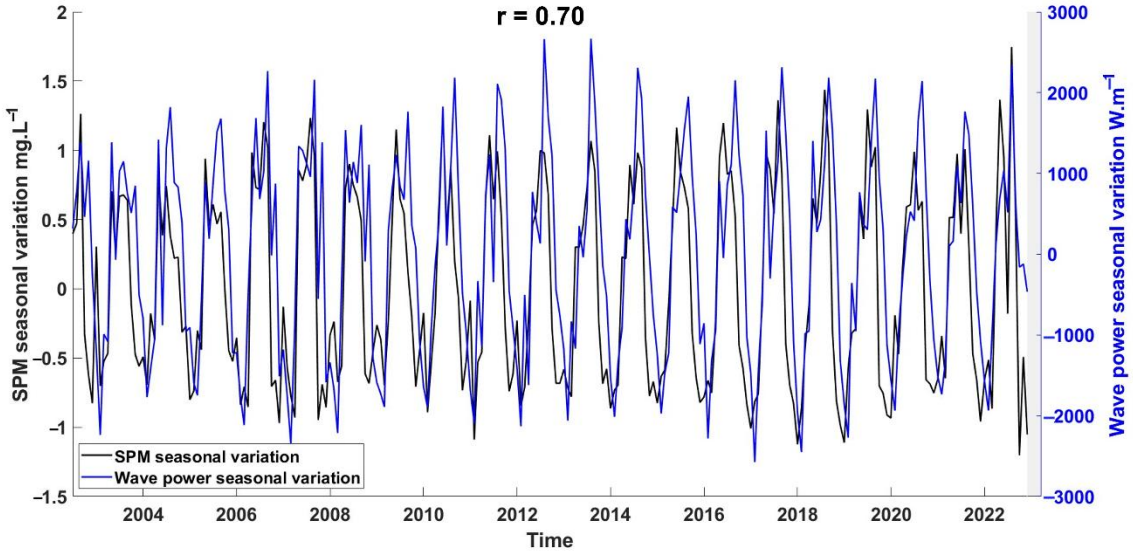

Figure A.2. Time series of Seasonal variation (X11 outputs) of SPM (black), and wave power (blue) extracted at Point A, located offshore (20 m depth) of Açu Port (Figure 5a).

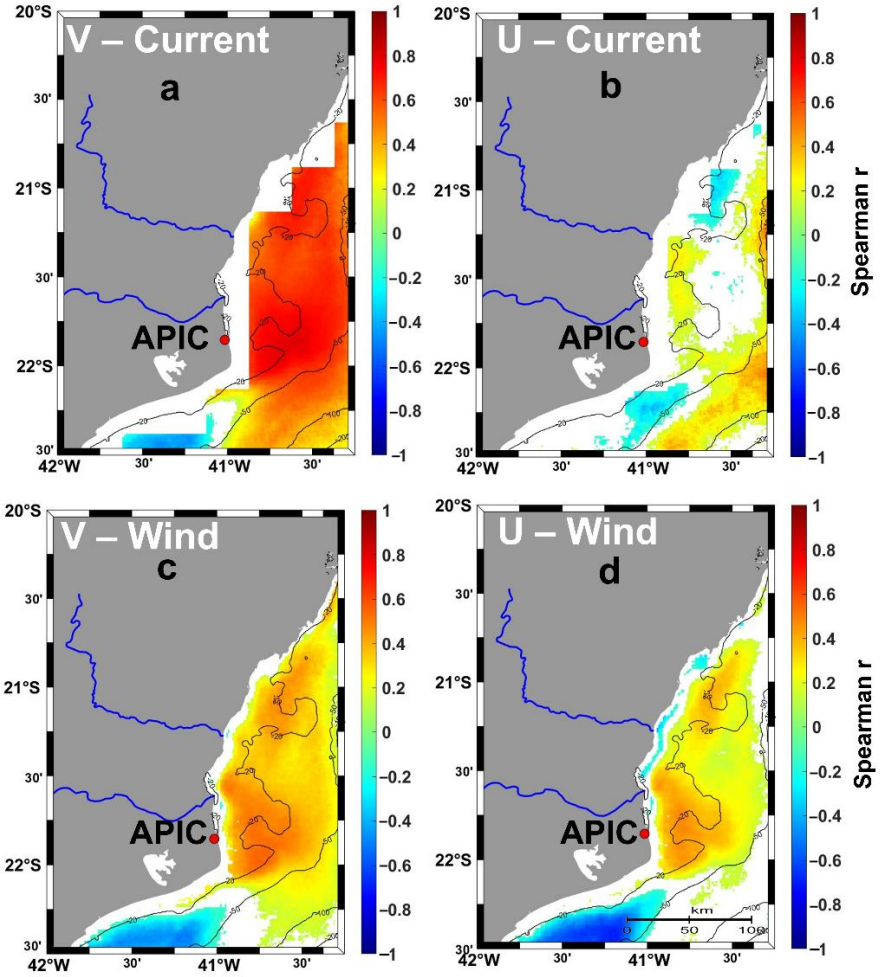

Figure A.3. Correlation maps between seasonal components of SPM, wind and current. (a) correlation map between seasonal components of SPM and meridional current (V). (b) correlation map between seasonal components of SPM and zonal current (U). (c) correlation map between seasonal components of SPM and meridional wind (V). (b) correlation map between seasonal components of SPM and zonal wind (U). Only significant correlations ($p < 0.05$, $N = 246$) are shown.

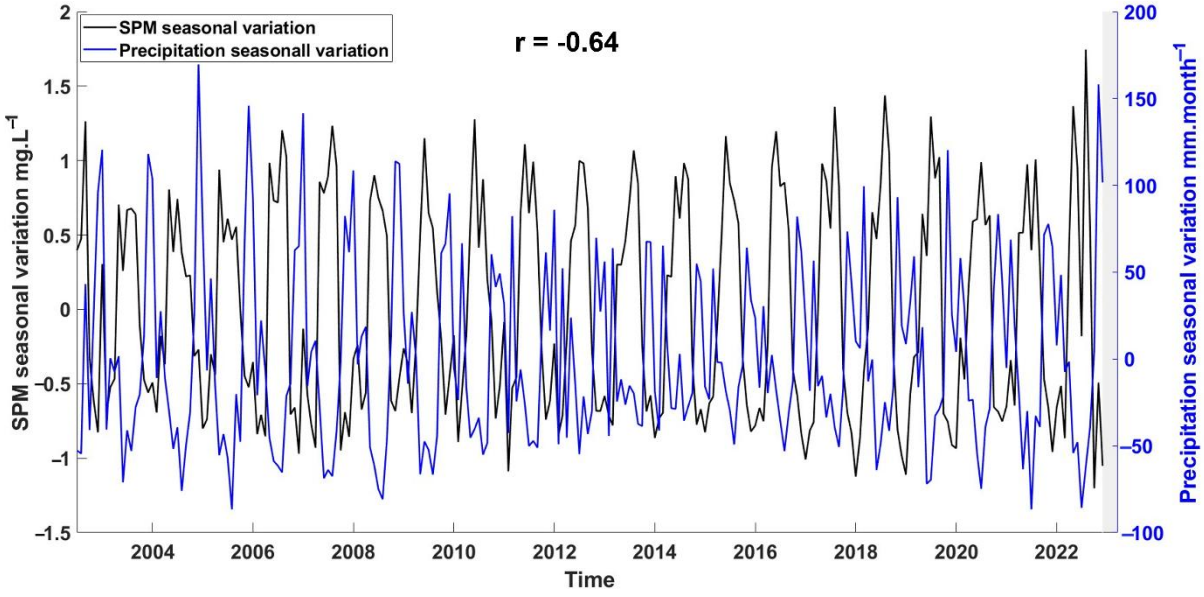

Figure A.4. Time series of Seasonal variation (X11 outputs) of SPM (black) extracted at Point A, located offshore (20 m depth) of Açu Port (Figure 5a), and precipitation (blue), averaged over Açu Port region.

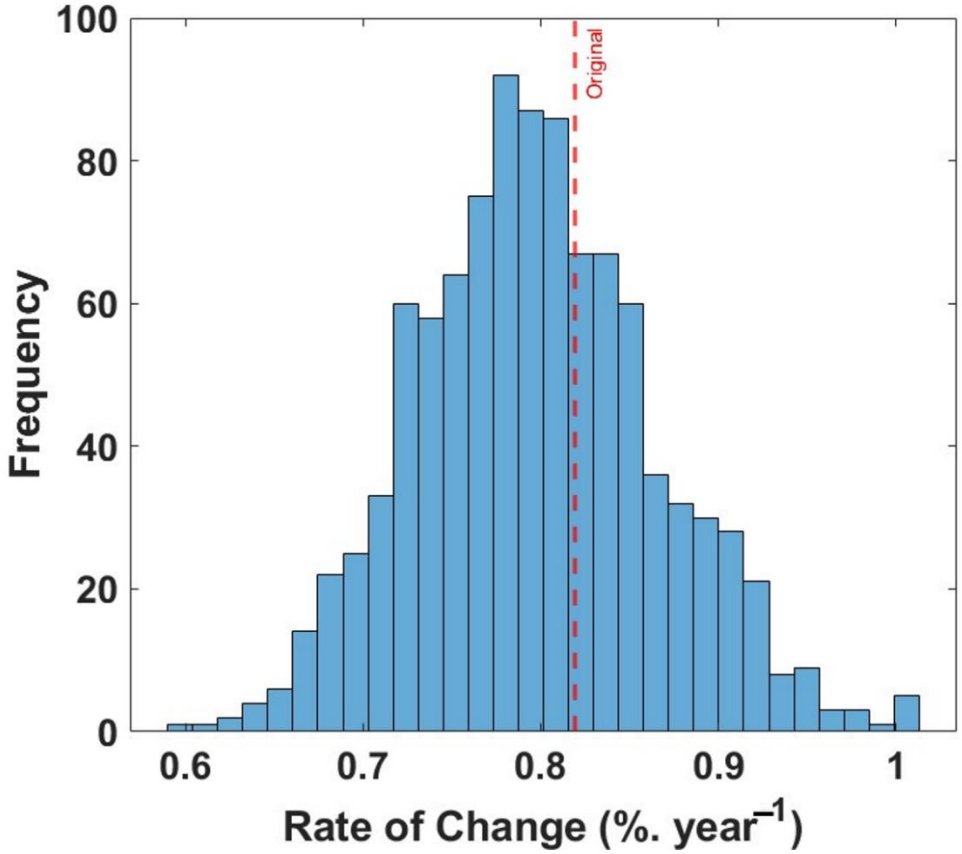

Figure A.5. Distribution of 1000 simulated SPM trends (%·year⁻¹) from the Monte Carlo uncertainty propagation analysis, showing how retrieval-error perturbations derived from in situ–MODIS (OC-SMART) matchups on the estimated Rate of Change (RC) near the APIC hotspot. The red vertical line indicates the original RC estimated from the unperturbed SPM time series.

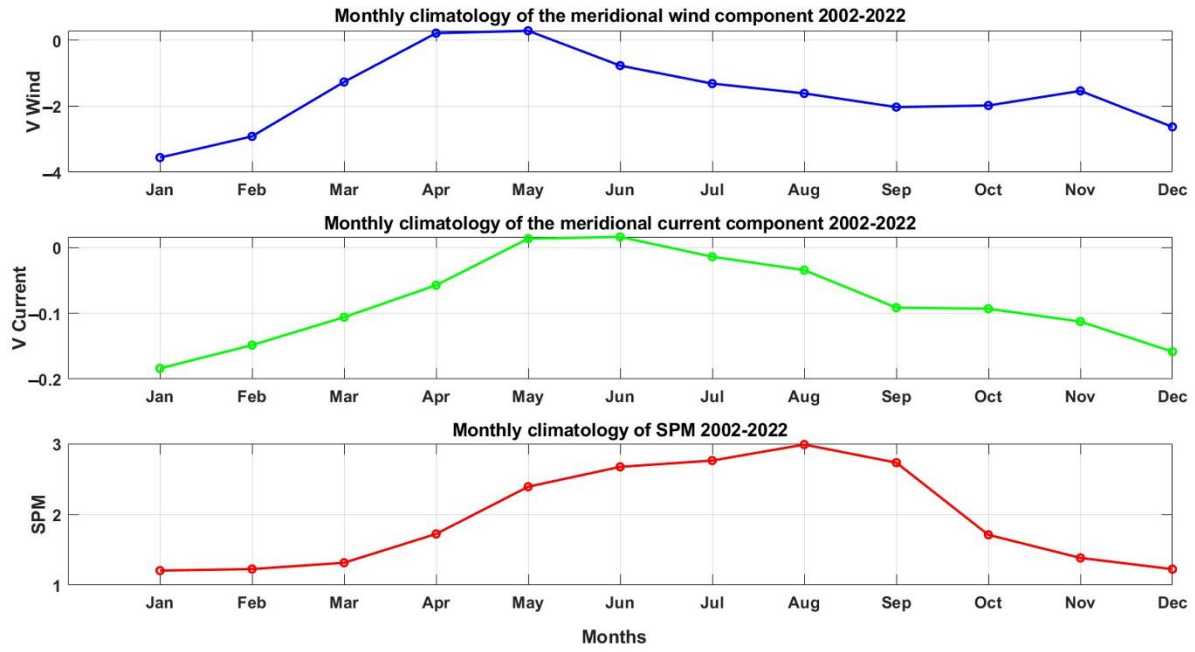

Figure A.6. Climatological monthly averages of (a) the meridional wind component (V-Wind), (b) the meridional current component (V-Current), and (c) SPM concentrations, illustrating the temporal lag between wind forcing and SPM variability.

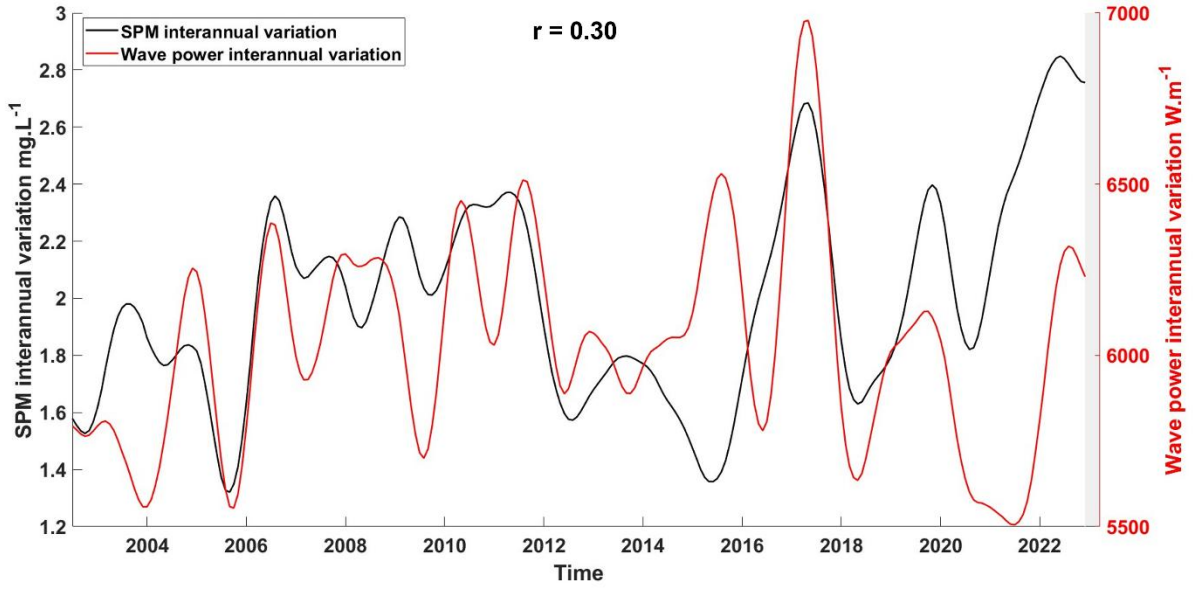

Figure A.7. Time series of Interannual variation (X11 outputs) of SPM (black), and power waves (red) extracted at Point A, located offshore (20 m depth) of Açu Port (Figure 5a).

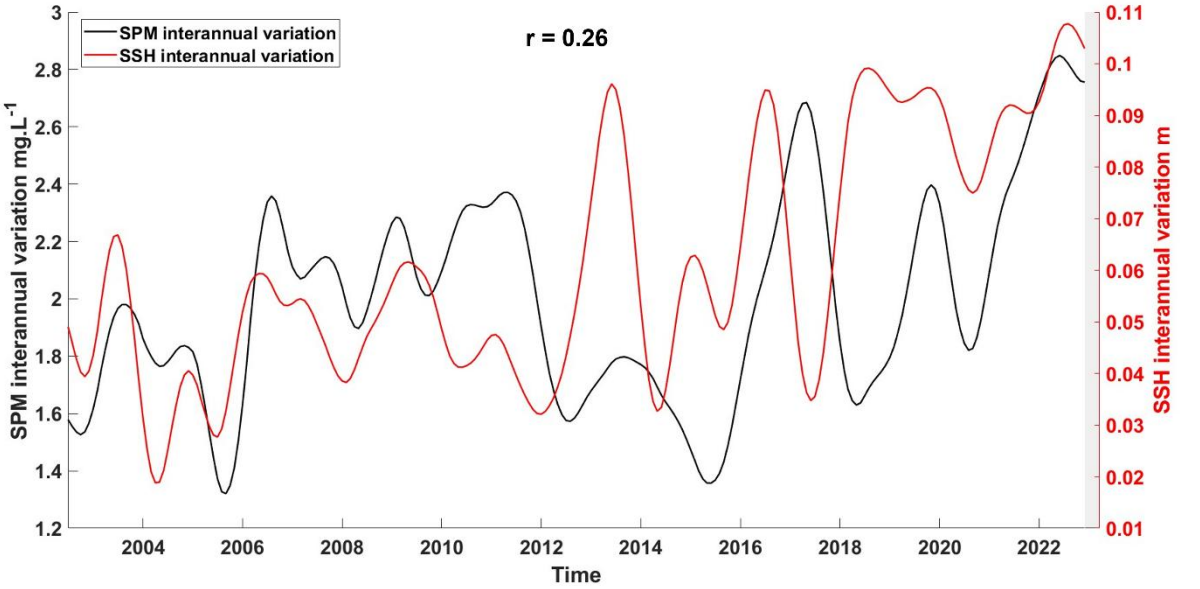

Figure A.8. Time series of Interannual variation (X11 outputs) of SPM (black), and SSH (red) extracted at Point A, located offshore (20 m depth) of Açu Port (Figure 5a).

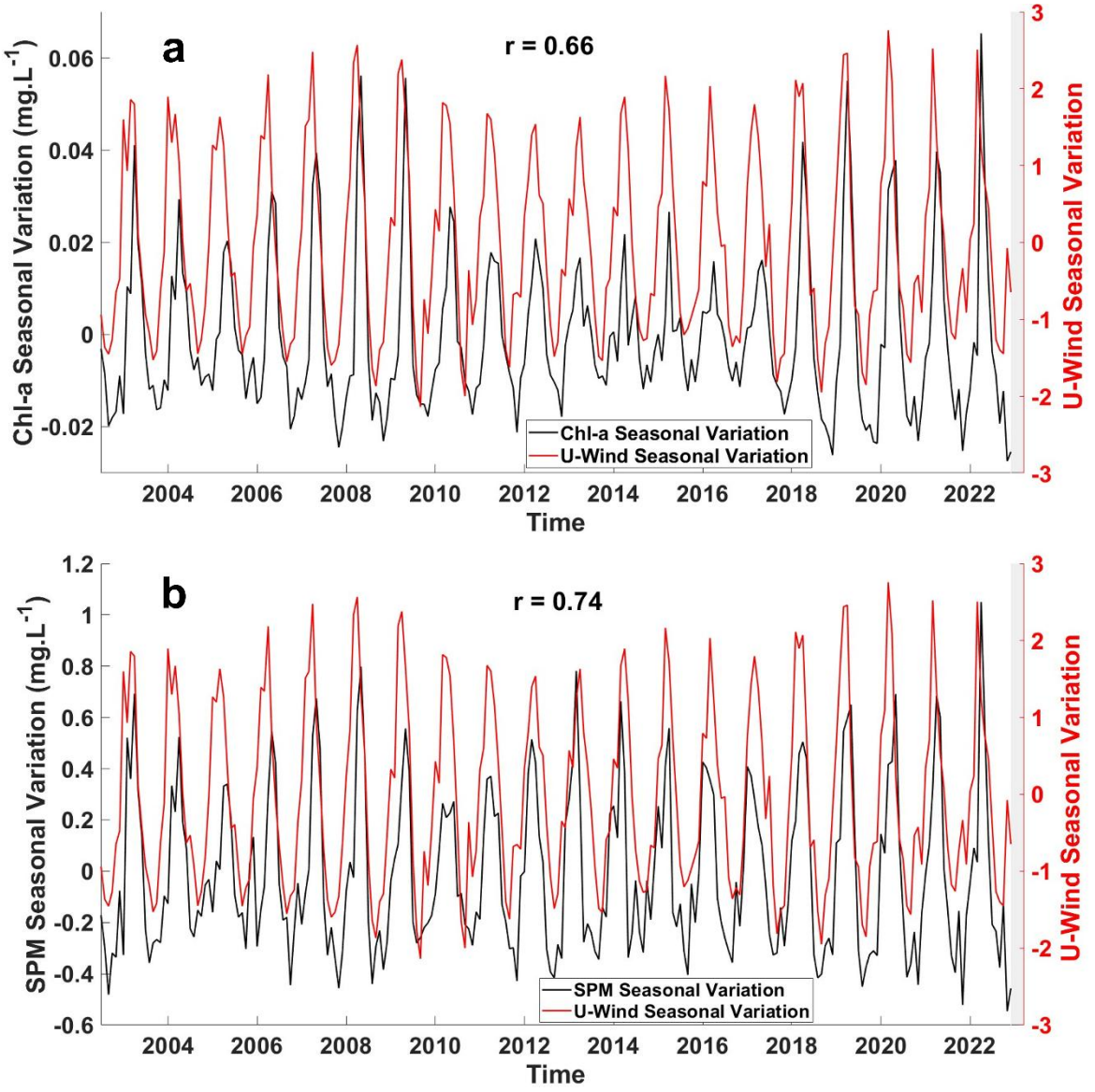

Figure A.9. Correlation between the seasonal variation (Census X-11 outputs) of U-wind and Chl-a and SPM over the western coast of Maranhão State: (a) time series of the seasonal variation of Chl-a (black) and seasonal variation of U-wind (red), (b) time series of the seasonal variation of SPM (black) and seasonal variation of U-wind (red), extracted at point A with the seasonal variation of river discharge (2002–2022).

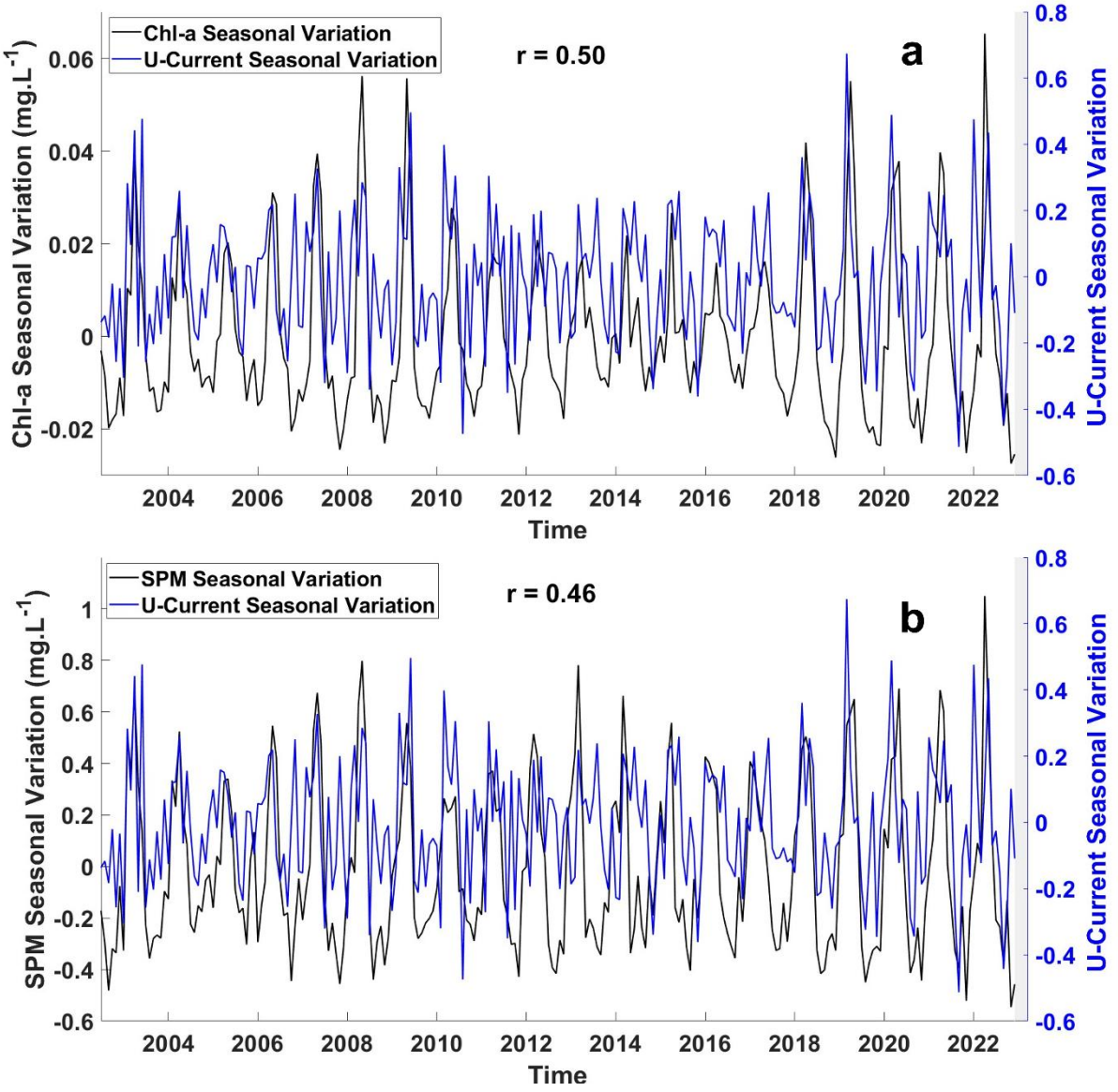

Figure A.10. Correlation between the seasonal variation (Census X-11 outputs) of U-Current and Chl-a and SPM over the western coast of Maranhão State: (a) time series of the seasonal variation of Chl-a (black) and seasonal variation of U- Current (blue), (b) time series of the seasonal variation of SPM (black) and seasonal variation of U- Current (blue), extracted at point A with the seasonal variation of river discharge (2002–2022).

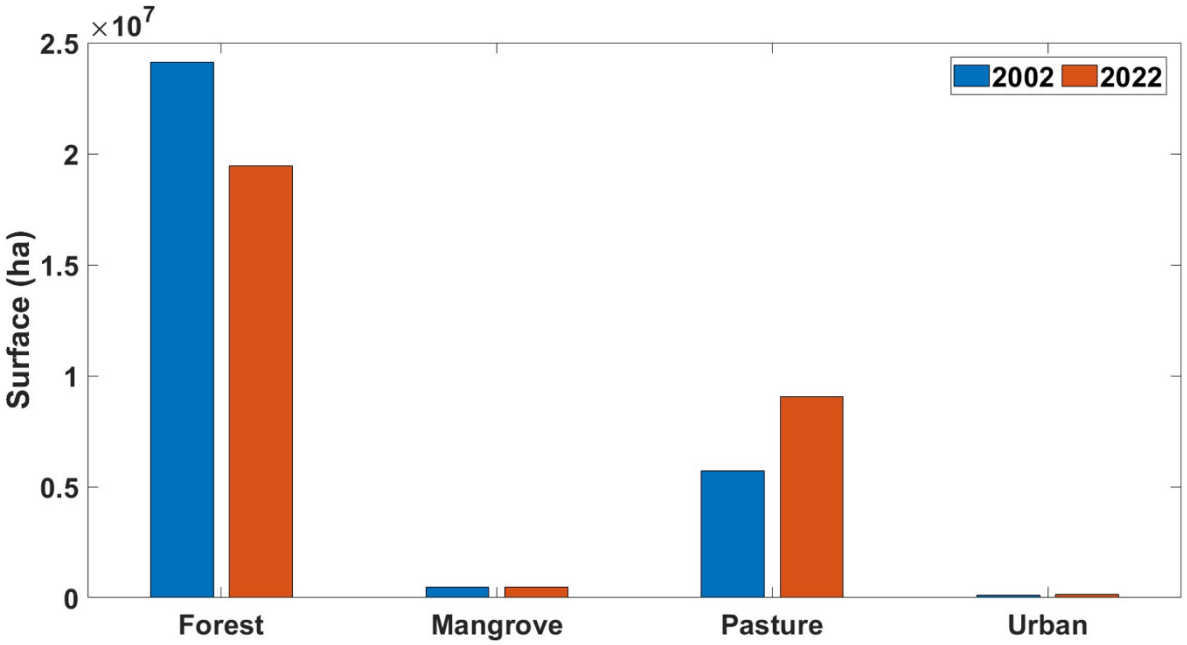

Figure A.11. Histograms of land use and land cover changes (Forest, Mangrove, Pasture and Urban surface in hectares) between 2002 and 2022.

Table A.1. Generalized Additive Model (GAM) results for interannual variability of Chl-a

Variable	F-Statistic	Contribution (%)
Pasture	**255.30**	**73.90**
River discharge	42.01	12.15
V-Current	33.08	9.60
V-Wind	9.50	2.75
U-Wind	5.59	1.60
U-Current	2.15	6.21×10^{-6}

Table A.2. Generalized Additive Model (GAM) results for interannual variability of SPM

Variable	F-Statistic	Contribution (%)
Pasture	**958.22**	**89.39**
V-Current	41.40	3.86
River discharge	27.77	2.59
U-Wind	24.54	2.29
U-Current	11.98	1.12
V-Wind	7.99	0.75

RÉSUMÉ SUBSTANTIEL EN FRANÇAIS

Introduction

Les zones côtières sont des interfaces dynamiques entre les continents et l'océan, jouant un rôle clé dans la régulation des flux de matière et d'énergie et soutenant une forte productivité biologique, malgré leur extension spatiale limitée (Longhurst et al., 1995; Gattuso et al., 1998; Bauer et al., 2013; Cloern et al., 2014).

Depuis plusieurs décennies, les systèmes côtiers sont profondément affectés par l'intensification des pressions anthropiques, notamment les changements d'usage des terres, l'urbanisation, la construction de barrages et le développement d'infrastructures industrielles. Ces perturbations accroissent les apports en sédiments, nutriments et matière organique vers l'océan et interagissent avec le changement climatique, via l'augmentation des températures et les modifications des régimes de précipitation et de débits fluviaux, compliquant l'attribution des changements observés (Beusen et al., 2005; Syvitski et al., 2005; Milliman et al., 2008; Doney et al., 2012; IPCC, 2022).

L'évaluation de la qualité des eaux côtières repose notamment sur l'analyse de la chlorophylle-a (Chl-a), des matières en suspension (SPM) et du carbone organique particulaire (POC), qui renseignent respectivement sur la biomasse phytoplanctonique, la turbidité et la dynamique particulaire, ainsi que le cycle du carbone côtier (Kineke et al., 1996; Kasprzak et al., 2008; Blair and Aller, 2012). Toutefois, le manque d'observations in situ continues limite fortement l'analyse des tendances à long terme dans de nombreuses régions côtières (Henson et al., 2016; Muller-Karger et al., 2018).

Dans ce contexte, la télédétection par couleur de l'océan constitue un outil essentiel en fournissant des observations synoptiques, cohérentes et de longue durée des propriétés biogéochimiques côtières (McClain, 2009; Siegel et al., 2013). Le capteur MODIS-Aqua offre la plus longue série temporelle continue actuellement disponible, bien que son application aux eaux côtières reste complexe en raison de leur forte hétérogénéité optique (IOCCG, 2000; Dierssen, 2010).

Le littoral brésilien représente un laboratoire naturel majeur, couvrant près de 8 000 km et soumis à de fortes pressions anthropiques, tout en restant insuffisamment documenté par des observations in situ de long terme (Castro and Miranda, 1998; Spalding et al., 2007; Brandini et al., 2018).

Cette thèse s'inscrit dans le cadre du projet COCOBRAZ, financé par la FAPESP et l'ANR, visant à analyser l'évolution à long terme de la qualité biogéochimique des eaux côtières

brésiliennes et à identifier les rôles respectifs des forçages naturels et anthropiques.

Dans ce contexte, cette thèse vise à répondre aux questions scientifiques suivantes :

1. Dans quelle mesure les observations de couleur de l'océan MODIS-Aqua, combinées à des corrections atmosphériques et des modèles bio-optiques adaptés, permettent-elles de représenter de manière fiable la dynamique de la Chl-a, des SPM et du POC dans les eaux côtières optiquement complexes du Brésil ?
2. Quels changements spatio-temporels et quels hotspots côtiers peuvent être identifiés dans les propriétés biogéochimiques des eaux côtières brésiliennes à partir des séries temporelles MODIS-Aqua à 1 km sur la période 2002–2022 ?
3. Quelle est l'importance relative des pressions anthropiques et des forçages climatiques dans les changements à long terme de la qualité des eaux côtières, à partir d'études de cas régionales le long du littoral brésilien ?

Pour y répondre, la thèse exploite plus de vingt ans de données MODIS-Aqua traitées avec la correction atmosphérique OC-SMART (Fan et al., 2021) et combinées à des algorithmes bio-optiques développés spécifiquement pour les eaux côtières, avec un accent particulier sur les approches fondées sur les Optical Water Types (Vantrepotte et al., 2012; Moore et al., 2014; Spyrakos et al., 2018). En combinant analyses à grande échelle et études de cas régionales ciblées, ce travail apporte de nouveaux éléments sur le fonctionnement biogéochimique des zones côtières brésiliennes et démontre le potentiel des séries satellitaires de long terme pour l'analyse des impacts anthropiques dans des environnements côtiers hautement dynamiques.

Chapitre 1 : Etat de l'art

1. Rôle et enjeux des zones côtières

Les zones côtières sont des environnements de transition majeurs où interagissent des processus terrestres, océaniques et atmosphériques, générant une forte variabilité physique et biogéochimique (Crossland et al., 2005; Ramesh et al., 2015). Malgré leur extension spatiale limitée, elles figurent parmi les écosystèmes les plus productifs de la planète et fournissent une part disproportionnée des services écosystémiques marins, tout en concentrant des usages humains intenses (Millennium Ecosystem Assessment, 2005; Luisetti et al., 2014). Cette combinaison de forte productivité, de pressions anthropiques et de sensibilité environnementale fait des zones côtières des régions prioritaires pour le suivi environnemental à long terme.

2. Le littoral brésilien : diversité physique et biogéochimique

Le littoral brésilien s'étend sur près de 8 000 km, depuis les régions équatoriales jusqu'aux latitudes subtropicales, couvrant une large gamme de contextes climatiques, hydrodynamiques

et biogéochimiques (Ab'Sáber, 2003; Bernardes et al., 2012). Cette extension latitudinale génère une forte hétérogénéité des environnements côtiers, allant des eaux très turbides et riches en matière organique sous l'influence des grands panaches fluviaux, notamment celui de l'Amazone, à des zones dominées par des masses d'eau océaniques plus claires et oligotrophes (Ekau and Knoppers, 1999; Ciotti et al., 2010; Brandini et al., 2018).

Les propriétés biogéochimiques des eaux côtières brésiliennes, telles que la chlorophylle-a, les matières en suspension et le carbone organique, présentent ainsi de forts gradients spatiaux et une variabilité temporelle marquée, résultant de l'interaction entre apports continentaux, circulation océanique, forçages climatiques et processus hydrodynamiques de méso-échelle.

3. Pressions anthropiques et limites des observations in situ

Les zones côtières brésiliennes concentrent une grande partie de la population et des activités économiques du pays. La déforestation, l'expansion agricole, l'urbanisation, la construction de barrages et le développement portuaire ont accru les flux de nutriments, de sédiments et de contaminants vers les milieux côtiers, avec des impacts documentés sur de nombreux écosystèmes (Bernardes et al., 2012; de Andrés et al., 2018; Cotovicz et al., 2021). Toutefois, l'évaluation de ces impacts à long terme reste limitée par la rareté et la discontinuité des réseaux d'observation in situ, qui ne permettent pas une couverture spatiale et temporelle suffisante à l'échelle nationale (Garcia et al., 2016; Brandini et al., 2018).

4. Apports de la télédétection par couleur de l'océan et rôle de MODIS

Dans ce contexte, la télédétection par couleur de l'océan constitue un outil central pour le suivi des environnements côtiers. Les observations satellitaires fournissent des mesures synoptiques, répétitives et cohérentes des propriétés optiques et biogéochimiques de surface, permettant d'analyser la variabilité saisonnière, interannuelle et les tendances à long terme (McClain, 2009; Blondeau-Patissier et al., 2014).

Parmi les capteurs disponibles, MODIS-Aqua occupe une place clé grâce à la longueur et à la continuité de sa série temporelle, offrant plus de deux décennies d'observations à résolution kilométrique adaptées aux analyses de variabilité et de tendance à grande échelle. Cependant, l'exploitation de MODIS en zone côtière reste complexe en raison de la forte hétérogénéité optique des eaux, où les contributions relatives du phytoplancton, des particules minérales et de la matière organique dissoute varient fortement dans l'espace et le temps (IOCCG, 2000).

5. Complexité optique, séries temporelles et besoins méthodologiques

La forte complexité optique des eaux côtières brésiliennes limite l'applicabilité directe des algorithmes globaux développés pour l'océan ouvert et introduit des incertitudes dans l'analyse des tendances à long terme (IOCCG, 2000; Mélin, 2016). Les approches fondées sur les types

optiques de masses d'eau offrent un cadre pertinent pour mieux représenter cette diversité et améliorer la robustesse des produits satellitaires en milieu côtier (Mélin and Vantrepotte, 2015; Spyrakos et al., 2018).

L'analyse des séries temporelles de couleur de l'océan repose par ailleurs sur des méthodes robustes permettant de séparer la variabilité saisonnière, interannuelle et les changements de long terme, tout en tenant compte de la forte variabilité naturelle et des discontinuités d'observation propres aux zones côtières (Vantrepotte and Mélin, 2011; Mélin et al., 2017).

6. Analyse des séries temporelles issues de la couleur de l'océan

L'analyse des séries temporelles de couleur de l'océan est essentielle pour étudier la variabilité et les changements à long terme des écosystèmes côtiers à partir des observations satellitaires. Les séries de variables biogéochimiques, telles que la chlorophylle-a ou les matières en suspension, permettent de caractériser la variabilité saisonnière, interannuelle et les tendances de long terme (Henson et al., 2010; Vantrepotte and Mélin, 2011). En zone côtière, leur interprétation est rendue complexe par une forte variabilité naturelle, des événements extrêmes, des discontinuités d'observation et des incertitudes liées aux algorithmes, ce qui nécessite des approches robustes adaptées aux données satellitaires (Mélin, 2016). Les méthodes de décomposition temporelle et les tests de tendance non paramétriques se sont ainsi imposés pour distinguer les signaux de changement des fluctuations naturelles (Vantrepotte and Mélin, 2011; Wang et al., 2020). Ce cadre analytique constitue le fondement méthodologique des analyses développées dans ce travail pour relier les évolutions observées aux forçages climatiques et aux pressions anthropiques.

7. Lacunes et perspectives

Dans l'ensemble, le State of the Art met en évidence un déficit d'évaluations satellitaires cohérentes, adaptées à la complexité optique des eaux côtières brésiliennes et couvrant des échelles spatiales et temporelles suffisantes. Le développement d'approches intégrées, combinant données MODIS de long terme, algorithmes adaptés aux eaux côtières et analyse multi-échelle des séries temporelles, apparaît essentiel pour améliorer la compréhension des dynamiques biogéochimiques côtières et soutenir les stratégies de gestion et de conservation à long terme.

Chapitre 2 : Développement de la base de données COCOBRAZ et la dynamique spatio-temporelle générale des eaux côtières brésiliennes (2002-2022)

1. Contexte et objectifs du chapitre

Ce chapitre s'inscrit dans le cadre du projet franco-brésilien COCOBRAZ, dont l'un des objectifs majeurs est de développer un cadre observationnel cohérent, homogène et accessible

pour l'étude des eaux côtières brésiliennes. Le littoral brésilien, long de près de 8 000 km, présente une diversité exceptionnelle de contextes hydrodynamiques, biogéochimiques et anthropiques, mais demeure insuffisamment documenté par des observations in situ continues et spatialement représentatives. Cette lacune limite la capacité à analyser la variabilité spatio-temporelle et les changements à long terme de la qualité des eaux côtières à l'échelle nationale. L'objectif principal de ce chapitre est donc double. D'une part, il vise à présenter le développement de la base de données COCOBRAZ, reposant sur l'intégration de données in situ hétérogènes et de plus de vingt ans d'observations satellitaires MODIS-Aqua traitées de manière cohérente. D'autre part, il fournit une première analyse à l'échelle nationale de la variabilité spatio-temporelle et de l'évolution à long terme de variables biogéochimiques clés, à savoir la chlorophylle-a (Chl-a), les matières en suspension (SPM) et le carbone organique particulaire (POC), en mettant en évidence les principaux hotspots de changement le long du littoral brésilien.

2. Constitution de la base de données in situ COCOBRAZ

La base de données in situ COCOBRAZ compile des observations issues de nombreuses campagnes océanographiques menées entre 2000 et 2023, couvrant l'ensemble du littoral brésilien. Elle regroupe 3 646 stations d'échantillonnage réparties dans des environnements contrastés, incluant estuaires, panaches fluviaux, zones côtières internes, plateaux continentaux et eaux océaniques adjacentes.

Les variables biogéochimiques compilées comprennent principalement la chlorophylle-a, les matières en suspension, le carbone organique particulaire et dissous, ainsi que la turbidité. La base met en évidence une variabilité extrême des conditions côtières brésiliennes, avec des concentrations de Chl-a allant d'eaux oligotrophes offshore à des systèmes hyper-productifs et très turbides, et des valeurs de SPM atteignant des niveaux exceptionnellement élevés dans les régions sous forte influence fluviale.

Bien que cette base in situ reste spatialement et temporellement hétérogène, elle constitue la compilation la plus complète à ce jour pour les eaux côtières brésiliennes. Dans le cadre de cette thèse, elle est utilisée comme support contextuel et comme élément de cohérence avec les cadres observationnels existants, tandis que l'analyse principale repose sur les séries satellitaires de long terme.

3. Développement de la base satellitaire MODIS-Aqua (2002–2022)

Le cœur du cadre observationnel COCOBRAZ repose sur le traitement systématique de l'ensemble des données MODIS-Aqua à 1 km de résolution couvrant la période 2002–2022. Environ 7 400 images journalières ont été traitées selon une chaîne homogène, garantissant la

cohérence spatiale et temporelle nécessaire aux analyses de long terme.

Les données brutes MODIS ont été traitées en utilisant la méthode de correction atmosphérique OC-SMART, spécifiquement conçue pour les environnements optiquement complexes (Fan et al., 2021). Cette correction permet d'obtenir des réflectances de surface fiables sur un large spectre de conditions côtières. Un traitement complémentaire NIR-SWIR a été appliqué dans les zones extrêmement turbides, telles que le panache de l'Amazone et la lagune de Patos, afin de pallier les limitations liées à la saturation des bandes rouges et proche infrarouge de MODIS.

Les réflectances ont ensuite été mosaïquées, reprojetées sur une grille régulière à 1 km, et agrégées mensuellement à l'aide d'une moyenne géométrique, afin de réduire l'influence des valeurs extrêmes et des lacunes d'échantillonnage. Ce jeu de données constitue une archive satellitaire continue et cohérente de deux décennies, unique pour l'étude des eaux côtières brésiliennes.

4. Production des variables biogéochimiques à partir de MODIS

À partir de la base MODIS traitée, plusieurs modèles bio-optiques ont été appliqués afin de générer des séries temporelles cohérentes de Chl-a, SPM, POC, DOC et absorption par la matière organique dissoute colorée.

La chlorophylle-a a été estimée à l'aide du modèle CONNECT, basé sur des réseaux de neurones adaptés aux eaux côtières et intégrant explicitement la diversité optique via les types optiques de masses d'eau (OWTs). Cette approche permet d'éviter les limitations des algorithmes globaux de type OCx, particulièrement sujettes à saturation et biais en milieux côtiers turbides.

Les concentrations de SPM et de POC ont été estimées à l'aide de nouveaux algorithmes développés dans le cadre de cette thèse, reposant sur une combinaison pondérée de modèles existants en fonction des OWTs. Cette stratégie permet d'assurer des performances robustes sur l'ensemble du continuum optique, depuis les eaux claires jusqu'aux environnements très turbides.

Les validations réalisées à partir de jeux de données in situ indépendants démontrent la robustesse de ces algorithmes, tant pour les estimations directes que pour les matchups satellite-in situ, confirmant leur applicabilité à l'analyse des séries temporelles de long terme.

5. Analyse des séries temporelles et détection des tendances

Les séries temporelles mensuelles de Chl-a, SPM et POC ont été analysées à l'aide d'un cadre méthodologique robuste combinant décomposition temporelle et tests de tendance. La méthode Census X-11 a été utilisée pour séparer les composantes saisonnières, interannuelles

et résiduelles, tandis que le test de Mann-Kendall saisonnier a permis de détecter des tendances monotones significatives sur la période 2002–2022. Lorsque des tendances significatives étaient détectées, leur amplitude a été estimée à l'aide de la pente de Sen.

Ce cadre analytique permet d'identifier des patterns cohérents à l'échelle nationale tout en tenant compte de la forte variabilité naturelle et de la saisonnalité marquée des systèmes côtiers brésiliens.

6. Représentation des écosystèmes côtiers et capacité de MODIS

L'analyse met en évidence la capacité de MODIS-Aqua à 1 km de résolution à représenter une large diversité de systèmes côtiers brésiliens, incluant plus de 40 estuaires et panaches fluviaux, 17 baies et 17 lagunes côtières. Bien que certaines structures internes fines ne soient pas résolues, MODIS permet de capturer de manière cohérente l'expression côtière des apports continentaux et des gradients biogéochimiques majeurs.

La comparaison avec des produits multi-capteurs (GlobColour, OC-CCI) montre que, bien que ces produits reproduisent les grandes structures spatiales, ils présentent des limitations importantes en milieux côtiers, notamment une perte de sensibilité, une forte hétérogénéité spatiale ou une saturation des algorithmes de chlorophylle-a. Les produits MODIS traités avec OC-SMART et CONNECT offrent une représentation plus cohérente et physiquement interprétable des gradients côtiers et des tendances à long terme.

7. Hotspots biogéochimiques et variabilité à long terme

L'analyse conjointe des tendances de Chl-a, SPM et POC met en évidence de nombreux hotspots le long du littoral brésilien, caractérisés par des évolutions significatives sur la période 2002-2022. Ces hotspots concernent des baies, des estuaires, des lagunes et des zones sous forte influence fluviale.

Les résultats révèlent des comportements contrastés selon les types de systèmes : augmentation généralisée des SPM dans de nombreuses baies, diminution du POC dans plusieurs estuaires, ou encore tendances opposées entre secteurs d'un même système lagunaire. Ces patterns reflètent l'interaction complexe entre forçages naturels et pressions anthropiques (Figure).

8. Exemples de pressions anthropiques et perspectives

Enfin, le chapitre illustre comment l'approche développée permet d'identifier et d'interpréter l'impact de pressions anthropiques majeures, telles que la déforestation liée à l'expansion des pâturages au Maranhão, la régulation fluviale par les barrages du São Francisco, ou encore l'industrialisation associée au port d'Açu. Ces exemples démontrent la capacité des séries satellitaires à détecter des signaux cohérents et à orienter des études régionales ciblées.

Ces hotspots constituent la base des analyses approfondies développées dans les chapitres suivants, consacrés à l'impact de l'industrialisation portuaire et des changements d'usage des terres sur la biogéochimie côtière.

Chapitre 3 : Impact de l'industrialisation sur la dynamique des matières en suspension : étude de cas du port d'Açu (2002-2022)

1. Contexte et objectifs

Ce chapitre analyse l'impact de l'industrialisation portuaire sur la dynamique des matières en suspension (SPM) le long de la côte nord de l'État de Rio de Janeiro, en se concentrant sur le complexe industrialo-portuaire d'Açu (APIC). Le port d'Açu constitue aujourd'hui le plus grand complexe portuaire privé d'Amérique latine et a connu une expansion rapide depuis le début de sa construction à partir de 2006-2007. Les activités associées, notamment le dragage, l'approfondissement des chenaux, la construction d'infrastructures offshore et la gestion des sédiments, sont susceptibles de modifier durablement les régimes sédimentaires côtiers.

L'objectif principal de ce chapitre est d'évaluer l'évolution spatio-temporelle des concentrations de SPM sur la période 2002-2022 à partir des observations MODIS-Aqua, et de distinguer l'influence relative des activités anthropiques liées au port et des forçages naturels (vents, courants, houle, précipitations). L'enjeu est d'identifier un signal anthropique robuste dans un environnement côtier fortement dynamique.

2. Données satellitaires et approche méthodologique

L'analyse repose sur l'exploitation de vingt ans de données MODIS-Aqua (2002-2022) à 1 km de résolution spatiale, traitées de manière homogène à l'aide de la correction atmosphérique OC-SMART, spécifiquement adaptée aux eaux côtières optiquement complexes. Afin d'estimer les concentrations de SPM, une approche originale fondée sur les Optical Water Types (OWTs) a été développée.

Cette méthode combine deux algorithmes bio-optiques optimisés en fonction des classes optiques dominantes : un algorithme adapté aux eaux claires à modérément turbides (OWTs 1-3) et un algorithme basé sur les bandes proche infrarouge pour les eaux fortement turbides (OWTs 4-5). Les deux modèles sont fusionnés à l'aide d'une pondération probabiliste, garantissant une transition continue entre conditions optiques contrastées. La robustesse de cette approche est validée à partir de la base de données in situ GLORIA et de jeux de données de matchup satellite in situ.

Les séries temporelles mensuelles de SPM sont analysées à l'aide d'un cadre statistique combinant la décomposition Census X-11 et le test saisonnier de Mann-Kendall, permettant de séparer la variabilité saisonnière, interannuelle et les tendances de long terme.

L'interprétation des évolutions observées est complétée par l'analyse de données auxiliaires incluant les vents de surface, les courants océaniques, l'état de la houle, les précipitations et les données d'occupation des sols, afin d'évaluer le rôle respectif des forçages naturels et des activités anthropiques dans la variabilité de la SPM.

3. Variabilité saisonnière des matières en suspension

Les cartes moyennes saisonnières issues de MODIS montrent une forte structuration saisonnière des concentrations de SPM. Les niveaux les plus élevés sont observés durant l'hiver austral, avec une extension offshore plus marquée que durant l'été. Les concentrations maximales restent systématiquement confinées aux zones côtières et de plateau interne, traduisant le rôle majeur des processus de resuspension et de transport côtier.

L'analyse des composantes saisonnières révèle une forte corrélation entre la variabilité saisonnière de la SPM et la composante méridienne des courants de surface, indiquant un transport préférentiellement orienté vers le nord. Les vents et la houle jouent un rôle complémentaire : la houle contribue à la remise en suspension des sédiments, tandis que les vents modulent indirectement la circulation côtière. En revanche, l'influence des apports fluviaux est limitée, en cohérence avec la régulation du débit du fleuve Paraíba do Sul.

4. Évolution interannuelle et tendances à long terme

L'analyse des tendances sur la période 2002-2022 met en évidence une augmentation marquée et spatialement cohérente des concentrations de SPM à proximité immédiate du port d'Açu. Les augmentations atteignent localement 20 à 60 % sur deux décennies, avec un taux moyen d'augmentation d'environ 0,8 % par an dans la zone la plus impactée. Ces tendances sont statistiquement significatives et persistent après prise en compte des incertitudes associées aux restitutions satellitaires, comme démontré par une analyse de propagation d'erreur de type Monte Carlo.

À l'inverse, aucune augmentation comparable n'est observée à l'embouchure du fleuve Paraíba do Sul, où une légère diminution des concentrations de SPM est même détectée, confirmant que la source principale de l'augmentation observée près de l'APIC n'est pas fluviale.

5. Extension spatiale du signal anthropique

Les analyses de corrélation spatiale montrent que la variabilité interannuelle de la SPM observée au voisinage immédiat du port est fortement corrélée à celle mesurée dans les zones côtières situées au nord de l'APIC. Cette continuité spatiale suggère une propagation du signal sédimentaire sous l'effet des courants côtiers dominants, confirmant que l'influence du port dépasse son emprise locale.

Bien que les tendances au nord du port soient plus faibles et parfois non significatives, leur cohérence spatiale indique que les activités portuaires modifient le régime sédimentaire régional par redistribution le long du littoral.

6. Rôle de l'industrialisation et des forçages naturels

L'évolution temporelle de la SPM est étroitement liée aux différentes phases de développement du port d'Açu. Trois grandes périodes sont identifiées : une phase pré-port caractérisée par des niveaux faibles et stables, une phase de construction marquée par une forte variabilité et une augmentation rapide de la SPM associée aux opérations de dragage, puis une phase opérationnelle durant laquelle les concentrations restent élevées et augmentent à nouveau lors de l'intensification des activités et des opérations de maintenance.

Les données d'occupation des sols issues de MapBiomas montrent une transformation profonde du territoire, avec une conversion massive de milieux naturels en surfaces industrialisées, confirmant l'ampleur de la perturbation anthropique. Les analyses croisées avec les vents, courants et vagues montrent que ces forçages naturels modulent la dispersion et la redistribution des sédiments, mais qu'ils ne présentent pas de tendance de fond susceptible d'expliquer l'augmentation observée de la SPM. L'industrialisation apparaît ainsi comme le facteur dominant du changement à long terme.

7. Conclusions et implications

Ce chapitre démontre pour la première fois, à partir d'une série satellitaire de vingt ans, l'existence d'un signal anthropique robuste lié au développement du port d'Açu sur la dynamique des matières en suspension côtières. Les résultats montrent que les activités industrielles augmentent durablement la disponibilité sédimentaire, tandis que les processus hydrodynamiques naturels contrôlent la dispersion spatiale de ce signal.

L'approche méthodologique développée, combinant correction atmosphérique avancée, algorithmes adaptés aux eaux côtières et analyse robuste des séries temporelles, met en évidence le potentiel des observations de couleur de l'océan pour détecter et quantifier les impacts humains dans des environnements côtiers complexes. Ces résultats constituent une base essentielle pour les chapitres suivants, dédiés à l'analyse d'autres pressions anthropiques le long du littoral brésilien.

Chapitre 4 : Impact de la déforestation et de l'expansion des pâturages sur la dynamique biogéochimique des eaux côtières du Maranhão (2002–2022)

1. Contexte et objectifs

Ce chapitre examine l'impact des changements d'usage et de couverture des sols, en particulier la déforestation et l'expansion des pâturages dans l'arrière-pays amazonien du

Maranhão, sur la variabilité et l'évolution à long terme des matières en suspension (SPM) et de la chlorophylle-a (Chl-a) dans les eaux côtières adjacentes. Le Maranhão constitue une région clé de l'Amazonian Equatorial Coast, caractérisée par une hydrodynamique macrotidale, une forte influence fluviale et une mosaïque d'écosystèmes côtiers, mais également par une pression anthropique croissante liée à l'élevage extensif et à la conversion des forêts.

L'objectif principal est d'identifier et de quantifier, à partir de séries satellitaires de long terme, la contribution relative des forçages naturels (précipitations, débits fluviaux, vents, courants) et des pressions anthropiques liées aux changements d'occupation des sols sur l'évolution de la qualité biogéochimique des eaux côtières entre 2002 et 2022.

2. Données satellitaires et cadre méthodologique

L'analyse repose sur vingt années de données MODIS-Aqua (2002-2022) à 1 km de résolution, traitées de manière homogène à l'aide de la correction atmosphérique OC-SMART, particulièrement adaptée aux eaux côtières turbides et optiquement complexes. Les concentrations de Chl-a et de SPM sont estimées à l'aide de modèles bio-optiques basés sur les Optical Water Types (OWTs), permettant d'adapter les algorithmes aux conditions optiques contrastées rencontrées le long de la côte du Maranhão.

Les séries temporelles mensuelles de Chl-a et de SPM sont analysées à l'aide d'un cadre statistique combinant la décomposition Census X-11 et le test saisonnier de Mann-Kendall, afin de séparer les composantes saisonnières, interannuelles et les tendances de long terme. L'interprétation des résultats est complétée par l'analyse de données auxiliaires incluant les débits fluviaux, les précipitations, les vents de surface, les courants océaniques et les données d'occupation des sols issues de MapBiomas. Enfin, des modèles additifs généralisés (GAMs) sont utilisés pour quantifier la contribution relative de ces différents facteurs à la variabilité interannuelle de Chl-a et de SPM.

3. Distribution spatiale et variabilité saisonnière de Chl-a et SPM

Les distributions climatologiques montrent des concentrations élevées de Chl-a et de SPM le long de la côte et de l'inner shelf, avec un contraste marqué entre la saison des pluies (décembre-mai) et la saison sèche (juin-novembre). Les maximas saisonniers sont observés durant la saison humide, en cohérence avec l'augmentation des apports fluviaux et du ruissellement continental.

Les coefficients de variation indiquent une forte variabilité saisonnière dans les zones côtières et estuariennes, tandis que la variabilité diminue vers le large. La circulation de surface, dominée par un flux côtier vers le nord-ouest associé au Courant Nord-Brésilien, favorise la rétention et le transport le long de la côte des eaux chargées en particules et nutriments.

4. Structure de la variabilité temporelle

La décomposition Census X-11 révèle que la composante saisonnière domine la variabilité totale de Chl-a et de SPM sur l'ensemble de la zone côtière. La composante interannuelle représente une fraction plus faible mais spatialement structurée de la variance, particulièrement marquée pour la SPM dans les zones sous forte influence fluviale. La composante irrégulière reste secondaire et associée à des événements ponctuels.

Ces résultats montrent que, bien que les cycles hydrologiques saisonniers contrôlent largement la dynamique biogéochimique, des signaux interannuels persistants émergent à l'échelle de deux décennies.

5. Tendances à long terme et évolution conjointe de Chl-a et SPM

L'analyse des tendances met en évidence une augmentation significative de Chl-a (~30 %) et de SPM (~50 %) entre 2002 et 2022 dans les eaux côtières peu profondes (< 50 m). Ces tendances sont spatialement cohérentes et statistiquement robustes. Les séries interannuelles normalisées montrent une forte variabilité d'une année à l'autre, mais une trajectoire globale ascendante sur l'ensemble de la période.

L'évolution différenciée de Chl-a et de SPM conduit à une diminution significative du ratio Chl-a:SPM sur l'inner shelf, indiquant que l'augmentation de la turbidité a été plus rapide que celle de la biomasse phytoplanctonique. Ce résultat suggère un renforcement progressif de la limitation lumineuse dans les eaux côtières.

6. Rôle des changements d'usage des sols et des forçages naturels

Les données MapBiomas montrent une conversion massive des forêts en pâturages dans les bassins versants drainant vers la côte du Maranhão entre 2002 et 2022. Les cartes de corrélation spatiale et les séries temporelles indiquent une relation positive et significative entre l'expansion des pâturages et les variations interannuelles de Chl-a et surtout de SPM.

Les modèles GAM confirment que l'expansion des pâturages est le facteur dominant expliquant la variabilité interannuelle, représentant la majeure partie de la variance expliquée pour Chl-a et SPM. Les débits fluviaux et la circulation océanique jouent un rôle secondaire, modulant la variabilité interannuelle sans présenter de tendance de fond sur la période étudiée. Lorsque l'effet des pâturages est retiré, le débit fluvial apparaît comme le principal contrôle naturel résiduel.

7. Implications et conclusions

Ce chapitre démontre que les changements d'usage des sols dans l'arrière-pays amazonien du Maranhão exercent un contrôle majeur sur l'évolution à long terme de la biogéochimie côtière. L'augmentation conjointe de Chl-a et de SPM, combinée à la baisse du ratio Chl-

a:SPM, indique un système de plus en plus dominé par les apports terrigènes et la turbidité, avec des conséquences potentielles sur la production primaire, le cycle du carbone et les écosystèmes côtiers.

L'approche intégrée combinant observations satellitaires MODIS-Aqua, données auxiliaires et modélisation statistique fournit un cadre robuste pour attribuer les changements observés aux pressions anthropiques. Ces résultats soulignent la vulnérabilité des côtes amazoniennes aux perturbations terrestres et constituent une base essentielle pour les stratégies de gestion intégrée terre-mer et pour les perspectives développées dans la conclusion générale de la thèse.

Conclusion and perspectives :

Cette thèse a analysé la variabilité spatio-temporelle et l'évolution à long terme de la biogéochimie côtière le long de la marge brésilienne à partir de plus de vingt ans d'observations satellitaires MODIS-Aqua (2002-2022). En combinant une correction atmosphérique adaptée (OC-SMART), des approches bio-optiques fondées sur les types optiques de masses d'eau (OWTs) et des méthodes statistiques robustes, ce travail fournit une évaluation cohérente et homogène de la dynamique de la qualité des eaux côtières dans des environnements optiquement complexes.

Les résultats montrent que le suivi fiable de la chlorophylle-a, des matières en suspension et du carbone organique particulaire nécessite des produits satellitaires adaptés et des stratégies de modélisation flexibles. Les algorithmes développés au cours de cette thèse, basés sur les OWTs, permettent des restitutions robustes sur l'ensemble du continuum terre–mer et confirment la pertinence de MODIS-Aqua pour l'analyse des tendances à long terme en zone côtière.

À l'échelle nationale, l'analyse des séries temporelles met en évidence une forte hétérogénéité spatiale des trajectoires biogéochimiques, avec l'identification de hotspots côtiers contrastés. Si la variabilité saisonnière et interannuelle est largement contrôlée par les forçages climatiques, les études de cas régionales démontrent que les pressions anthropiques dominent les évolutions de long terme dans certains contextes. Le développement du port d'Açu entraîne une augmentation localisée et durable des matières en suspension, tandis que la déforestation et l'expansion des pâturages dans le Maranhão sont associées à une augmentation progressive de la turbidité et de la biomasse phytoplanctonique côtière.

Ces résultats soulignent le potentiel des observations satellitaires de long terme pour détecter, quantifier et attribuer les impacts anthropiques sur les systèmes côtiers. Les principales perspectives concernent la continuité des séries satellitaires au-delà de MODIS-Aqua,

l’intégration de données à plus haute résolution spatiale, le couplage avec des modèles hydrologiques et hydrodynamiques, et le développement d’analyses biogéochimiques multivariables pour mieux quantifier les flux et les stocks de matière et de carbone dans les zones côtières.

Characterization of the biogeochemical dynamics of Brazilian coastal waters through the analysis of ocean color satellite archives

ABSTRACT

Coastal zones are highly dynamic environments where natural processes and human activities interact across multiple spatial and temporal scales. Despite their ecological and socio-economic importance, long-term assessments of coastal biogeochemical variability remain limited in many regions, particularly in optically complex coastal waters. This PhD thesis investigates the spatiotemporal variability and long-term evolution of coastal biogeochemical properties along the Brazilian margin using satellite ocean color observations.

The analysis is based on more than two decades (2002-2022) of MODIS-Aqua ocean color data at 1 km resolution, processed using the OC-SMART atmospheric correction method. To account for the strong optical heterogeneity of Brazilian coastal waters, bio-optical retrievals of chlorophyll-a (Chl-a), suspended particulate matter (SPM), and particulate organic carbon (POC) rely on approaches based on Optical Water Types (OWTs), including dedicated OWT-based algorithms developed during this thesis for SPM and POC. Long-term variability and trends are analyzed using robust statistical frameworks combining Census X-11 seasonal decomposition, seasonal Mann-Kendall trend tests and generalized additive models (GAMs).

At the national scale, the results reveal strong spatial heterogeneity in coastal biogeochemical trajectories, with pronounced seasonal and interannual variability driven primarily by hydroclimatic forcing and riverine inputs. Long-term trend analyses identify contrasted coastal hotspots of change, highlighting regions characterized by stability, variability, or sustained biogeochemical modification over the last two decades. Comparisons with multi-sensor ocean color products demonstrate that MODIS-Aqua, when processed with adapted methodologies, provides more consistent and robust representations of coastal waters in highly turbid environments.

Two regional case studies further investigate the relative roles of anthropogenic pressures and natural forcing. In southeastern Brazil, the development of the Açu Port Industrial Complex is associated with a strong and spatially localized long-term increase in SPM, consistent with dredging and port expansion activities. Along the Amazonian Equatorial Coast of Maranhão, long-term increases in SPM and Chl-a are closely linked to land-use changes, particularly

deforestation and pasture expansion within contributing river basins, indicating a dominant anthropogenic control on coastal biogeochemical evolution.

Overall, this thesis demonstrates the relevance of an integrated framework combining long-term satellite observations, OWT-based bio-optical modeling, and robust time-series analysis for monitoring and attributing coastal biogeochemical changes in optically complex environments. The results provide new insights into the functioning of Brazilian coastal waters and highlight the potential of satellite ocean color observations to support long-term environmental assessment and coastal management.

Keywords: Ocean color, remote sensing, coastal biogeochemistry, MODIS-Aqua, spatiotemporal variability, Brazilian coast, anthropogenic pressures, Optical Water Types.

Caractérisation de la dynamique biogéochimique des eaux côtières brésiliennes via l'analyse des archives satellites « couleur de l'eau »

RÉSUMÉ

Les zones côtières sont des environnements dynamiques où interagissent des processus naturels et des activités humaines à différentes échelles spatiales et temporelles. Malgré leur importance écologique et socio-économique, l'analyse à long terme de la variabilité biogéochimique côtière reste limitée dans de nombreuses régions, en particulier dans les eaux côtières optiquement complexes. Cette thèse de doctorat étudie la variabilité spatio-temporelle et l'évolution à long terme des propriétés biogéochimiques le long de la marge brésilienne à partir d'observations satellitaires de couleur de l'océan.

L'étude repose sur plus de vingt ans (2002-2022) de données MODIS-Aqua à 1 km de résolution, traitées à l'aide de la correction atmosphérique OC-SMART. Afin de prendre en compte la forte hétérogénéité optique des eaux côtières brésiliennes, les restitutions de la chlorophylle-a (Chl-a), des matières en suspension (SPM) et du carbone organique particulaire (POC) s'appuient sur des approches fondées sur les types optiques de masses d'eau (OWTs), incluant le développement d'algorithmes spécifiques pour la SPM et le POC dans le cadre de cette thèse. La variabilité et les tendances à long terme sont analysées à l'aide de méthodes statistiques robustes combinant la décomposition Census X-11, le test saisonnier de Mann–Kendall et des modèles additifs généralisés (GAMs).

À l'échelle nationale, les résultats mettent en évidence une forte hétérogénéité spatiale des trajectoires biogéochimiques côtières, dominées par une variabilité saisonnière et interannuelle liée aux forçages hydro-climatiques et aux apports fluviaux. L'analyse des tendances révèle des hotspots côtiers contrastés, caractérisés par des dynamiques de stabilité, de variabilité ou de changement soutenu sur les deux dernières décennies. La comparaison avec des produits multi-capteurs montre que MODIS-Aqua, lorsqu'il est traité avec des approches adaptées, offre une représentation plus cohérente et robuste des eaux côtières fortement turbides.

Deux études de cas régionales permettent d'évaluer le rôle relatif des pressions anthropiques et des forçages naturels. Dans le sud-est du Brésil, le développement du complexe industrialo-portuaire d'Açu est associé à une augmentation durable et spatialement localisée des concentrations de SPM, en lien avec les activités de dragage et d'expansion portuaire. Sur

la côte équatoriale amazonienne du Maranhão, les augmentations à long terme de la SPM et de la Chl-a sont fortement liées aux changements d'usage des sols, notamment à la déforestation et à l'expansion des pâturages, indiquant un contrôle anthropique dominant sur l'évolution biogéochimique côtière.

Cette thèse démontre ainsi l'intérêt d'un cadre intégré combinant observations satellitaires de long terme, modélisation bio-optique fondée sur les OWTs et analyses robustes de séries temporelles pour le suivi et l'attribution des changements biogéochimiques côtiers. Elle apporte de nouveaux éléments sur le fonctionnement des eaux côtières brésiliennes et souligne le potentiel de la couleur de l'océan satellitaire pour soutenir l'évaluation environnementale et la gestion des zones côtières.

Mots-clés : Couleur de l'eau, télédétection, biogéochimie côtière, MODIS-Aqua, variabilité spatio-temporelle, côtes brésiliennes, pressions anthropiques, types optiques.